THE GEOCHEMISTRY OF A SUITE OF ECLOGITE XENOLITHS FROM THE RIETFONTEIN KIMBERLITE, SOUTH AFRICA

CLARE M. APPLEYARD

DEPARTMENT OF GEOLOGICAL SCIENCES
UNIVERSITY OF CAPE TOWN

JANUARY 2000

Dissertation submitted to the University of Cape Town in fulfilment of the requirements for the degree of Master of Science.

Declaration

I hereby declare that all the work presented in this dissertation is my own except where otherwise stated in the text

Clare Appleyard

January 2000 Signed by candidate

Signature removed

ABSTRACT

The Rietfontein kimberlite is an off-craton kimberlite pipe, located west of the Kaapvaal Craton at 26.75°S, 20.04°E and hosts a range of xenocryst lithologies, including peridotite, eclogite and a suite of megacryst minerals. This study focuses on a suite of eclogite xenoliths, which were subject to a detailed petrographical and geochemical study, aimed at their characterisation and comparison to eclogites from on-craton and other off-craton localities. Garnet, clinopyroxene, accessory and secondary minerals were analysed for major element compositions using electron microprobe techniques and garnet and clinopyroxene trace element compositions were determined by Laser Ablation Inductively-Coupled-Plasma Mass Spectrometry (LA-ICP-MS) techniques. Oxygen isotopic compositions of five garnet samples were obtained using laser flourination techniques, followed by analysis by gas source mass spectrometry.

Three petrographically distinct eclogite groups can be identified *viz.* bimineralic, opx-bearing and kyanite eclogites. The kyanite eclogites are markedly fresher than the bimineralic and opx-bearing eclogites and contain fewer accessory and secondary minerals. Many of the bimineralic and opx-bearing eclogites are highly altered, with orthopyroxene generally showing more alteration than garnet or clinopyroxene. Triple junctions in many samples indicate good equilibration. Accessory minerals in the eclogites include sulphides, ilmenite and rutile, whereas micas and amphiboles are common secondary minerals. The accessory minerals occur mostly interstitially, whereas the secondary minerals most commonly form alteration rims around the primary minerals. One sample shows an excellent example of garnet exsolution from clinopyroxene. Texturally, both Group I and Group II eclogites can be identified, although Group II eclogites dominate the suite. The modal proportions of garnet:clinopyroxene in the samples vary from 70:30 to 30:70, with an average ratio of 49:51, although small sample sizes and large degrees of alteration often made estimates of modal proportions erroneous. Kyanite and orthopyroxene both reach a maximum of 20 volume %.

The kyanite eclogites are geochemically distinct from the remaining eclogites with regards to both major and trace element compositions. Garnets from the kyanite eclogites are richer in Ca and are Cr-depleted relative to garnets from the bimineralic and opx-bearing eclogites, which tend to be more magnesian. Clinopyroxenes from the kyanite eclogites are more sodic, with higher Al_2O_3 and lower MgO contents than the bimineralic and opx-bearing eclogites. The

higher Na_2O and lower MgO contents in clinopyroxenes from the kyanite eclogites result in these eclogites being classified as Group B eclogites, whereas the bimineralic and opx-bearing eclogites classify as Group A and Group B eclogites. Low Na_2O_{gt} and K_2O_{cpx} concentrations mean that the majority of the Rietfontein eclogites are also Group II eclogites. All primary minerals are homogeneous, indicating compositional equilibrium within the samples. Garnets from both the bimineralic and opx-bearing eclogites show smoothly varying REE patterns and are relatively depleted in LREE, whereas clinopyroxenes show enrichment in LREE. Garnets and clinopyroxenes from the kyanite eclogites have distinctly different patterns. Garnets exhibit a positive Eu anomaly and clinopyroxenes have an overall convex upwards REE pattern and both are extremely depleted in LREE. Garnets from the kyanite eclogites have Sr, Sm and Nd contents greater than the bimineralic and opx-bearing eclogites, whereas clinopyroxenes from the kyanite eclogites have lower REE, Sc and Y abundances than the remaining eclogites. Partitioning of trace elements between clinopyroxene and garnet in the Rietfontein eclogites is shown to be primarily dependent on the Ca content of garnet, with the more Ca-rich garnets having greatest REE concentrations. Whole-rock compositions of the eclogites have been reconstructed from mineral compositions and are largely basaltic. The kyanite eclogites are richer in Na and Al than the bimineralic and opx-bearing eclogites, which are more magnesian. The kyanite eclogites exhibit compositional similarities to oceanic gabbros and most of the eclogites show strong similarities to boninites. The kyanite eclogites show distinctly different whole-rock REE patterns, with strong LREE depletion and positive Eu anomalies. The bimineralic and opx-bearing eclogites exhibit a range of patterns, mostly flat or showing a regular transition from relative LREE enrichment to relative HREE depletion. Oxygen isotope compositions of garnets from the Rietfontein eclogites range from 5.16-6.84‰, which fall within mantle defined $\delta^{18}O$ values and provide no clear evidence of a crustal precursor.

The major element compositions of garnet, clinopyroxene and, in the case of the opx-bearing eclogites, orthopyroxene, were used to calculate equilibration pressures and temperatures of the Rietfontein eclogites. The results indicate derivation from mantle depths, with temperatures of 733-1000°C (Krogh, 1988) and pressures of 24-39kb (Brey & Köhler, 1990) having been estimated. This large range in equilibration pressures and temperatures represents a significant range in mantle stratigraphy and the higher average equilibration temperatures of the kyanite eclogites provide evidence for derivation of these eclogites from greater depths than that of the bimineralic and opx-bearing eclogites. Geotherms constructed from the temperature and

pressure estimates of the opx-bearing eclogites yield heat flow approximations of 41-44mW.m^{-2}, most similar to geotherms for established on-craton areas.

The unambiguous differences in composition and equilibration conditions between the kyanite eclogites and the bimineralic/opx-bearing eclogites indicate that the Rietfontein eclogites represent samples from two distinct eclogite bodies situated at depth. A model is proposed whereby all three groups of eclogites originate as unrelated remnants of oceanic crustal material, with one body represented by the kyanite eclogites, the other by the bimineralic and opx-bearing eclogites. Subduction of plagioclase-rich, basaltic oceanic crust to eclogite facies depths would yield eclogites with compositional characteristics similar to those of the Rietfontein kyanite eclogites, *viz.* positive Eu anomalies and Na- and Al-rich whole rock compositions. In contrast, subduction, hydrothermal alteration and metamorphism to eclogite of an oceanic crustal section consisting of basalt, gabbro and boninite is suggested to be the source of the Rietfontein bimineralic and orthopyroxene-bearing eclogites. Underplating of the continental lithosphere by these unrelated eclogite bodies would then allow the Rietfontein kimberlite to separately sample each eclogite body as it ascended towards the surface.

ACKNOWLEDGEMENTS

An great number of acknowledgements need to be made at the end of a project that has taken almost two years to complete and a number of people have contributed towards this, both on a working level and on a more personal level.

Firstly, I must thank two sterling supervisors, Professor Anton le Roex and Dr Dave Bell who have constantly urged me to do my best, guided me in the right direction, and provided hours of useful discussion and insight into the finer details of mantle geochemistry. The reading of, and comments on, a seemingly endless stream of dissertation chapters were much appreciated, as were the constant words of encouragement when there seemed to be no light at the end of the tunnel. Drs Clive Stowe, Dave Reid and Ben Harte are also thanked for their useful discussions with regards to various aspects of the project. Thanks must also go to the NRF (formerly the FRD) for the financial assistance provided throughout the duration of the project.

A geochemical project can not exist without samples, and over half the samples in this project had previously been collected by Dr John Gurney. A more recent sampling trip to Rietfontein took place in August 1998, for which Drs Bell and Gurney must be thanked - they have a far keener eye for eclogites than myself.

The analytical data on which this project is based could not have been obtained without the help of a number of people. Thanks must go to Prof. le Roex and the late Dick Rickard for assisting in the use of the electron microprobe; Dr Andreas Späth and Prof. le Roex for their help on the LA-ICP-MS; Dr Chris Harris for the running of oxygen isotope analyses; and Shireen Govender for her watchful eye when cleaning samples with HF acid. David Wilson expertly prepared what seemed like an infinite number of microprobe sections and grain mounts.

An essential part of a geochemical study is to compare data with previously recorded data, and in this regard, a number of people were indispensable. Eva Anckar expertly runs the Kimberlite Data Base at UCT and she willingly and efficiently handled all my data queries and gave of her time to listen when needed. Petrus le Roux very kindly donated his entire MORB database to me, thus saving me an infinite number of hours, for which I am decidedly grateful. When it came to exploring the intricacies and potential of CoPlot and CoDraw, Petrus was indispensable,

and many of the graphs reflect his knowledge in this field. Any computer problems I stumbled across were graciously sorted out by Dr Dave Reid, who also kindly allowed use of his slide scanner.

Editing a manuscript this size must be everybody's worst nightmare, but I did manage to find a few people willing to take on the mammoth task. Bernadette, Bronwyn and Lisa did a fabulous job of correcting my typographical, grammatical and formatting errors, and their input was much appreciated.

My family played a vital role in providing words of support and encouragement and kept me going through the tough times over the past two years. Numerous people have been indispensible and deserve to be credited for making the last two years what they have been. Paul, you've been an absolute star, and I couldn't have made it without you; Bronwyn, thanks for being a great friend over the past 10 years, and for providing wonderful entertainment as a flatmate; the geology folk (Bernadette, Kalle, Petrus and Stewart) for making the long hours bearable and sociable; and finally, Virginia, Marchelle, Lisa and all the others for making the year as entertaining and unforgettable as it has been. Should I have forgotten anybody, apologies, and know that everything has been much appreciated.

TABLE OF CONTENTS

1. INTRODUCTION

1.1 Mantle samples

Crustal rocks, comprising igneous, sedimentary and metamorphic rocks, are commonly exposed on the Earth's surface, often *in situ*. The upper mantle is defined as the segment below the crust, extending to depths of 660 km (Haggerty, 1995), and examples of mantle derived samples are rarely, if ever, exposed *in situ*. For this reason, mantle xenoliths, together with other mantle derived rocks, have long been a source of interest in geological studies. Harte & Hawkesworth (1989) identified four major mantle domains, namely oceanic mantle lithosphere, continental mantle lithosphere, convecting upper mantle and convecting lower mantle. Each domain may provide material for magmatic rocks, thus providing us with samples of the upper mantle. The convecting upper mantle comes to the surface at mid-ocean ridges (Harte & Hawkesworth, 1989) and is thus sampled in the form of mid-ocean ridge basalts (MORB). Subduction of oceanic lithosphere may result in this material accreting to the continental mantle lithosphere (Harte & Hawkesworth, 1989). Oceanic and continental lithosphere can thus be intimately associated with each other and are both sampled at the surface of the Earth.

Xenoliths represent fragments of country rock adjacent to magmatic intrusions. These fragments are broken off and incorporated into the magma as it forces itself upwards through the mantle and crust. Mantle xenoliths in kimberlites and alkali basalts, together with ophiolite complexes, alpine peridotites and sea floor fault blocks, provide geologists with natural occurrences of upper mantle rock types (Harte, 1983). Four main groups of mantle-derived xenoliths have been recognised (Harte, 1983), namely peridotites and pyroxenites; eclogites; megacrysts or discrete nodules; and glimmerites and MARID-suite (Mica-Amphibole-Rutile-Ilmenite-Diopside) xenoliths. Alkali basalts commonly contain xenoliths of high pressure partial melts (websterites, wehrlites and pyroxenites but excluding eclogites), whereas peridotites, eclogites and dunites are more common in kimberlites (Haggerty, 1995). Whereas kimberlites can occur in both on- and off-craton settings, alkali basalts are mostly restricted to non-cratonic continental localities (McDonough, 1994).

1.2 The xenolith record in South Africa

South Africa has a large number of known kimberlite occurrences, both on and off the Kaapvaal Craton (Dawson, 1989). As a result of these abundant kimberlite occurrences, mantle-derived xenoliths are well sampled in southern Africa. Peridotite is the dominant xenolith observed at most southern African kimberlite localities (Gurney *et al.*, 1991). These peridotite xenoliths are diverse, comprising granular and sheared varieties and various types of metasomatised peridotite (Harte, 1983). Modal metasomatism is common in many South African peridotites and pyroxenites, and may affect mineralogy and composition in the xenoliths. Eclogites are also known to be widely distributed throughout South Africa (Rickwood *et al.*, 1969) and pyroxenites are best represented at Matsoku, where most are coarse grained, but some are occasionally deformed and metasomatised (Gurney *et al.*, 1991). Although megacrysts are common in a number of Southern African kimberlites, such as Monastery, Frank Smith, Kimberley, Orapa and Jagersfontein (Gurney *et al.*, 1991), Cr-rich megacrysts are rare. A number of MARID xenoliths have also been recorded from the Kimberley kimberlite pipes (Erlank *et al.*, 1987). Many South African kimberlite pipes are diamondiferous, and these diamonds are occasionally xenolith hosted. Diamonds, when enclosed in xenoliths, are predominantly found within eclogites and peridotites (Kirkley *et al.*, 1991), with eclogite the most common xenolith host, and garnet harzburgite the most common peridotitic host (Gurney, 1989).

Whereas many southern African kimberlites are located within the confines of the Kaapvaal Craton (approximately 770 - Gurney *et al.*, 1991), and have been intensively studied, many off-craton kimberlites have been noted, which also frequently contain mantle derived xenoliths. Studies of off-craton peridotites (Mitchell, 1984) have indicated that such mantle derived xenoliths originate, on average, at shallower depths than those from on-craton kimberlites of the Kaapvaal Craton. The greater depth of origin for high temperature peridotites within the craton margins, as opposed to those from outside the craton, suggests a deeper lithosphere in cratonic regions (MacGregor, 1975; Boyd & Gurney, 1986). Some differences can be noted between on- and off-craton peridotites, such as a higher enstatite Al content in orthopyroxene from off-craton garnet peridotites, when compared to on-craton peridotites (Gurney & Harte, 1980). Pearson *et al.* (1994) note that off-craton peridotites from Namibia have higher average diopside contents and lower Mg#'s than on-craton peridotites from Siberia. One of the most notable differences between on- and off-craton kimberlite localities, and their xenoliths, is the essential confinement

of diamondiferous kimberlites to the Kaapvaal Craton (Gurney, 1990). The barren nature of off-craton kimberlites is considered to be a consequence of derivation from shallower depths than on-craton kimberlites (Nixon, 1980). Heat flow is lowest in Archaean cratons, such as the Kaapvaal Craton, and increases away from the craton in the surrounding Proterozoic mobile belts (Nyblade and Pollack, 1993). One possible explanation for heat flow differences is the reduced lithospheric thickness below off-craton areas (Boyd & Gurney, 1986), which means that the asthenosphere is closer to the surface than it is beneath the craton. The position of Rietfontein in an off-craton mobile belt could suggest a shallower kimberlitic origin (considering previous studies), and a higher heat flow could be expected in the region.

1.3 Eclogite in the mantle

What is an eclogite?

The term "eclogite" was first applied to a metamorphic rock found in Bavaria, consisting of green omphacite and pink pyrope, by Haüy (1822). The discovery of eclogites as inclusions in kimberlites resulted in notable differences being observed between the metamorphic eclogites and kimberlitic eclogites, and it was suggested that the term "griquaites" be applied to the kimberlitic eclogites (Beck, 1899). This term was never really globally accepted (Dawson, 1980), and currently, eclogite as a petrographic rock name is restricted to rocks of broadly basaltic composition which lack primary plagioclase and have a predominant (>70 volume %) assemblage of garnet and jadeite-bearing clinopyroxene (Carswell, 1990). Numerous other anhydrous minerals have been observed as accessory minerals in eclogites, with quartz, kyanite, orthopyroxene and rutile being among the most common. Eclogites can be found in a number of geological settings, from high-pressure, high-temperature xenolith inclusions in kimberlites and other alkali magmas, to metamorphic eclogites found in gneissic terrains or alpine-type metamorphic rocks (Carswell *et al.*, 1965).

It has already been mentioned that coarse peridotite is the most frequently recorded mantle xenolith retrieved from kimberlite pipes. However, at select southern African kimberlite localities, eclogites are seen to dominate the xenolith suite. Such localities include Roberts Victor, Newlands and Bellsbank. Rietfontein is an off-craton kimberlite possessing a significant proportion of eclogite xenoliths. Despite the dominance of eclogites at Roberts Victor, the upper mantle at this locality, as represented by the kimberlite concentrate, is 85 volume % garnet peridotite, and the amount of eclogite in the upper 200km of subcontinental upper mantle is

estimated to be <1 volume % overall (Schulze, 1989). Previous estimates of the eclogite component at Roberts Victor ranged from 80% (MacGregor & Carter, 1970) to more than 98% (Hatton, 1978). The overall greater proportion of peridotite has led to the conclusion that peridotite is the most important, and volumetrically the greatest upper mantle constituent, but locally significant concentrations of eclogite do occur (Schulze, 1989). An eclogite dominated xenolith suite may result from structural weakening and subsequent disaggregation of peridotite xenoliths after metasomatism.

Abundant eclogite xenoliths have been noted in kimberlites off the Kaapvaal Craton, and along the craton margins (*eg.* Robey, 1981; Pearson *et al.*, 1995). A number of differences can be noted between on- and off-craton eclogite xenoliths. Robey (1981) believed the off-craton eclogites of the Central Cape Province to be fragments of Namaqua-Natal metamorphic rocks, and consequently proposed a crustal origin. Eclogites from off-craton localities are commonly associated with mafic garnet granulites, which are generally uncommon in on-craton kimberlites (Griffin *et al.*, 1979). Off-craton eclogites have been observed to be finer-grained and more granuloblastic than on-craton eclogites and the equilibration pressures of 10-23 kb (Robey, 1981) are much lower than those for many on-craton eclogites, where the presence of diamond can indicate minimum equilibration pressures of 45 kb (Gurney *et al.*, 1991). Equilibration temperatures for off-craton eclogites from the Cape Province were found to overlap completely with equilibration temperatures from on-craton eclogites (Pearson *et al.*, 1995), with most temperatures being greater than 930°C.

The proposed origin of eclogites as metamorphosed subducted oceanic crust (*eg.* Helmstaedt & Doig, 1975; MacGregor & Manton, 1986), together with the presentation of data (Ireland *et al.*, 1994) suggesting a link between eclogites derived from the deep lithosphere of an Archaean craton (greater than 150 km) and the crustal rocks (most notably tonalites, trondhjemites and granodiorites) of that craton, provides direct evidence of crust-mantle interactions and makes eclogite an important indicator of such relationships. The occurrence of deep subduction processes during the Archaean has been indicated by eclogites of mid-Archaean age that appear to be high-pressure melting residues of subducted oceanic crust (Pearson *et al.*, 1994). MacGregor (1975) believes that the Cretaceous lithosphere is thickest below Kimberley and thins to the east and west, a theory which was subsequently agreed upon by a number of authors,

including Boyd & Gurney (1986), who suggest a cratonic lithospheric thickness of 150-200km. Whereas the cratonic lithosphere is peridotite-rich, eclogite plays an important role in its structure, and age relationships between eclogites and peridotites suggest that the pre-existing peridotitic keel of the Kaapvaal Craton may have been periodically underplated by diamondiferous eclogite (Gurney, 1990). Processes resulting in the growth of continental lithosphere are uncertain, but the addition of new mantle material and recycling of crustal material back into the mantle can all contribute to the growth and modification of the lower cratonic lithosphere (Harte & Hawkesworth, 1989).

1.4 Project aims and relevance of the Rietfontein eclogite suite

Eclogite studies over the years have concentrated mainly on the better known on-craton eclogite suites, and, to a certain extent, off-craton eclogites have been neglected. As a result, far more is known about the lithospheric structure, crust-mantle interactions and the nature of the mantle under cratonic areas. Rietfontein is an off-craton kimberlite locality with a well represented xenolith suite. A comprehensive study of such an off-craton suite can substantially improve our knowledge of crust-mantle interactions, and the structure and nature of the lithosphere in these lesser studied areas. The aims of this study of the Rietfontein eclogites are thus as follows:

- to petrographically characterise the Rietfontein eclogite suite,
- to investigate the major and trace element compositions of the eclogites,
- to compositionally characterise petrographic groupings within the eclogite suite,
- to compare the Rietfontein eclogites to other off- and on-craton eclogites, and to note any similarities or differences,
- to determine the temperatures (and, where possible) pressures of equilibration of the Rietfontein eclogites,
- to investigate the thermal structure of the lithosphere surrounding Rietfontein,
- to reconstruct, and characterise the whole-rock compositions of the eclogite suite,
- to record the oxygen isotope characteristics of the eclogites,
- to determine whether the eclogites are crustal or mantle derived, and
- to determine which petrogenetic model best fits the characteristics expressed by the Rietfontein eclogites.

2. THE RIETFONTEIN KIMBERLITE

2.1 The Rietfontein kimberlite and associated xenoliths

Rietfontein is an off-craton locality, situated west of the Kaapvaal Craton. Its occurrence was first noted in 1913 (Wagner, 1914) and it is located close to the present day Namibia-South Africa border, at 26.75°S, 20.04°E (*Figure 2.1*). The pipe was initially believed to be diamondiferous (Gurney *et al.*, 1971), but this impression was later found to be incorrect (Dawson, 1989) and the pipe is, in fact, barren. The non-diamondiferous nature of this off-craton kimberlite is consistent with the confinement of most diamondiferous kimberlites to cratonic regions (Gurney, 1990). The Rietfontein kimberlite pipe has a surface area of approximately 2 hectares and a kimberlite dyke, extending almost 1.5km in a north-easterly direction, is associated with the pipe. U-Pb dating of zircons derived from the Rietfontein kimberlite yielded an age of 71.9 Ma, whereas a repeat analysis yielded an age of 71.1 Ma (Davis, 1977).

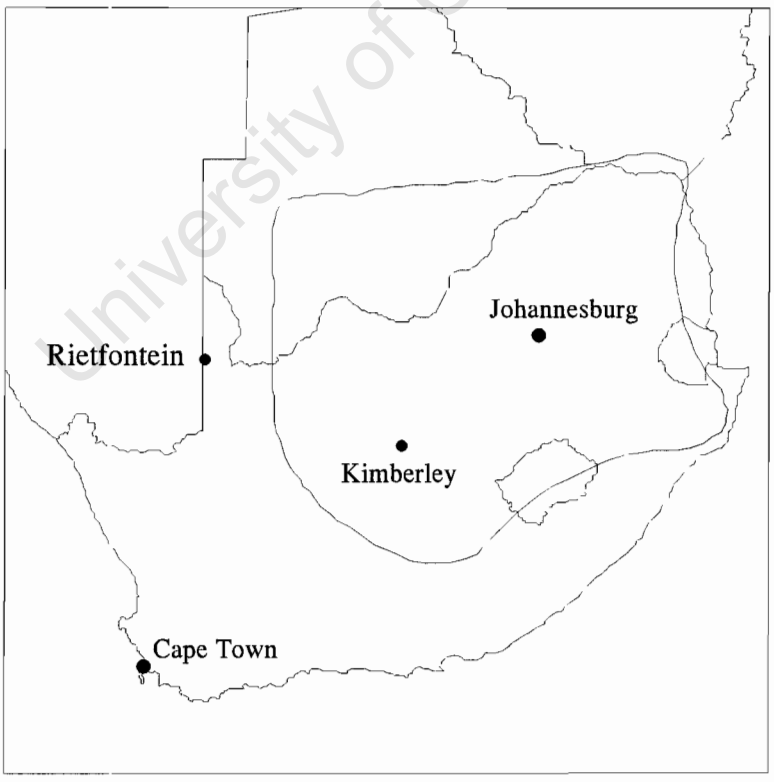

Figure 2.1 *Locality of the Rietfontein kimberlite, relative to the Kaapvaal Craton (outlined).*

The Rietfontein kimberlite consists of macrocrysts and country rock xenoliths set in a fine-grained, phlogopite-bearing matrix. Olivine is the most abundant macrocryst but chrome-diopside, enstatite, phlogopite and garnet are also visible. These macrocrysts reach a maximum size of approximately 3 mm, and are mostly rounded. The olivine macrocrysts are highly fractured, with serpentinised rims, although occasionally entire grains have been serpentinised. Oxide minerals are sparsely scattered throughout the fine-grained groundmass. Phlogopite is common within the groundmass but is not abundant enough to classify the kimberlite as a Group II variety. The kimberlite is thus a Group I kimberlite, after the classification of Smith (1983), having initially been described as a "basaltic" (non-micaceous) kimberlite (Gurney *et al.*, 1971).

Eclogites, including orthopyroxene-bearing and kyanite eclogites, are common xenoliths found within the Rietfontein kimberlite, but peridotites and pyroxenites are also present. The xenolith suite is thus diverse, covering a large range of mantle lithologies. Kyanite, garnet, pyroxenes, ilmenite, rutile, olivine, zircon and pyrite occur in the heavy mineral concentrate (Gurney *et al.*, 1971). Very few studies have been carried out on the Rietfontein kimberlite. Petrographic and major element characteristics of kyanite eclogites from the xenolith suite were recorded by Gurney *et al.* (1971) and the hydroxyl and major element composition of garnets from Rietfontein eclogites were analysed by Bell & Rossman (1992).

2.2 Tectonic setting

Crustal evolution in southern Africa has been complex, and can be traced back to approximately 3.8Ga (Tankard *et al.*, 1982). A number of crustal evolutionary stages are represented by southern African geology and these form a well-defined sequence of events. A brief overview of these stages yields the following basic history. A period of Archaean crustal development gave rise to a number of crystalline massifs, namely the Kaapvaal, Limpopo and Zimbabwe provinces. During the early Proterozoic this basement was buried beneath mostly sedimentary cover, broken by basic magma intrusions forming the Bushveld Igneous Complex and the Great Dyke. In the southern and western parts of the subcontinent a number of Proterozoic orogens had their basement and supracrustal cover tectonically reworked. Accumulation of geosynclinal deposits and emplacement of granitoid intrusions by partial melting of older crust also occurred during this period. Aborted rifting and continental sedimentation mark the Paleozoic Gondwana Era and eventual Mesozoic fragmentation of Gondwana was preceded by continental rift

volcanism, together with the injection of kimberlites, carbonatites and other alkaline intrusions. Sedimentation during this period was limited to the subcontinental margins and depressed interior regions (Tankard *et al.*, 1982).

The Kaapvaal Craton forms the nucleus of South African geology and was established over a period of approximately 1Ga (3.7-2.6Ga; de Wit *et al.*, 1992). Early continental nuclei, from which the Kaapvaal Craton could have developed, may have originated through regional intra-oceanic obduction, giving rise to stacking, tectonic loading and subsidence of the hydrated oceanic thrust stacks (de Wit *et al.*, 1992). Basement rocks within the Kaapvaal Craton consist of granitoids and gneisses (both massive and folded), together with deformed relicts of basic and ultrabasic volcanic and sedimentary sequences (Tankard *et al.*, 1982). Crustal amalgamation within the craton at 3.2Ga (de Wit *et al.*, 1992) was followed by the accumulation of the epicontinental Pongola Supergroup - evidence of cratonisation within the Kaapvaal Province (Tankard *et al.*, 1982). A wide orogenic belt formed along the northern margin of the craton as a result of northwards thrusting during an extended period of tectonic accretion of oceanic and continental fragments (de Wit *et al.*, 1992).

Proterozoic mobile belts bound the Kaapvaal Craton to the south and west. Intense orogenic activity in the southern and western parts of the subcontinent gave rise to these Proterozoic mobile belts (Tankard *et al.*, 1982). The Namaqua-Natal belt is one such belt, bounding the Kaapvaal Craton to the west and south (*Figure 2.2*). The Namaqua (western) part of this belt can be divided into three parts, namely the Gordonia, Richtersveld and Bushmanland Subprovinces (Hartnady *et al.*, 1985), which are thought to have accreted to the African continent as a unit approximately 1400-1200Ma ago (Joubert, 1986). This mobile belt extends around into Namibia, where no Archaean continental crust has yet been identified (Reid *et al.*, 1997), resulting in the description of such areas as "off-craton". The Namaqua Province may represent the deeply eroded infrastructure in the over-riding plate of a cordilleran-type orogeny incorporating the successively accreted Gordonia and Bushmanland Subprovinces (Stowe, 1986). The north-eastern contact zone between the Namaqua belt and the Rehoboth Subprovince is known as the "Namaqua Front" and was activated at a late stage as a zone of transcurrent shearing, granite intrusion and uplift (Stowe, 1983). The Richtersveld Subprovince is suggested to have formed between 2.0-1.9Ga as an island-arc complex that was later

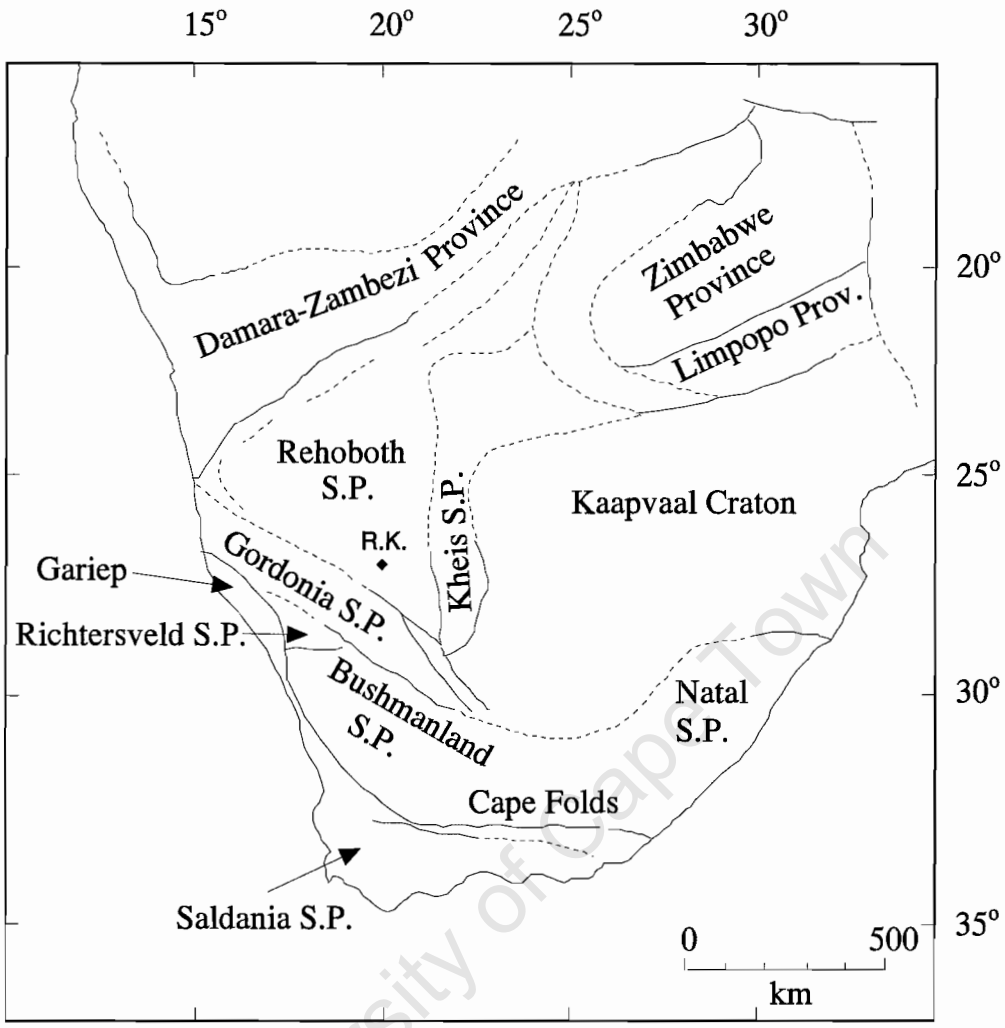

Figure 2.2 *Tectonic provinces and subprovinces (S.P.) of southern Africa (after Hartnady et al., 1985). The Rietfontein kimberlite (R.K.) is seen to be located within the Rehoboth Subprovince, west of the Kaapvaal Craton.*

mobilized at depth along an active continental margin (Hartnady *et al.*, 1985). The Gordonia Subprovince was initially a zone of convergent thrusting and folding, followed by metamorphism and retrograde shearing at around 1.2Ga and 1.1Ga respectively (Hartnady *et al.*, 1985). These subprovinces were later fused to the Kaapvaal provinces by cratonization.

The Kheis Subprovince is located directly west of the Kaapvaal Craton (*Figure 2.2*). The northern extension of this subprovince is not known, due to burial beneath Kalahari and Karoo cover (Stowe, 1986). It developed in a 2.0Ga quartzite-phyllite and amphibolite sequence, and is a thin-skinned fold and thrust belt (Hartnady *et al.*, 1985), which was joined to the Kaapvaal Craton approximately 1900Ma ago (Stowe, 1983). The Kheis Subprovince is underlain by

continental basement on the east side and may have been the margin of a large orogenic belt which evolved between 2100-1360Ma ago (Stowe, 1983). Excessive thrusting within the Kheis Subprovince has produced a tectono-stratigraphic succession consisting of five major thrust sheets (Hartnady *et al.*, 1985). Directly west of the Kheis Subprovince is the Rehoboth Subprovince. Very little is known about this subprovince as it is almost entirely covered by relatively undeformed cover sequences (Hartnady *et al.*, 1985). As a result, the basement composition of this area is unknown. It may consist of early Proterozoic material or could be a deep sedimentary basin into which thick strata (8km) of Nama Group sediments were deposited (C.W.Stowe, *personal communication*). It is within this puzzling, off-craton area that the Rietfontein kimberlite is located (*Figure 2.2*).

2.3 Regional geology

As mentioned in *Section 2.2*, the Rietfontein kimberlite is intruded through rocks and supracrustal cover comprising the Rehoboth Subprovince. Whilst little is known about the basement rocks in this area, including their origin or ages, outcrops of Nama Group and Karoo sediments are visible. Outcrops of Dwyka tillite, a glacial diamictite deposited between 300-350Ma, occur and over much of the Karoo basin this Dwyka rests unconformably on rocks of early Paleozoic to Precambrian age (Tankard *et al.*, 1982). Sedimentation of the Ecca and Beaufort Groups of the Karoo sediments was dominated by fluvial and shoal-water deltaic environments (Tankard *et al.*, 1982). Beneath the Karoo sediments, lie sediments of the Nama Group. These strata cover an extensive area in the southern and central portions of Namibia and adjacent areas of South Africa and formed at the end of a major geotectonic cycle (Germs, 1983). The Nama Group consists of a mostly marine, carbonate and siliciclastic lower part (Kuibis and Schwarzrand Subgroups) and a fluvial upper part (the Fish River Subgroup) (Germs, 1983). Nama Group sediments are older than 510Ma, and were deposited in a broad basin fringed in the north and west by the Damara and Gariep geosynclines during the last stages of orogeny (Tankard *et al.*, 1982). Nama sediments generally lie unconformably over crystalline Kalahari basement, although they may rest conformably or paraconformably on the uppermost Gariep strata (Tankard *et al.*, 1982). These two groups of sediments are the only two groups outcropping in the Rehoboth Subprovince in the vicinity of the Rietfontein kimberlite and, as a result, it is impossible to predict the basement rock composition in the area.

3. PETROGRAPHY

3.1 Introduction

Forty-six eclogite xenoliths collected from the Rietfontein kimberlite have been examined in this study. Most samples were between 1 and 5cm in diameter but two, CMA 1 and JJG 2104, were approximately 6 and 10cm in diameter respectively. The larger samples are all rounded and spheroid in shape, whereas the smaller samples exhibit more angular and irregular shapes. This is most likely due to the fact that these smaller eclogites are not complete samples, but represent fragments that have broken off larger samples. On the basis of petrography, three types of Rietfontein eclogites have been identified, namely:

- bimineralic eclogites
- kyanite eclogites
- orthopyroxene-bearing eclogites (*i.e.* websterites).

Whereas olivine-bearing mantle xenoliths have been comprehensively classified on a textural basis (*eg.* Harte, 1977), only one scheme exists for the textural classification of eclogites, and descriptions of eclogites refer mainly to relative grain sizes within a sample, for example "equigranular". Over the years a number of classification schemes have been developed and used to identify different groups of eclogites. One of these is based purely on textural features - that of MacGregor & Carter (1970). Following this scheme, Group I eclogites contain coarse-grained, subhedral to rounded garnets set in a matrix of anhedral to interstitial clinopyroxene. Group II eclogites contain irregular, anhedral garnet and clinopyroxene grains that together have a tightly interlocking fabric. Group I garnets are cloudy relative to Group II garnets which are generally clear and unaltered. Group II clinopyroxenes tend to be significantly less altered than those of Group I eclogites. Other textural eclogite descriptions include "cumulate" eclogites, which correspond to MacGregor and Carter's (1970) Group I eclogites, whereas an interlocking fabric relates to Group II eclogites (Dawson, 1980). Group II eclogites are also accepted as having a metamorphic granoblastic texture, where straight grain boundaries and triple junctions are common. To compensate for a lack of textural eclogite classifications, authors often describe textures in their own unique manner, for example, Griffin *et al.* (1990) describe eclogites from the Eastern Margin of the Australian Craton as having a "fish-net" texture.

Textural variations within eclogites can be recognised on the basis of (a) fabric differences due to the presence or absence of mineral banding, (b) differences in the proportions and colours of the primary minerals garnet and clinopyroxene, (c) textural variations as a result of metasomatic alteration and (d) the presence of distinctive accessory minerals such as kyanite and diamond (Dawson, 1980; Dawson & Carswell, 1990). Layering is common in eclogite xenoliths and may take the form of mineral layering (such as interbanding of bimineralic eclogite and kyanite eclogite) or textural layering, where, for example "cumulate-textured" eclogite may grade into eclogite with an interlocking fabric (Lappin & Dawson, 1975). A large number of accessory minerals have been observed in eclogites and may be used to characterise eclogite groups. They include quartz and its high-pressure polymorph coesite, plagioclase, sanidine, orthopyroxene, olivine, amphibole, kyanite, sillimanite, corundum, phlogopite, rutile, ilmenite, sulphides (commonly pyrrhotite and pyrite), diamond and graphite (Dawson, 1980).

A number of difficulties arose when attempting to apply the MacGregor & Carter (1970) classification scheme to the Rietfontein eclogites. The first problem was that many of the samples are too small, and the grains sometimes too large for one to obtain an objective view of the texture. The second problem relates to the alteration observed in many samples, which often resulted in distortion of grain boundaries, hence making classification according to the MacGregor & Carter (1970) classification difficult. These same problems also made approximations of modal proportions difficult. Where possible then, the Rietfontein eclogites were classified according to the MacGregor & Carter (1970) scheme and modal proportions were visually estimated as volume percentages (*Table 3.1*). A general discussion of the salient features of the Rietfontein eclogites follows, whereas detailed descriptions for individual samples can be found in Appendix II.

3.2 Petrographic descriptions

3.2.1. Bimineralic eclogites

The bimineralic eclogites contain garnet and clinopyroxene as the primary mineral phases, and account for the majority (76%) of eclogite samples recovered from Rietfontein. Just over half (54%) the bimineralic eclogites can be classified as Group II eclogites but following the discussion in the introduction, the Rietfontein eclogites will be grouped on the basis of their

Table 3.1 *Modal proportions (volume %) of the major and accessory minerals of the Rietfontein eclogites. Proportions determined visually to the nearest 5 %, point counting was not undertaken. Where possible, groups have been assigned according to the scheme of MacGregor & Carter (1970).*

	Group	Garnet	Cpx	Opx	Kyanite	Ilmenite	Rutile	Sulphides	Amphibole
JJG 105	I	60	40					<<1	
Rtfn 48-2	I	50	50						
Rtfn 55-1	I	60	40						
Rtfn 55-2	I	80	20						
CMA 7	I	50	50				<<1		
CMA 9	I	70	30			<<1			
JJG 2104	II	20	60		20				
PC3	II	60	40					<<1	
PC 5.2/2	II	40	60						
PC12	II	30	70						
Rtfn 31-2	II	50	50						
Rtfn 31-3	II	45	55			<<1	<<1		
Rtfn 43-1	II	60	40			<<1	<<1		
Rtfn 43-9	II	40	60						
Rtfn 48-1	II	55	45				<<1		
Rtfn 54-1	II	60	30		10				
Rtfn 54-2	II	30	60		10		<<1		
Rtfn 54-3	II	45	45		10				
Rtfn 54-4	II	30	60		10		<<1	<<1	
Rtfn 55-4	II	30	70						
Rtfn 56-1	II	58	37	5					
Rtfn 57-1	II	50	50						
Rtfn 57-2	II	40	60						
Rtfn 57-3	II	50	50					<<1	
CMA 1	II	30	70						<<1
CMA 2	II	40	60						<<1
CMA 3	II	30	50	20					
CMA 6	II	35	65						
CMA 8	II	50	50						<<1
CMA 12	II	45	45	10					
CMA13	II	35	60	5			<<1		
CMA 15	II	40	60			<<1			
CMA 17	II	70	30						
CMA 18	II	60	40						
PC1		70	30						
PC 5.2/1		65	35					<<1	
Rtfn 31-1		45	55					<<1	<<1
Rtfn 43-10		45	55						
Rtfn 43-7		40	60				<<1		
Rtfn 55-3		50	50						
CMA 4		40	60						
CMA 5		50	50						
CMA 10		50	50			<<1	<<1		
CMA 11		60	35	5					
CMA 14		40	60				<<1		<<1
CMA 16		50	50						<<1

primary mineralogy. The garnet:clinopyroxene modal proportions in these samples ranges from 30:70 to 80:20, with an average ratio of 50:50. Some of the samples consist of almost entirely garnet, or in one case, clinopyroxene, with only a few discrete grains of clinopyroxene or garnet respectively. These samples are all small (approximately 1-1.5cm in diameter) so it is possible that they are merely fragments of larger specimens, and thus not representative of the modal proportions as a whole. Garnets in the bimineralic eclogites show varying colours, from orange, to a darker brown-orange through to purple. Clinopyroxenes occur in various shades of green, from light green to a darker emerald green. Garnets show a large range in size, from 1mm grains to the largest grains which reach approximately 1.5cm in diameter. Clinopyroxenes tend to be smaller than the garnet grains, varying in diameter from 0.5mm - 1cm. Whereas some samples are equigranular, others show bimodal grain size groupings (*Plate 3.1*). Fine grained alteration material (mostly micas and amphiboles) is common along the grain boundaries and fractures within the mineral grains. Replacement of garnet and pyroxenes by metasomatic mica and amphibole is a common feature in eclogites (Dawson & Carswell, 1990) and is seen to have occurred in some of the bimineralic Rietfontein eclogites. Garnet and clinopyroxene occur both as fresh and altered (cloudy) grains, however, in any given sample the garnet generally has a fresher appearance than the clinopyroxene. Kelyphite rims around garnets are visible in some samples, and some clinopyroxenes show "spongy" rims, which are composed of very fine grained, disseminated material, probably clinopyroxene (*Plate 3.2*). These spongy rims follow the outline of the clinopyroxene grains and fresh clinopyroxene cores grade progressively into the altered rims.

Clinopyroxene commonly exhibits strain in the form of undulose extinction, and triple junctions are common in samples containing cumulus clinopyroxene. The minerals commonly show extensive fracturing and embayed grains are not unusual. Both curved and straight grain boundaries occur. Veins containing rounded vesicles of carbonate material are observable in many samples. Similar veins have been attributed to decompression melting during rapid ascent within the kimberlite (Dawson & Carswell, 1990). Garnets in four eclogites contain microscopic inclusions of rutile needles, which are randomly orientated (*Plate 3.3*).

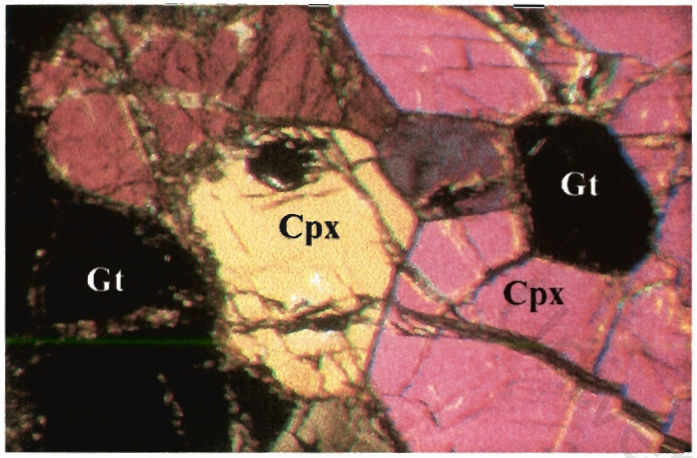

Plate 3.1 *Variable garnet (gt) and clinopyroxene (cpx) grain sizes in sample CMA 1, with triple junctions visible between some grains. 2.5x magnification, XPL, field of view (fov) = 3mm.*

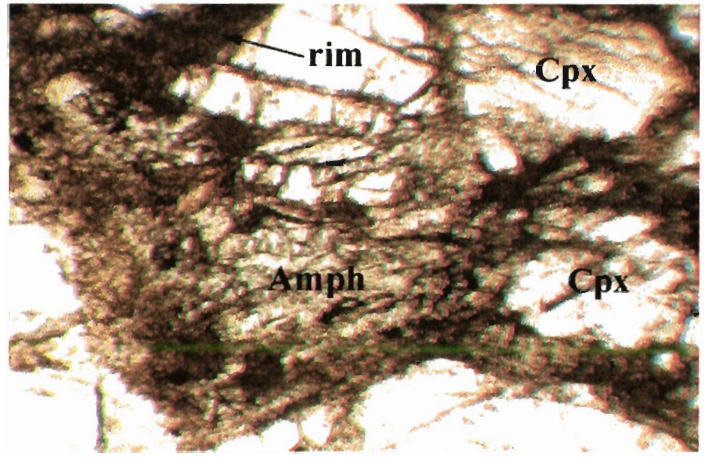

Plate 3.2 *"Spongy" rims around clinopyroxene cores, and secondary amphibole (amph), both the result of metasomatism, in CMA 1. 4x magnification, PPL, fov = 1.8mm.*

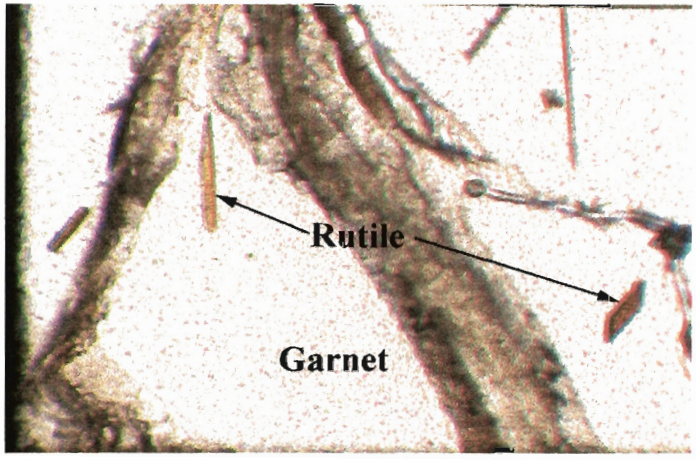

Plate 3.3 *Randomly oriented rutile inclusions in a garnet grain from sample Rtfn 48.1. 10x magnification, fov = 1mm.*

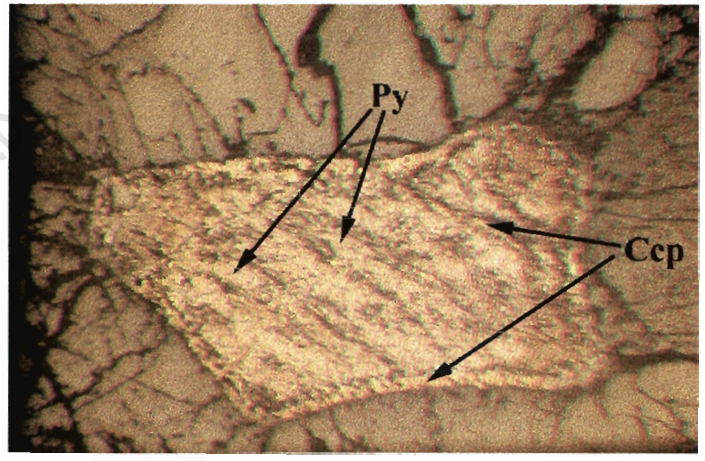

Plate 3.4 *Interstitial sulphide inclusion in JJG 105. This sulphide is well zoned, with a chalcopyrite (Ccp) rim, and a predominantly pyrite (Py) core. Areas of Ccp also observed in the core. 2.5x magnification, reflected light, fov = 3mm.*

Accessory minerals in the Rietfontein bimineralic eclogites include sulphides (pyrite and chalcopyrite), rutile and ilmenite, whereas secondary minerals comprise phlogopite and amphibole (actinolite, edenite and hornblende). Most of the eclogites contain at least one accessory mineral, and very few are fresh enough to contain no secondary minerals. The amphiboles occur as fine grained, irregular laths and subhedral grains with a pleiochroic green colour (*Plate 3.2*), although a few larger, continuous plates are occasionally observed. The phlogopite and amphibole both occur in the form of fine grained, disseminated plates, rimming garnet and pyroxene grains. Such phlogopite rims surrounding garnets have been described as secondary (Carswell, 1970) and may have a number of origins. MacGregor & Manton (1986) believe that such secondary phases are an integral part of the eclogite bulk chemistry, whereas others (*eg.* Caporuscio & Smyth, 1987) believe that they were introduced by external metasomatising fluids. Jerde *et al.* (1993*a*) believe secondary phases such as serpentine, phlogopite, ilmenite and amphibole to be alteration products of high pressure-temperature assemblages. Whereas phlogopite and amphibole are secondary minerals, it is difficult to say whether the oxide and sulphide minerals are primary or secondary, due to their common occurrence in areas of alteration. Rutile and ilmenite most commonly take the form of interstitial blebs, and sulphides also occur interstitially, although a few inclusions within garnet were observed. The sulphides are often heterogeneous, showing distinctly different core and rim compositions, and even different compositions within the core itself (*Plate 3.4*). Such zoning and intergrowth of different sulphide minerals may indicate unmixing from a higher temperature monosulphide solid solution. Many of the eclogites exhibit alteration to varying degrees, and much of this appears to be a direct result of entrainment within the kimberlite, with minerals such as calcite, serpentine, micas, chlorite, and brucite developing as a consequence of this interaction. These minerals appear mostly in large patches, and occasionally in veins, between the garnet and clinopyroxene grains and exhibit a texture very similar to that shown by kimberlites.

One sample shows the unusual textural feature of garnet exsolution within clinopyroxene *(Plate 3.5*). These exsolution lamellae are approximately 0.25 to 0.5mm in diameter and reach lengths of 1 to 1.5cm. The garnet lamellae are fresh, and up to 4 or 5 lamellae can occur in a single, optically continuous clinopyroxene grain. Exsolution of garnet from clinopyroxene in eclogites

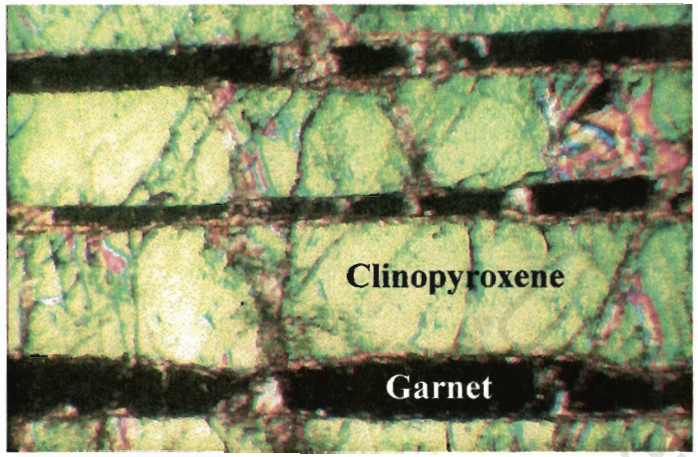

Plate 3.5 *Garnet exsolution lamellae in clinopyroxene, sample CMA 1. Lamellae can be up to 0.5mm in diameter. Garnet has exsolved from a large, optically continuous cpx grain. 2.5x magnification, XPL, fov = 3mm.*

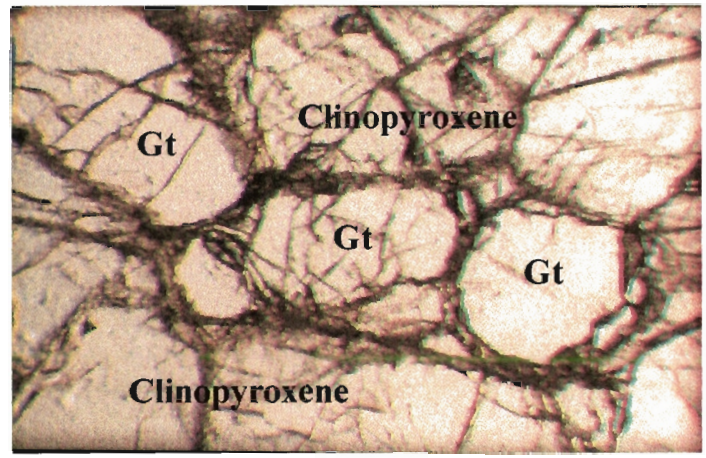

Plate 3.6 *Granular garnets in CMA 1, forming a texture similar to a "necklace" texture. 2.5x magnification, PPL, fov = 3mm.*

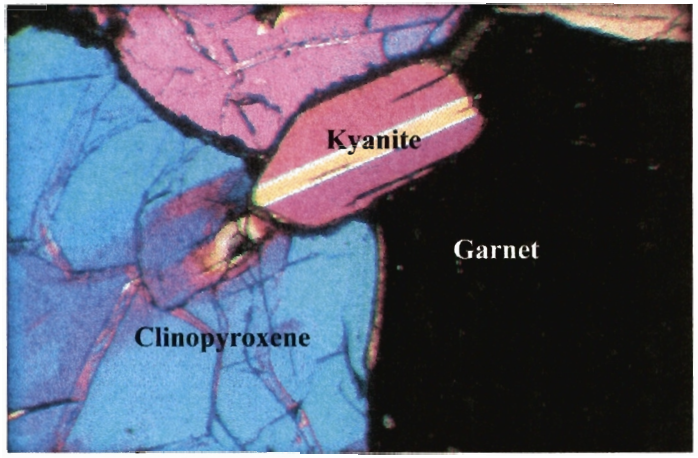

Plate 3.7 *Fresh kyanite eclogite, showing interlocking texture between kyanite, garnet and clinopyroxene. 2.5x magnification, XPL, fov = 3mm.*

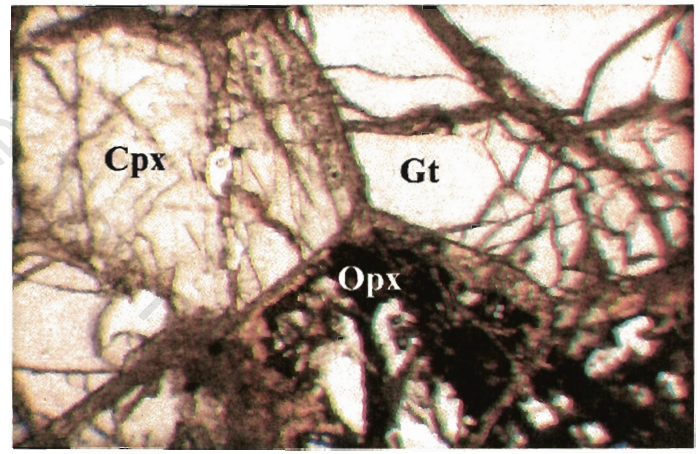

Plate 3.8 *Triple junction in an opx-bearing eclogite, between clinopyroxene (cpx), orthopyroxene (opx) and garnet (gt). 2.5x magnification, PPL, fov = 3mm.*

has been described by Harte & Gurney (1975), Smyth *et al.* (1989) and Jerde *et al.* (1993) and is commonly attributed to cooling of a sample from near-solidus conditions to normal mantle lithosphere temperatures (Harte & Gurney, 1975). This particular sample (CMA 1) also shows fresh, rounded granular garnets, up to 2mm in diameter, forming an interlocking texture with the clinopyroxene grains (*Plate 3.6*).

3.2.2 Kyanite eclogites

Five kyanite eclogites have been described in this study and all can be classified as Group II eclogites (*Table 3.1*). The samples are all relatively fresh, showing very little sign of alteration relative to the bimineralic and orthopyroxene-bearing eclogites (*Plate 3.7*). Garnet, clinopyroxene and kyanite are all equigranular, with an average grain diameter of 1.5 - 2mm. Garnets are orange in colour, clinopyroxenes are pale green and kyanite shows a distinctive pale blue colour. The kyanite grains are mostly euhedral, sometimes rounded, and simple twinning is common. Triple junctions among the three phases are common, indicating that the minerals are well equilibrated. Garnet grain shapes are variable, ranging from rounded, to euhedral, to irregular, and some contain inclusions of clinopyroxene. Clinopyroxene tends to be irregularly shaped, fractured and shows slight alteration along the rims of the grains, similar to the spongy rims described in the bimineralic eclogites. Such altered rims are commonly attributed to metasomatic processes (Taylor & Neal, 1989). Serpentinization is common along fractures and both curved and straight grain boundaries occur between the primary minerals. Accessory minerals are scarce, with only interstitial rutile (present in two samples) and pyrite (present in one sample) having been identified. The modal abundance of kyanite in these rocks ranges between 5 and 20 volume % (*Table 3.1*).

3.2.3 Orthopyroxene-bearing eclogites

Six of the Rietfontein eclogites were found to contain orthopyroxene and, due to the relatively low modal proportions of orthopyroxene in these rocks (from less than 5% to a maximum of 20%; *Table 3.1*), these eclogites are referred to as orthopyroxene-bearing eclogites, rather than garnet websterites. A garnet websterite will consist of primary clinopyroxene and orthopyroxene with accessory garnet. However, the Rietfontein orthopyroxene-bearing eclogites consist of primary garnet and clinopyroxene with mostly accessory orthopyroxene. It will also

be seen in this chapter, and in subsequent chapters, that there are neither petrological nor compositional factors distinguishing the orthopyroxene-bearing eclogites from the bimineralic eclogites. For these reasons, the term "orthopyroxene-bearing eclogite" has been favoured over the term "garnet websterite".

Although some of the orthopyroxene-bearing samples are identifiable as Group II eclogites, it is difficult to group others into MacGregor & Carter's (1970) classification scheme, due mainly to the degree of alteration. Garnet is consistently the freshest mineral and orthopyroxene the most altered. The eclogites are medium to coarse grained, with garnet grains reaching a maximum diameter of 1cm. Garnets show a colour range of dark orange to rose pink, whereas clinopyroxenes are all dark to emerald green in colour. Subhedral, rounded and irregular garnet and clinopyroxene grain shapes can be observed. Serpentinization is common along fractures and grain boundaries. Triple junctions indicate equilibration within the samples (*Plate 3.8*) and form the basis of the classification as Group II eclogites. Embayed edges are also a feature of some of the clinopyroxenes, as is replacement of clinopyroxene by secondary minerals, such as serpentine. Clinopyroxene in some of these orthopyroxene-bearing samples exhibit "spongy" rims and decompression melting veins occasionally occur, as described for the bimineralic eclogites. Orthopyroxene in most of the samples is highly altered along fractures and grain boundaries, having been replaced by a dark reddish-brown mineral, similar in appearance to the kelyphite rims often found around garnets, although fresh cores of orthopyroxene still remain in most cases. This high degree of alteration makes it difficult to petrographically distinguish the original grain outlines. Pyrite is present as an interstitial accessory mineral in one sample and accessory rutile is the only oxide mineral observed. Fine grained, pleiochroic green amphibole is found rimming the primary mineral grains, and in alteration veins running through the samples.

3.3 Discussion

Despite the small sample size of most of the Rietfontein eclogites, many samples can still be identified (on a textural basis) as Group I or Group II eclogites, based on the classification scheme of MacGregor & Carter (1970). However, some samples were too small, or too coarse-grained, to confidently be classified according to this scheme. Group II eclogites are the

dominant variety at Rietfontein, accounting for 61% of the sampled suite, whereas Group I eclogites account for 13% of the samples. The remaining 26% of the suite were not classified, due to the small sample size, coarse grain size or degree of alteration. The compositional classification of the eclogites as Group I or Group II eclogites, following McCandless & Gurney (1989), will be discussed in *Chapter 4*. Since not all samples could be classified according to the MacGregor & Carter (1970) scheme, the eclogites will be classified as either bimineralic, orthopyroxene-bearing, or kyanite eclogites. All of the Rietfontein eclogite groups contain accessory minerals, although secondary minerals such as phlogopite and amphibole are not found in the kyanite eclogites.

Petrographically, very few differences seem to exist between on-craton and off-craton eclogites. Textures are often very similar, and the same accessory minerals are found in both on- and off-craton eclogites. Lower crustal eclogites from Australia (Griffin & O'Reilly, 1986) and Cape Province off-craton eclogites (Robey, 1981; Pearson *et al.*, 1995) are commonly associated with granulites and garnet pyroxenites, whereas on-craton localities are dominated by mantle peridotite samples. Other xenoliths reported from Rietfontein include peridotite and pyroxenite (Gurney *et al.*, 1971), suggesting that the xenolith suite is dominantly a mantle-derived suite, similar to on-craton localities, and lacking the lower crustal xenoliths such as granulites found in Cape Province off-craton localities.

The Rietfontein eclogites show similarities to both on- and off-craton localities. Granoblastic grain boundaries and triple junctions are common in lower crustal eclogites from Australia (Griffin & O'Reilly, 1986) and South African on-craton localities such as Bellsbank (Taylor & Neal, 1989). None of the Rietfontein eclogites show any sign of foliation or layering however, despite these features commonly being observed in eclogites (Dawson, 1980; Dawson & Carswell, 1990). Again, this may be a direct consequence of the small sample sizes. Spongy reaction rims around clinopyroxene grains are commonly reported from off-craton (Robey, 1981; Pearson *et al.,* 1995) and on-craton (Taylor & Neal, 1989; Beard *et al.*, 1996; Snyder *et al.*, 1997) eclogites and are commonly attributed to metasomatism, as are the frequently observed rims of secondary mica and amphibole around garnet grains (Taylor & Neal, 1989). Pearson *et al.* (1995) report aggregates of exsolved clinopyroxene from Cape Province off-craton eclogites,

which is not reported in the literature for on-craton eclogites. Corundum has been found in eclogites from a number of on-craton localities (Ater *et al.*, 1984; Taylor & Neal, 1989; Viljoen, 1994) but is not observed in the Rietfontein eclogites.

Some textural differences can be observed between the Rietfontein eclogites and other off-craton localities. Kyanite in the Rietfontein kyanite eclogites always forms an interlocking textural arrangement with the garnet and clinopyroxene. Robey (1981) describes kyanite from the Cape Province eclogites as inclusions in garnet and clinopyroxene, acicular intergrowths with quartz, and as needle-like laths defining a foliation. Orthopyroxene from the Rietfontein eclogites is often altered, and is clearly different to the relict orthopyroxene and "wormy" trails of orthopyroxene found within clinopyroxene from other off-craton eclogites, such as the Cape Province suite (Robey, 1981). Pearson *et al.* (1995) describe mineral banding, randomly oriented kyanite tablets and symplectite-like re-growths on clinopyroxene in eclogites from off-craton localities (*eg.* Kalkput, Lovedale, Abrahamskraal and Pampoenpoort) around the Kaapvaal Craton. The secondary amphibole reported in Cape Province eclogites by Robey (1981) is interpreted to be of a retrograde origin during hydration of the rocks prior to entrainment by the kimberlite. This type of amphibole is also observed in the Rietfontein eclogites and is interpreted to have formed due to similar metasomatic processes.

The Rietfontein eclogites show textures indicative of equilibrated rocks. Triple junctions are identifiable in many of the samples, together with straight grain boundaries. These triple junctions can be observed in all three groups of eclogite, *viz* bimineralic, orthopyroxene and kyanite eclogites. Triple junctions are representative of a metamorphic recrystallisation texture, and the granoblastic polygonal textures represent a close approach to textural equilibrium (Yardley *et al.*, 1990). Replacement textures are not exhibited by the Rietfontein eclogites and the described textures, together with homogeneous mineral grains, suggest that the xenolith suite is well equilibrated.

The kyanite eclogites are the freshest group of eclogites found at Rietfontein. This contradicts observations by Dawson (1980), who notes that an almost characteristic feature of kyanite eclogites is their high degree of alteration. Whereas the bimineralic and orthopyroxene eclogites

show varied degrees of alteration, and often contain secondary minerals such as phlogopite and amphibole, the kyanite eclogites only contain rutile and, in one instance, pyrite as accessory minerals. Spongy clinopyroxene rims which are present in some of the bimineralic and orthopyroxene eclogites are also absent in the kyanite eclogites. Taylor & Neal (1989) attribute these spongy margins to the reaction of primary clinopyroxene with a metasomatic fluid, and amphibole and phlogopite are inferred to form by metasomatic fluid percolating through the eclogites and reacting with the primary minerals. The lack of these minerals and textures in the kyanite eclogites, suggests that these eclogites did not undergo the same metasomatic event to which the bimineralic and orthopyroxene eclogites were subjected. This may mean that the kyanite eclogites were derived from a different part of the mantle than the other eclogites, or were incorporated at a different time.

The presence of kyanite as a primary mineral in some of the eclogites hints at a very different precursor to the kyanite eclogites than the precursors to the bimineralic and orthopyroxene eclogites. The presence of large amounts of kyanite (up to 20 volume % in one case) in the Rietfontein kyanite eclogites suggests that the protolith rocks must have been particularly rich in aluminium. Jerde *et al.* (1993*b*) suggest that kyanite eclogites may represent protoliths that contained abundant plagioclase, which on an increase in pressure would have formed kyanite, in addition to aluminous pyroxene. The clinopyroxene of the Rietfontein kyanite eclogites is indeed Al-rich, more so than that of the bimineralic eclogites (see *Chapter 4*, *Section 4.2.2*), suggesting that the idea of a plagioclase-rich precursor to the kyanite eclogites may be applicable to the Rietfontein suite. Jerde *et al.* (1993*b*) argue further that during the course of exsolution, the Ca-Tschermakite portion of the pyroxene formed the garnet and some primary kyanite may have been consumed by this late-crystallising garnet. No exsolution features are visible in the suite of kyanite eclogites from this study, suggesting full equilibration within the rocks.

Clues to the origin of the Rietfontein eclogites may be obtained from the textures and petrography of the eclogites. Some of the Rietfontein eclogites (those tentatively identified as Group I eclogites) exhibit igneous, cumulus textures. The large rounded garnets are set in a matrix of interstitial clinopyroxene and such eclogites were interpreted by MacGregor & Carter (1970) to be sets of crystals that formed as a result of fractional crystallisation in a high pressure

magma chamber. The second eclogite texture identified in the Rietfontein eclogites, the granoblastic texture with straight grain boundaries and triple junctions, is more compatible with a metamorphic origin for the rocks and MacGregor & Carter (1970) suggest that these eclogites formed during the fractional crystallisation of sets of liquids. Further studies have however led to other interpretations of the eclogite group textures. MacGregor & Manton (1986) propose a subduction theory for the development of both Group I and Group II eclogites, suggesting that Group I eclogites are derived from a series of cumulate oceanic crust gabbros, whilst Group II eclogites represent subducted altered basalts. Hatton & Gurney (1987) show that Group I Roberts Victor eclogites are a chemically and texturally related suite of rocks and interpret the formation of this group as a result of igneous processes within a single body. They also agree with the subduction theory of MacGregor & Manton (1986), stating that the metamorphic textures in Group II eclogites may be indicative of metamorphosed oceanic basalts. Smyth *et al.* (1989) and Caporuscio & Smyth (1990) believe that bimineralic eclogites and grospydites are related through the continuous fractionation of a single evolving magma, and that the eclogites represent the clinopyroxene cumulate portion of the melt system.

When considering the textures of the Rietfontein eclogites in the context of descriptions by others, it seems that there may be a number of possible origins of these eclogites. The coarse grained, cumulus textured eclogites (all bimineralic eclogites) may be the result of fractional crystallisation and accumulation within a magma chamber, whilst the finer grained eclogites exhibiting the granoblastic, metamorphic textures may be representative of metamorphosed subducted crust material.

The garnet exsolution texture exhibited by sample CMA 1 provides further information with regard to mantle processes in the Rietfontein area at the time of eclogite formation. Processes causing exsolution bear directly on the pressure-temperature paths and tectonic histories of samples (Jerde *et al.*, 1993). Garnet exsolution within eclogites is common, having been reported from a number of localities, both on-craton (Roberts Victor - Harte & Gurney, 1975; Bellsbank - Shervais *et al.*, 1988; Smyth *et al.*, 1989; Colorado - Ater *et al.*, 1984 and Kaalvallei - Viljoen, 1994) and off-craton (Cape Province - Pearson *et al.*, 1995). Exsolution of orthopyroxene from clinopyroxene has also been reported from Bellsbank (Shervais *et al.*, 1988

and Taylor & Neal, 1989), but no orthopyroxene exsolution is visible in the Rietfontein eclogites.

Harte & Gurney (1975) studied an eclogite from Roberts Victor showing three sets of garnet lamellae exsolved from clinopyroxene and attributed the textural features to slow cooling at depth from near-solidus conditions (1400°C and 34-28kb) towards normal mantle lithosphere temperatures. Sautter & Harte (1988) re-examined in greater detail the xenolith described by Harte & Gurney (1975), to obtain information on the exsolution microtextures and diffusion gradients. They concur with Harte & Gurney (1975) that the exsolution is as a result of cooling from high temperatures. Lappin (1978) and Smyth *et al.* (1984) both cite exsolution phenomena in clinopyroxene to suggest that more calcic eclogites may have recrystallised from near solidus temperatures at pressures in excess of 3 GPa. Smyth *et al.* (1989) use garnet exsolution from clinopyroxene as an indication of a high pressure igneous origin for the Bellsbank eclogites. Jerde *et al.* (1993*b*) agree that any process involving an increase in pressure or a decrease in temperature may result in the exsolution of garnet from pyroxene. The re-equilibration of aluminous pyroxene from higher temperatures has been suggested by Pearson *et al.* (1995) to account for the exsolution of garnet in eclogites from the Kaapvaal Craton margin. Taking previous studies into account, sample CMA 1 illustrates that at some stage during their geological history, the Rietfontein eclogites experienced significant cooling at depth, possibly in conjunction with a pressure increase, resulting in exsolution of garnet from aluminous clinopyroxene. The absence of exsolution in all the other eclogites again suggests that there may be more than one suite of eclogites represented at Rietfontein, with differing geological histories.

Thus, to summarise, the textures exhibited by the Rietfontein eclogites suggest that there may be more than one origin for this suite. The cumulus textured rocks may be the result of fractional crystallisation in a magma chamber, whilst the granoblastic eclogites may represented subducted, metamorphic crustal fragments. The kyanite eclogites indicate the presence of a protolith that originally contained plagioclase, and the presence of secondary minerals, such as phlogopite and amphibole, illustrates that the Rietfontein eclogites experienced some form of metasomatism, or alteration by the kimberlite. Metasomatism, should this be the cause of the secondary minerals, probably occurred before entrainment of the xenoliths. Undulose extinction in the

pyroxenes of many samples indicates that the eclogites were subjected to strain at some stage during their geological history. Samples not showing evidence of strain, but instead containing triple junctions, have been recrystallised and annealed, resulting in the metamorphic granoblastic texture which is observed. The garnet exsolution lamellae present in one sample suggests cooling of the sample towards mantle lithosphere temperatures. The lack of diamond in the Rietfontein eclogites may mean that the samples were not derived from depths within the diamond stability field and the absence of graphite suggests that the area may have been depleted in carbon.

4. Major Element Mineral Chemistry

4.1 Introduction

Eclogites are found in a number of geological settings, as noted by Coleman *et al.* (1965), who devised one of the first classification schemes for massif eclogites, proposing three groups, (A, B and C) based on different modes of occurrence of eclogites: Group A eclogites occur as xenoliths in kimberlite pipes, basalts, or layers within ultramafic rocks; Group B eclogites are found as lenses in high-grade migmatitic gneiss terranes and Group C eclogites occur as bands or lenses within alpine-type metamorphic rocks. Although this scheme was based on the geological setting of the eclogites, Coleman *et al.* (1965) found that each group had distinctive garnet and clinopyroxene compositions, with the pyrope content of garnet decreasing from Group A to Group C, and the jadeite content increasing from Group A to Group C. These compositional differences in different garnets and clinopyroxenes were noted by Dawson & Stephens (1975) and Stephens & Dawson (1977) respectively. Classifications were based on the TiO_2, Al_2O_3, Cr_2O_3, FeO, MgO, CaO and Na_2O contents of the minerals. A compositional continuum can be observed from deep-red high-pyrope garnets, through pyrope-almandines, to garnets with higher Ca contents, which are orange to yellow in colour in peraluminous eclogites and grospydites (Dawson & Carswell, 1990).

For many years, the favoured origin for high-pressure eclogitic rocks was that of cumulates, formed by fractionation of mantle magmas (*eg.* O'Hara & Yoder, 1967; MacGregor & Carter, 1970; Hatton, 1978). A second origin, that of metamorphosed, subducted oceanic crust, was suggested by Helmstaedt & Doig (1975), after a petrographical and compositional study of eclogites from the Colorado Plateau showed that they were similar to Franciscan eclogites. High Na contents in these eclogites are believed to strongly imply an oceanic crustal origin. MacGregor & Manton (1986) reached a similar conclusion with regard to eclogite petrogenesis after investigating the major element mineral compositions and oxygen isotope compositions of Roberts Victor eclogites. Debate still centres around a mantle cumulate/subducted oceanic crust origin, and Hatton & Gurney (1987) used CaO_{gt} and Na_2O_{cpx}, and correlations within these discriminants, to interpret the formation of Group I and Group II Roberts Victor eclogites as the result of igneous processes within a single body. Smyth *et al.* (1989) believe major element

compositional continuity between different eclogite groups to be indicative of a crystal fractionation origin.

The Group I and Group II petrographic classification of the Roberts Victor eclogites (MacGregor & Carter, 1970) formed the basis of a geochemical study by McCandless & Gurney (1989). This study used Na_2O_{gt} and K_2O_{cpx} to compositionally distinguish Group I and Group II eclogites, and it was shown that Group I eclogites have an average K_2O_{cpx} value of $\geq$ 0.08 wt% and $Na_2O_{gt} \geq$ 0.09 wt%, whereas Group II garnet and clinopyroxenes have Na_2O and K_2O concentrations below these levels. Diamondiferous eclogites show Na_2O_{gt} and K_2O_{cpx} contents similar to those of Group I eclogites, suggesting that Group I eclogites formed under conditions similar to those required for diamond genesis (McCandless & Gurney, 1989).

Further studies on the major element compositions of kimberlite-hosted eclogites have yielded the separation of eclogites into three groups, *viz* Group A, B & C (Taylor & Neal, 1989). These groups are distinct, and different to the A, B & C grouping of Coleman *et al.* (1965). Compositional differences between the three groups are clear, with Group A eclogites containing Mg- and Cr-rich garnets, and clinopyroxenes with a low jadeite (expressed in terms of Na) content. Fe-rich garnets and clinopyroxenes of intermediate jadeite composition constitute Group B, whilst Group C eclogites have the most Ca-rich (grossular) garnets and clinopyroxenes with the highest jadeite component (Jerde *et al.*, 1993*a*). Group A eclogites are generally believed to have an origin as mantle cumulates (Smyth *et al.*, 1989; Taylor & Neal, 1989; Neal *et al.*, 1990), but the origin of Group B and Group C eclogites is still being debated, with origins as both mantle cumulates (Smyth *et al.*, 1989) and metamorphosed oceanic crust (Helmstaedt & Doig, 1975; MacGregor & Manton, 1986; Taylor & Neal, 1989; Jerde *et al.*, 1993*a*) being suggested. Although much evidence for the origin of eclogites is drawn from trace and rare earth element geochemistry, and oxygen isotopes, basic classification schemes rely heavily on mineral major element compositions.

4.2 Aims

With three petrographic groups within the Rietfontein eclogites already having been identified (*Chapter 3*), it is necessary to compositionally classify these groups, and to determine the major

element compositional differences between them. One of the main aims of this dissertation is to compare the Rietfontein eclogites to other off-craton and on-craton eclogites. Griffin *et al.* (1990) were unable to distinguish between clinopyroxenes from garnet granulites and those from eclogites, based on the jadeite versus Tschermak contents of the clinopyroxenes, but differences between the Rietfontein eclogites and other settings may be apparent. Knowledge of the major element mineral composition of the Rietfontein eclogites will allow classification of the eclogites according to pre-existing schemes, and, as such, a direct comparison with other eclogites. From these schemes, suggestions can be made as to the nature of the eclogite protolith. It is also essential to determine whether the Rietfontein eclogites are crust or mantle derived. Garnet granulites are crustal rocks (Griffin & O'Reilly, 1986; Griffin & O'Reilly, 1987; Pearson *et al.*, 1995), and if the pyroxenes contained in these rocks are similar to those in mantle eclogites, it may be difficult to classify the Rietfontein eclogites as being crust or mantle-derived, based solely on the major element chemistry.

4.3 Methods

The major element compositions of garnet, clinopyroxene and accessory minerals from the Rietfontein eclogites were determined at the University of Cape Town using the Cameca-Camebax electron microprobe. Details of this analytical technique, together with the detection limits and precision can be found in Appendix I. Major element chemistry of the minerals observed in the Rietfontein eclogites will be presented and discussed in this chapter. Tables of individual analyses can be found in Appendix II, whilst representative analyses of the primary minerals are provided in *Tables 4.1-4.4*. In each sample, at least two grains of each of the primary minerals were analysed, and each grain was analysed at least twice, with core and rim analyses being obtained where possible. Fe^{3+} contents were calculated for ilmenite using the method of Droop (1987). This method uses an equation derived using stoichiometric criteria, and the number of Fe^{3+} ions per X oxygens in the mineral formula F, is given by $F = 2X(1-T/S)$, where T is the ideal number of cations per formula unit, and S is the observed cation total per X oxygens calculated assuming all iron to be Fe^{2+}.

4.4 Mineral Chemistry

4.4.1 Garnet

Representative analyses of garnets from the Rietfontein eclogites are reported in *Table 4.1*, whereas the full data set may be found in Appendix II. The Rietfontein garnets show large variations in Ca (= 100Ca/[Ca+Mg+Fe]), Mg (= 100Mg/[Ca+Mg+Fe]) and, to a lesser extent, variation in Fe (=100Fe/[Ca+Mg+Fe]), as illustrated in *Figure 4.1*. Most of the garnets from the bimineralic and orthopyroxene-bearing eclogites are pyrope, having Mg values of 50-75. Only one eclogite, kyanite eclogite JJG 2104, contains garnet with greater than 50% grossular component. Garnets from the three sample groups exhibit similar proportions of almandine, and in the kyanite eclogites, this proportion is similar to the proportion of pyrope. A visual comparison of the end-member components of the Rietfontein eclogitic garnets with garnets from on- and off-craton eclogites (*Figure 4.1*) is inconclusive. There is much overlap between off-craton eclogites, represented by the Cape Province off-craton suite, and on-craton eclogites, represented by the Roberts Victor eclogites. All garnets from the Rietfontein eclogites fall within the Roberts Victor field, with a number falling within the off-craton field. *Figure 4.2* illustrates the end-member compositions of the Rietfontein eclogitic garnets relative to garnets from the Kaalvallei (Viljoen, 1995) eclogites, and Rietfontein garnets analysed by Bell & Rossman (1992). Similar compositions were obtained by Bell & Rossman (1992) for the bimineralic, orthopyroxene-bearing and kyanite eclogites as were obtained in this study. Many of the Rietfontein garnets fall into the area of overlap between Group I and Group II Kaalvallei garnets, whereas a number of the more grossular-rich bimineralic and orthopyroxene-bearing eclogites fall within the Group I field. The Rietfontein kyanite eclogites do not seem to have any compositional similarities with either the Group I or Group II garnets from Kaalvallei.

MgO and CaO show the largest inter-sample variation (6.35 - 20.82 wt%, and 3.64 - 19.42 wt% respectively) in the Rietfontein eclogites, whereas FeO shows less variability (7.11 - 16.26 wt%). Garnets from the kyanite eclogites have the highest CaO contents, and the lowest MgO contents. Three bimineralic eclogites contain garnets that are substantially different to garnets from the other bimineralic eclogites. The CaO and MgO contents of these garnets are similar to those observed in garnets from the kyanite eclogites. Although no kyanite has been observed in these samples, it is possible that the small sample sizes are not representative of the sample as a whole,

Table 4.1 *Selected representative analyses of garnets from the Rietfontein eclogites*

Mg# = 100Mg/(Mg+Fe), Ca = 100Ca/(Ca+Mg+Fe*), Mg = 100Mg/(Ca+Mg+Fe*), Fe = 100Fe/(Ca+Mg+Fe*), Fe* - all iron calculated as* Fe^{2+}.

	Bimineralic eclogites					**Kyanite eclogites**			**Opx-bearing eclogites**		
Sample	**CMA 1** (lamellae)	**CMA 1** (granular)	**CMA 2** (core)	**PC 3** (core)	**Rtfn 57.3** (core)	**JJG 2104** (core)	**Rtfn 54.4** (rim)	**Rtfn 55.3** (core)	**CMA 3** (core)	**PC 5.2/1** (core)	**CMA 12** (core)
SiO_2	40.63	41.03	40.83	42.12	41.26	39.88	39.13	39.56	40.16	41.39	40.73
TiO_2	0.08	0.07	0.06	0.12	0.10	0.09	0.11	0.25	0.07	0.08	0.13
Al_2O_3	23.21	23.21	23.19	24.52	23.70	22.66	22.71	22.59	22.12	23.45	23.64
Cr_2O_3	0.40	0.40	0.47	0.34	0.64	0.02	0.05	0.02	0.81	0.26	0.18
FeO*	11.19	11.28	12.84	7.84	8.85	11.03	14.95	14.76	16.48	13.23	12.82
MnO	0.41	0.43	0.41	0.39	0.36	0.20	0.28	0.27	0.68	0.33	0.39
MgO	14.66	14.62	16.03	20.65	20.45	6.59	9.37	9.66	14.43	17.77	18.12
CaO	9.00	9.12	6.20	4.14	4.47	19.56	13.08	12.72	4.91	3.71	3.84
Na_2O	0.01	0.01	0.01	0.05	0.11	0.06	0.04	0.07	0.01	0.04	0.06
Total	**99.58**	**100.17**	**100.03**	**100.16**	**99.94**	**100.11**	**99.71**	**99.90**	**99.68**	**100.25**	**99.91**
*** Cations calculated on the basis of 12 oxygens ***											
Si	2.971	2.983	2.970	2.968	2.940	2.987	2.946	2.965	2.982	2.983	2.946
Ti	0.004	0.004	0.003	0.006	0.005	0.005	0.006	0.014	0.004	0.004	0.007
Al	2.000	1.989	1.989	2.036	1.990	2.000	2.015	1.995	1.936	1.992	2.015
Cr	0.012	0.011	0.013	0.009	0.018	0.001	0.002	0.001	0.024	0.007	0.005
Fe*	0.685	0.686	0.781	0.462	0.527	0.691	0.941	0.925	1.023	0.797	0.775
Mn	0.025	0.027	0.025	0.023	0.022	0.013	0.018	0.017	0.043	0.020	0.024
Mg	1.599	1.584	1.738	2.169	2.173	0.736	1.052	1.079	1.597	1.909	1.954
Ca	0.706	0.711	0.484	0.313	0.342	1.572	1.057	1.023	0.391	0.286	0.298
Na	0.002	0.002	0.002	0.006	0.016	0.008	0.006	0.011	0.002	0.005	0.009
Sum	**8.003**	**7.997**	**8.006**	**7.993**	**8.032**	**8.012**	**8.042**	**8.029**	**8.001**	**8.005**	**8.034**
Mg #	70.0	69.8	69.0	82.4	80.5	51.6	52.8	53.8	61.0	70.5	71.6
Ca	23.6	23.8	16.1	10.6	11.2	52.4	34.6	33.8	13.0	9.6	9.8
Mg	53.5	53.2	57.9	73.7	71.4	24.6	34.5	35.7	53.1	63.8	64.6
Fe	22.9	23.0	26.0	15.7	17.3	23.1	30.9	30.6	34.0	26.6	25.6

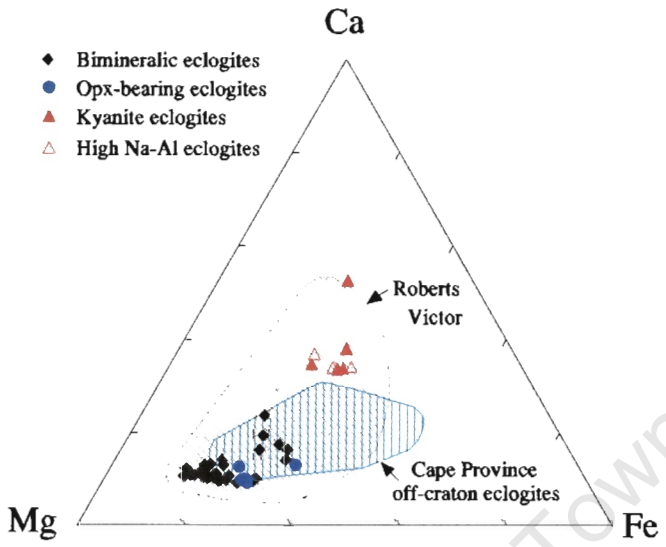

Figure 4.1 *Ca-Mg-Fe ternary diagram for garnets from the Rietfontein eclogites. Data for the off-craton field from Robey (1981); Roberts Victor data from Hatton (1978); MacGregor & Manton (1986); Ongley et al. (1987); McCandless & Gurney (1989); Bell & Rossman (1992).*

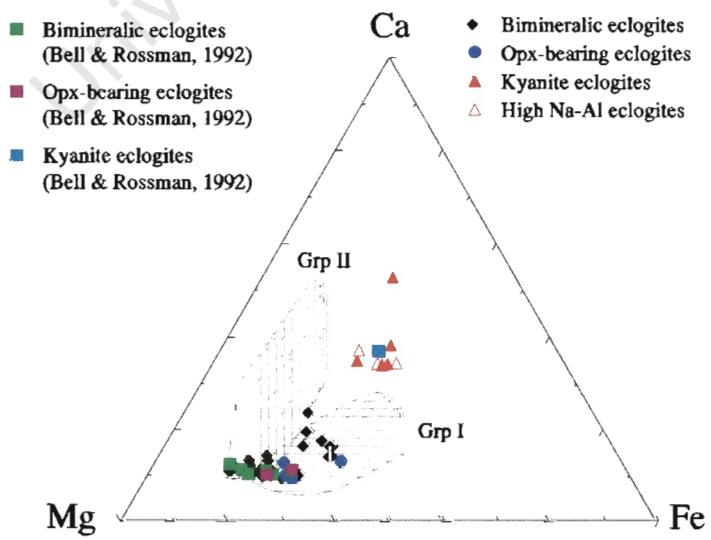

Figure 4.2 *Ca-Mg-Fe ternary diagram for the Rietfontein garnets, showing the compositions relative to the Rietfontein garnets of Bell & Rossman (1992) and Kaalvallei (Viljoen, 1994).*

and kyanite may have been observed had larger sample sizes been available. In all aspects of their chemistry, these three bimineralic eclogites (Rtfn 55.3, CMA 4 & CMA 17) show similarities to the kyanite eclogites. For this reason, these samples have been grouped with the kyanite eclogites in the variation diagrams, and throughout the text, references to the kyanite eclogites will include these samples, unless they are referred to individually as the "High Na-Al eclogites".

The Rietfontein garnets are relatively homogeneous, and no distinct zoning, or core-rim variations can be observed. Most differences within grains occur in Al_2O_3, FeO, MgO and CaO and are less than 0.5 wt% absolute, although rare variations of up to 2 wt% relative (CaO, MgO and FeO) within a grain have been observed. These appear to be random heterogeneities, and not zoning patterns, as there is no constant pattern across the core-rim-core of the grain. There are no differences in the major element chemistry between the exsolved garnet lamellae and the granular garnets of sample CMA 1, both are Mg-rich (pyrope), with approximately equal proportions of Fe and Ca.

Figures 4.3a & b illustrate that the main difference between garnets of the kyanite eclogites and other garnets lies in the concentrations of Mg and Ca, whereas minor elements such as Mn and Ti occur in very similar concentrations. Garnets from the orthopyroxene-bearing eclogites do not show any significant differences in major element chemistry to the bimineralic eclogites. Two garnets show Ti abundances elevated above those of the other garnets (*Figure 4.3b*). A comparative plot of the TiO_2-Cr_2O_3 abundances of the rutile-bearing and rutile-free eclogites is inconclusive (*Figure 4.4*). Rutile in the Rietfontein eclogites is seen to contain varying amounts of TiO_2 and Cr_2O_3, although the presence of rutile seems to have no bearing on the garnet compositions. The highest TiO_2 contents in Rietfontein garnets (*Figure 4.4*) belong to rutile-free eclogites, and garnets from both rutile-bearing, and rutile-free eclogites have similar TiO_2 and Cr_2O_3 abundances.

Na_2O contents of the Rietfontein eclogites are very low, with only 3 samples containing more than 0.09 wt% Na_2O. Thus, combined with the K_2O contents of the clinopyroxenes (*Section 4.2.2*), the Rietfontein eclogites can be classified as Group II eclogites after McCandless & Gurney (1989) (*Figure 4.5*). Two of the high Na garnets are bimineralic eclogites, whereas the third is

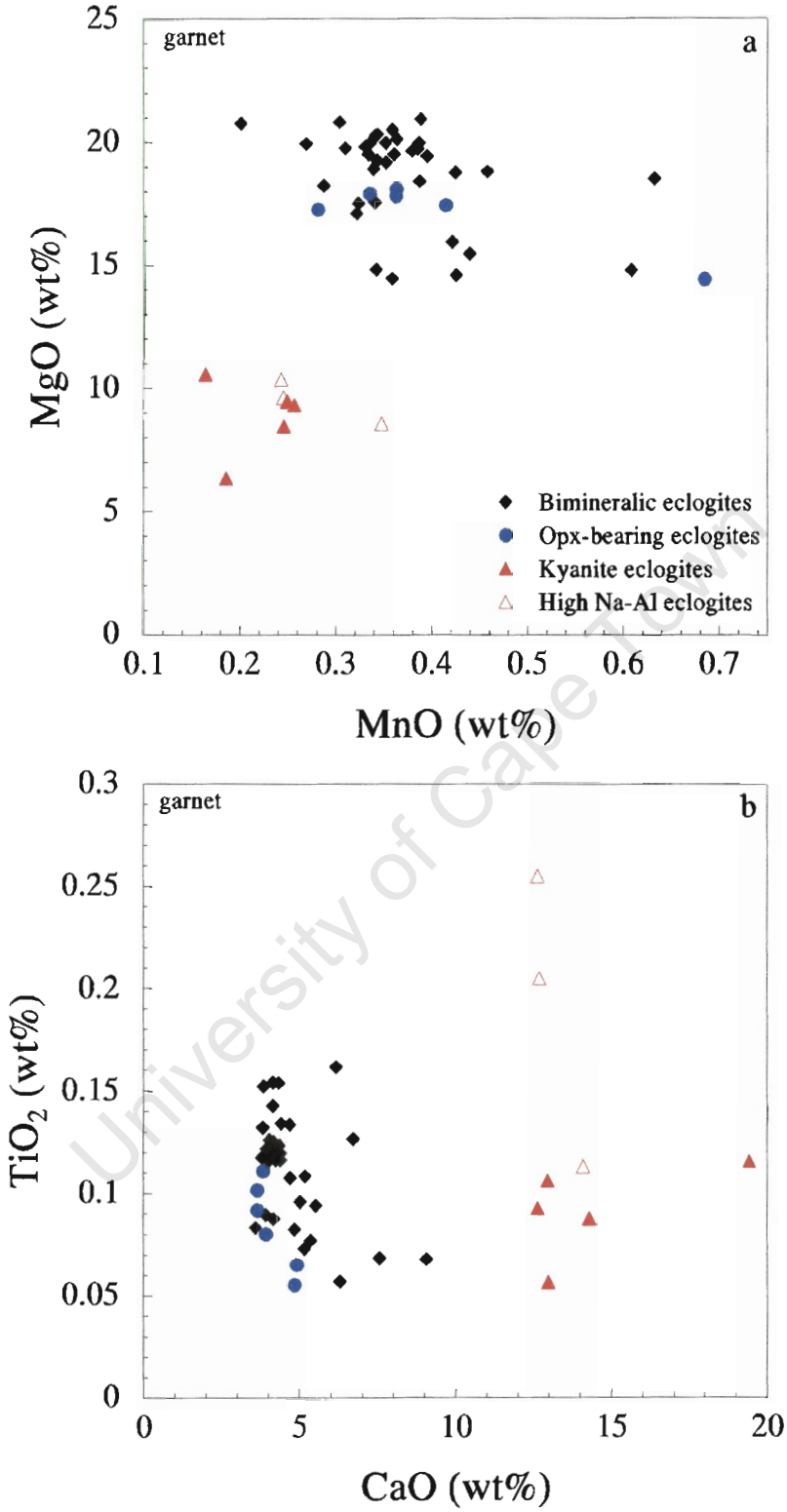

Figure 4.3 *MgO vs MnO* ***(a)****, and* TiO_2 *vs CaO* ***(b)*** *for garnets from the Rietfontein eclogites. Minor elements such as Mn and Ti are similar for all groups, but distinct differences can be seen in Mg and Ca compositions.*

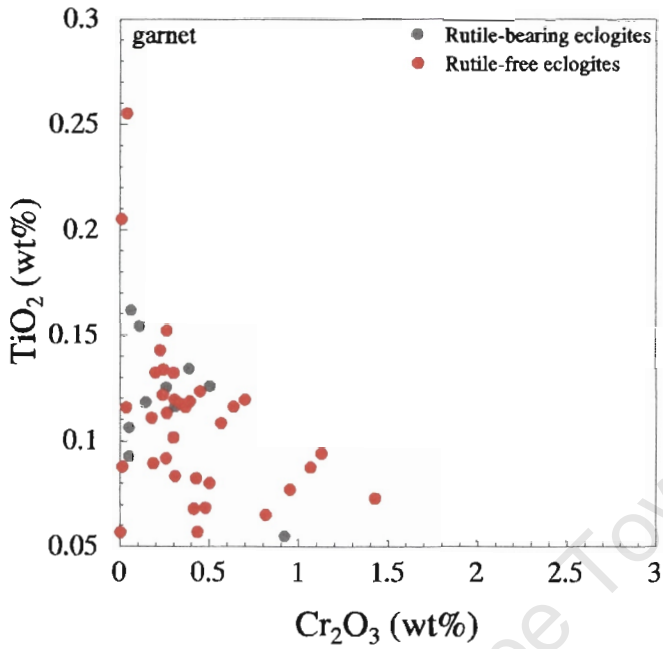

Figure 4.4 *TiO_2 and Cr_2O_3 contents of garnets from rutile-bearing and rutile-free Rietfontein eclogites.*

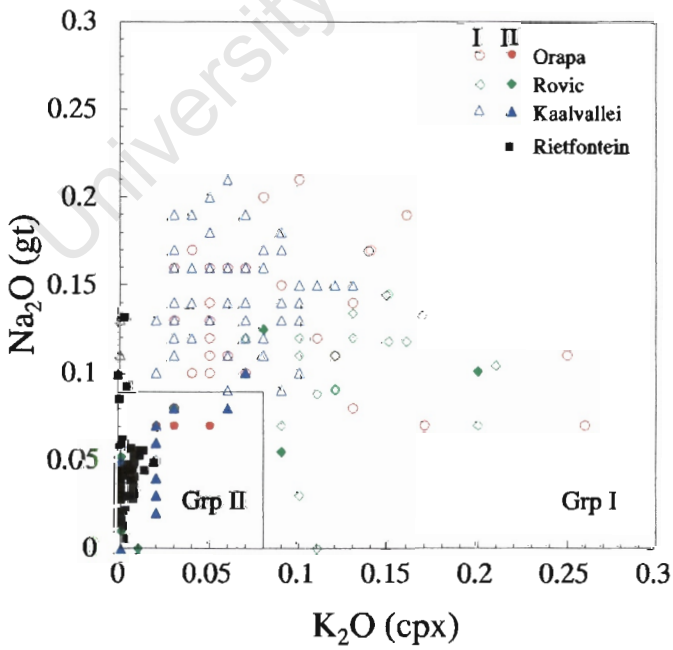

Figure 4.5 *Na_2O_{gt} vs K_2O_{cpx} (both wt%) for the Rietfontein eclogites. Following the classification of McCandless & Gurney (1989), most are Group II eclogites. Literature data: Orapa (Shee, 1978); Deines et al. (1991); Kaalvallei (Viljoen, 1994); Roberts Victor (Hatton, 1978; MacGregor & Manton, 1986).*

from a high Na-Al eclogite (CMA 17). CMA 17 is the only eclogite with elevated Na contents to contain elevated Ti contents (*Figure 4.6*). Na is known to have a positive correlation with Ti in garnet (Reid *et al.*, 1976), and diamondiferous eclogites contain garnets enriched in Na_2O (Reid *et al.*, 1976; McCandless & Gurney, 1989). Higher TiO_2 contents could thus be used to imply a greater pressure of formation, within the garnet stability field.

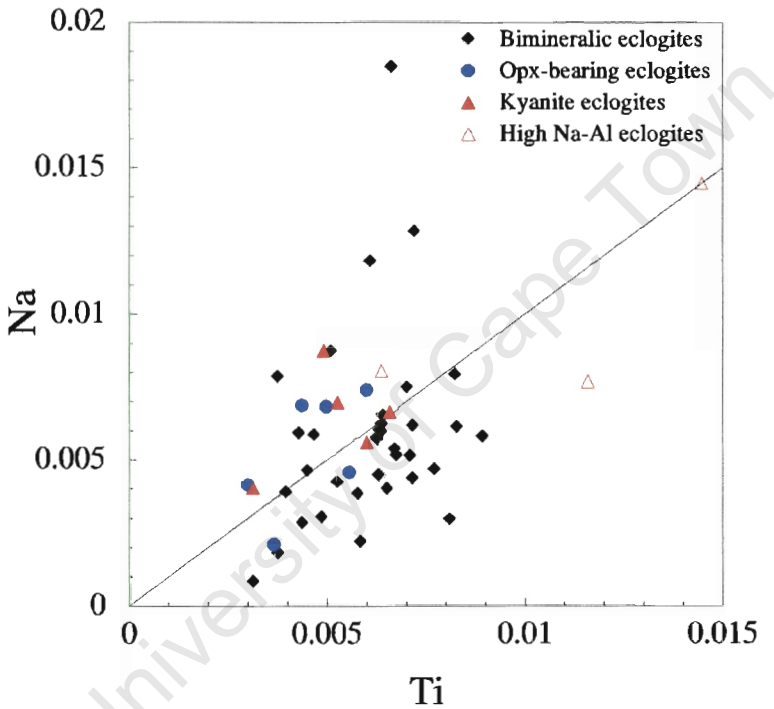

Figure 4.6 *Atomic Na vs Ti for garnets from the Rietfontein eclogites. A broad linear correlation between the two can be observed, it is not however as well constrained as that of Reid et al. (1976).*

Most of the garnets (approximately 70%) have low (<0.5 wt%) Cr_2O_3 contents. However, some of the eclogites contain garnets with higher Cr_2O_3 contents: these garnets seem to reflect more of a peridotitic chemical signature (Snyder *et al.*, *1997*). A comparison of the Rietfontein eclogitic garnets with peridotitic garnets is illustrated in *Figure 4.7*. Garnets from the kyanite eclogites contain the lowest Cr/(Cr+Al) ratios, whereas some of the bimineralic eclogites tend towards higher ratios. Garnets from peridotites exhibit much higher Cr/(Cr+Al) ratios, although garnets with lower values overlap the range of values exhibited by some of the Rietfontein

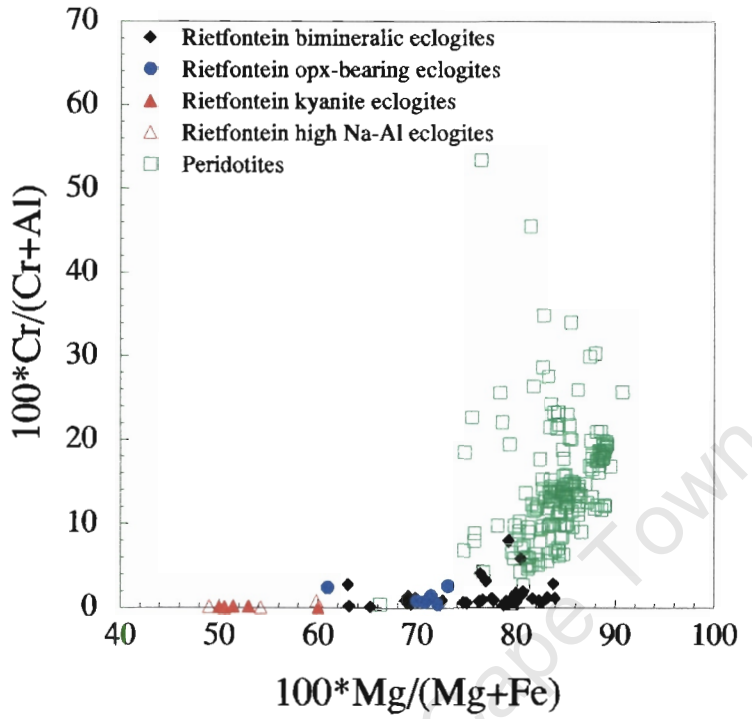

Figure 4.7 *Cr/(Cr+Al) vs Mg# for garnets from the Rietfontein eclogites, compared to abundances exhibited by peridotitic garnets. Peridotite data from Lawless (1978); Smith (1981); Moore (1986); Waters (1987); Hill (1989); Hops (1989); Nowicki (1990).*

bimineralic eclogites.

4.4.2 Pyroxenes

Selected representative analyses of clinopyroxenes from the Rietfontein eclogites are presented in *Table 4.2*, whereas the full data set can be found in Appendix II. Clinopyroxenes from the Rietfontein eclogites show less Ca-Mg-Fe variation than the garnets (*Figure 4.8*). The clinopyroxenes plot within a tightly constrained field, and the compositions of clinopyroxene from the bimineralic, orthopyroxene-bearing and kyanite eclogites are not vastly different with regard to Ca, Mg and Fe. Kyanite eclogites have a slightly higher proportion of Ca, and a slightly lower proportion of Mg than the bimineralic and orthopyroxene-bearing eclogites, whereas the proportion of Fe in all three groups is identical. On a simple Ca-Mg-Fe plot, the clinopyroxenes fall within the diopside and augite fields as defined by Morimoto (1988), and the orthopyroxenes are classified as enstatite. Whereas the major chemical variation in the Rietfontein garnets can be

Table 4.2 *Selected representative analyses of clinopyroxenes from the Rietfontein eclogites*

Mg# = 100Mg/(Mg+Fe), Ca = 100Ca/(Ca+Mg+Fe*), Mg = 100Mg/(Ca+Mg+Fe*), Fe = 100Fe/(Ca+Mg+Fe*), Fe* - all Fe calculated as* Fe^{2+}

	Bimineralic eclogites				Kyanite eclogites				Opx-bearing eclogites		
Sample	**PC 1** (core)	**PC 3** (core)	**Rtfn 31.2** (core)	**CMA 7** (rim)	**Rtfn 54.1** (core)	**Rtfn 54.3** (core)	**Rtfn 54.4** (rim)	**CMA 17** (rim)	**PC 5.2/1** (core)	**CMA 3** (core)	**CMA 13** (core)
SiO_2	54.70	54.32	54.83	54.21	53.52	53.99	53.57	53.68	55.12	54.20	54.25
TiO_2	0.14	0.28	0.31	0.28	0.28	0.22	0.23	0.46	0.24	0.10	0.11
Al_2O_3	1.54	3.23	5.26	3.39	14.55	12.08	13.27	10.41	5.30	1.66	1.55
Cr_2O_3	0.13	0.31	0.17	0.14	0.03	0.03	0.05	0.00	0.36	0.35	0.43
FeO*	1.86	1.59	3.30	2.65	2.77	1.99	2.38	3.40	3.36	4.21	2.33
MnO	0.00	0.03	0.02	0.07	0.02	0.00	0.02	0.03	0.05	0.11	0.06
MgO	17.83	16.60	14.71	16.12	8.43	10.46	9.20	10.17	14.28	16.74	16.90
CaO	23.07	21.37	18.32	20.91	14.28	16.16	14.52	15.60	17.81	21.56	22.68
Na_2O	0.74	1.79	3.28	2.32	5.92	5.16	6.35	5.84	3.64	1.33	1.05
K_2O	0.02	0.02	0.02	0.02	0.02	0.02	0.02	0.02	0.02	0.02	0.02
Total	**100.04**	**99.53**	**100.21**	**100.09**	**99.80**	**100.10**	**99.61**	**99.59**	**100.16**	**100.26**	**99.36**
*** Cations calculated on the basis of 6 oxygens ***											
Si	1.976	1.965	1.968	1.960	1.898	1.914	1.908	1.930	1.979	1.972	1.980
Ti	0.004	0.008	0.008	0.008	0.007	0.006	0.006	0.012	0.006	0.003	0.003
Al	0.065	0.138	0.223	0.145	0.608	0.505	0.557	0.441	0.224	0.071	0.067
Cr	0.004	0.009	0.005	0.004	0.001	0.001	0.002	0.000	0.010	0.010	0.012
Fe*	0.056	0.048	0.099	0.080	0.082	0.059	0.071	0.102	0.101	0.128	0.071
Mn	0.000	0.001	0.001	0.002	0.001	0.000	0.001	0.001	0.001	0.003	0.002
Mg	0.961	0.895	0.787	0.869	0.446	0.553	0.488	0.545	0.764	0.908	0.920
Ca	0.894	0.829	0.706	0.811	0.543	0.615	0.555	0.602	0.686	0.842	0.888
Na	0.052	0.126	0.228	0.162	0.407	0.354	0.439	0.407	0.253	0.094	0.074
K	0.001	0.001	0.001	0.001	0.001	0.001	0.001	0.001	0.001	0.001	0.001
Sum	**4.013**	**4.019**	**4.025**	**4.041**	**3.995**	**4.006**	**4.027**	**4.042**	**4.026**	**4.033**	**4.017**
Mg#	94.5	94.9	88.8	91.6	84.4	90.4	87.3	84.2	88.3	87.6	92.8
Ca	46.8	46.8	44.3	46.0	50.7	50.1	49.8	48.1	44.2	44.8	47.2
Mg	50.3	50.5	49.5	49.4	41.6	45.1	43.9	43.7	49.3	48.4	49.0
Fe	2.9	2.7	6.2	4.6	7.7	4.8	6.4	8.2	6.5	6.8	3.8

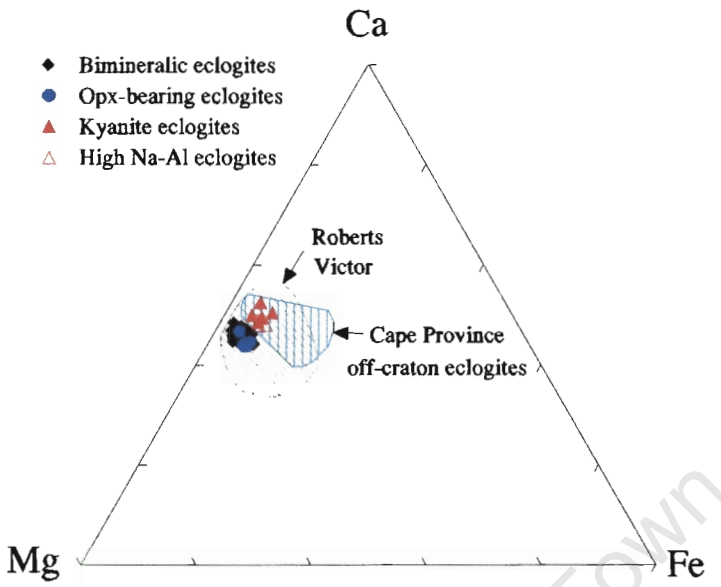

Figure 4.8 *Ca-Mg-Fe ternary diagram for clinopyroxenes from the Rietfontein eclogites. Data for the off-craton field from Robey (1981); Roberts Victor data from Hatton (1978); MacGregor & Manton (1986); Ongley et al. (1987); McCandless & Gurney (1989); Bell & Rossman (1992).*

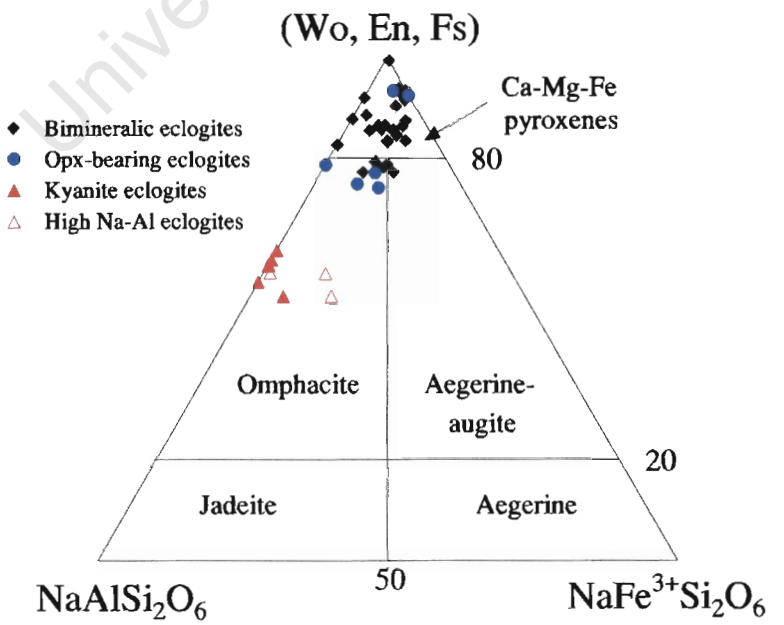

Figure 4.9 *Classification of the Rietfontein clinopyroxenes with respect to Na and Fe^{3+} content. Fe^{3+} calculated using the method of Droop (1987); diagram and fields after Morimoto (1988).*

expressed in terms of Ca and Mg, the variations in the Rietfontein clinopyroxenes are described by the diopside ⇌ jadeite substitution, and the Ca-Mg-Fe variations are of little magnitude. This is illustrated in *Figure 4.9*, where is can be seen that although the majority of the Rietfontein eclogites (>50%) consist of Ca-Mg-Fe pyroxenes, many contain a significant omphacite component, as is to be expected in eclogites. The kyanite eclogites all contain significant omphacite, as do a number of bimineralic and orthopyroxene-bearing samples.

Figure 4.10 illustrates the large variation in Na_2O in the Rietfontein eclogites, from 0.8-6.3 wt%. MgO contents in the pyroxenes vary from less than 10 % in some of the kyanite eclogites, to greater than 15 % in most of the bimineralic eclogites (*Figure 4.10*). The omphacitic pyroxenes have higher Al_2O_3 than the pyroxenes in the bimineralic and orthopyroxene-bearing eclogites, reaching almost 14 wt %. FeO within the clinopyroxenes varies between 1.4 and 4.1 wt%, and Cr_2O_3 contents are all below 0.80 wt% (*Table 4.2*). *Figure 4.10* illustrates that on the basis of their clinopyroxene Na_2O and MgO compositions, two eclogite groups can be identified. The first group contains moderate to high MgO concentrations, and low to moderate Na_2O levels. This group comprises the bimineralic and orthopyroxene-bearing eclogites, and falls within the Group A and lower Group B fields as defined by Taylor & Neal (1989). The second group comprises the kyanite eclogites, contains low MgO concentrations and high Na_2O concentrations, and also falls within the Group B eclogite field of Taylor & Neal (1989), but closer to the Group B - Group C boundary. K_2O contents in the Rietfontein eclogites are very low, with most concentrations below the detection limits (0.02 wt%) of the electron microprobe (*Table 4.2*). This reinforces the classification of the Rietfontein eclogites as Group II eclogites according to the scheme of McCandless & Gurney (1989) (*Figure 4.5*).

Clinopyroxenes from the orthopyroxene-bearing eclogites do not show any distinct chemical differences to those of the bimineralic and kyanite eclogites, except slightly higher FeO contents. Overall the clinopyroxenes show more intra-grain variation than the garnets. One particular sample shows absolute differences of up to 2.5 wt% in CaO and Al_2O_3 in different parts of a grain, but in general, differences are less than 0.5 wt% absolute between the cores and rims of grains. Like the garnets, these differences seem to reflect minor heterogeneities, rather than zoning patterns.

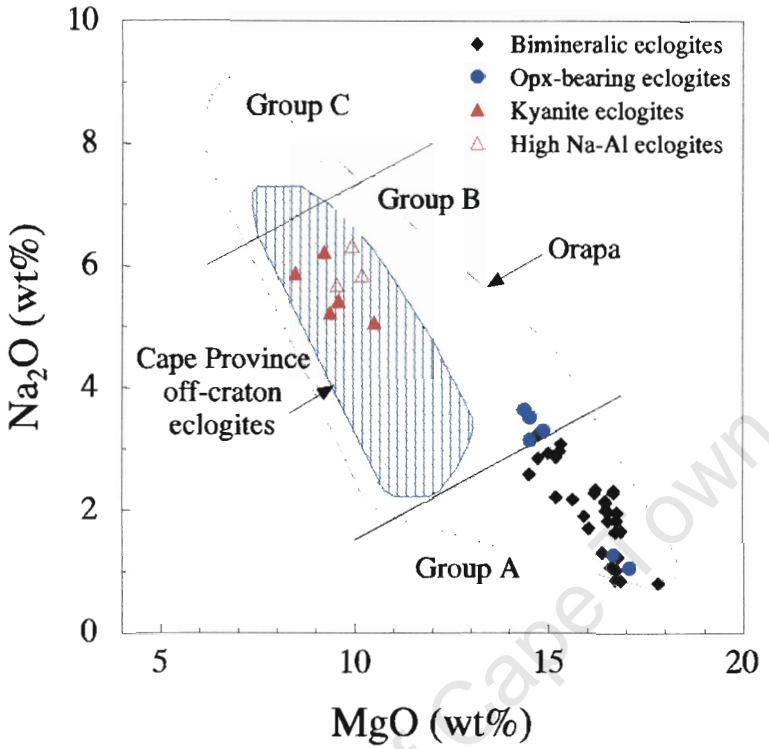

Figure 4.10 *Na_2O (wt%) vs MgO (wt%) for Rietfontein clinopyroxene. Orapa data from Shee (1978), Deines et al. (1991); off-craton data from Robey (1981). Group A, B & C fields are based on the composition of the Bellsbank eclogites, defined by Taylor & Neal (1989).*

Orthopyroxenes within the Rietfontein eclogites are commonly altered around grain boundaries, and along fracture zones. The orthopyroxenes are high-Mg enstatites, with Mg#'s of 82 - 89. Al_2O_3, Cr_2O_3, TiO_2 and Na_2O contents of the orthopyroxenes are all low (*Table 4.3*). FeO is variable between samples, with minimum and maximum concentrations of 7.0 and 11.76 wt% respectively. MgO shows a similar degree of variability, with contents falling between 30.47 and 34.1 wt%. Like the garnets and clinopyroxenes, the orthopyroxenes are homogeneous, with no compositional zoning. Comparisons of the Rietfontein eclogitic orthopyroxenes with peridotitic orthopyroxenes are illustrated in *Figure 4.11*. *Figure 4.11a* compares the Al_2O_3 abundances and Mg#'s of the two orthopyroxene types. Orthopyroxenes from the Rietfontein eclogites have much lower Mg#'s, and lower Al_2O_3 contents than most of the peridotitic orthopyroxenes. CaO and Na_2O abundances in the Rietfontein orthopyroxenes also tend towards the lower concentrations exhibited by the peridotitic orthopyroxenes (*Figure 4.11b*). Despite the fact that

Table 4.3 *Major element compositions of orthopyroxenes from the Rietfontein eclogites Mg# = 100Mg/(Mg+Fe*), Ca = 100Ca/(Ca+Mg+Fe*), Mg = 100Mg/(Ca+Mg+Fe*), Fe = 100Fe/(Ca+Mg+Fe*), Fe* - all Fe calculated as* Fe^{2+}

Sample	PC 5.2/1	Rtfn 56.1	CMA 3	CMA 11	CMA 12	CMA 13
SiO_2	57.09	57.41	55.82	55.72	56.95	57.77
TiO_2	0.06	0.04	0.06	0.06	0.09	0.07
Al_2O_3	0.73	0.78	0.58	0.70	0.70	0.72
Cr_2O_3	0.02	0.05	0.04	0.04	0.00	0.10
FeO*	9.32	8.95	11.99	8.80	8.31	7.57
MnO	0.09	0.08	0.19	0.09	0.12	0.11
MgO	32.46	32.26	30.47	33.92	33.53	33.79
CaO	0.32	0.31	0.32	0.28	0.31	0.28
Na_2O	0.10	0.10	0.04	0.12	0.17	0.09
K_2O	0.02	0.03	0.00	0.02	0.03	0.00
Total	**100.20**	**99.99**	**99.52**	**99.74**	**100.21**	**100.49**
*** Cations calculated on the basis of 6 oxygens ***						
Si	1.988	1.998	1.984	1.952	1.977	1.990
Ti	0.001	0.001	0.002	0.001	0.002	0.002
Al	0.030	0.032	0.024	0.029	0.029	0.029
Cr	0.001	0.001	0.001	0.001	0.000	0.003
Fe*	0.271	0.261	0.356	0.258	0.241	0.218
Mn	0.003	0.002	0.006	0.003	0.004	0.003
Mg	1.685	1.674	1.614	1.772	1.735	1.735
Ca	0.012	0.011	0.012	0.010	0.011	0.010
Na	0.007	0.007	0.003	0.008	0.012	0.006
K	0.001	0.001	0.000	0.001	0.001	0.000
Sum	**3.999**	**3.988**	**4.003**	**4.036**	**4.013**	**3.996**
Mg#	86.1	86.5	81.9	86.8	87.6	89.3
Ca	0.6	0.6	0.6	0.5	0.6	0.5
Mg	85.6	86.0	81.4	86.4	87.1	88.8
Fe	13.8	13.4	18.0	13.1	12.3	10.7

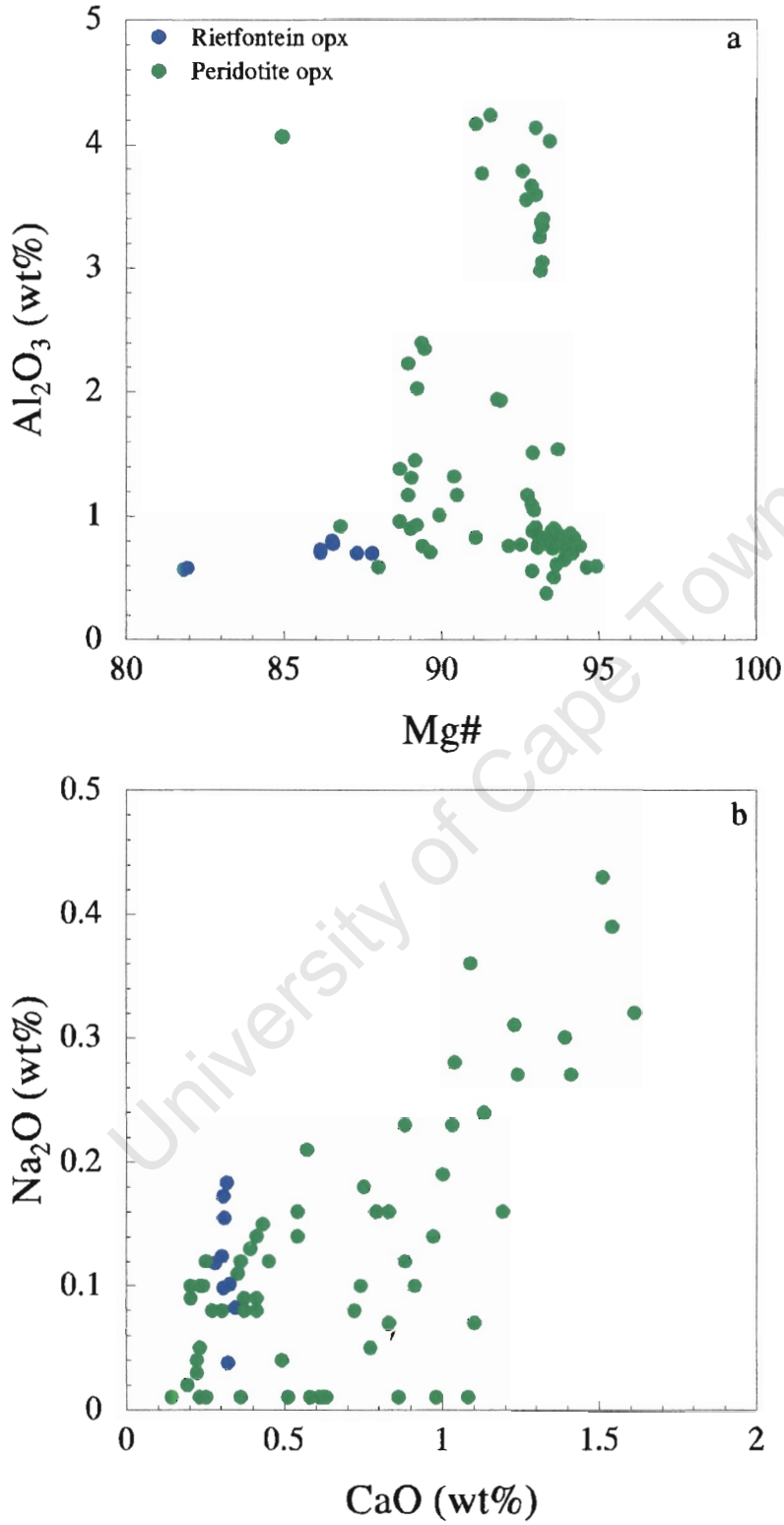

Figure 4.11 a) *Al_2O_3 (wt%) vs Mg#, and* ***b)*** *Na_2O vs CaO for Rietfontein orthopyroxenes, compared orthopyroxenes from on-craton peridotites. Peridotite data from Lawless (1978); Bell (1981); Smith (1981); Moore (1986); Waters (1987); Winterburn (1987); Hill (1989); Hops (1989).*

the Rietfontein orthopyroxenes show some similarities to peridotitic orthopyroxenes, they do form a compositionally distinct group.

4.4.3 Accessory and secondary minerals

4.4.3.1 Kyanite and sulphides

Representative analyses of accessory minerals (kyanite, ilmenite, rutile and sulphides) and secondary minerals (amphibole and phlogopite) are presented in *Table 4.4*. Kyanites from the 5 kyanite eclogites are uniform, and contain minor amounts (less than 0.2 wt%) of TiO_2, Cr_2O_3, FeO, MnO, MgO, CaO and Na_2O. Sulphides, many of which are altered, are a common accessory mineral in the Rietfontein eclogites. The degree of alteration and exsolution made representative analyses difficult to obtain (*Table 4.4*). However, it was possible to determine that the sulphides were not homogeneous, as many showed visibly different cores and rims. It was also noted that the sulphides showed significant chemical variation within the cores, so the grains are entirely heterogeneous. Variable proportions of Fe, Cu and Ni were measured in the sulphides, illustrated in *Figure 4.12*. This diagram also illustrates the amount of heterogeneity within each sulphide grain. Minor amounts of Zn (0-0.3 wt%) and Co (0.1-1.4 wt%) are noted in the sulphides.

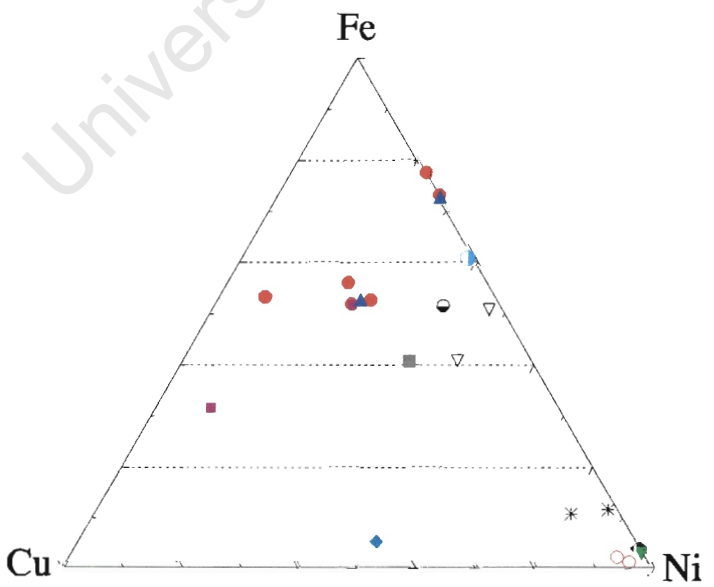

Figure 4.12 *Fe-Ni-Cu ternary diagram for sulphide minerals in the Rietfontein eclogites. The wide compositional spread is obvious, as is heterogeneity within single sulphides (each sulphide has a different marker).*

Table 4.4 *Representative major element analyses of accessory minerals from the Rietfontein eclogites*

	Kyanite		Ilmenite		Rutile		
Sample	**JJG 2104**	**Rtfn 54.2**	**CMA 9**	**CMA 15**	**Rtfn 54.2**	**Rtfn 48.1**	**Rtfn 31.1**
SiO_2	37.15	36.49	0.01	0.00	0.03	0.01	0.01
TiO_2	0.01	0.01	56.02	48.98	98.26	95.16	94.83
Al_2O_3	62.55	62.90	0.34	0.26	1.60	0.50	0.08
Cr_2O_3	0.07	0.11	0.59	1.19	0.10	1.46	0.45
Fe_2O_3			3.56	9.59			
FeO	0.12	0.19	25.20	31.86	0.49	1.97	3.02
MnO	0.03	0.03	0.37	0.37	0.02	0.06	0.01
MgO	0.02	0.00	13.92	6.77	0.03	0.48	0.64
CaO	0.02	0.07	0.02	0.00	0.02	0.10	0.05
Na_2O	0.01	0.00					
Total	**99.97**	**99.79**	**100.03**	**99.03**	**100.54**	**99.76**	**99.09**

	Amphibole				Phlogopite	
Sample	**Rtfn 31.1**	**CMA 1**	**CMA 2**	**CMA 14**	**Rtfn 55.3**	**Rtfn 55.3**
SiO_2	45.45	43.31	42.77	53.21	39.08	42.09
TiO_2	0.56	0.17	0.24	0.25	0.88	1.19
Al_2O_3	11.70	15.41	15.12	1.42	18.81	13.99
Cr_2O_3	0.25	0.37	0.41	0.08	0.03	0.20
FeO	6.11	7.50	8.92	3.86	8.54	5.56
MnO	0.05	0.16	0.20	0.08	0.01	0.00
MgO	17.23	16.15	15.57	16.34	20.43	23.86
CaO	9.16	10.46	9.89	21.07	0.03	0.09
Na_2O	4.12	3.88	4.06	1.66	1.11	0.50
K_2O	1.23	0.97	0.68	0.00	8.27	9.43
F					0.43	0.50
Total	**95.85**	**98.38**	**97.85**	**97.97**	**97.62**	**97.39**

	Sulphides						
Sample	**JJG 105** (1-core)	**JJG 105** (1-rim)	**JJG 105** (2-core)	**JJG 105** (2-rim)	**PC 5.2/1** (core)	**PC 3** (inclusion)	**Rtfn 57.3** (rim)
S	33.82	30.59	32.38	31.75	25.80	29.06	33.96
Fe	47.95	34.07	48.76	34.13	2.89	3.07	7.11
Cu	0.07	15.24	0.00	14.21	0.52	27.07	5.45
Ni	18.00	15.51	14.22	16.58	70.90	30.45	53.18
Zn	0.29	0.10	0.00	0.00	0.16	0.28	0.18
Co	0.17	0.36	0.17	0.20	0.12	1.39	0.02
Total	**100.32**	**95.87**	**95.53**	**96.87**	**100.39**	**91.33**	**99.89**

4.4.3.2 Amphibole

Amphiboles in the Rietfontein eclogites can be identified as hornblende, actinolite and edenite. Hornblende has variable Al_2O_3 contents, of 9.5-17.7 wt%, and Na_2O contents of 3-5 wt%. Na_2O contents of actinolite are lower (1-2 wt%), and CaO contents are much higher than in hornblende, 20-21 wt% (*Table 4.3*). *Figure 4.13* illustrates the compositions of the Rietfontein accessory amphiboles, compared to amphiboles of peridotites and other off-craton eclogites. The Rietfontein amphiboles have lower TiO_2 contents than the off-craton eclogitic amphiboles of Robey (1981), and lower average Cr_2O_3 contents than peridotitic amphiboles (*Figure 4.13a*). *Figure 4.13b* illustrates the unique occurrence of tremolite (low Na_2O, low Al_2O_3) in the Rietfontein eclogites, and the higher average Na_2O of the Rietfontein amphiboles when compared to amphiboles from peridotites and the Cape Province off-craton eclogites.

4.4.3.3 Mica

The mica identified in the Rietfontein eclogites is phlogopite, with MgO contents of 20 - 24 wt% and K_2O contents of approximately 9 wt%. A TiO_2-Mg# diagram (*Figure 4.14*) illustrates the phlogopite composition of the mineral in the Rietfontein eclogites, relative to other phlogopite compositions. The Mg# of the Rietfontein phlogopites is lower than phlogopites from on-craton eclogites and peridotites, and similar to that of primary phlogopites from the Cape Province off-craton eclogites (Robey, 1981). The Rietfontein phlogopites exhibit TiO_2 contents lower than the other off-craton peridotites, but similar to those of on-craton eclogites and peridotites.

4.4.3.4 Oxide minerals

Ilmenites generally exhibit high MgO (11.7 - 13.9 wt%) contents, typical of upper-mantle derived ilmenites (Haggerty, 1991), although ilmenites in one sample have lower, more moderate MgO (~ 6 wt%) contents. The high-Mg ilmenites compare favourably to ilmenites found in peridotites (*Figure 4.15a*), whereas the low-Mg ilmenites are similar to those found in Kaalvallei on-craton eclogites. The low MgO ilmenites also contain the highest proportion of Fe_2O_3 (9 wt%) and FeO (~32 wt%), and the lowest TiO_2 contents (49 wt%). The high MgO ilmenites have TiO_2 contents between 48 and 56 wt%, FeO contents of 25-32 wt%, and Fe_2O_3 contents of 3-9 wt%. A large number of eclogites also contain accessory rutile. These rutiles contain variable

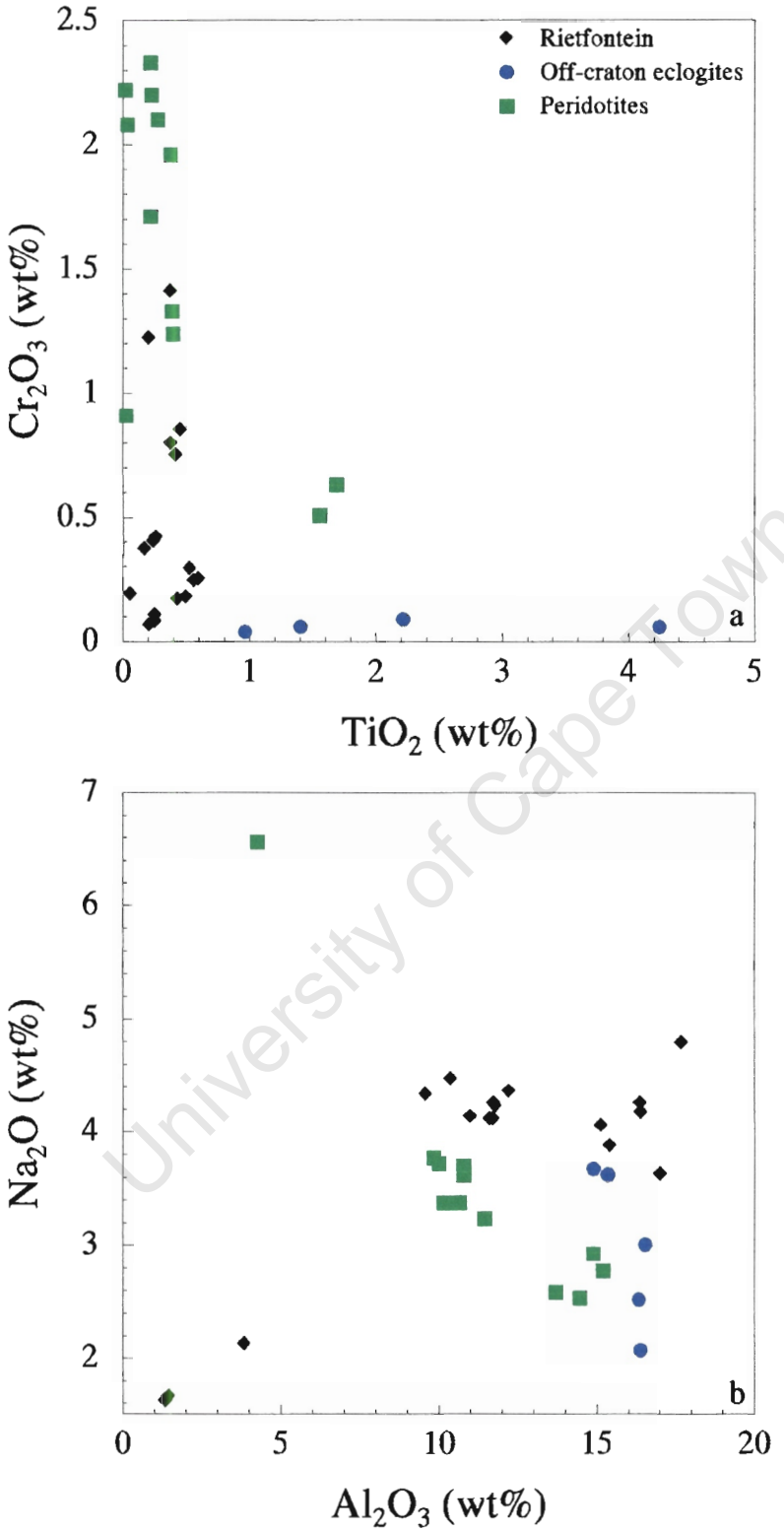

Figure 4.13 a) *Cr_2O_3 vs TiO_2, and* ***b)*** *Na_2O vs Al_2O_3 (all wt%) for amphiboles from the Rietfontein eclogites, compared to amphiboles from off-craton eclogites (Robey, 1981) and peridotites (Waters, 1987; Nowicki, 1990).*

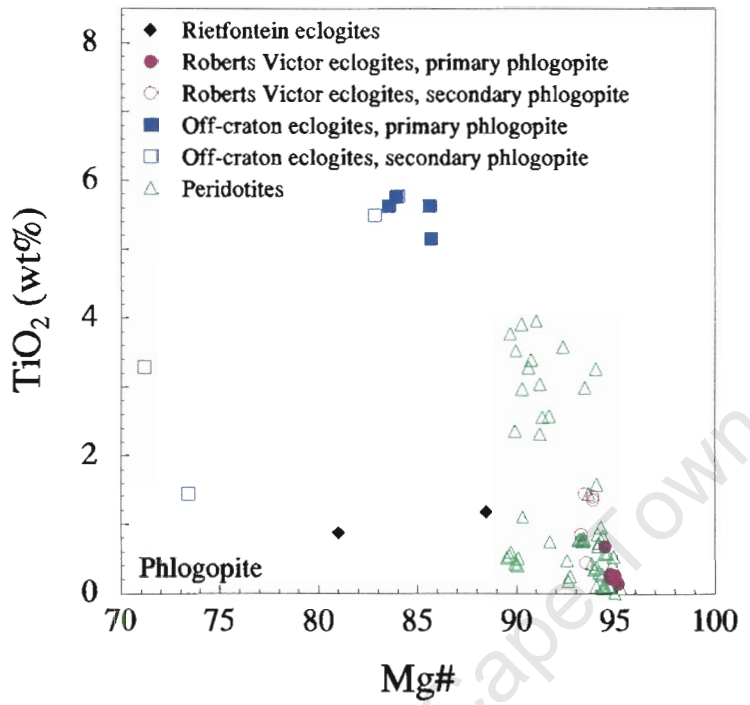

Figure 4.14 *TiO_2 vs Mg# for Rietfontein phlogopites, compared to phlogopites from Roberts Victor eclogites (Carswell, 1975), off-craton eclogites (Robey, 1981) and peridotites (Lawless, 1978; Waters, 1987; Winterburn, 1987; Hops, 1989)*

amounts of TiO_2, from 84-99 wt %. Other oxides occurring in significantly measurable amounts include Al_2O_3 (0.08-1.5 %), Cr_2O_3 (0.1-1.5 %), FeO (0.5-3.0 %) and MgO (up to 0.6 %). *Figure 4.15b* illustrates the lower average Cr_2O_3 and higher average Al_2O_3 contents of the Rietfontein eclogites.

4.5 Discussion

4.5.1 On- and off-craton eclogite comparisons

Figures 4.1 & 2 illustrate the major (Ca, Mg, Fe) compositional relations of garnets from Rietfontein relative to off-craton and on-craton eclogites. The Rietfontein eclogites plot within the on-craton field, although a number of bimineralic and orthopyroxene-bearing eclogites plot within the area of overlap with the off-craton field, as defined by eclogites from the Central Cape Province (Robey, 1981). The kyanite eclogites plot only within the on-craton (Roberts Victor) field however, and show compositional differences to the Kaalvallei eclogitic garnets. *Figures*

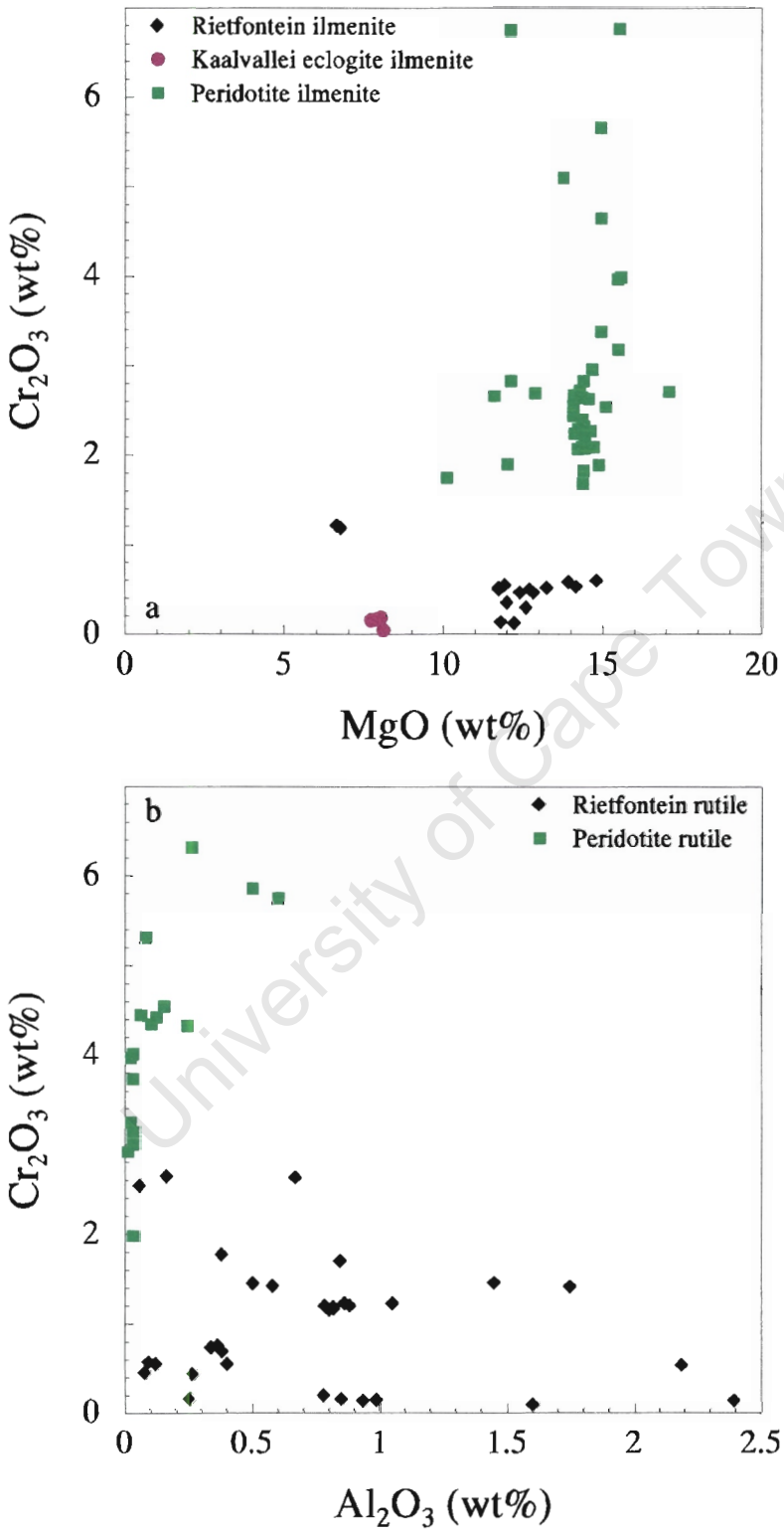

Figure 4.15 a) *Cr_2O_3 vs MgO for the Rietfontein ilmenites, compared to ilmenites from the Kaalvallei eclogites (Viljoen, 1994), and peridotites. b) Cr_2O_3 vs Al_2O_3 for rutiles from the Rietfontein eclogites, compared to peridotitic rutile. Peridotite data from Lawless (1978); Waters (1987), Gurney (unpublished).*

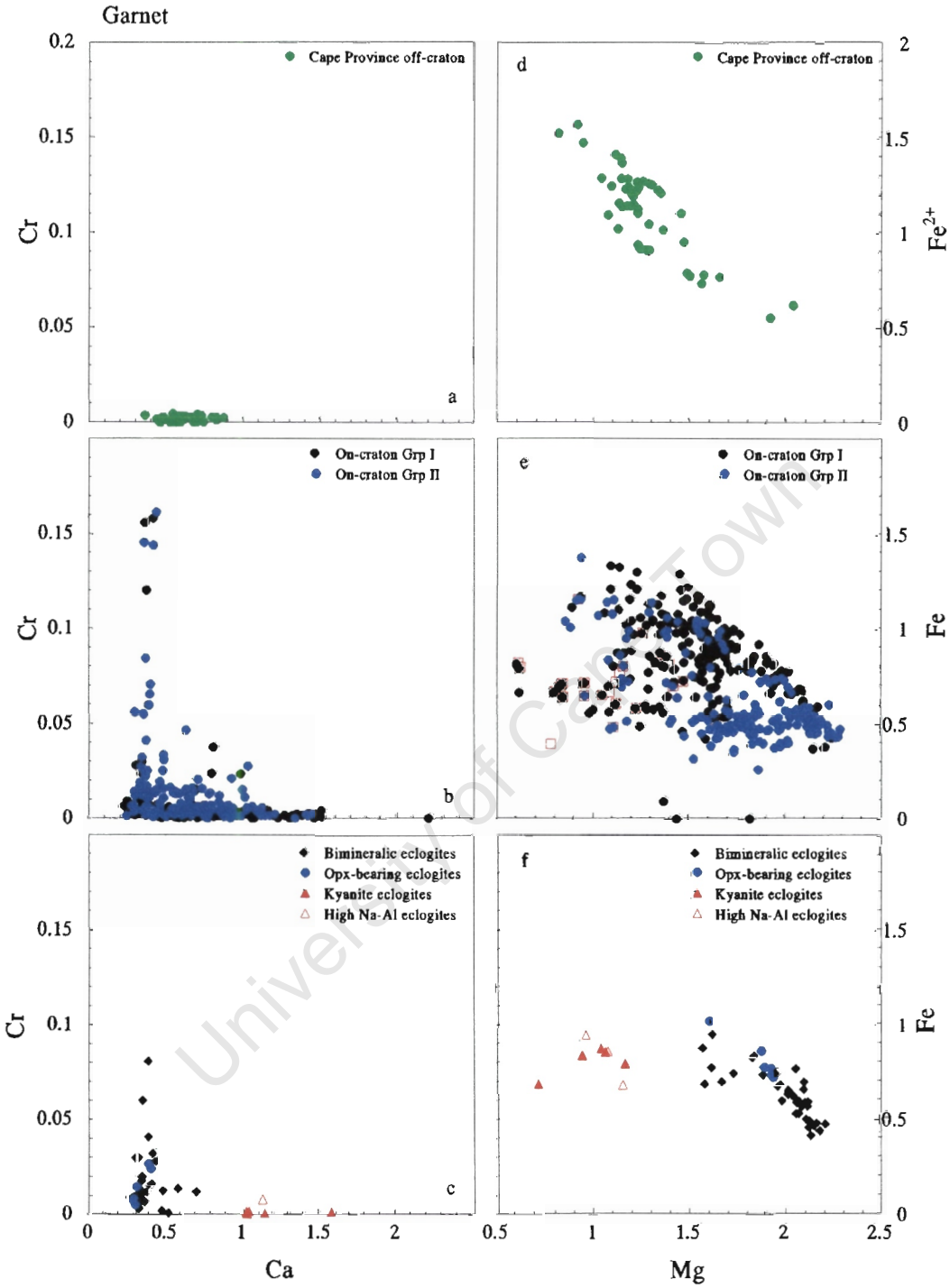

Figure 4.16 *Cr vs Ca and Fe vs Mg cation plots for the Rietfontein eclogites (**c** & **f**) compared to data for on-craton eclogites (**b** & **e**), and off-craton eclogites (**a** & **d**). Data for off-craton eclogites from Robey (1981); on-craton eclogite data from Orapa (Shee, 1978; Deines et al., 1991), Kaalvallei (Viljoen, 1994), Bellsbank (Caporuscio & Smyth, 1986; Taylor & Neal, 1989; Neal et al., 1990) and Roberts Victor (Reid et al., 1976; Hatton, 1978; MacGregor & Manton, 1986; Ongley et al., 1987; McCandless & Gurney, 1989; Bell & Rossman, 1992; Harte & Kirkley, 1997).*

4.16 a, b and *c* indicate differences in the Cr and Ca cations of garnets from on-craton and off-craton localities, and Rietfontein. Off-craton garnets show very restricted, low Cr contents in contrast to garnets from on-craton localities which show a much wider range in both Cr and Ca. The Cr contents of many on-craton eclogites tend towards more peridotitic (higher Cr) compositions. Garnets with the highest Cr contents contain the lowest Ca abundances. Garnets from the Rietfontein eclogites show a distribution very similar to that exhibited by the on-craton eclogites, with a trend of increasing Cr content at lower Ca abundances. An Fe-Mg plot for garnets (*Figure 4.16 d, e* and *f*) again illustrates the similarities in compositional fields for on- and off-craton eclogites. In *Figure 4.16 d & f* it can be seen that the off-craton and Rietfontein bimineralic and orthopyroxene-bearing samples form broadly linear trends. The kyanite eclogites from Rietfontein form a separate group away from this linear trend. In a similar manner, kyanite eclogites from on-craton localities (indicated by red squares on *Figure 4.16e*) also form a distinct, separate group at lower Mg abundances. Fe-Mg and Cr-Ca trends in the Rietfontein garnets show more similarities to garnets from on-craton eclogites than they do to the Cape Province off-craton eclogites.

Figure 4.8 shows off-craton and on-craton (Roberts Victor) fields for purposes of comparison on a Ca-Mg-Fe pyroxene plot. Clinopyroxenes from Rietfontein eclogites show major element compositions that fall well within the Roberts Victor on-craton field, whereas the kyanite eclogites plot within the area of overlap. The extensive overlap is also evident in *Figure 4.10*, where the two fields are very similar, with the on-craton field (represented by Orapa eclogites) showing a larger compositional diversity. *Figure 4.17* illustrates Cr-Al and Na-Al comparative diagrams for clinopyroxenes from eclogites. Al contents of clinopyroxenes show a large compositional range, with the Rietfontein bimineralic and orthopyroxene-bearing eclogites showing values consistent with those observed mostly in Group II on-craton eclogites. On-craton eclogites show a trend of increasing Cr with decreasing Al content, whilst off-craton eclogites show mostly restricted Cr contents. On a Na-Al diagram, clinopyroxenes from the Rietfontein bimineralic and orthopyroxene-bearing eclogites show a positive linear trend along the stoichiometric line, a trend which is also exhibited by the on-craton eclogites. At higher Na and Al contents however, the clinopyroxenes fall away from this line, as indicated by the Rietfontein kyanite eclogites. A similar pattern is illustrated by both Group I and Group II on-craton eclogites, although off-craton

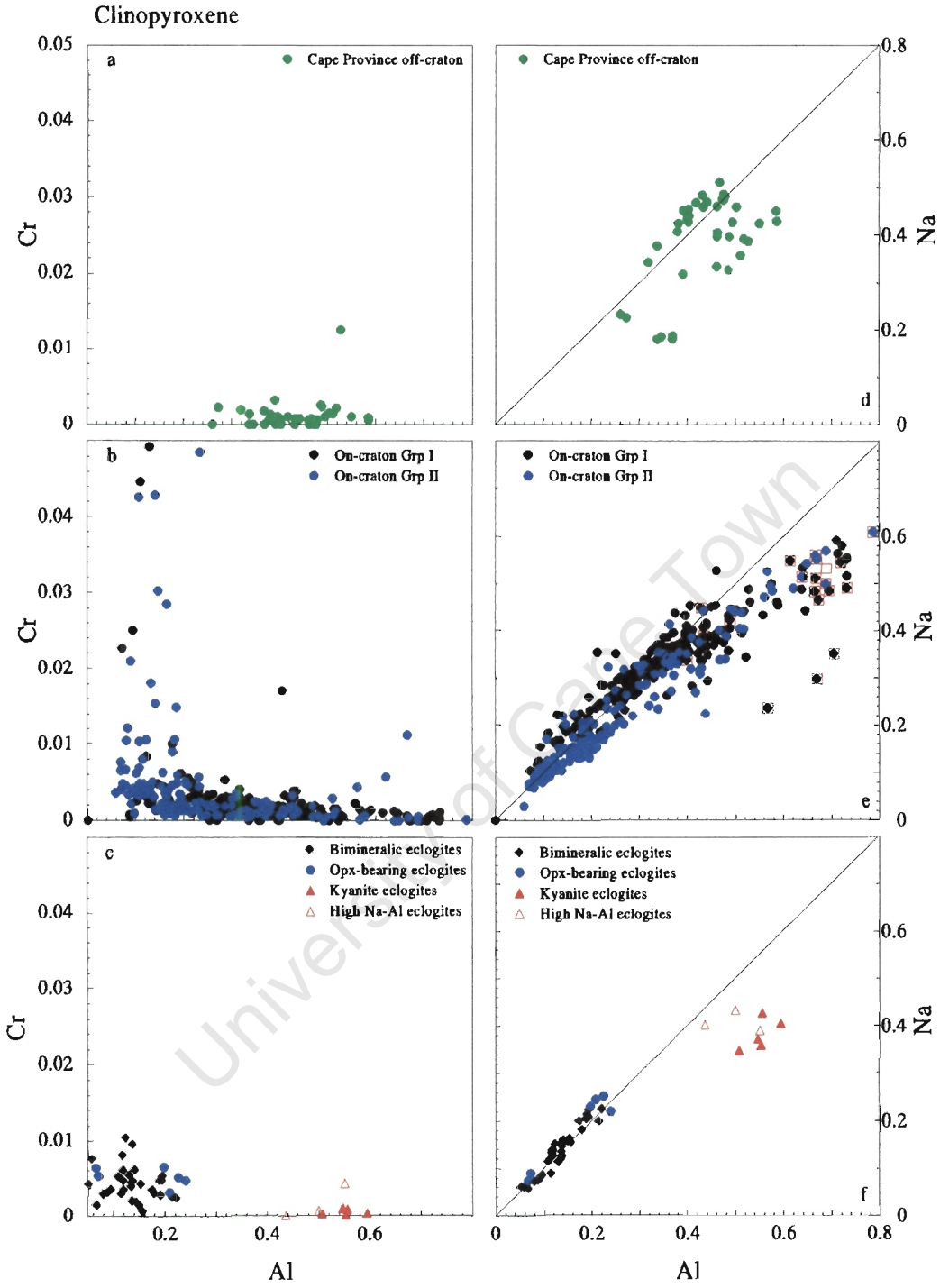

Figure 4.17 *Cr vs Al and Na vs Al cation plots for the Rietfontein clinopyroxenes (**c** & **f**) compared to data for on-craton eclogites (**b** & **e**), and off-craton eclogites (**a** & **d**). Data for off-craton eclogites from Robey (1981); on-craton eclogite data from Orapa (Shee, 1978; Deines et al., 1991), Kaalvallei (Viljoen, 1994), Bellsbank (Caporuscio & Smyth, 1984; Taylor & Neal, 1989; Neal et al., 1990) and Roberts Victor (Reid et al., 1976; Hatton, 1978; MacGregor & Manton, 1986; Ongley et al., 1987; McCandless & Gurney, 1989; Bell & Rossman, 1992; Harte & Kirkley, 1997).*

eclogites do not seem to conform to this trend. Kyanite eclogites from on-craton localities (illustrated by open red squares in *Figure 4.17e*) deviate from the stoichiometric line, in a similar fashion to the kyanite eclogites from Rietfontein. Off-craton eclogites show more compositional spread than the Rietfontein eclogites, and the stoichiometric trend is not as tightly constrained, with samples falling off the line at both low and high Na and Al values.

The comparative major element plots for garnet and clinopyroxene illustrate that in most cases, compositional fields for on-craton and off-craton eclogites show significant overlap, although off-craton eclogites show less variation than the on-craton eclogites. The Rietfontein eclogites show garnet and clinopyroxene compositions that always plot within the on-craton fields, and due to field overlap, very often within the off-craton fields. However, with regard to compositional trends within these fields, the Rietfontein eclogites seem to bear a greater resemblance to the on-craton eclogites than they do to the off-craton eclogites. The marked similarities to on-craton eclogites would also imply a mantle, rather than crustal origin for the eclogites, as opposed to the Cape Province off-craton eclogites, which are believed to be of a crustal origin (Robey, 1981).

4.5.2 Equilibrium state of the Rietfontein eclogites

Whereas garnet and clinopyroxene from the Rietfontein eclogites show no obvious zoning, Pearson *et al.* (1995) report zoning in both clinopyroxene and garnet in eclogites from the South-West margin of the Kaapvaal craton. Many on-craton localities have eclogites with homogeneous garnet and clinopyroxene grains (*eg.* Smyth & Caporuscio, 1984; Ater *et al.*, 1984; Sautter & Harte, 1988; Taylor & Neal, 1989; Beard *et al.*, 1996; Snyder *et al.*, 1997), although zoning has been observed in a few specimens from the Colorado Plateau (Ater *et al.*, 1984) and Roberts Victor (Lappin & Dawson, 1975; Sautter & Harte, 1988). The presence of homogeneous minerals indicates generally well-equilibrated samples (Gurney, 1990) and Beard *et al.* (1996) suggests that compositional zoning in garnet is most likely produced by metasomatism immediately prior, or subsequent to, incorporation into the kimberlite. The good equilibration within eclogites from Rietfontein is indicated by homogenous grains, with samples showing very little inter- or intra-grain variation.

Further evidence for the degree of equilibration of the Rietfontein eclogites can be drawn from the compositions of exsolved and granular garnet within sample CMA 1. In this sample, there are no visible differences between the composition of the exsolved garnet lamellae and the granular garnets, and no differences exist between clinopyroxenes containing garnet lamellae and those without. This is in contrast to studies on exsolution lamellae from other localities. For example, a Roberts Victor eclogite contains three types of garnet lamellae, each of which show relatively constant compositions, but marked compositional variations occur between different garnet lamellae and granular garnets (Harte & Gurney, 1975). Sautter & Harte (1988) found that, in this same sample, clinopyroxene is homogeneous between the narrowest garnet lamellae, but elsewhere the grains are zoned, showing marked variations with respect to Al_2O_3, SiO_2 and MgO. These compositional variations suggest that each garnet lamellae or granular grain formed under fairly constant conditions, but with variation in conditions between periods of garnet exsolution (Harte & Gurney, 1975). The lack of variation within the Rietfontein eclogite indicates that the exsolution lamellae have equilibrated with the other garnets, suggesting chemical exchange within the sample. This equilibration consequently took place prior to entrainment within the kimberlite, indicating a substantial mantle residence period for the xenolith. Should the xenolith have been entrained shortly after the process of exsolution, diffusion gradients within the sample would have been observed (Jerde *et al.*, 1993*b*).

4.5.3 Eclogite classification and mineral composition implications

Petrographically, the Rietfontein eclogites can tentatively be classified as Group I or Group II eclogites, although some are difficult to classify, due to sample size and degree of alteration (see *Chapter 3*). On the basis of Na_2O_{gt} and K_2O_{cpx} content, three Rietfontein eclogites can be recognised as Group I eclogites, but petrographically do not classify as Group I eclogites. McCandless & Gurney (1989) report that only 96% of the Roberts Victor Group II eclogites have less Na_2O contents less than 0.09 wt% in garnet, so the apparent petrographic-compositional classification discrepancy in the Rietfontein eclogites is not unusual. McCandless & Gurney (1989) found that diamondiferous eclogites and Group I eclogites have almost identical Na_2O_{gt} and K_2O_{cpx} contents, which suggests that Group I eclogites may have formed under conditions similar to those required for diamond genesis. The critical depth for diamond genesis under equilibrium conditions is approximately 150km below the surface (Gurney, 1990), thus Group I

eclogites are inferred to form at deeper levels (higher pressures) than Group II eclogites (McCandless & Gurney, 1989). The low Na_2O_{gt} and K_2O_{cpx} contents of the Rietfontein eclogites imply formation at shallower lithospheric depths than diamondiferous Group I eclogites.

The Rietfontein eclogites can be classified as Group A and Group B eclogites after Taylor & Neal (1989). Group B eclogites include the kyanite and orthopyroxene-bearing eclogites, with the bimineralic eclogites forming the bulk of the Rietfontein Group A eclogites (*Figure 4.10*). The presence of pyrope garnets and low Na_2O_{cpx} in Group A eclogites are a few of the geochemical signatures which led Shervais *et al.* (1988) and Taylor & Neal (1989) to suggest an origin for these rocks as mantle cumulates. Many of the Rietfontein Group A eclogites contain garnets and clinopyroxenes with relatively high Cr_2O_3 contents (> 0.4-0.5 wt%), a feature also noted by Taylor & Neal (1989), indicating a slight peridotitic signature (Jerde *et al.*, 1993*a*). A lack of Cr_2O_3 in mantle minerals is uncharacteristic of minerals that have precipitated from primary or near-primary melts (Ater *et al.*, 1984). By inference then, it is unlikely that the Rietfontein eclogites, whose garnets, for the most part, have depleted Cr_2O_3 contents, crystallised directly from mantle magmas. The presence of kyanite in some eclogites (*Chapter 3*) implies the involvement of an Al-rich protolith, and indeed the clinopyroxenes of the Rietfontein kyanite eclogites have elevated Al_2O_3 concentrations. High Na contents in eclogitic pyroxenes have been regarded as a characteristic implying derivation of eclogites from ocean floor rocks (*eg.* Helmstaedt & Doig, 1975), and a number of authors (*eg.* MacGregor & Manton, 1986; Shervais *et al.*, 1988; Taylor & Neal, 1989; Neal *et al.*, 1990) suggest that Group B and C eclogites may respectively represent the basaltic and feldspathic cumulate portions of the oceanic crust. The high Na-, high Al-clinopyroxenes of the Rietfontein kyanite eclogites, combined with the presence of kyanite itself, seems to unequivocally suggest a metamorphosed oceanic crustal origin for this group of eclogites. Further discussion of petrogenetic models, and origins of the Rietfontein eclogites will be dealt with once trace element compositions (and hence whole rock compositions) and oxygen isotopes have been considered.

5. GEOTHERMOBAROMETRY

Abbreviations used throughout this chapter are as follows:
CFMAS - CaO-FeO-MgO-Al_2O_3-SiO_2
FMAS - FeO-MgO-Al_2O_3-SiO_2
CMAS - CaO-MgO-Al_2O_3-SiO_2
CMS - CaO-MgO-SiO_2
MAS - MgO-Al_2O_3-SiO_2
X_{Ca} - Ca/(Ca+Mg+Fe)
Mg# - Mg/(Mg+Fe)

5.1 Introduction

Mineral assemblages have compositional variables that are sensitive to changes in the pressure and temperature of their geological setting (Boyd, 1973). Experimental calibration of these compositional responses to pressure and temperature provide geothermometers and geobarometers which can be applied to natural rock samples to determine pressures and temperatures of origin of these samples. In this chapter, thermobarometric methods are applied to the Rietfontein eclogites to determine from what depth these eclogites originate - are they crust or mantle derived? Once pressures and temperatures have been obtained for a particular xenolith suite, a geotherm for that particular area may be defined. Boyd (1973) defined a fossil geotherm for Lesotho using pressure-temperature points from garnet lherzolites. The derivation of a geotherm for the Rietfontein area, and subsequent details of the thermal structure of the Rietfontein lithosphere will be addressed in *Chapter6*.

The equilibrium of reactions within a chemical system can be used to determine pressures and temperatures of such equilibrations. The P-T slope (dP/dT) of such a reaction will determine whether or not it will make a good geothermometer or barometer, and is given by the Clausius-Clapeyron equation:

$$dP/dT = \Delta S/\Delta V$$

where ΔS refers to the change in entropy and ΔV refers to the volume change within a system. A good geothermometer will have a large dP/dT, and generally involves reactions with a small ΔV, whereas a good geobarometer has a small dP/dT, and is generally a reaction with a large ΔV. Geothermometers can be based on exchange reactions, or solvus relations between mineral pairs.

Divariant solid-solid reactions, such as those occurring between garnet and orthopyroxene, make useful geobarometers, due to the commonly large ΔV.

The limited number of minerals found in eclogites means that, compared to peridotites, there are relatively few equilibrium reactions applicable to eclogites. For this reason, geothermometers based on the exchange of Fe^{2+} and Mg between garnet and clinopyroxene are especially relevant in eclogite studies (*eg.* Ellis & Green, 1979; Krogh, 1988). Other geothermometers based on Fe^{2+}-Mg exchanges between other minerals (*eg.* garnet-orthopyroxene, garnet-olivine, olivine-spinel), the pyroxene solvus, and the Ni contents of olivine are all applicable to peridotites, but not eclogites. Although there are currently a number of methods of deriving the temperatures of equilibration of mantle xenoliths, methods of calculating equilibration pressures are limited, and most are based on the solubility of Al in orthopyroxene coexisting with garnet (*eg.* Nickel & Green, 1985). As a result of these calibrations using orthopyroxene and garnet, it is not possible to determine absolute pressures of eclogite formation. An exception to this rule would occur should an eclogite contain orthopyroxene, as is the case for some of the Rietfontein eclogites. Attempts at calibrating geobarometers for eclogites have however been made, the most recent using the solubility of CaTs in clinopyroxene coexisting with garnet (Simakov, 1999). However, these geobarometers have not been investigated fully, or tested for accuracy, and determination of absolute equilibration pressures for eclogites remains uncertain. It is possible though, to infer minimum equilibration pressures in eclogites containing coesite or diamond, using the phase transition equilibria of quartz $\rightleftharpoons$ coesite and graphite $\rightleftharpoons$ diamond, which occur at known positions in pressure-temperature space (Carswell, 1990).

A number of compositional effects, assumptions and common problems must be considered when applying thermobarometric methods. Uncertainties in Fe^{3+}/Fe^{2+} abundances in pyroxenes and garnet can cause large errors in temperatures in calibrations based on Fe^{2+}-Mg partitioning. The recalculation of Fe^{2+} and Fe^{3+} from stoichiometry (Droop, 1987) in Fe-poor pyroxenes is meaningless due to uncertainties in the proportions of more abundant cations such as Si (Giaramita & Day, 1990). Ambiguities in the site assignments of Al in pyroxenes may lead to uncertainties in calculated pressures and temperatures (Smith, 1999). Extrapolation of calibrations beyond those of the experimental conditions may lead to significant errors in

calculated pressures and temperatures, and a lack of thermodynamic data used in the formulation of thermodynamic expressions may lead to uncertainties in the thermobarometric calibrations. Substandard microprobe analyses will lead to erroneous pressure and temperature estimations for a suite of rocks. When calculating pressures and temperatures, it is also assumed that the minerals are in equilibrium with each other.

5.2 Aims

Eclogites occur within the Earth's upper mantle over a large pressure-temperature range (Dawson, 1980). Wide ranges in equilibration temperatures (and, where possible, pressures) have been reported from individual localities such as Bellsbank, Roberts Victor and Kaalvallei, and collectively, these result in a wide range of possible equilibration conditions for both mantle and crustal derived eclogites. Roberts Victor eclogites are known to span a temperature range of 900-1300°C, although most of the eclogites fall within a 200°C window, of 1100-1200°C (MacGregor & Manton, 1986). Large temperature ranges have also been reported for Orapa and Premier eclogites (1028-1380°C and 1189-1365°C respectively) (Shee & Gurney, 1979; Robinson *et al.*, 1984 and Gurney *et al.*, 1985). Eclogites retrieved from the Bellsbank kimberlite exhibit minimum temperatures of approximately 800°C (Shervais *et al.*, 1988), to a maximum temperatures of 1150°C (Viljoen, 1995), and Pearson *et al.* (1995) report a temperature range of 760-1050°C for eclogites occurring on the south-west margin of the Kaapvaal Craton, although the majority of these eclogites have equilibration temperatures greater than 930°C.

The large range of temperatures exhibited by eclogites are important, and serve to justify further thermobarometric studies on eclogite suites. The temperature range may be interpreted in a number of ways, one of which is the belief that the range reflects derivation of eclogite samples from a considerable depth range within the mantle. Equilibration temperatures will provide information as to whether xenoliths are crustal or mantle derived, with higher temperatures and pressures being associated with mantle conditions. Higher equilibration temperatures are indicative of a mantle origin, whereas lower temperatures may be used to infer a possible crustal origin for rocks. The primary aim of this chapter is thus to determine the temperatures and, where possible, pressures of equilibration of the Rietfontein eclogites and to hence decide whether they are crustal- or mantle-derived. It may be possible that the three eclogite groups identified at

Rietfontein have different equilibration temperatures, indicating derivation from different areas within the crust and/or mantle. A comparison of equilibration temperatures with those of on-craton and other off-craton eclogite suites will highlight differences in depths of origin of suites, and the structure of the thermal lithosphere in different areas.

5.3 Review of applicable geothermometers and geobarometers

5.3.1 Fe-Mg exchange thermometers

Fe-Mg exchange thermometers are based on the exchange of Fe^{2+} and Mg between two co-existing minerals in a rock. The exchangeable atoms in these reactions are usually elements of a similar charge and ionic radius, leading to small volume changes and large entropy changes. Garnet-olivine (*eg.* O'Neill & Wood, 1979), garnet-clinopyroxene (*eg.* Ellis & Green, 1979) and garnet-orthopyroxene (*eg.* Harley, 1984*a*) are all forms of geothermometers based on Fe^{2+}-Mg exchanges.

5.3.1.1 Garnet-clinopyroxene thermometry

The temperature sensitive Fe-Mg exchange equilibrium between garnet and clinopyroxene can be expressed as follows:

$$\underset{\text{pyrope}}{\tfrac{1}{3}Mg_3Al_2Si_3O_{12}} + \underset{\text{hedenbergite}}{CaFeSi_2O_6} \leftrightarrows \underset{\text{almandine}}{\tfrac{1}{3}Fe_3Al_2Si_3O_{12}} + \underset{\text{diopside}}{CaMgSi_2O_6}.$$

For this reaction, K_D is the partitioning coefficient for Fe and Mg between garnet and clinopyroxene, and is commonly defined as:

$$K_D = \frac{(Fe^{2+} / Mg)^{Gt}}{(Fe^{2+} / Mg)^{Cpx}}.$$

A number of garnet-clinopyroxene thermometers have been developed over the years (*eg.* Råheim & Green, 1974; Mori & Green, 1978; Ganguly, 1979; Ellis & Green, 1979; Saxena; 1979; Krogh, 1988; Pattison & Newton, 1989; Ai, 1994; Berman *et al.*, 1995).

Råheim & Green (1974) were the first to calibrate a relationship between K_D, temperature and pressure in order to form a geothermometer, based on experimental runs carried out between 600-

1500°C, and 20-40kb, in a system of bulk chemical composition $6.2 < 100Mg/(Mg+Fe) < 85$. This study concluded that K_D decreases with an increase in temperature within a system. Mori & Green (1978) performed further experiments in the CFMAS system, between 30-40kb and 950-1500°C, and found that their linear regression curves differed from those of Råheim & Green (1974) when Mg/(Mg+Fe) exhibited values between 0.06 and 0.85. Ganguly (1979) reviewed available data, and developed an expression accounting for the effect of the Mn content of garnet on the value of K_D. Ellis & Green (1979) developed a geothermometer (T_{EG}) based on the crystallisation of compositions within the system CFMAS at temperatures between 750°-1300°C, and pressures of 24-30kb. It was also found that K_D is dependent on the Ca-content, and independent of the Mg/(Mg+Fe) content of clinopyroxene and garnet. Krogh (1988) re-interpreted the existing experimental data of Råheim & Green (1974), Mori & Green (1978) and Ellis & Green (1979), deriving a new expression for the garnet-clinopyroxene exchange thermometer (T_{Kr}). The introduction of a curvilinear relationship between LnK_D and X_{Ca} in T_{Kr} meant that the effect of the grossular component of garnet in the range $X_{Ca} = 0.10\text{-}0.50$ was better approximated. Pattison & Newton (1989) found distribution ratios to be strongly dependent on the Mg# of garnet, and fitted new experimental data to a 3rd order polynomial equation to account for this effect, which they consider applicable to rocks with a Mg# of 12.5-60 (T_{PN}). Pearson *et al.* (1995) noted that T_{PN} produced temperatures 50-300°C lower that T_{EG}, and emphasised problems in extrapolating Pattison & Newton (1989) isotherms to high Mg#'s. Ai (1994) found that both the Mg# and Ca content of garnet has a significant effect on K_D and added a $Mg\#_{gt}$ term, in addition to an X_{Ca}^{Gt} term, to the thermometric equation (T_{Ai}).

Smith (1999) found that the formulation of Krogh (1988) is widely used and that temperatures calculated using T_{Kr} reproduced the experimental conditions of Brey & Köhler (1990) to within ± 62°C. The Ai (1994) formulation was found to be more sensitive to pressure than T_{Kr}, and yields unreasonably high temperatures for high pressure xenoliths (Smith, 1999). Although the Berman *et al.* (1995) calibration was found to yield plausible results for garnet peridotites (Smith, 1999), it is not an appropriate formulation to apply to the Rietfontein peridotites. A comparison of temperatures calculated using the T_{EG}, T_{Kr}, T_{Ai} and T_{Ber} calibrations yields similar temperatures for all but the kyanite eclogites. For the bimineralic and orthopyroxene-bearing eclogites, temperature differences between T_{Ber}, T_{EG} and T_{Kr} are within 100°C, but for the kyanite eclogites

this difference is 200-300°C (*Figure 5.1*). T_{Ber} is based on the T_{PN} geothermometer and one of the possible error sources in the Pattison & Newton (1989) study was uncertainty with regard to the effects on K_D of variable Na, Ca and Al contents in clinopyroxene, which were not constrained during their experiments (Aranovich & Pattison, 1995). Also, product clinopyroxene compositions contained only small amounts of Na and the authors (Aranovich & Pattison, 1995) have admitted that variable Al and Ca contents in clinopyroxene may be a problem. When formulating a new geothermometer, Berman *et al.* (1995) state that net-transfer equilibria constraining the thermodynamic properties of clinopyroxene components ($CaAl_2SiO_6$, $NaAlSi_2O_6$, $Mg_2Si_2O_6$) other than those in the garnet-clinopyroxene Fe-Mg exchange reaction were not considered. This means that the equilibria of Na were not considered. These omissions and possible errors in the T_{Ber} calibration could be the cause of temperature underestimations for the Rietfontein kyanite eclogites, which contain high-Ca garnets and high-Na, high-Al clinopyroxenes. This large discrepancy thus renders the T_{Ber} calibration unsuitable for use on the Rietfontein suite of eclogites. Thus, due to this apparent error in the T_{Ber} calibration with regard to eclogites containing high-Ca garnets, the pressure sensitivity of the T_{Ai} geothermometer, and the underestimation of T_{PN}, the T_{EG} and T_{Kr} geothermometers will be used to calculate and discuss equilibration temperatures of all the Rietfontein eclogites.

5.3.1.2 Garnet-orthopyroxene thermometry

The distribution of Fe^{2+} and Mg between garnet and orthopyroxene can be described by an exchange reaction as follows:

$$\frac{1}{3}Mg_3Al_2Si_3O_{12} + \frac{1}{2}Fe_2Si_2O_6 \leftrightarrows \frac{1}{3}Fe_3Al_2Si_3O_{12} + \frac{1}{2}Mg_2Si_2O_6$$

pyrope ferrosilite almandine enstatite

Harley (1984*a*) experimentally investigated Fe-Mg partitioning between garnet and orthopyroxene within the pressure range 5-30kb and temperature range 800-1200°C, in the FMAS and CMAS systems. Although the geothermometer of Harley (1984*a*) (T_{Har}) is the most commonly used garnet-orthopyroxene geothermometer, others such as those of Lee & Ganguly (1988) and Ganguly *et al.* (1996) exist. Fe^{3+}, Cr^{3+} and Mn are potentially important minor constituents not considered in the Harley (1984*a*) calibration of this geothermometer, and T_{Har} yields lower temperatures than T_{EG}. At temperatures greater than 1000°C, this difference is between 50 -

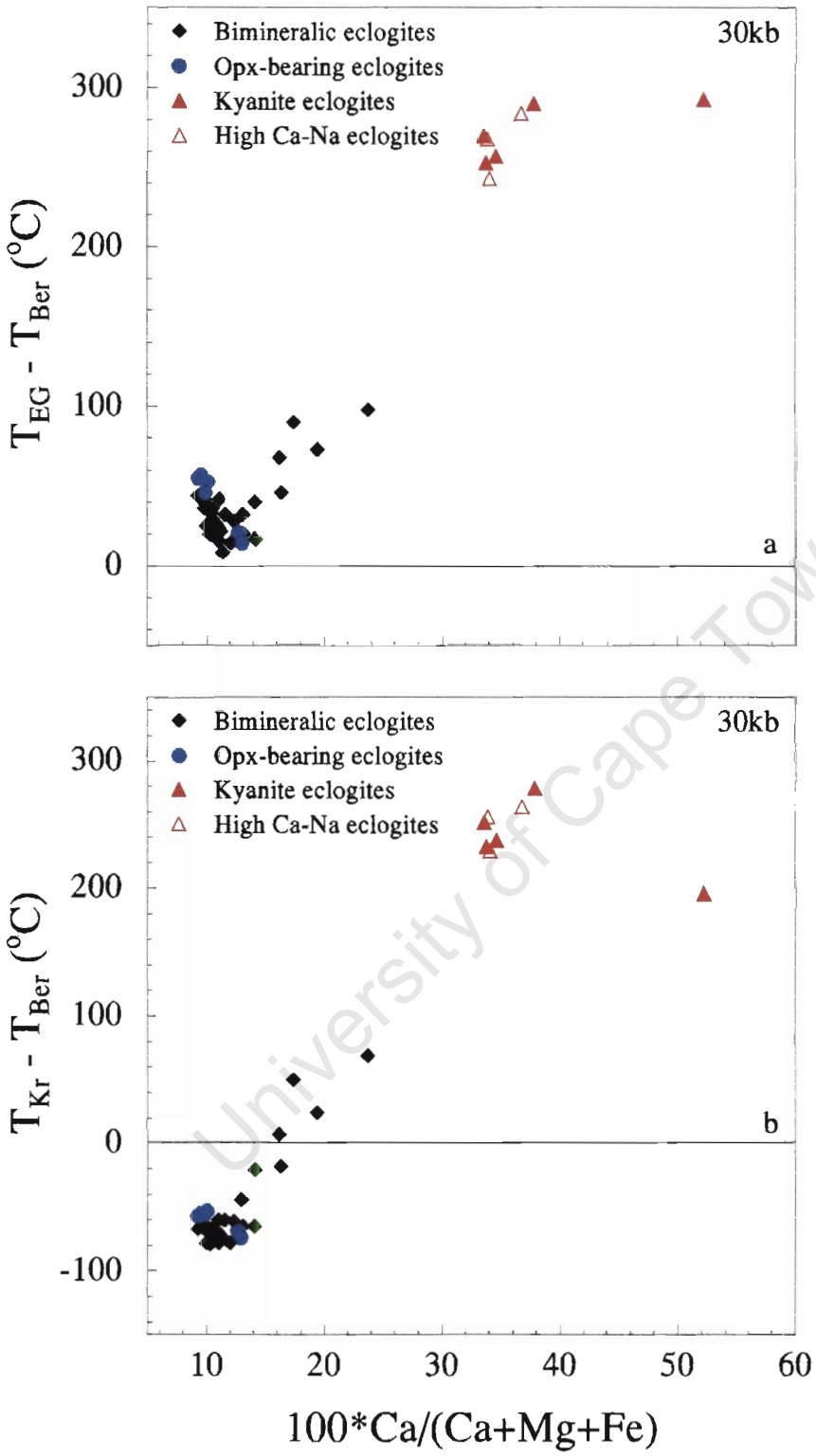

Figure 5.1 *Temperature differences between garnet-clinopyroxene thermometers for the Rietfontein eclogites. It can be see that T_{Ber} increasingly underestimates temperatures with increasing Ca-content of garnet. For the bimineralic and orthopyroxene-bearing eclogites, the difference between T_{Ber} and either T_{EG} or T_{Kr} is ± 100 °C, whereas for the kyanite eclogites it is between 200-300 °C. T_{EG}, T_{Kr} and T_{Ber} refer to the calibrations of Ellis & Green (1979), Krogh (1988) and Berman et al. (1995) respectively.*

130°C, whereas the difference is less than 50°C at lower temperatures. The orthopyroxene-garnet geothermometer is pressure dependent, with changes in temperature of 25-30°C/5kb, although the effect of Fe^{3+} is less pronounced than in other geothermometers. This form of geothermometer may thus not be suitable for eclogites with very high pressure origins. Limitations to this geothermometer are as a result of large relative errors in the experimental and natural rock data used in the calibration (Harley, 1984*a*). T_{Har} will be applied to the Rietfontein orthopyroxene-bearing eclogites, as it is the most commonly used garnet-orthopyroxene geothermometer, and can provide a good comparison of various Fe^{2+}-Mg exchange reactions.

5.3.2 Two-Pyroxene thermometers

Two-pyroxene thermometers are based on solvus relations existing between co-existing orthopyroxene and clinopyroxene. Some mineral pairs with similar structures exhibit continuous solid solution at high temperatures, but at lower temperatures they may exhibit an expanding miscibility gap. Miscibility gaps are strongly temperature dependent, and can thus make good geothermometers. Due to the general shape of the solvus, small changes in mineral compositions correspond to large temperature differences along steep limbs, but correspond to moderate temperature differences near the crest of the solvus. Thus, as temperature increases, solvus geothermometers become more sensitive indicators (Bucher & Frey, 1994).

5.3.2.1 The pyroxene solvus

The use of the miscibility gap between orthopyroxene and clinopyroxene as a geothermometer was first proposed by Davis & Boyd (1966), who investigated the binary join in the $Mg_2Si_2O_6$-$CaMgSi_2O_6$ system at 30kb. Above 800°C, the diopside limb of the solvus is temperature dependent. Natural pyroxenes rarely belong to the binary join $Mg_2Si_2O_6$-$CaMgSi_2O_6$, so a major problem with the use of this thermometer is the use of correction terms to account for other components in the system. Since the early work of Davis & Boyd (1966), a number of calibrations of this geothermometer have been devised, such as those of Wood & Banno (1973), Boyd (1973), Lindsley & Dixon (1976), Wells (1977), Bertrand & Mercier (1985) and Brey & Köhler (1990).

The calibration of Brey & Köhler (1990) ($T_{BK\text{-}2pyx}$) is the most recently formulated and widely used 2-pyroxene geothermometer (Smith, 1999), and can best reproduce experimental results (Brey & Köhler, 1990). The Wells (1977) geothermometer does not take pressure effects into account, and would thus not be a suitable geothermometer to apply to the Rietfontein eclogites. Use of the 2-pyroxene method with regard to Rietfontein eclogites is limited, as only six of the samples contain orthopyroxene. The Brey & Köhler (1990) geothermometer is formulated for use in peridotites, so application to eclogites should be used with caution as small, but important, compositional differences exist between the two rock types. Pyroxene solvus thermometers are also hampered by the insensitivity of pyroxenes to temperatures less than 900°C (Griffin & O'Reilly, 1987), and a lack of knowledge with regards to the effect of Fe^{2+} on the system may also lead to uncertainties in temperatures calculated using this method.

5.3.2.2 Ca-in-orthopyroxene thermometry

An alternative pyroxene thermometer can be obtained by the use of the Ca content of orthopyroxene equilibrated with clinopyroxene. This method uses the remaining limb of the two-pyroxene solvus used by Boyd (1973). Sachtleben & Seck (1981) used the experimental data of Lindsley & Dixon (1976) to calculate temperatures using the solubility of CaO in orthopyroxene co-existing with clinopyroxene. A disadvantage of this thermometer is the relatively low amount of CaO dissolved in the orthopyroxene structure at low temperatures (Sachtleben & Seck, 1981). However, orthopyroxene contains less Al, Cr, Na and Ti than co-existing clinopyroxene, and may thus be less affected by bulk compositional variations (Smith, 1999). Brey & Köhler (1990) fitted available reversed experiments in the CMS system, as a function of pressure and reciprocal temperature and note that the Ca-in-opx thermometer ($T_{BKCa\text{-}opx}$) yields different results when applied to Kaapvaal Craton garnet peridotites than their 2-pyroxene thermometer yields. It was found that Na^{opx} distribution is very similar to Ca^{opx} distribution, suggesting that Na^{opx} may also be temperature dependent, and may thus influence the Ca content of orthopyroxene. A correction scheme for this influence has not yet been derived, and as a result, Brey & Köhler (1990) suggest caution when using this geothermometer.

5.3.3 Al-in-orthopyroxene geobarometer

Garnet-orthopyroxene geobarometry is based on the pressure sensitivity of Al in orthopyroxene coexisting with garnet and was first calibrated by MacGregor in 1974, based on the following exchange reaction:

$$Mg_2Si_2O_6 + MgAl_2SiO_6 \leftrightharpoons Mg_3Al_2Si_3O_{12}$$

orthopyroxene solid soln. pyrope

Garnet-orthopyroxene barometry is sensitive to temperature estimations and temperature overestimations will cause pressure overestimations, and vice versa (Nickel & Green, 1985). A number of geobarometers based on the Al-in-opx method are currently available (*eg.* Wood, 1974; MacGregor, 1974; Harley, 1984*b*; Nickel & Green, 1985; Brey & Köhler, 1990).

MacGregor (1974) experimentally studied the solubility of Al within the MAS system, at pressures of 5-40kb and 900-1600°C. Wood (1974) carried out experiments in the FMAS and CFMAS systems, between 8-30kb and 800-1250°C, taking into account the effects of Ca and Fe^{2+} on the system. Harley (1984*b*) determined the pressure-temperature-compositional (P-T-X) dependence of Al solubility in the FMAS system, at P-T ranges of 5-30kb and 800-1200°C. These results were then extended into the CFMAS system to determine the effect of the Ca content of garnet on the Al content of the co-existing orthopyroxene. Nickel & Green (1985) refined the existing Al-in-orthopyroxene geobarometers (P_{NG}) by investigating the influence of Cr on the system. Pressures calculated using the Harley (1984*b*) geobarometer (P_{Har}) are lower than those calculated using P_{NG} (Nickel & Green, 1985). The most commonly used Al-in-orthopyroxene geobarometer is that of Brey & Köhler (1990) (P_{BKN}), who treat orthopyroxene as a two-site solid solution with ideal mixing on M2, and assume ideal mixing of Fe and Mg in garnet.

Three geobarometric calibrations have been applied to the Rietfontein eclogites, for comparative purposes. These are the P_{Har}, P_{NG} and P_{BKN} calibrations, and each provides a range of equilibration pressures. Smith (1999) reports coherent arrays for African xenoliths to which the P_{BKN} and Finnerty & Boyd (1984) (a revision of the MacGregor (1974) calibration) geobarometers have been applied. As a result of these good comparisons, and the ability of P_{BKN} to reproduce the experimental data of Brey *et al.* (1990) to within ± 2.2kb, P_{BKN} has been selected for application

with two geothermometers ($T_{BK\text{-}2pyx}$ and T_{Kr}), although P_{Har} and P_{NG} will also be applied for comparative purposes.

5.4 Methodology

All of the Rietfontein eclogite suite sampled in this study have been subjected to thermometric calculations. For each sample, all acceptable (oxide total = 99.5-100.5%) garnet and clinopyroxene analyses were combined, including both core and rim compositions, to give an average garnet and an average clinopyroxene composition. Orthopyroxenes from the orthopyroxene-bearing eclogites were averaged in the same manner. Such an averaging procedure will alleviate intra- and inter-grain compositional differences and give the best compositional estimate for a particular mineral species. Fe^{3+} was not calculated, due to the large errors associated with such a calculation in Fe-poor pyroxenes. All Fe was thus assumed to be Fe^{2+}. These compositional averages for garnet, clinopyroxene and orthopyroxene were then used to calculate equilibration pressures and temperatures using the FORTRAN programme of Doug Smith, TP97v.2 (Smith, 1999). All temperatures are reported in degrees Celsius (°C), and pressures are reported in kilobars (kb).

5.5 Results

5.5.1 Equilibration temperatures

For the purpose of comparisons amongst the eclogites, an assumed pressure of 30kb has been used when applying the garnet-clinopyroxene geothermometers, as it is an average value of pressures calculated for the Rietfontein eclogites (*Section 5.5.2*). A detailed table of temperature results, calculated over a range of pressures and using a number of geothermometers is presented in *Table 5.1*.

The application of two garnet-clinopyroxene thermometers (T_{EG} & T_{Kr}) to the Rietfontein eclogites yields slightly different temperature distributions. The minimum temperature obtained using the T_{EG} calibration is 815°C, whilst the T_{Kr} approximation is 733°C, both at an assumed pressure of 30kb. Both thermometers obtain a minimum temperature on the same sample, a bimineralic eclogite, CMA 15. Whereas there is an 82°C difference between the two minimum temperatures, the maximum temperatures obtained for the Rietfontein eclogites are very similar,

Table 5.1 *Equilibration temperatures (^{o} C) at set pressures (kb) for the Rietfontein eclogites.*
EG = Ellis & Green (1979); Kr = Krogh (1988); BKN_{2pyx} = 2pyx thermometer, Brey & Kohler (1990); BK_{opx} = Ca-in-opx thermometer, Brey & Kohler (1990); Har = Harley (1984a).

	P = 20kb					P=30kb					P=40kb				
	EG	Kr	BKN_{2pyx}	BK_{opx}	Har	EG	Kr	BKN	BK_{opx}	Har	EG	Kr	BKN	BK_{opx}	Har
JJG 105	873	762				908	801				943	839			
JJG 2104	930	832				957	860				983	888			
PC 1	813	717				846	753				879	788			
PC 12	851	747				885	784				919	822			
PC 3	815	711				848	746				881	782			
PC 5.2/1	882	766	874	836	854	917	805	888	879	913	953	844	906	921	973
PC 5.2/2	898	786				933	826				969	866			
Rtfn 31.1	857	746				891	784				926	822			
Rtfn 31-2	903	788				939	828				975	868			
Rtfn 31-3	856	749				890	787				925	825			
Rtfn 43-1	902	805				938	844				974	884			
Rtfn 43-10	923	879				957	917				992	954			
Rtfn 43-7	883	780				918	819				953	858			
Rtfn 43-9	869	762				903	800				938	838			
Rtfn 48-1	889	786				925	825				960	864			
Rtfn 48-2	927	829				964	869				1000	910			
Rtfn 54-1	982	967				1012	1000				1043	1033			
Rtfn 54-2	863	841				891	871				920	902			
Rtfn 54-3	877	856				906	887				935	918			
Rtfn 54-4	876	856				905	887				934	918			
Rtfn 55-1	891	791				926	830				961	869			
Rtfn 55-2	866	771				901	809				935	846			
Rtfn 55-3	917	903				947	935				978	968			
Rtfn 55-4	797	747				828	779				858	812			
Rtfn 56-1	851	736	985	830	818	886	774	1001	873	875	920	811	1021	915	933
Rtfn 57-1	905	798				941	838				976	878			
Rtfn 57-2	825	733				857	768				890	804			
Rtfn 57-3	870	770				904	808				939	846			
CMA 1	838	807				868	839				898	872			

Table 5.1 continued

	P = 20kb					P=30kb					P=40kb				
	EG	Kr	BKN	BK_{opx}	Har	EG	Kr	BKN	BK_{opx}	Har	EG	Kr	BKN	BK_{opx}	Har
CMA 2	796	729				827	763				858	796			
CMA 3	792	701	839	843	806	824	735	853	886	862	856	769	871	929	919
CMA 4	914	893				944	924				973	956			
CMA 5	895	786				931	825				967	865			
CMA 6	809	721				841	756				873	790			
CMA 7	920	818				957	858				993	899			
CMA 8	953	889				990	929				1026	969			
CMA 9	896	816				931	855				965	893			
CMA 10	885	788				920	826				955	865			
CMA 11	863	753	805	814	817	897	791	815	855	874	932	829	831	896	932
CMA 12	931	825	806	830	814	968	866	819	873	871	1004	907	837	915	928
CMA13	793	701	762	811	782	825	735	770	851	837	857	769	784	893	892
CMA 14	829	765				861	800				893	835			
CMA 15	784	700				815	733				846	767			
CMA 16	951	847				988	889				1026	930			
CMA 17	917	901				947	934				977	966			
CMA 18	956	868				993	909				1030	951			

1012°C (T_{EG}) and 1000°C (T_{Kr}). As is the case with the minimum temperature, both geothermometer calibrations give a maximum reading on the same sample, this time a kyanite eclogite (Rtfn 54.1).

Figure 5.2 shows histograms of the distribution of temperatures within the Rietfontein eclogites. It can be seen that according to the T_{Kr} geothermometer, the most common temperature range in the Rietfontein eclogites is 800-850°C, whereas the most frequent temperature range according to T_{EG} is 100 degrees higher, from 900-950°C. It is clear that temperatures calculated using the T_{Kr} span a much larger range than those calculated using T_{EG}. It can be seen that, according to both calibrations, the orthopyroxene-bearing eclogites span a smaller temperature range (200°C) than the bimineralic eclogites. However, it should be remembered that only six orthopyroxene-bearing samples have been analysed, so a sample population of the size of the bimineralic eclogites would probably yield a similar range in temperatures. T_{EG} and T_{Kr} both indicate equilibration temperatures of less than 1000°C for the bimineralic eclogites. These histograms illustrate the observation that T_{EG} temperatures are, on average, higher than T_{Kr} temperatures.

For the six orthopyroxene-bearing eclogites retrieved from Rietfontein, $T_{BK\text{-}2pyx}$, $T_{BK\text{-}Ca\text{-}opx}$ and T_{Har} may also be used to estimate temperature. $T_{BK\text{-}2pyx}$ shows a large temperature range for the Rietfontein eclogites, namely 770-1001°C (at 30kb). $T_{BK\text{-}Ca\text{-}opx}$ and T_{Har} yield relatively smaller temperature ranges (851-886°C and 837-913°C respectively), and, with the exception of $T_{BK\text{-}2pyx}$, these ranges are smaller than those expressed by T_{EG} & T_{Kr} for the same samples. *Figure 5.3 a* and *b* illustrate the range in temperatures provided by these geothermometers, and it can be seen that for $T_{BK\text{-}2pyx}$, the large temperature range is caused by the presence of an outlier, sample Rtfn 56.1, which exhibits a temperature far higher than the other orthopyroxene-bearing eclogites. There is no such outlier on the $T_{BK\text{-}Ca\text{-}opx}$ or T_{Har} graphs, suggesting that the reason for this outlier may lie within the clinopyroxene terms of $T_{BK\text{-}2pyx}$. A careful study of the major element chemistry of this sample reveals that it has a lower Ca^{*}_{cpx} ($Ca^{M2}/[1\text{-}Na^{M2}]$) value than the other samples, leading to a much larger K^{*}_{D}, and hence an elevated temperature. This suggests that the wide temperature range in the Rietfontein eclogites, calculated using $T_{BK\text{-}2pyx}$ may be both a function of the calibration of the geothermometer and the composition of the samples. The major element mineral composition of this sample is no different to the other samples, and it can be concluded

that $T_{BK\text{-}2pyx}$ is extremely sensitive to stoichiometric variations and site allocations in clinopyroxene.

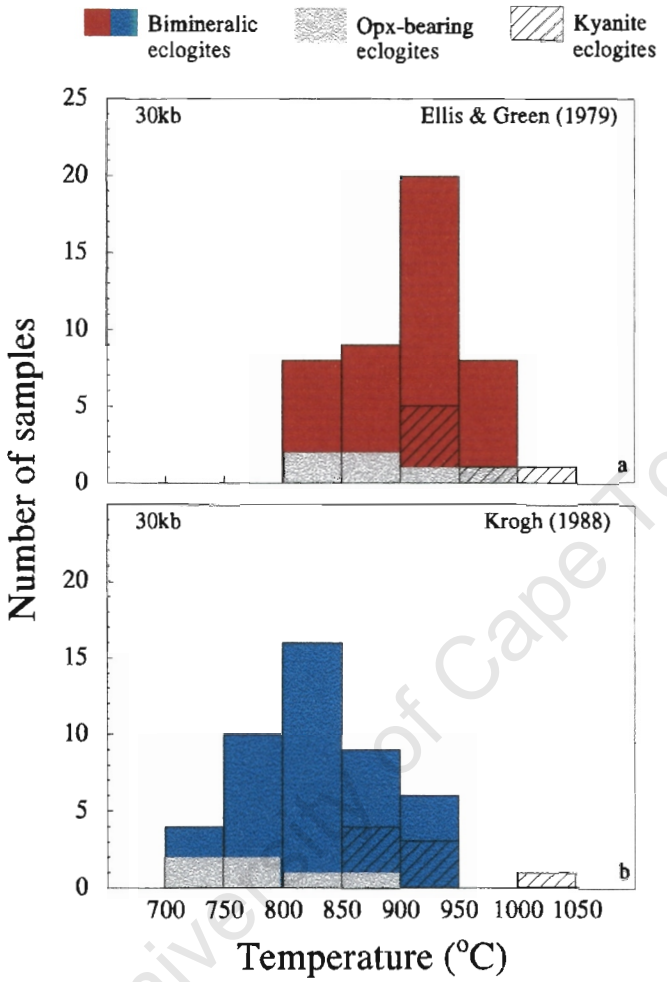

Figure 5.2 *Distribution of equilibrium temperatures within the Rietfontein eclogites at an assumed pressure of 30kb, using the garnet-clinopyroxene thermometers of Ellis & Green (1979) (top) and Krogh (1988)(bottom).*

5.5.2 Equilibration pressures

Table 5.2 presents combined pressure and temperature estimates for the Rietfontein orthopyroxene-bearing eclogites. All geobarometers used in estimating the equilibration pressures of the Rietfontein eclogites use the method of Al-in-orthopyroxene co-existing with garnet (P_{Har}, P_{NG} and P_{BKN}). At a fixed temperature of 800°C, P_{Har} provides the lowest pressure estimations for the Rietfontein eclogites, between 26.8 and 28.1 kb. P_{NG} gives pressures of 27.7 - 32.6 kb, whereas estimations obtained using P_{BNK} give similar pressures, of 30.6 - 32.6 kb. This means

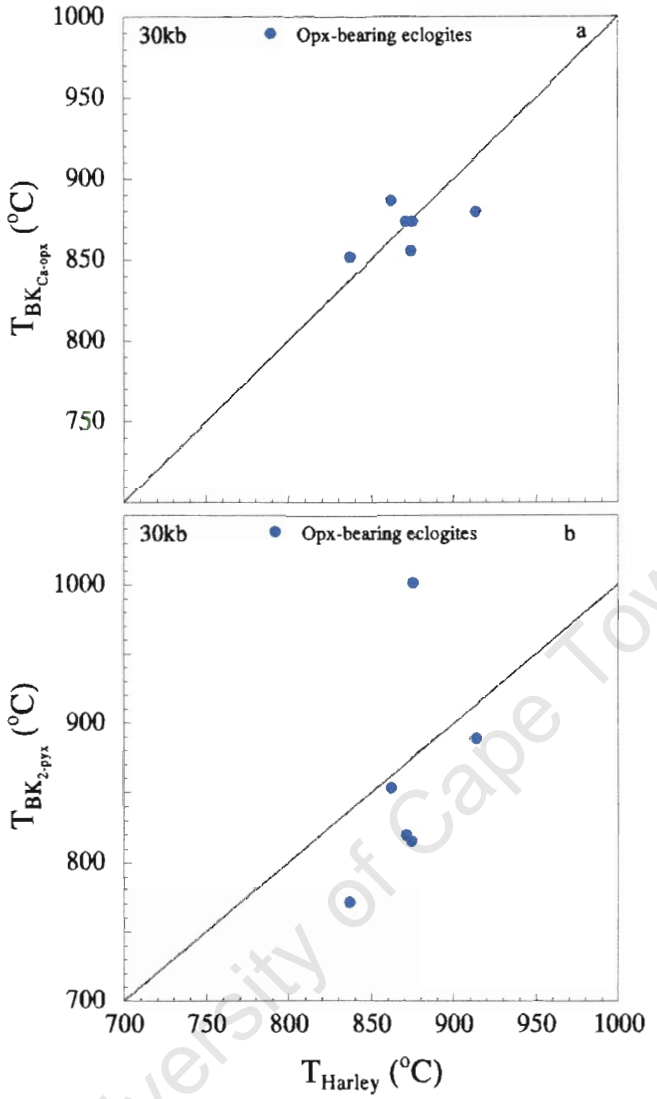

Figure 5.3 a) *Temperatures calculated using Brey & Köhler's (1990) Ca-in-opx thermometer, compared to the temperatures of the Harley (1984a) gt-opx thermometer;* ***b)*** *temperatures calculated using Brey & Köhler's (1990) 2-pyroxene thermometer, compared to the temperatures of Harley (1984a).*

that at a fixed temperature, P_{NG} provides the largest spread of pressures, whereas P_{Har} results in the smallest spread. One of the possible reasons for this is that P_{NG} uses the greatest number of terms in the geobarometric equation, and accounts for minor elements such as Cr, Ti and Na, whereas P_{Har} has the smallest number of variable terms in the equation, and fails to account for the possible effects of Cr, Ti, Na or Mn. Thus, the use of a larger number of chemical variables may lead to a larger pressure range, and vice versa.

Table 5.2 *Combined pressure (kb) and temperature (^{o} C) estimates for the Rietfontein opx-bearing eclogites. P_{BKN} = Brey & Kohler (1990); T_{Kr} = Krogh (1988); $T_{BKN2pyx}$ = 2 pyroxene thermometer, Brey & Kohler (1990); T_{BKopx} = Ca-in-opx temperature, Brey & Kohler (1990); T_{Har} = Harley (1984a); P_{Har} = Harley (1984b); T_{Wells} = Wells (1977); P_{NG} = Nickel & Green (1985).*

	T_{Kr}	P_{BKN}	$T_{BKN2pyx}$	P_{BKN}	T_{BKopx}	P_{BKN}	T_{Har}	P_{BKN}
PC 5.2/1	821	34.1	910	39.5	921	40.2	1005	45.5
Rtfn 56-1	774	30.2	1037	46.3	906	38	929	39.5
CMA 3	714	23.9	867	35.3	928	40	911	38.6
CMA 11	798	31.8	828	33.6	884	37.1	932	40.1
CMA 12	903	39.1	832	34.9	912	39.7	934	41
CMA13	720	25.7	776	29.2	875	35.5	824	27.6

	T_{Har}	P_{Har}
PC 5.2/1	932	33.2
Rtfn 56-1	873	29.6
CMA 3	858	29.3
CMA 11	879	30.8
CMA 12	876	30.9
CMA13	824	27.6

	T_{Wells}	P_{NG}	$T_{BKN2pyx}$	P_{NG}
PC 5.2/1	841	30.3	913	34.5
Rtfn 56-1	924	34.5	1028	40.4
CMA 3	877	36.5	923	39.3
CMA 11	803	29	836	30.9
CMA 12	795	28.9	835	31.2
CMA13	828	32.8	793	30.7

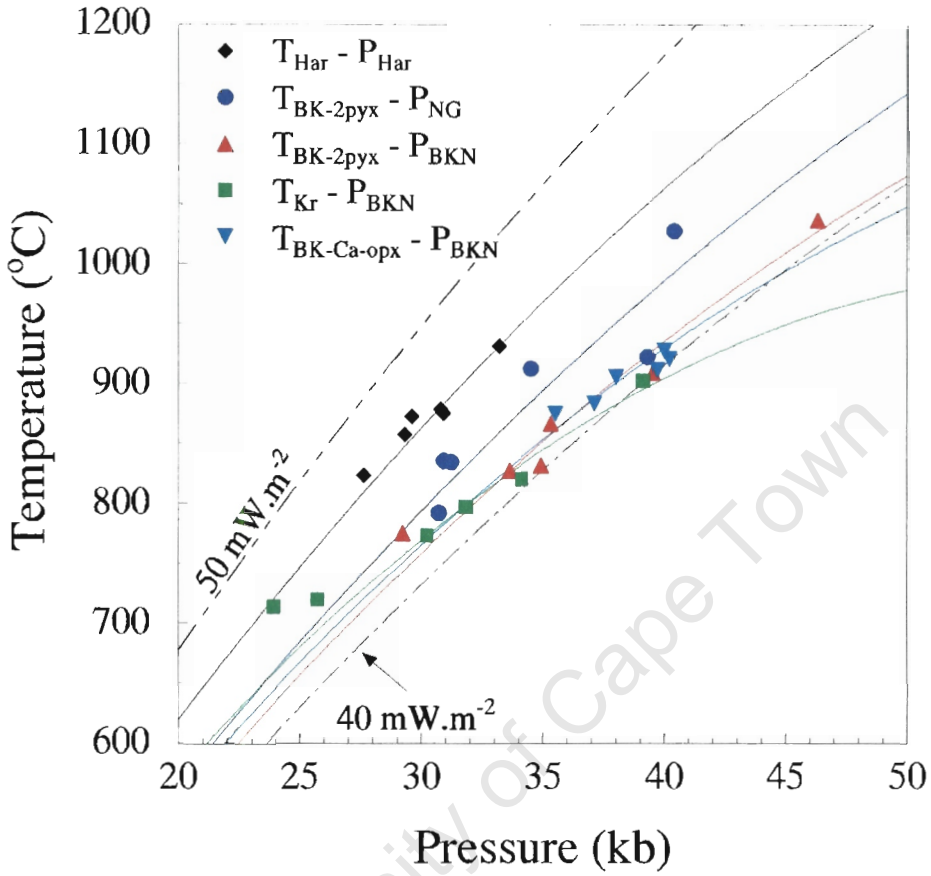

Figure 5.4 *Combined pressure and temperature estimations for the Rietfontein orthopyroxene-bearing eclogites. T_{Har} & P_{Har} - Harley (1984a,b); $T_{BK\text{-}2pyx}$ - 2 pyroxene thermometer of Brey & Köhler (1990); P_{NG} - Nickel & Green (1985); P_{BKN} - Brey & Köhler (1990); T_{KR} - Krogh (1988); $T_{BK\text{-}Ca\text{-}opx}$ - Ca-in-opx thermometer of Brey & Köhler (1990). 40 & 50 mW.m^{-2} cratonic geotherms after Pollack & Chapman (1977).*

A combination of $T_{BK\text{-}2pyx}$ - P_{BKN} results in a large spread of estimated pressures and temperatures. Temperatures range from 776 - 1037°C, a difference of 261°C, and pressures vary by 17.1 kb (from 29.2 - 46.3kb). T_{Har} - P_{Har} leads to the smallest range in pressure and temperature estimations, with temperatures falling in the range 824-932°C, and pressures from 27.6 - 33.2 kb. The use of P_{NG} with $T_{BK\text{-}2pyx}$ provides very similar results to those obtained using $T_{BK\text{-}2pyx}$ and P_{BKN}. There is a wide range in both the temperature and pressure estimations, with large differences between the minimum and maximum approximations (235°C and 9.7 kb respectively). The use of T_{Kr} with P_{BKN} yields intermediate temperatures of 714 - 903°C, and pressures of 23.9 - 39.1 kb. $T_{BK\text{-}Ca\text{-}opx}$ used in combination with P_{BKN} yields a tightly constrained range of pressures and

temperatures, 35.5-40.2kb and 875-921 °C respectively. These pressure and temperature ranges are illustrated in *Figure 5.4*, together with approximate geotherms. These geotherms will be discussed and interpreted in *Chapter 6*. These pressure results indicate that the Rietfontein eclogites originate from depths of between 80 and 140km, and thus represent a large stratigraphic mantle range of almost 50km.

5.6 Discussion

One of the most important aspects to be considered when reporting and discussing equilibration conditions in eclogites is the amount of error associated with the calculation of pressure and temperature. Uncertainties in reported equilibration temperatures and pressures will occur as a direct result of errors associated with the microprobe analyses of major elements in the relevant minerals, *i.e.* garnet, clinopyroxene and orthopyroxene. The 1σ errors on microprobe garnet and clinopyroxene analyses are reported in *Table I.1*, *Appendix I.* Accounting for these errors within the T_{EG} formula produced varying results. Sample Rtfn 57.2, which contains clinopyroxene with a low percentage of FeO (1.4 wt%) yielded temperatures 20° higher and 18° lower than the uncorrected equilibration temperature. Sample CMA 3, which contains clinopyroxene with a high percentage of FeO (4.15 wt%) yielded temperatures within 7° of the uncorrected equilibration temperature reported in *Table 5.1.* It can thus be seen that the microprobe errors do not significantly affect the calculated equilibration temperatures and, as such, the presented data may be considered accurate.

In *Section 5.5.1*, it was reported that garnet-clinopyroxene temperatures for the Rietfontein eclogites fell within the range 733 - 1012°C, using T_{EG} and T_{Kr}. *Figure 5.5* compares the equilibration temperatures of the Rietfontein eclogites (*a*) with temperatures from the Cape Province off-craton eclogites (*b*), and on-craton localities Bellsbank (*c*), Udachnaya (*d*), Roberts Victor (*e* & *f*) and Kaalvallei (*g* & *h*). For all localities, temperatures were calculated using T_{EG} at an assumed pressure of 30kb. The range of temperatures, and temperature distribution of the Rietfontein eclogites is very similar to that of the Cape Province off-craton eclogites of Robey (1981). Both exhibit temperature distribution maximums between 900 and 950°C, but the Cape Province eclogites extend to lower equilibration temperatures (755°C) than the Rietfontein eclogites. The Bellsbank eclogites (*c*) have a restricted temperature range (although this may be

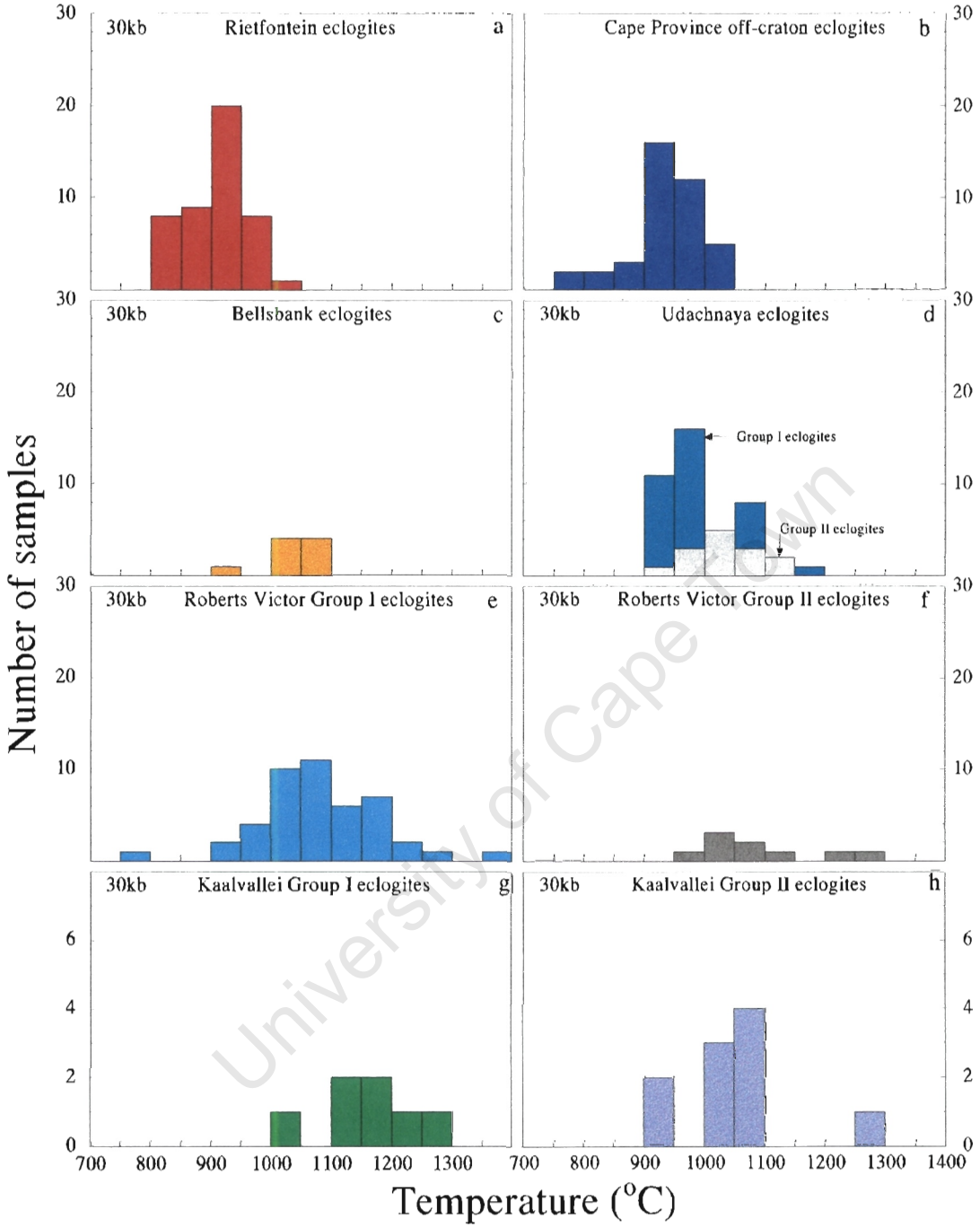

Figure 5.5 *Comparative histograms of equilibration for temperatures from off-craton, and a variety of on-craton eclogite localities. All temperatures calculated using Ellis & Green (1979), at an assumed pressure of 30kb. Literature data from Robey (1981); MacGregor & Manton (1986); Viljoen (1994, 1995); Jacob et al. (1994); Sobolev et al. (1994); Snyder et al. (1997)*

due to a restricted number of temperature determinations), with most temperatures ranging from 1000-1100°C. On-craton Russian eclogites, represented by Udachnaya (*d*), extend to higher temperatures than the South African off-craton eclogites and most temperatures fall between 950-1000°C. Roberts Victor eclogites (*e* & *f*) show the largest temperature distribution, from 770-1363°C, at 30kb, although the majority of temperatures range from 1050-1100°C. Eclogites from Kaalvallei also exhibit a wide temperature range, with a maximum temperature distribution from 1050-1100°C. *Figure 5.5* illustrates the greater range of equilibration temperatures and higher average temperatures of on-craton eclogites, when compared to Rietfontein. There are however, marked similarities between the Rietfontein and Cape Province off-craton eclogites, based on equilibration temperatures, and the distribution thereof. This marks the first characteristic of the Rietfontein eclogites that is most similar to other off-craton eclogites, rather than on-craton eclogites.

Griffin & O'Reilly (1986) suggest that xenoliths from east Australia which have equilibration temperatures less than 850°C may be regarded as crustal xenoliths. A number of Rietfontein eclogites have equilibration temperatures less than this, but, if these were crustal xenoliths, there should be petrographical and chemical differences between these eclogites and those which are likely to be mantle-derived. However, no such differences are observed, and it is thus likely that the Rietfontein eclogites are all mantle-derived.

Whereas equilibrium pressures can be calculated directly for the orthopyroxene-bearing eclogites, it is only possible to infer pressures and depths of origin for the bimineralic and kyanite eclogites from Rietfontein. When one considers temperatures calculated using T_{Kr}, at an assumed pressure of 30kb, bimineralic eclogites show temperatures between 733-929°C, orthopyroxene-bearing eclogites between 735-866°C, and kyanite eclogites between 860-1000°C. Whereas the orthopyroxene-bearing eclogites exhibit the lowest temperatures expressed by the Rietfontein eclogites, and can thus be used to infer the shallowest level of derivation of the eclogites, the bimineralic and, most notably, the kyanite eclogites extend to far higher temperatures of equilibration. The maximum pressure expressed by the orthopyroxene-bearing eclogites would thus not be the maximum depth of origin of the Rietfontein eclogites and on the basis of equilibration, the kyanite eclogites represent the deepest mantle sampled by the Rietfontein

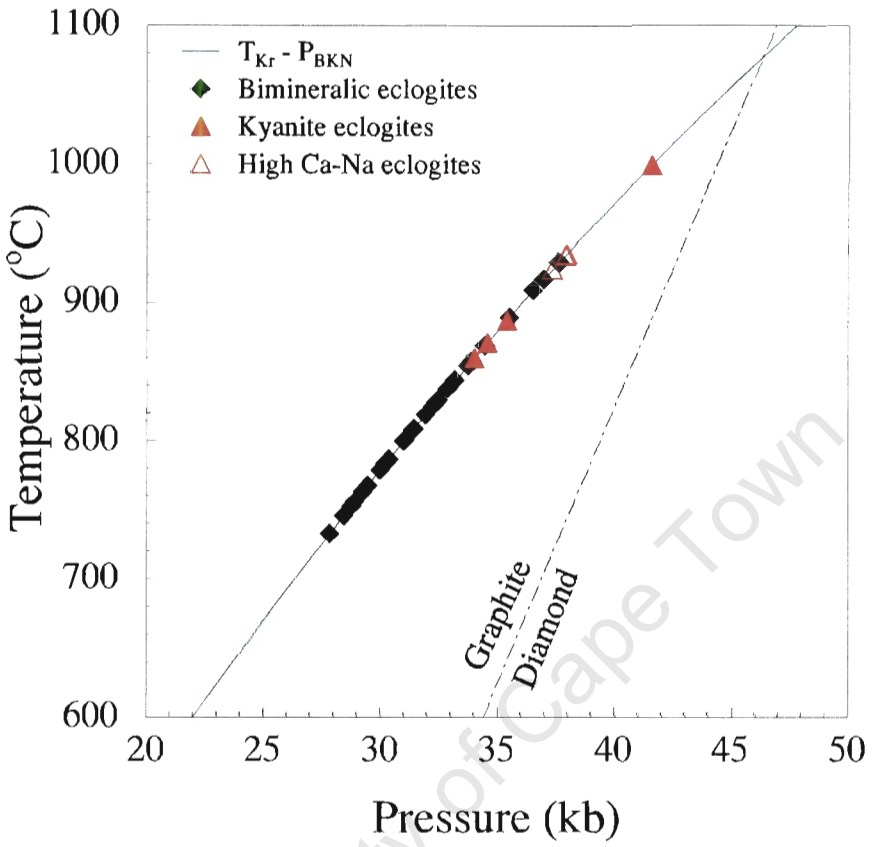

Figure 5.6 *T_{Kr} temperature estimations for the Rietfontein bimineralic and kyanite eclogites extrapolated on the T_{Kr}-P_{BKN} geotherm obtained from the orthopyroxene-bearing eclogites, in order to estimate equilibration pressures. Diamond-graphite boundary after Kennedy & Kennedy (1976).*

kimberlite. By using an approximate geotherm, calculated using T_{Kr}, in combination with the P_{BKN} pressures of the orthopyroxene-bearing eclogites, it is possible to obtain approximate equilibration pressures for the bimineralic and kyanite eclogites. Extrapolation of T_{Kr} temperatures for the bimineralic and kyanite-bearing eclogites onto this geotherm results in pressures of approximately 28-42kb, or depths of 84-126km (*Figure 5.6*). The higher temperatures of the kyanite and some bimineralic eclogites can be used to infer either higher geothermal gradients at the time of equilibration, or greater depths of origin. The higher equilibration pressures for the kyanite eclogites with regards to most of the bimineralic eclogites are clearly visible in *Figure 5.6*, and these higher pressures could be taken as further confirmation that the Rietfontein eclogites are indeed mantle-derived. The maximum pressure for any

Rietfontein eclogite yields a depth of origin of approximately 140km and this would thus represent the minimum depth from which the Rietfontein kimberlite could be derived.

Temperatures and pressures of equilibration of the Rietfontein eclogites thus indicate that they are mantle derived, having originated at depths of between 80-140km and representing a significant range in mantle stratigraphy of 40-50km. Pressure estimates suggest that the lithosphere under Rietfontein extends to depths of at least 140km, but probably deeper, and 140km would thus be the minimum depth sampled by the Rietfontein kimberlite. Ranges of equilibration temperatures are similar for all three eclogite groups, although the kyanite eclogites do show higher average temperatures, implying a deeper mantle origin.

6. THERMAL STRUCTURE OF THE RIETFONTEIN LITHOSPHERE

6.1 Introduction

6.1.1 Heat flow

The thermal structure of the lithosphere may be deduced in a number of ways. Conductive heat flow measurements may be used to construct geotherms for particular parts of the lithosphere, and these geotherms can then be used to infer thermal differences within the structure of the lithosphere, together with proposed lithosphere-asthenosphere boundaries. A second method of geotherm construction involves the determination of pressure-temperature equilibration points on suites of mantle derived xenoliths. Xenoliths may be used to map the thermal structure of the upper mantle at the time of kimberlite intrusion and reconstruct the petrological, rheological and chemical characteristics of a region. Boyd (1973) studied garnet lherzolite samples from Lesotho kimberlite pipes, and interpreted that the pressure-temperature points for these lherzolites form a trend defining a fossil geotherm. Thermal conductivity is controlled by a number of factors such as composition, temperature and pressure effects (Chapman, 1986). Furthermore, a number of differences can be noted between heat flow measurements from on- and off-craton areas. Ballard *et al.* (1987) noted that from 12 sites within the Archaean Kaapvaal-Zimbabwe Craton and Limpopo Belt, the average heat flow was 47±4 $mW.m^{-2}$ and that a trend of increasing heat flow, from less than 40 $mW.m^{-2}$ within the cratonic nucleus to almost 60 $mW.m^{-2}$ at the edges, existed. Proterozoic and Pan African mobile belts surrounding the craton yield a mean of 66±3 $mW.m^{-2}$, increasing from approximately 60 $mW.m^{-2}$ at the cratonic margin to more than 70 $mW.m^{-2}$ several hundred kilometres away. Heat flow also differs between the western and eastern margins of the Kaapvaal Craton, and measurements of 38±7 $mW.m^{-2}$ and 53±4 $mW.m^{-2}$ have been recorded, and the average heat flow in the Namaqua-Natal Belt (just south of Rietfontein) is 61±10 $mW.m^{-2}$ (Smith, 1999).

A number of suggestions have been proposed to account for the heat flow differences between stable Archaean cratons and Proterozoic mobile belts. Nyblade & Pollack (1993) noted a widespread global spatial pattern between heat flow and the proximity of Archaean cratons.

They suggested that the presence of a thicker lithosphere beneath the craton impedes the flow of mantle heat through the craton, forcing more deep mantle heat to escape through the thinner mobile belt lithosphere. A second suggestion is that the heat flow is not dependent on the thickness of the lithosphere, and is instead due to lower crustal heat production in cratonic areas (Lenardic, 1997). The elevated geotherms of young fold belts and rift zones relative to cratons implies large lateral variations in temperatures at the base of the crust, and thus in the relative stability of eclogite and granulite mineral assemblages (Griffin *et al.*, 1990).

6.1.2 Geotherms

The reconstruction of geotherms using thermobarometric data from xenoliths was first attempted by Boyd (1973), who found that coarse, "cold" peridotites from Lesotho defined a shallower geotherm than the sheared, "hot" peridotites. Such "inflected" geotherms have since been noted from a number of localities, including off-craton areas such as the Gibeon kimberlite province in Namibia (Franz *et al.*, 1996*a* & *b*), where the low-temperature peridotites are interpreted to represent cool, non-convecting lithospheric mantle (Pearson *et al.*, 1994*a*). The high temperature xenoliths have been interpreted to represent thermal anomalies caused by convective movements in the lithosphere, with eruptions originating at the base of the lithosphere, or they may have formed in contact aureoles enveloping magma chambers within the lithosphere (Boyd & Gurney, 1986). The transition from cold to hot peridotites, and the subsequent expression in the form of an inflected geotherm, is interpreted to represent the position of the lithosphere-asthenosphere boundary at the time of kimberlite eruption (Boyd & Gurney, 1986). The depth to this transition is seen to vary from within the craton to off-craton regions. MacGregor (1975) notes that the depth to the top of the low velocity (asthenospheric) zone varies, from 140km in Namibia, 180km in Lesotho to 195km under the Kimberley region, interpreted as delineating a root for the Kaapvaal Craton (Boyd & Gurney, 1986). Pressure-temperature conditions of Namibian peridotites indicate thermal gradients of 44-50 $mW.m^{-2}$, lower than those of the adjacent Kaapvaal Craton (Franz *et al.*, 1996a). Temperatures at the root of the Kaapvaal Craton in Archaean time were near those calculated for a present-day shield geotherm (Pollack & Chapman, 1977), which, given the greater radioactive heat production in the Archaean, is surprising (Boyd & Gurney, 1986). The similarity of xenolith and diamond inclusion equilibrium conditions with shield geotherms indicates that the xenolith pressure-

temperature conditions were ambient, having changed little in 3Ga (Boyd, 1985). Crustal and mantle ages across southern Africa correspond to each other, demonstrating long term crust-mantle coupling and indicating a stable mechanical boundary layer down to 200km beneath cratons (Pearson *et al.*, 1994*a*).

6.2 Aims

Rietfontein is a known off-craton kimberlite and geothermobarometric information derived from its eclogite suite can be used to attempt to further understand the differences in heat flow between Archaean cratons and post-Archaean mobile belts. Due to the known differences in heat flow, and thus geotherms between on- and off-craton localities, it may also be possible to confirm Rietfontein as an off-craton locality, and draw further comparisons between these eclogites and other on- and off-craton xenoliths. Heat-flow has been estimated for the mobile belts surrounding Rietfontein (Jones, 1999), although so far, no geotherms have been calculated for Rietfontein itself, due to the lack of previous studies on this eclogite suite. This chapter thus aims to use pressures and temperatures of equilibration of the Rietfontein orthopyroxene-bearing eclogites to estimate a geotherm for the area. Similarities and differences will be noted between the Rietfontein geotherm and geotherms from other on- or off-craton localities, and a heat flow estimate will be presented.

6.3 Results

Figure 6.1 illustrates the positions in pressure-temperature space of the orthopyroxene-bearing Rietfontein eclogites, according to a number of combined geothermometer and geobarometer calibrations (discussed in *Chapter5*). *Figure 6.1a* plots temperatures according to the Brey & Köhler (1990) 2-pyroxene thermometer (T_{BK}) and Al-in-opx barometer (P_{BKN}), whilst *Figure 6.1b* illustrates T_{BK} plotted with pressures calculated using the Nickel & Green (1985) barometer (P_{NG}). In *Figure 6.1c*, garnet-clinopyroxene temperatures of Krogh (1988) (T_{Kr}) are plotted with pressures calculated according to P_{BKN}, and temperatures and pressures calculated using the Harley (1984*a* & *b*) geothermobarometer (T_{Har} - P_{Har}) are plotted in *Figure 6.1d*. In total, three geothermometers are used, together with three geobarometers, and explanations as to the use of these can be found in *Chapter 5*.

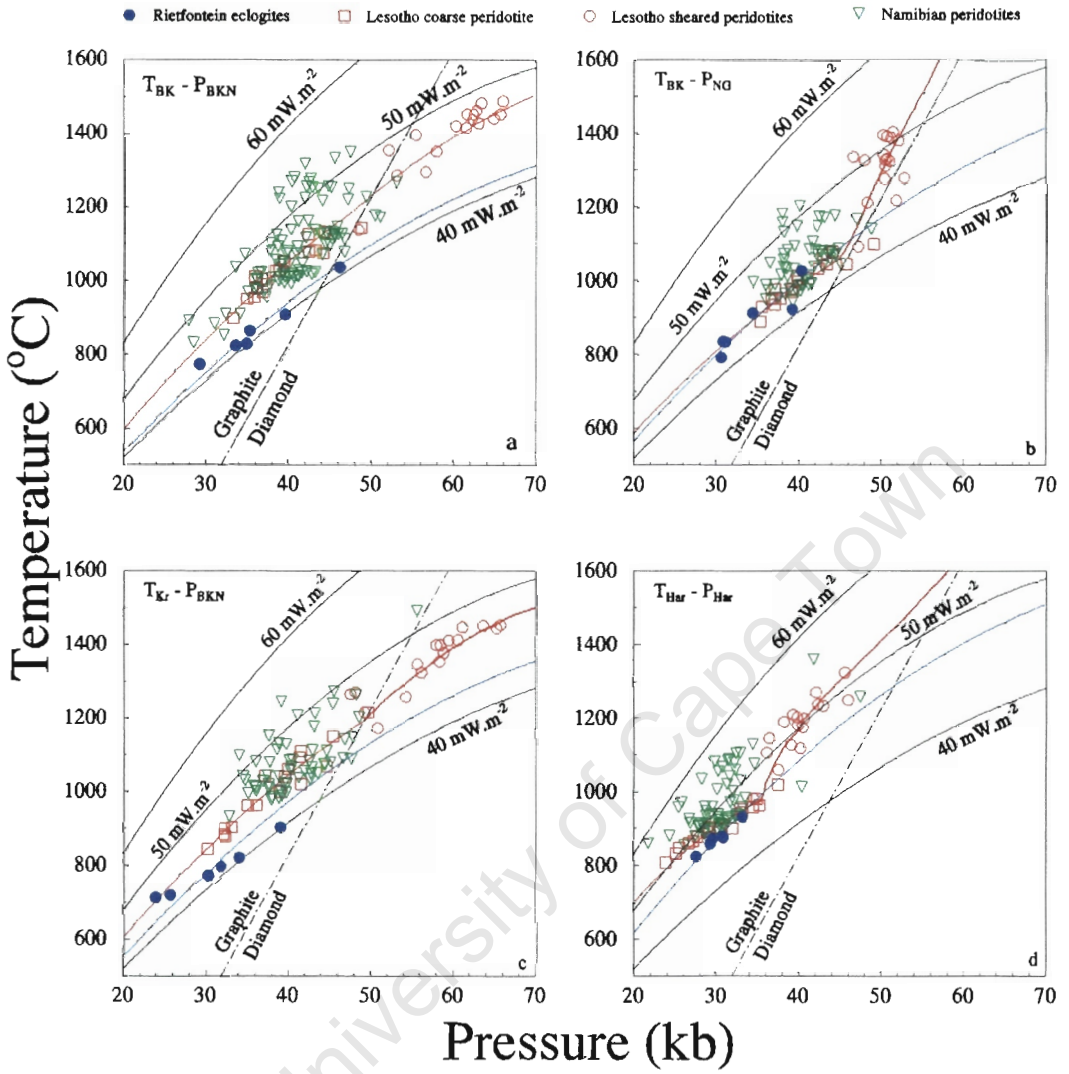

Figure 6.1 *Approximate geotherms for the Rietfontein eclogites through pressure temperature points calculated using a) Brey & Köhler's (1990) 2-pyx thermometer and Al-in-opx barometer, b) Brey & Köhler's (1990) 2-pyx thermometer and Nickel & Green's (1985) Al-in-opx barometer, c) Krogh's (1988) gt-cpx thermometer and Brey & Köhler's (1990) Al-in-opx barometer and d) Harley's (1984a & b) thermobarometer. Lesotho data from Nixon & Boyd (1973); Bloomer & Nixon (1973); Whitelock (1973); Rolfe (1973); Cox et al. (1973). Namibia data from Mitchell (1984); Bell & Rossman (1992); Franz et al. (1996a & b); Bell (unpublished data). Continental geotherms after Pollack & Chapman (1977) and diamond-graphite boundary after Kennedy & Kennedy (1976).*

Figure 6.1 illustrates that all thermobarometric calibrations, with the exception of T_{Har} - P_{Har}, result in pressure-temperature approximations for the Rietfontein eclogites that plot on, or very close to the 40 $mW.m^{-2}$ continental geotherm of Pollack & Chapman (1977). *Figure 6.1d* (T_{Har} - P_{Har}) shows the Lesotho coarse peridotite geotherm intersecting the 50 $mW.m^{-2}$ geotherm, and the Namibian peridotites plotting very close to the 60 $mW.m^{-2}$ geotherm, higher than geotherms approximated using other thermobarometers. It can be seen that in *Figure 6.1d*, both the peridotite and eclogite temperatures, and hence the geotherms, are displaced to higher values than those obtained using other geothermobarometers. This could be due to the pressure dependence of the garnet-orthopyroxene thermometer, or the general dependence of Fe-Mg thermometers on ferric iron (*Chapter5*). Non-equilibration between garnet and pyroxenes may also lead to anomalously high temperatures. The Lesotho geotherm according to T_{Har} - P_{Har} estimates much higher heat flow than that measured on the Kaapvaal Craton, indicating that it may be erroneous to approximate heat flow for Rietfontein based on T_{Har} - P_{Har} measurements.

The inflected geotherm of the Lesotho peridotites is visible on the diagrams, with the sheared peridotites illustrating a steeper sloped geotherm than the coarse peridotites. All the Rietfontein eclogites, and most of the Namibian peridotites plot within the geothermal area indicated by the Lesotho coarse peridotites. A small amount of overlap occurs between the higher temperature Namibian peridotites, and the Lesotho sheared peridotites, which may indicate that some of the Namibian peridotites originate close to the lithosphere-asthenosphere transitional zone. Whereas the Lesotho coarse peridotites define a well-constrained trend on a P-T diagram and can be used to define geotherms of approximately 45±2 $mW.m^{-2}$, the Namibian peridotites show considerable scatter, and cannot be used to plot a single accurate geotherm. Rather, these peridotites plot between geotherms representing heat flow of 42 and 55 $mW.m^{-2}$ (*Figure 6.1a-c*). The similarity in geotherms between Rietfontein and the Lesotho peridotites is clearly illustrated in *Figure 6.1.* The Rietfontein orthopyroxene eclogites can be used to define a geotherm of approximately 43±2 $mW.m^{-2}$. This heat flow approximation is most similar to the approximations of the Lesotho peridotites than it is to the Namibian peridotites. A relatively tightly constrained set of temperatures and pressures are exhibited by the Rietfontein eclogites, compared to the peridotite ranges, indicating sampling of a smaller range of mantle stratigraphy. It should however be noted

that the peridotite data takes a number of localities into account, whereas Rietfontein is a single locality.

6.3 Discussion

Although Rietfontein is an off-craton locality, the heat-flow and thermal structure of the lithosphere beneath Rietfontein shows greater similarity to that observed at localities found within the Kaapvaal Craton, than it does to off-craton localities. An estimate of heat flow in the Rietfontein area, according to *Figure 6.1a-c*, would be approximately 41-45 $mW.m^{-2}$. Harley's (1984*a* & *b*) thermobarometer leads to a slightly higher heat flow estimation of approximately 46 $mW.m^{-2}$. These approximate geotherms contrast sharply with the measured heat flow around the Rietfontein area, which averages 61±10 $mW.m^{-2}$ in the Namaqua-Natal belt, and 63±6 $mW.m^{-2}$ in the Ghanzi-Chobe belt (Jones, 1999). Heat flow approximated by geotherms in Namibia give a range of values. Peridotites from Louwrensia indicate a geotherm close to 44 $mW.m^{-2}$ (Pearson *et al.*, 1995) and Anis Kubub peridotites yield geotherms of 44-50 $mW.m^{-2}$ (Franz *et al.*, 1996*a*). These are all slightly higher than the accepted Kaapvaal Craton estimates of ≤42 $mW.m^{-2}$ (Rudnick *et al.*, 1997). Despite being located in a post-Archaean belt, in which higher heat flow is common (Rudnick *et al.*, 1997), Rietfontein seems to exhibit a heat flow more similar to that observed within the margins of the Kaapvaal Craton.

These studies show that whereas there is a general increase in heat flow from on- to off-craton areas, heat flow in off-craton areas is not always as high as reported averages for Proterozoic mobile belts. Franz *et al.* (1996*b*) attempted to account for this by suggesting that parts of old cratonic lithosphere may still be present beneath Namibia, forming a wedge shaped continuation of the Kaapvaal Craton towards the west, or as a set of small lithospheric slices. During hotspot activity and upwelling of the asthenosphere, parts of this cratonic mantle could have been strongly deformed and finally erupted within the kimberlites (Franz *et al.*, 1996*b*). If such a process could account for the decreased heat flow under Namibia, it could most certainly account for the depressed heat flow at Rietfontein, which is closer to the Kaapvaal Craton than the Gibeon kimberlite province of Namibia.

The progression of coarse to sheared peridotites is believed to mark the transition from lithosphere to asthenosphere within the mantle (Boyd & Gurney, 1986). All of the Rietfontein orthopyroxene-bearing eclogites plot close to the lower, coarse peridotite limb of the Lesotho peridotite geotherm, suggesting that the eclogites are derived from the middle to lower layers of the lithosphere, rather than the upper asthenosphere. However, the geotherm of the Rietfontein eclogites indicates an unequivocal mantle origin, rather than a crustal origin. Geothermal gradients of 44-50 $mW.m^{-2}$ in the Gibeon area of Namibia imply that the lithospheric thickness in this area does not exceed 160km (Franz *et al.*, 1996*a*). Considering the maximum depth estimate of the Rietfontein eclogites, approximately 140km, and the geothermal gradient of 41-45 $mW.m^{-2}$, the lithospheric thickness around Rietfontein is probably similarly 160km, a suggestion corroborated by many xenolithic suites (Boyd *et al.*, 1985). The absence of an inflected geotherm around Rietfontein may be due either to a limited suite of samples, or it could imply that the convective asthenospheric movements which affected other mantle areas were not operative in the Rietfontein area. The similarity of the Rietfontein eclogite geotherms to those constructed using present day heat measurements (Pollack & Chapman, 1977) indicates a lithosphere which has been relatively stable, remaining unmixed and having been sustained by mantle convection processes (Basu *et al.*, 1986).

Thus, the lithosphere which was sampled by the Rietfontein kimberlite had relatively low heat flow, more similar to that of the Kaapvaal Craton than other Proterozoic mobile belts. The eclogites all have similar equilibration pressures and temperatures to coarse Lesotho peridotites and their position on the lower limb of the inflected geotherm indicates derivation from lithospheric source regions. The similarity of the mantle geotherm from Rietfontein to current shield geotherms indicates a lithosphere that has remained stable for millions of years.

7. TRACE ELEMENT MINERAL CHEMISTRY

Abbreviations used throughout this chapter are as follows:
REE - Rare earth elements
LREE - Light rare earth elements (La - Nd)
MREE - Middle rare earth elements (Sm - Tb)
HREE - Heavy rare earth elements (Ho - Yb)
D_i - clinopyroxene/garnet partitioning coefficient for element i
D_{i*} - molar clinopyroxene/garnet partition coefficient for element i
P-T-X - pressure - temperature - composition

7.1 Introduction

Trace elements are present in rocks in quantities of less than 0.1% and have important applications in petrogenetic studies. Rare earth elements (REE) are geochemically very similar and their abundances in upper mantle rocks can provide a record of upper mantle processes such as melting, metasomatism and melt segregation. They are also useful in defining compositional heterogeneity in the upper mantle (McDonough & Frey, 1989). As such, an investigation into the trace element abundances of garnet and clinopyroxene from the Rietfontein eclogites can assist in answering a number of pertinent questions.

Distinct REE characteristics have been identified for different the eclogite groups. Group A eclogites contain LREE enriched clinopyroxenes, Group B eclogites contain extremely LREE depleted and HREE enriched garnets and Group C eclogitic minerals typically display positive Eu anomalies and low overall REE abundances (Taylor & Neal, 1989). It has also been noted that in the case of Siberian eclogites, those containing exsolved garnet have no prominent Eu anomalies and have steeper positive REE slopes than eclogites without exsolved garnets (Jerde *et al.*, 1993*b*). A comparison of the trace element abundances and REE patterns of the Rietfontein eclogites with eclogitic minerals from on- and off-craton localities will further establish any similarities between eclogites from the two settings. It has already been ascertained (*Chapter 4*) that the major element mineral compositions of the kyanite eclogites are significantly different to those of the other eclogites. It is important to consider whether these differences extend to the trace element abundances. The partitioning of trace elements between mantle phases can often affect the abundances of elements within these phases and an investigation into the partitioning

of elements within the eclogites will determine the main controls on partitioning in this area – whether it be temperature or composition controlled.

In addition, the fractionation of REE relative to each other can be used to determine the geneses of rock suites. As such, REE concentrations have been used over the years to substantiate theories on eclogite petrogenesis (*eg.* Shervais *et al.*, 1988; Taylor &Neal, 1989; Smyth *et al.*, 1989). Jagoutz *et al.* (1984) use low HREE contents and positive Eu anomalies to argue against a MORB-type basalt derivation for their "Type A" eclogites. Smyth *et al.* (1989) believe that positive Eu anomalies in eclogites can be accounted for by accumulation in a magma chamber at high pressure, whereas other authors (*eg.* Shervais *et al*, 1988; Taylor & Neal, 1989; Neal *et al.*, 1990; Jerde *et al.*, 1993; Taylor & Neal, 1993; Snyder *et al.*, 1997) believe the REE abundances and positive Eu anomalies of some eclogites are consistent with the subduction and metamorphism of oceanic crust. Therefore a secure knowledge of REE patterns in eclogitic minerals can contribute to a better understanding of the origin of eclogites and assist in identifying possible protoliths.

Indirect approaches to determining trace element compositions of mantle rocks may lead to a number of problems. Trace elements are often normalised using chondritic meteorites but chondritic meteorites are not uniform in composition and the Earth has non-chondritic abundances of volatile elements (Frey, 1984). Trace element studies on eclogites should also consider the possibility of REE mobility during metamorphic processes. REE analysis of mineral separates is the most reliable method for determining upper mantle REE abundances as kimberlitic inclusions often contain late-stage alteration minerals (Frey, 1984). Mineral grains selected for trace element analyses should be inclusion- and crack-free and unaltered to avoid possible contamination by common mantle processes such as alteration and metasomatism.

7.2 Methods

Trace elements abundances of garnets and clinopyroxenes from the Rietfontein eclogites were analysed at UCT using the Perkin Elmer Elan 6000 Inductively Coupled Plasma - Mass Spectrometer, coupled to a CETAC LSX-200 UV laser. Details of this analytical technique, together with 1σ errors and detection limits may be found in *Appendix I.* Of the 49 samples

retrieved from the Rietfontein kimberlite, 20 were selected for a more detailed trace element study. These 20 samples are representative of the three eclogite groups found at Rietfontein (bimineralic, orthopyroxene-bearing and kyanite eclogites) and cover the full chemical compositional range exhibited by the eclogites. Two garnet and two clinopyroxene grains were analysed from each eclogite sample, with replicate (2-4) analyses being performed on each grain. The analyses for each sample were then averaged out to give one garnet and one clinopyroxene trace element value for each sample. For the purposes of REE diagrams, ppm values were chondrite normalised using the C1 chondrite values of Sun & McDonough (1989).

7.3 Garnet trace element chemistry

7.3.1 Sc, Ni, Sr, Y, Zr abundances

Sc is one of the most variable trace elements found in garnets of the Rietfontein eclogites, with concentrations of 17.2-157 ppm being measured. Zr and Sr also show strong variations (2.24-23.5 ppm and 0.079-3.51 ppm, respectively), whereas Ni and Y concentrations are fairly well constrained (14.2-40.8 ppm and 8.26-26.9 ppm, respectively) (*Table 7.1*). As is the case with major element mineral compositions (*Chapter 4*), marked differences may be observed between the kyanite and bimineralic/orthopyroxene-bearing eclogites. *Figure 7.1* illustrates some of the trends and groups within the eclogites which can be identified using trace element compositions.

It was mentioned previously that the garnets of the kyanite eclogite group have lower Mg #'s than garnets of the bimineralic and orthopyroxene-bearing eclogites (*Chapter 4*), and this is clearly seen on the trace element - Mg# diagrams of *Figure 7.1a-d, h*. On a plot of Ni vs Mg# (*Figure 7.1a*), the Rietfontein eclogite groups can be separated only on the basis of Mg#, the Ni abundances in garnets of all groups are similar. Sc abundances in many of the bimineralic and orthopyroxene-bearing eclogites are similar to those exhibited by the kyanite eclogites *(Figure 7.1b*), although 7 samples show slightly elevated (> 60 ppm) Sc contents. The high-Ca garnets of the kyanite eclogites have Sr abundances much greater than those of garnets from the other Rietfontein groups (*Figure 7.1c*). These kyanite eclogites form a distinct array at higher Sr and lower Mg#'s on this diagram and a broad trend of decreasing Sr with decreasing Mg# can be identified. This trend is however, based on the position of sample CMA 4, and without it, the

Table 7.1 *Representative trace element analyses for garnet and clinopyroxene grains from the Rietfontein eclogites. Concentrations reported in ppm. La/Yb ratios chondrite normalised after Sun & McDonough (1989). n.d. = not detected*

Eclogite type	Bimineralic eclogites			Kyanite eclogites		Opx-bearing eclogites	
Garnet	**CMA 1**	**CMA 8**	**Rtfn 57.1**	**JJG 2104**	**CMA 4**	**PC 5.2/1**	**CMA 3**
Sc	157	89.8	48.7	17.2	32.5	48.5	145
Ni	24.3	23.1	24.7	28.1	39.5	40.8	21.2
Sr	0.65	0.46	0.12	1.49	3.51	0.12	0.67
Y	18.2	11.8	10.6	8.26	13.1	11.6	17.2
Zr	3.37	19.9	4.48	2.24	5.65	4.26	6.83
La	0.009	0.020	0.003	n.d.	0.003	0.007	n.d
Ce	0.046	0.13	0.064	0.072	0.083	0.037	0.028
Nd	0.14	0.53	0.35	1.27	2.67	0.21	0.13
Sm	0.28	0.67	0.29	0.92	1.70	0.44	0.17
Eu	0.18	0.36	0.19	0.80	0.91	0.25	0.12
Gd	1.26	1.52	0.95	1.26	1.87	1.02	0.69
Dy	3.00	1.89	1.79	1.40	2.26	1.70	2.32
Er	2.09	1.28	1.27	0.95	1.51	1.29	2.32
Yb	1.83	1.18	1.23	0.84	1.98	1.40	2.57
$(La/Yb)_n$	0.0035	0.0120	0.0020		0.0011	0.0037	

Eclogite type	Bimineralic eclogites			Kyanite eclogites		Opx-bearing eclogites	
Clinopyroxene	**CMA 1**	**Rtfn 48.2**	**Rtfn 57.1**	**JJG 2104**	**Rtfn 54.4**	**CMA 12**	**PC 5.2/1**
Sc	41.3	24.4	19.2	4.57	9.76	22.0	16.4
Ni	442	324	353	419	226	293	508
Sr	26.0	417	208	138	372	241	328
Y	0.62	2.16	1.52	0.074	0.38	3.82	1.70
Zr	2.25	44.7	14.1	3.30	11.6	32.7	18.3
Nb	0.01	n.d.	1.00	0.44	n.d.	0.09	0.75
Th	0.06	n.d.	0.26	n.d.	n.d.	0.45	0.49
La	1.13	25.3	7.80	0.008	0.069	11.2	9.03
Ce	2.48	62.7	19.2	0.18	0.93	28.3	20.3
Nd	1.24	28.0	9.91	0.72	3.28	13.9	11.6
Sm	0.40	4.00	1.89	0.22	0.73	3.06	2.37
Eu	0.11	1.06	0.54	0.078	0.27	0.93	0.68
Gd	0.41	2.30	1.13	0.068	0.29	2.48	1.49
Dy	0.24	0.77	0.47	0.041	0.13	1.27	0.60
Er	0.062	0.20	0.10	0.053	0.038	0.23	0.11
Yb	0.050	0.069	0.051	0.021	0.017	0.13	0.045
$(La/Yb)_n$	16.22	263.75	109.61	0.27	2.96	60.97	144.19

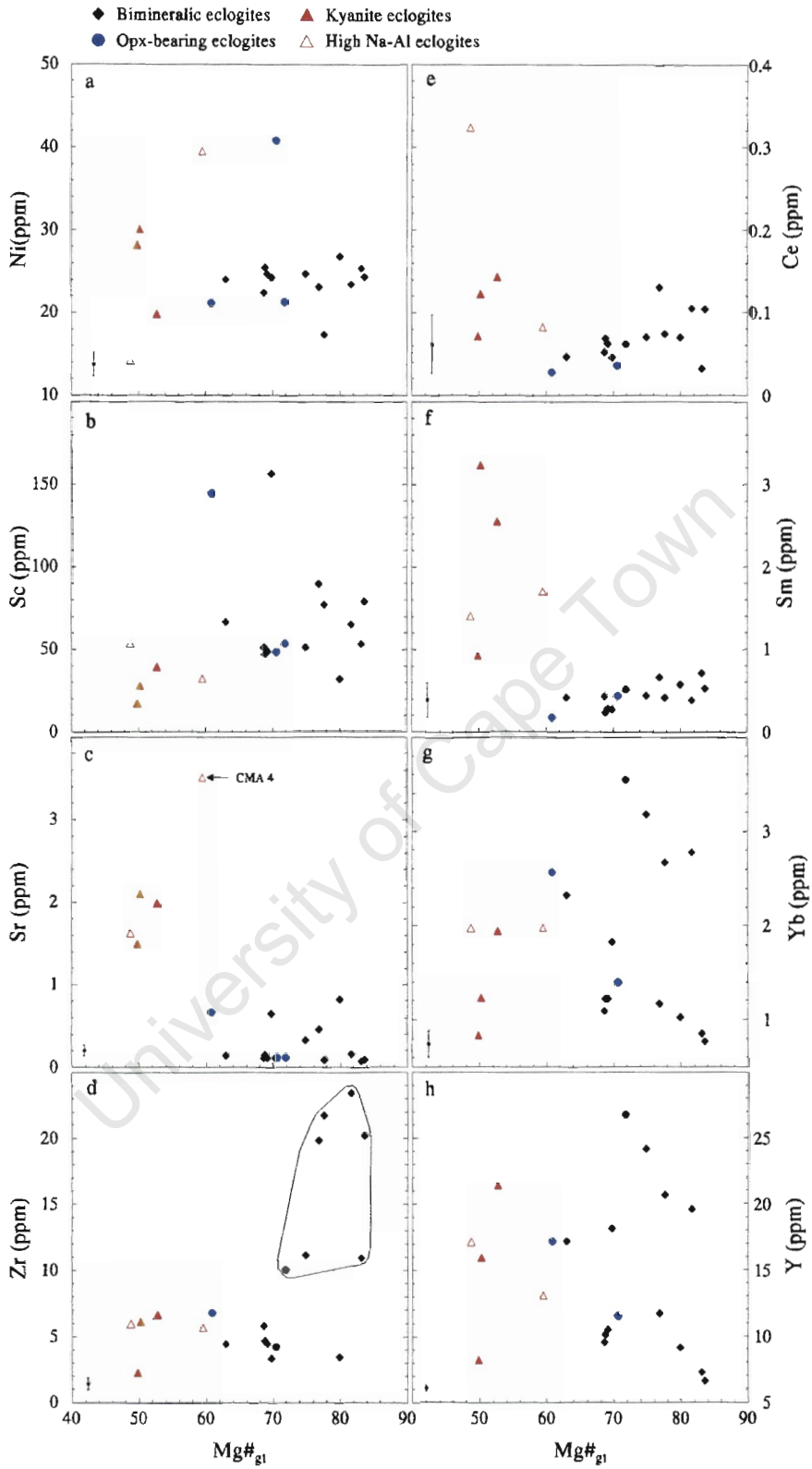

Figure 7.1 *Selected trace element abundances in garnets from the Rietfontein eclogites, plotted as a function of Mg#. All abundances reported in ppm and 1 σ error bars appear in the bottom left corner of the diagrams.*

kyanite eclogites would only form a separate group to the other eclogites. The bimineralic and orthopyroxene-bearing eclogites form a group with a wide range of Mg#'s (60-84), whose garnets all show Sr concentrations of less than 1 ppm. As with Sc in the Rietfontein garnets, similar Zr abundances occur in the kyanite and half of the bimineralic/orthopyroxene-bearing eclogites (*Figure 7.1d*). Again, a group of predominantly bimineralic eclogites exists with elevated Zr contents (> 10 ppm) and many of the elevated Zr garnets also have elevated Sc contents. No differences in Y concentrations exist between the three eclogite groups (*Figure 7.1h*).

7.3.2 REE abundances

The REE abundance variations with major element (Mg#) composition for garnets are illustrated in *Figure 7.1(e-g)*. *Figure 7.1e* illustrates the similar Ce abundances found in the three eclogite groups, and only one high Na-Al eclogite shows higher Ce concentrations (> 0.2ppm). Sm abundances (*Figure 7.1f*) in the kyanite eclogites are elevated above those of bimineralic and orthopyroxene-bearing eclogites, whereas Yb concentrations for the groups are similar , with the bimineralic and orthopyroxene-bearing eclogites exhibiting a larger range in concentration. *Figure 7.2* is a plot of Nd *vs* Zr/Y for garnets from the Rietfontein eclogites. It can be seen that whereas there is a broad positive correlation between the two for the bimineralic eclogites, the kyanite eclogites exhibit a trend of increasing Nd at fairly constant Zr/Y ratios.

Figure 7.3 illustrates REE patterns for selected bimineralic, orthopyroxene-bearing and kyanite eclogites. For the bimineralic eclogites, two subtly different trends can be observed (*Figure 7.3, top*). All samples show the LREE depletion and moderate HREE enrichment expected in garnet co-existing with clinopyroxene. The first trend is a generally smooth curvi-linear increase from the LREE, through the MREE to the HREE (CMA 1, CMA 14). However, some of the eclogites exhibit a smoothly increasing pattern from LREE to MREE, which then flattens out towards the HREE (CMA 8). A slight variation on this flattened HREE trend is exhibited by sample Rtfn 55.2, which shows a steeper light to middle REE pattern, and a slight concave-downwards pattern from Sm to Dy, which then flattens out towards Er and Yb. It is possible however, that this anomalous pattern may be due to analytical errors, and if one considers the 2σ errors associated with garnet analyses (see *Appendix I, Figure I.1a*), the actual REE pattern may be smoother than

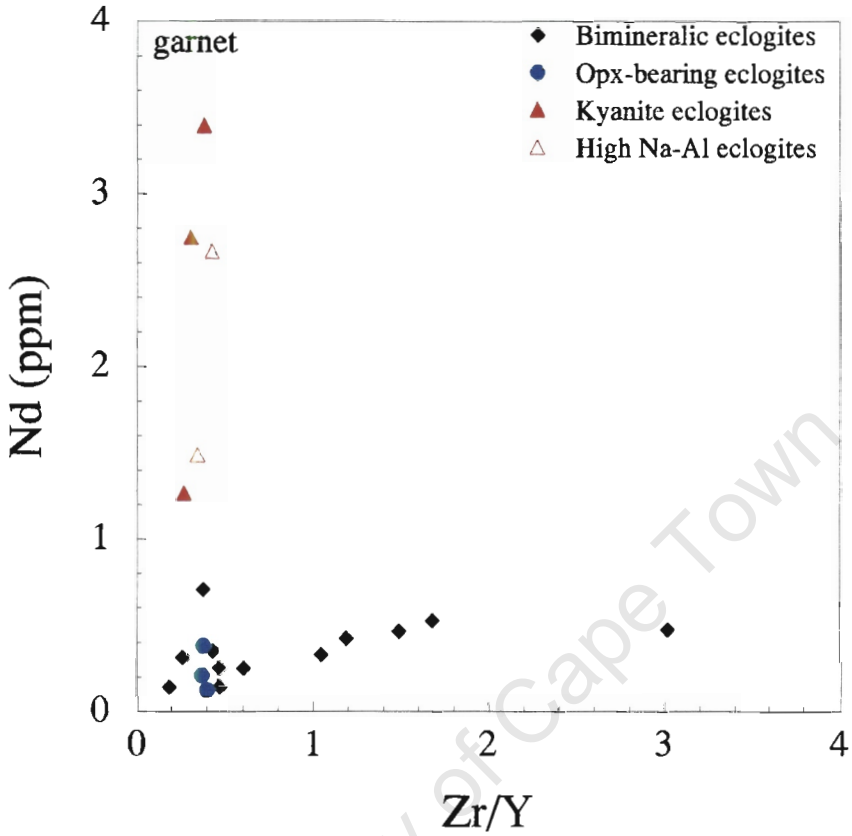

***Figure** 7.2 Nd vs Zr/Y for garnets from the Rietfontein eclogites. The higher Nd contents of the kyanite eclogites are clearly visible.*

illustrated. CMA 1 is the sample containing exsolved garnet lamellae, and it can be seen from the plots that there is no significant difference between the REE abundances of this eclogite and the abundances in the other bimineralic eclogite garnets. No significant trace element differences were noted within either the garnet lamellae themselves, or between the lamellae and the granular garnets, indicating good equilibrium within the samples.

The orthopyroxene-bearing eclogites exhibit REE trends (*Figure 7.3, middle*) almost identical to those observed in the bimineralic eclogites, with both regular curvi-linear patterns and flattened MREE to HREE patterns being observed. Garnets from the bimineralic and orthopyroxene-bearing eclogites show MREE and HREE abundances of 1-10x chondrite, with a maximum concentration of 15x chondrite being reached.

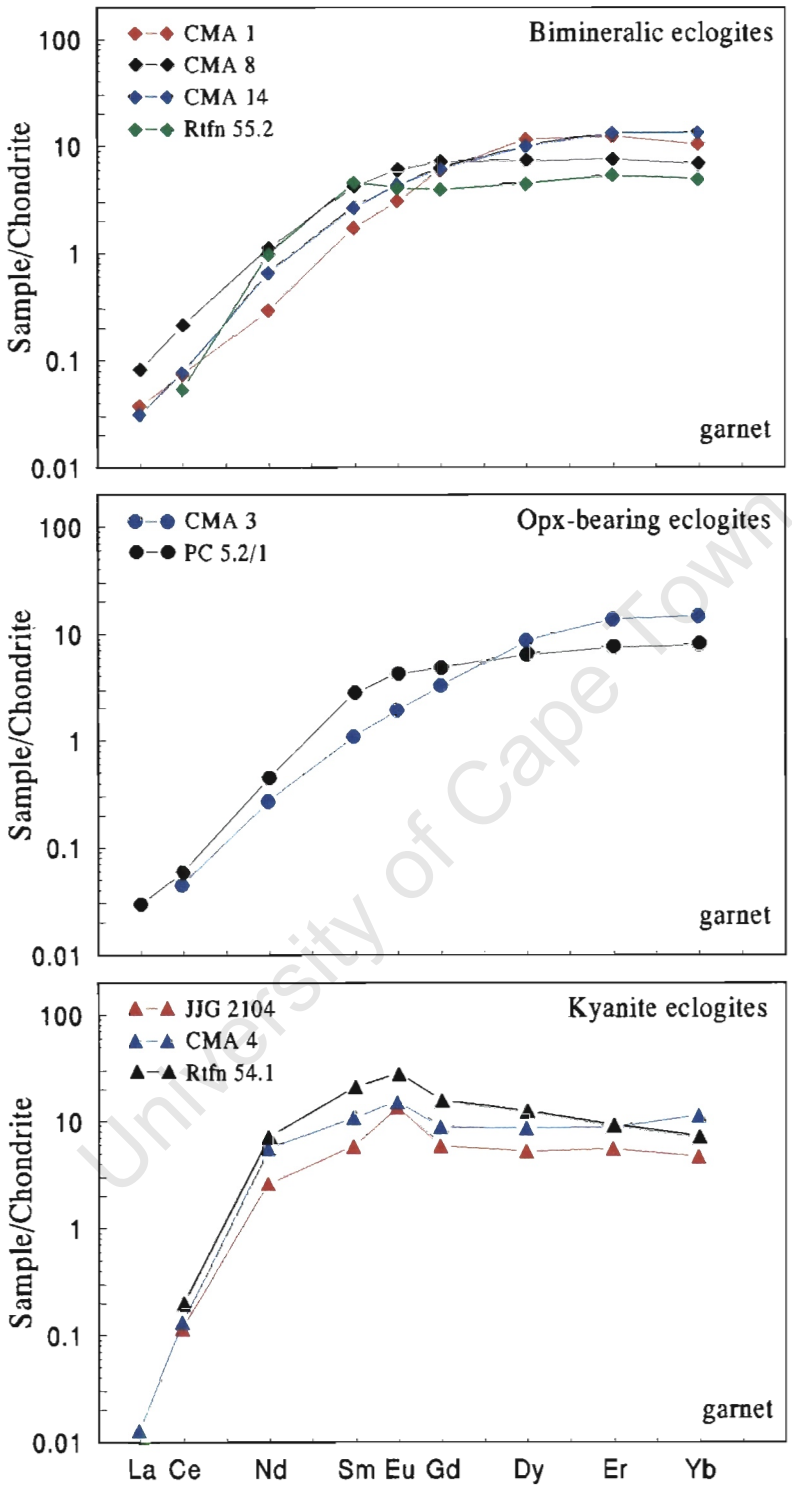

Figure 7.3 *REE diagrams for garnets from selected Rietfontein eclogites - bimineralic eclogites (top), opx-bearing eclogites (middle) and kyanite eclogites (bottom). REE abundances are chondrite normalised after Sun & McDonough (1989). 2σ error bars for REE analyses are illustrated in Appendix I, Figure I.1.*

The kyanite eclogites exhibit vastly different REE patterns to the other samples (*Figure 7.3, bottom*). Garnets from these eclogites are strongly depleted in LREE, and show an overall convex-upwards pattern over the range of LREE to HREE. However HREE in these garnets are depleted *relative* to the MREE, and have concentrations of 5-10x chondritic values. The MREE are 5-30x more enriched than chondrites. Positive Eu anomalies are also present in most of the kyanite eclogites, some more pronounced than others (*eg.* JJG 2104). Overall, the MREE (Sm, Eu & Gd) are more enriched in the kyanite eclogites, than in the bimineralic or orthopyroxene bearing eclogites. Garnets in all samples were homogeneous, with no significant intra- or inter-grain variations.

7.4 Clinopyroxene trace element chemistry

7.4.1 Sc, Ni, Sr, Y, Zr abundances

Sr within the Rietfontein clinopyroxenes is very variable, with a factor of 16 variation being noted (26 - 417 ppm). Ni also shows a small amount of variation (149-508 ppm), whereas Sc shows more variation (4.5 - 47.7 ppm). Zr exhibits the most trace element variation in the Rietfontein clinopyroxenes, with a factor of 20 variation being observed (2.25 - 44.7 ppm). Clinopyroxenes from the kyanite eclogites show the lowest concentrations of all measured trace elements, when compared to those of the bimineralic and orthopyroxene-bearing eclogites (*Table 5.1*).

Figure 7.4a-d & h illustrate the variation of select trace elements with Ca/(Ca+Na) contents in the Rietfontein clinopyroxenes. The kyanite and bimineralic/orthopyroxene-bearing eclogites are easily separated on the basis of the $Ca/(Ca+Na)_{cpx}$ contents, the kyanite eclogites possessing a lower ratio due to the higher Na abundances in the clinopyroxene. *Figure 7.4a* illustrates the even spread of Ni contents between the kyanite and bimineralic/orthopyroxene-bearing eclogites. Clinopyroxenes of the kyanite eclogites have the lowest Sc concentrations (*Figure 7.4b*), whereas Sr abundances are similar in all groups (*Figure 7.4c*), unlike the Sr in garnet, which is higher in the kyanite eclogites. Most of the kyanite eclogite clinopyroxenes have Sc abundances of less than 10ppm, whereas the bimineralic and orthopyroxene-bearing eclogite clinopyroxenes have concentrations greater than 15ppm. Whereas most clinopyroxenes have Sc contents of less than 30 ppm, two eclogite samples have higher than average Sc contents (41 and 48 ppm).

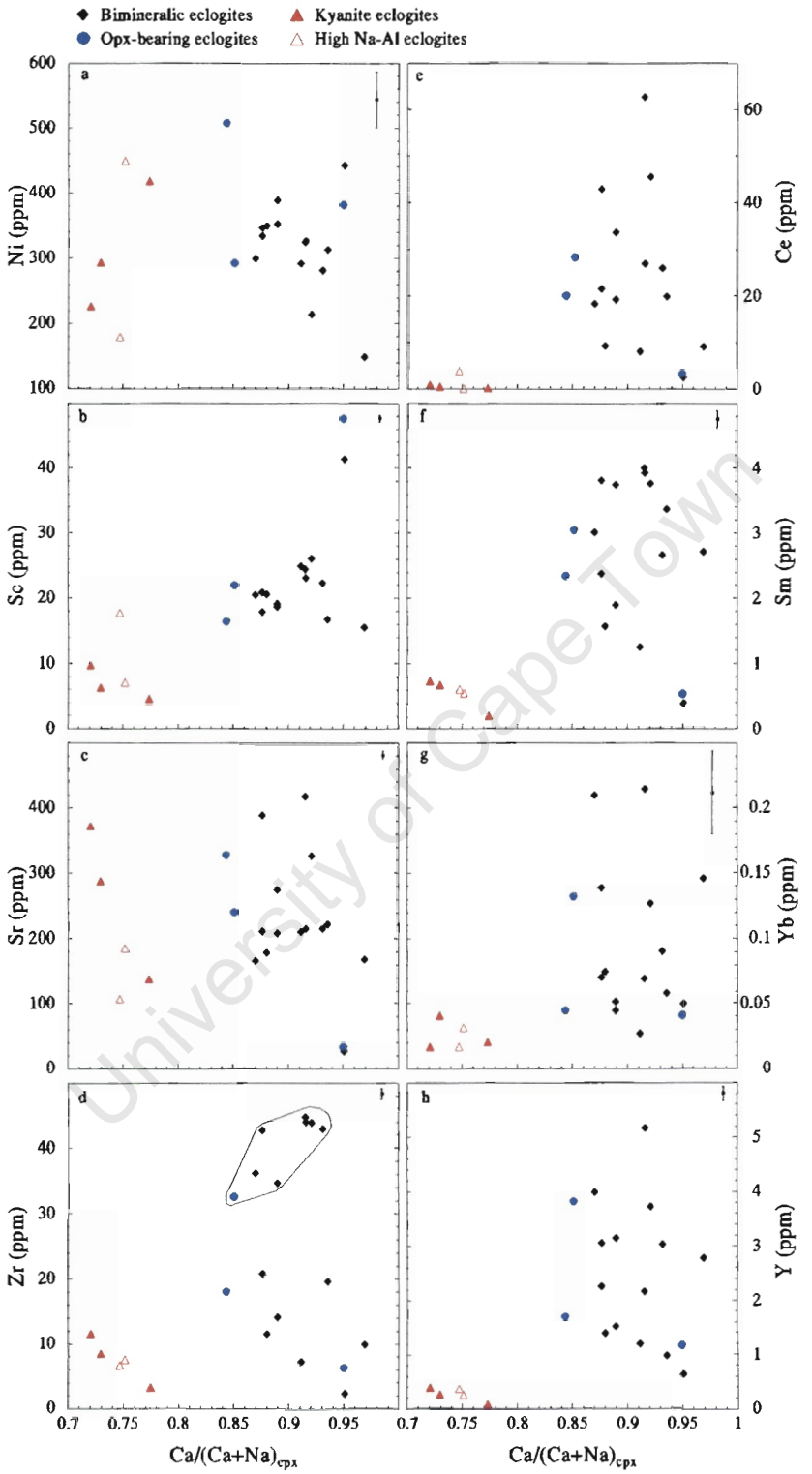

Figure 7.4 *Trace element abundances for clinopyroxenes from the Rietfontein eclogites, plotted as a function of* $Ca/(Ca+Na)_{cpx}$. *All values reported in ppm, 1σ error bars illustrated in the top right corner of the diagrams.*

In *Section 7.3.1* it was noted that a group of garnets from bimineralic eclogites contain elevated Zr concentrations. A similar grouping is exhibited by the clinopyroxenes, where a group of seven bimineralic and one orthopyroxene-bearing eclogite have elevated (>30ppm) Zr contents (*Figure 7.4d*). With the exception of two samples (Rtfn 57.1 and JJG 105), the samples that contain high-Zr clinopyroxenes also have high-Zr garnets. This indicates the geochemical similarities that exist between the garnets and clinopyroxenes of the Rietfontein eclogites. A broad negative correlation between Zr_{cpx} and Ca/(Ca+Na) is visible in *Figure 7.4d*. The overall lower trace element abundances of the kyanite eclogites is again illustrate in *Figure 7.4h*, where the Y concentrations in the kyanite eclogites are seen to be far lower than those of the other eclogite groups.

7.4.2 REE abundances

Variations in select REE with major element chemistry for the clinopyroxenes are visible in *Figure 7.4 e-g*, and the overall lower REE abundances in the kyanite eclogites are clearly illustrated. A small field of overlap can be seen in the Ce (*Figure 7.4e*), Sm (*Figure 7.4f*) and Yb (*Figure 7.3g*) abundances of the kyanite eclogites and the lower REE abundance bimineralic and orthopyroxene-bearing eclogites. *Figure 7.4f* also illustrates a well-constrained negative correlation between Sm and $Ca/(Ca+Na)_{cpx}$. A plot of Sc *vs* Zr/Y for clinopyroxenes (*Figure 7.5*) highlights a broad negative correlation between the two variables. The kyanite eclogites have distinctly higher Zr/Y ratios that the bimineralic and orthopyroxene-bearing eclogites.

Two samples (JJG 105 and Rtfn 57.1) exhibit intra-grain compositional variations, the first evidence of possible disequilibrium in the eclogites. These are not large differences however, and overall the REE patterns are the same, with only slight differences in REE abundances between grains (*Figure 7.6*). REE patterns for clinopyroxenes from the Rietfontein eclogites are presented in *Figure 7.7*. The bimineralic and orthopyroxene-bearing eclogites exhibit trends expected of clinopyroxene in equilibrium with garnet, namely enrichment of LREE *relative* to HREE. From the three bimineralic eclogites illustrated (*Figure 7.7, top*), it is clear that more inter-sample variation occurs in the clinopyroxenes than the garnets of the Rietfontein eclogites. Sample Rtfn 43.1 is highly LREE enriched, with concentrations of up to 100x chondrite. Within the group of bimineralic eclogite clinopyroxenes, it can be seen that the slopes of the curves are variable, the

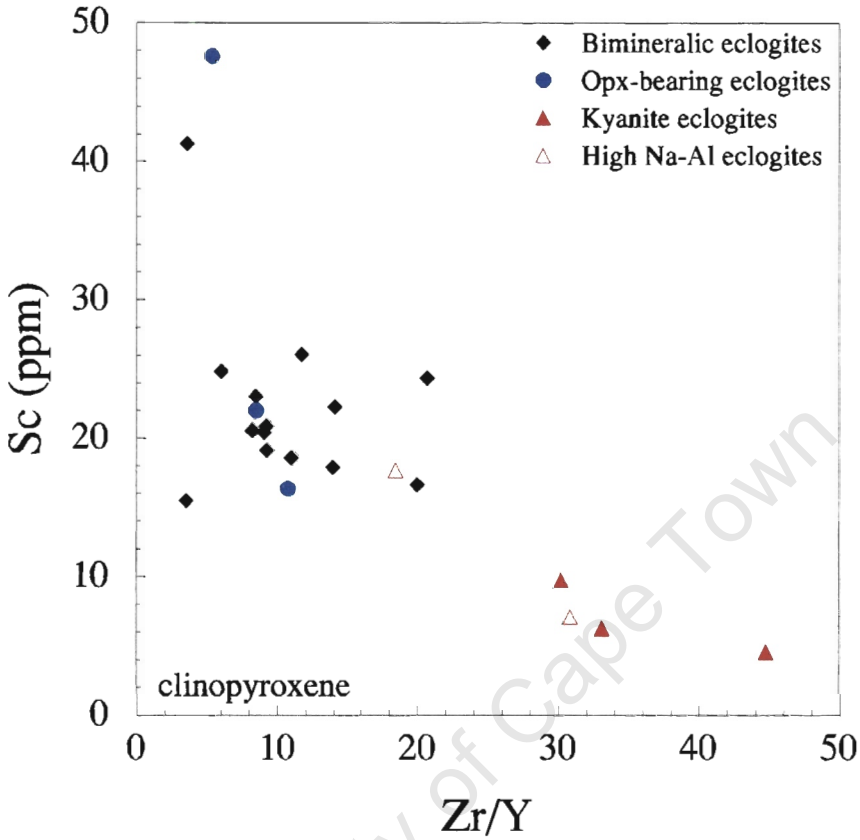

Figure 7.5 *Sc vs Zr/Y for Rietfontein clinopyroxenes. A broad negative correlation is visible and the kyanite eclogites have much higher Zr/Y ratios than the other eclogites.*

LREE to MREE slope of sample Rtfn 43.1 being much steeper than that of Rtfn 31.1. Rtfn 31.1 has a much shallower, almost flat LREE pattern. CMA 1 shows a slight negative Eu anomaly, together with a gradual LREE slope but the general trends exhibited by this exsolved eclogite are similar to those of the other bimineralic eclogites.

Clinopyroxenes from the orthopyroxene-bearing eclogites (*Figure 7.7, middle*) show very similar patterns to the bimineralic eclogites. LREE enrichment is not as pronounced, with values of 40x chondrite being reached, but HREE depletion reaches the same levels (0.3x chondrite). The negative Eu anomaly exhibited by bimineralic sample CMA 1 is also seen in orthopyroxene-bearing eclogite CMA 3.

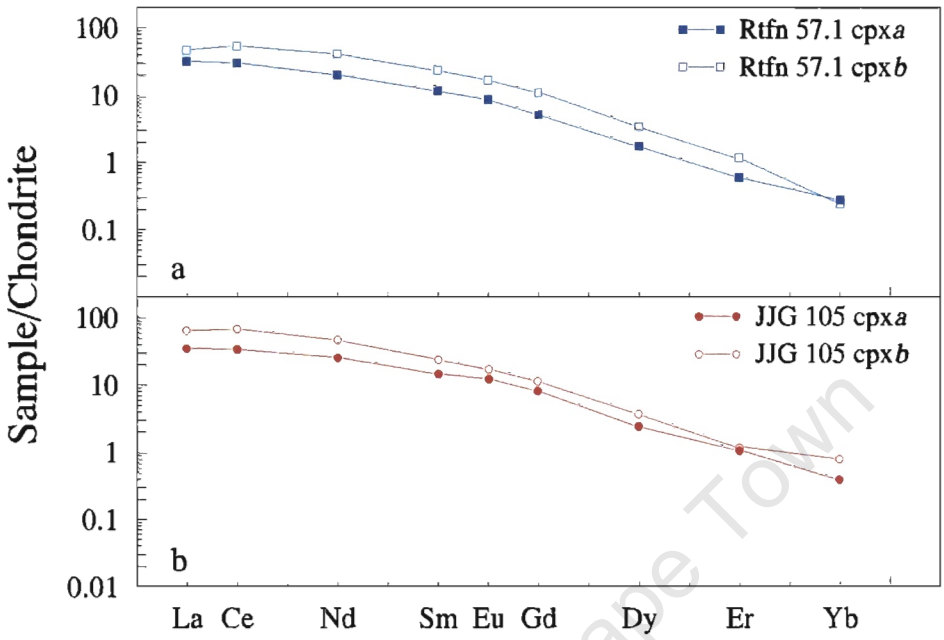

Figure 7.6 *REE diagrams illustrating intra-grain variation within clinopyroxenes from two Rietfontein eclogites.*

Clinopyroxenes from the kyanite eclogite group show marked differences to those discussed above (*Figure 7.7, bottom*). These eclogites show both LREE and HREE depletion, with LREE depletion being the most extreme (0.01 - 0.12x chondrite). All kyanite eclogites show a similar range of HREE values, but there is considerably more scatter when looking at the LREE. CMA 17 shows LREE enrichment relative to chondrites and the other kyanite eclogites, and the overall trend is more similar to that of the bimineralic eclogites. This may be due to the fact that this sample is a bimineralic eclogite, but in major element compositional aspects, is similar to the kyanite eclogites. The garnet REE pattern of this sample is also similar to the bimineralic eclogite signatures, suggesting that the similarities of CMA 17 to the kyanite eclogites extend only as far as the major element chemistry. The remaining kyanite eclogites show distinct convex upward LREE to MREE patterns, with a peak REE concentration occurring at Nd. Whilst there is an

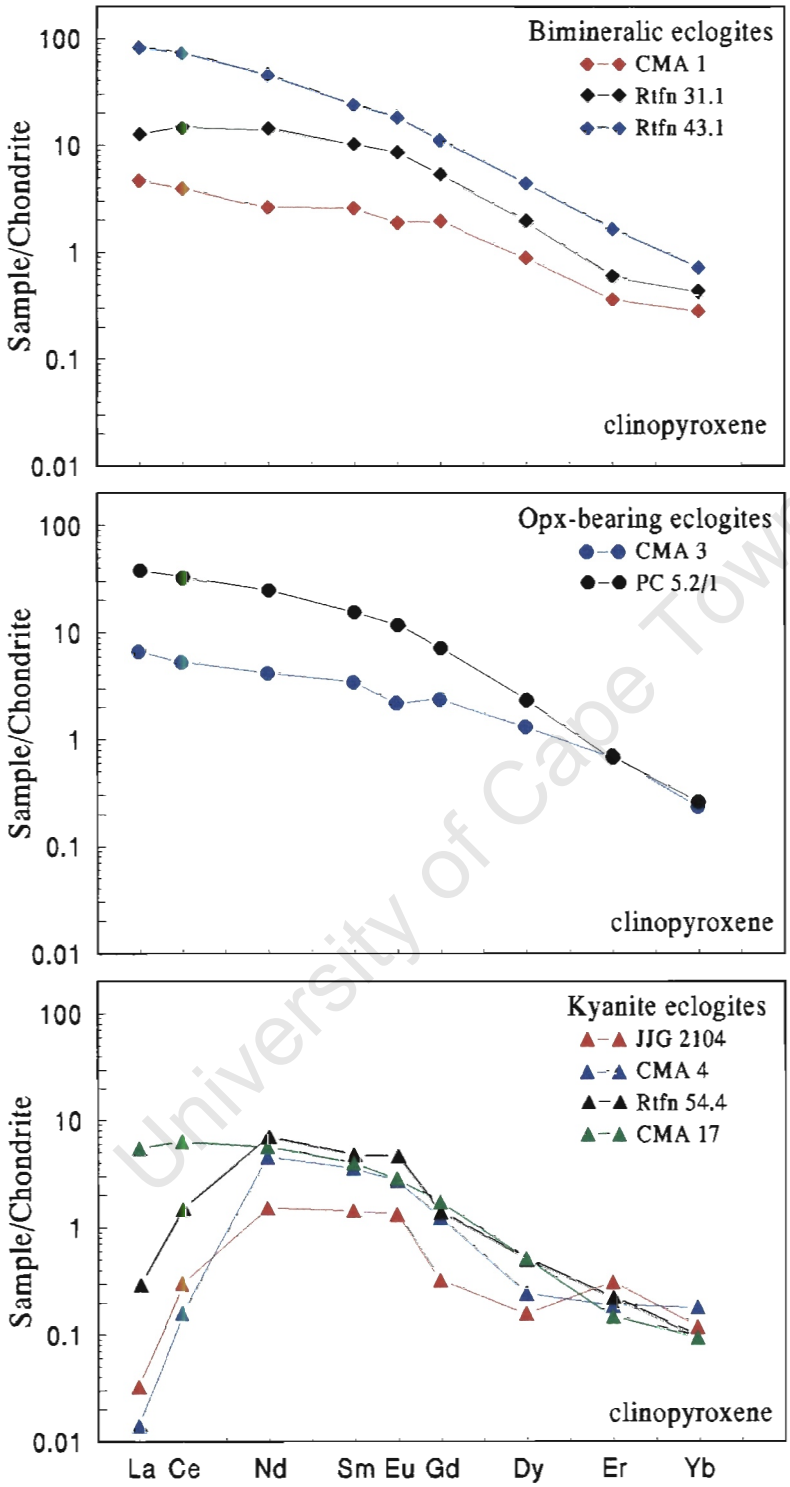

Figure 7.7 REE *diagrams for clinopyroxenes from selected Rietfontein eclogites. Top - bimineralic eclogites, middle - opx-bearing eclogites and bottom - kyanite eclogites. REE abundances are chondrite-normalised after Sun & McDonough (1989). 2σ errors on analysed elements are illustrated in Appendix I, Figure I.1.*

overall trend of steep LREE and HREE slopes, the MREE slopes are more gradual (even flat in the case of JJG 2104). Most slopes decrease steadily towards the heaviest REE, occasionally flattening out (CMA 4). JJG 2104 however exhibits an anomalous, higher Er concentration, yielding a somewhat different pattern to the other kyanite eclogites.

$[La/Yb]_N$ ratios of the Rietfontein clinopyroxenes range between 0.08 and 263 (bimineralic eclogites = 16.2-263, opx-bearing eclogites = 27.9-144, kyanite eclogites = 0.08-56.3) (*Table 7.1*). This exceeds the range of values reported in the classification scheme of Taylor & Neal (1989), rendering it inapplicable to the Rietfontein eclogites into Groups A, B and C.

7.5 Trace element partitioning

Partition coefficients for a variety of trace elements have been calculated for coexisting clinopyroxene and garnet in the Rietfontein eclogites. Element partitioning between co-existing mineral phases provides important data fundamental to crystal chemistry, geothermobarometry and the mathematical modelling of processes such as partial melting, fractional crystallisation and metasomatism (O'Reilly & Griffin, 1995). The majority of the upper mantle trace element budget is contained within the mineral phases garnet and clinopyroxene, and the partitioning of trace elements between these two phases has application to both systems that have melt present, and those in which it is absent (Harte & Kirkley, 1997). Due to the relative rigidity of cation sites in some solids, the mineral phases in these solids may exert greater influence over the variation of partition coefficients than the composition of the melt phase (Blundy & Wood, 1991). It is necessary to determine which compositional parameters and/or pressure-temperature controls are responsible for trace element partitioning within the Rietfontein eclogites. *Table 7.2* gives calculated partition coefficients for relevant trace elements in the Rietfontein eclogites, where D represents clinopyroxene/garnet (in ppm) for a particular trace element. Partition coefficients for the REE are seen to decrease with decreasing atomic radius of an element (see *Table 7.2*), for example $D_{Ce} > D_{Nd} > D_{Sm} > D_{Eu}$.

Figure 7.8a and *b* illustrates the partitioning of Nd, Eu and Y (*a*) and Zr and Ni (*b*) as a function of the Ca content of garnet. The kyanite eclogites are distinguished from the bimineralic and orthopyroxene-bearing eclogites by their higher garnet Ca contents. Due to the large differences

Table 7.2 *Calculated partition coefficients for co-existing clinopyroxene and garnet in the Rietfontein eclogites.* $D_i = i^{cpx}/i^{gt}$, *where "i" refers to any given element*

	CMA 1	CMA 3	CMA 4	CMA 5	CMA 8	CMA 12	CMA 14
D_{Zr}	0.67	0.92	1.34	3.23	2.21	3.24	1.60
D_{Sr}	40.0	50.4	52.8	496	462	1986	1445
D_{Sc}	0.26	0.33	0.22	0.40	0.26	0.41	0.37
D_{Ni}	18.2	18.1	11.4	12.1	14.1	13.8	12.2
D_{Y}	0.034	0.068	0.019	0.16	0.44	0.14	0.069
D_{Ce}	53.8	118	1.21	256	205	449	169
D_{Nd}	8.75	15.7	0.80	48.3	30.6	36.5	16.1
D_{Sm}	1.45	3.15	0.33	6.75	5.87	5.87	2.97
D_{Eu}	0.61	1.13	0.18	3.18	3.31	3.03	1.50
D_{Gd}	0.33	0.73	0.14	1.45	2.20	1.21	0.65
D_{Dy}	0.079	0.15	0.028	0.332	0.87	0.31	0.14
D_{Er}	0.030	0.051	0.021	0.11	0.34	0.081	0.050
D_{Yb}	0.027	0.016	0.016	0.066	0.18	0.037	0.012

	CMA 17	JJG 105	JJG 2104	PC 1	PC 5.2/1	Rtfn 31.1	Rtfn 43.1
D_{Zr}	1.13	9.07	1.47	2.83	4.29	1.97	2.01
D_{Sr}	65.7	2492	92.4	204	2818	1473	3380
D_{Sc}	0.33	0.38	0.26	0.48	0.34	0.40	0.34
D_{Ni}	12.6	13.6	14.9	5.56	12.4	15.6	12.3
D_{Y}	0.021	0.30	0.009	0.30	0.15	0.15	0.18
D_{Ce}	12.1	617	2.55	127	556	174	605
D_{Nd}	1.79	155	0.57	13.1	54.4	26.6	65.2
D_{Sm}	0.44	15.8	0.24	4.66	5.41	3.57	8.92
D_{Eu}	0.23	5.64	0.097	1.36	2.73	2.07	3.61
D_{Gd}	0.15	3.20	0.054	1.94	1.47	1.30	1.63
D_{Dy}	0.043	0.63	0.030	0.56	0.35	0.34	0.40
D_{Er}	0.014	0.18	0.055	0.20	0.087	0.094	0.12
D_{Yb}	0.008	0.11	0.025	0.14	0.032	0.068	0.047

	Rtfn 48.2	Rtfn 54.1	Rtfn 54.4	Rtfn 55.1	Rtfn 55.2	Rtfn 57.1
D_{Zr}	2.21	1.39	1.75	1.83	1.78	3.14
D_{Sr}	4207	137	188	1288	2793	1763
D_{Sc}	0.31	0.23	0.25	0.34	0.31	0.39
D_{Ni}	13.3	9.76	11.4	12.0	12.3	14.3
D_{Y}	0.32	0.016	0.018	0.15	0.13	0.14
D_{Ce}	595	4.28	6.45	244	594	302
D_{Nd}	59.0	0.79	1.19	32.6	37.3	28.2
D_{Sm}	7.49	0.21	0.29	6.81	4.69	6.63
D_{Eu}	5.04	0.15	0.20	4.13	2.54	2.84
D_{Gd}	2.46	0.12	0.086	1.59	1.41	1.19
D_{Dy}	0.69	0.020	0.031	0.34	0.33	0.26
D_{Er}	0.30	0.023	0.016	0.099	0.096	0.083
D_{Yb}	0.088	0.033	0.009	0.032	0.067	0.041

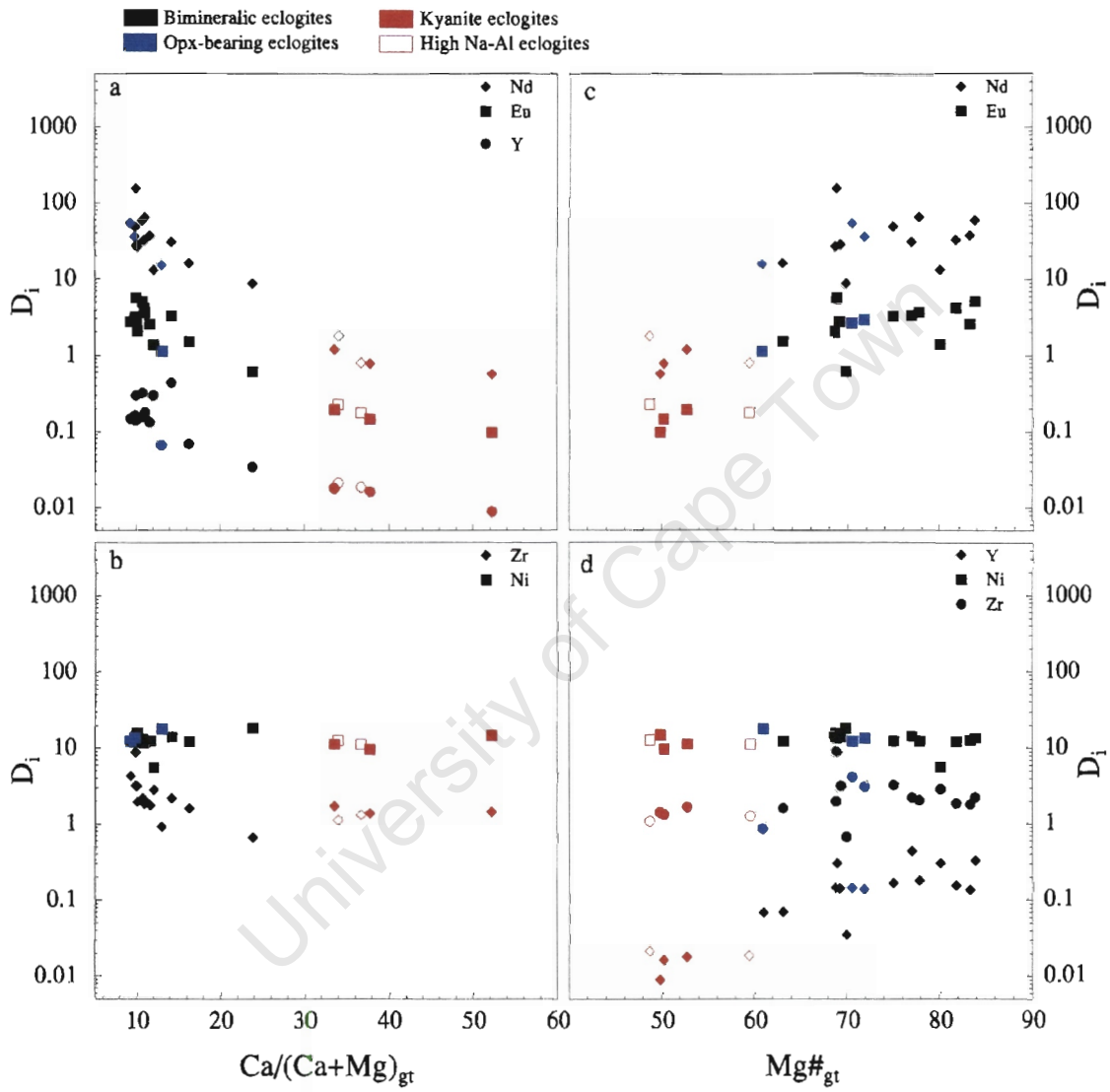

Figure 7.8 *Calculated cpx/gt partition coefficients for selected trace elements from the Rietfontein eclogites. Each marker on the graphs represents a particular element, listed in the legend.* ***a)*** *Partition coefficients for Nd, Eu and Y illustrated as a function of the Ca content of garnet;* ***b)*** *Zr and Ni partition coefficients plotted against the Ca content of garnet; c) Nd and Eu partition coefficients plotted as a function of* $Mg\#_{gt}$*;* ***d)*** D_Y*,* D_{Ni} *and* D_{Zr} *illustrated as a function of* $Mg\#_{gt}$

in Ca contents between the different eclogite groups, molar Ca serves as a good basis on which partition coefficient trends may be identified and distinguished. The same can be said about the Mg# of garnet - garnets from kyanite eclogites have lower Mg#'s than garnets from the other eclogites, and the variation of partition coefficients with Mg# is illustrated in *Figures 7.8c* and *d*. *Figure 7.8a* shows well defined trends of partition coefficient variations for Nd, Eu and Y, with each element showing a decrease in partition coefficient *(i.e.* increased tendency to preferentially enter garnet) with an increase in $Ca/(Ca+Mg)_{gt}$. Some elements show more scatter than others, although the general trend is the same. It can be seen that for all elements, with the exception of Zr and Ni, the lowest partition coefficient for a particular element is always found in the kyanite eclogites, suggesting that the more Ca-rich the garnet, the more likely it is that it will preferentially incorporate trace elements into its structure. Whereas the partition coefficients for the kyanite eclogites are much lower than those of the bimineralic and orthopyroxene-bearing eclogites, the orthopyroxene-bearing eclogites fall within the range defined by the bimineralic eclogites. There are substantial differences in the partition coefficients within the groups of bimineralic and orthopyroxene-bearing eclogites though, for example the partition coefficients for Nd and Eu range between 8-155 and 0.6-5.6 respectively, for bimineralic eclogites, and 15.7-54 and 1.1-3 respectively, for orthopyroxene-bearing eclogites. D_{Ni} remains constant at approximately 10 across the entire range of Ca/(Ca+Mg) (*Figure 7.8b*), and Zr shows only a slight tendency for decreasing D_i with increasing $Ca/(Ca+Mg)_{gt}$, although this is only applicable to the bimineralic and orthopyroxene-bearing eclogites, not the kyanite eclogites.

Broad trends of increasing D_i with increasing $Mg\#_{gt}$ are defined for Nd, Eu and Y (*Figure 7.8c* and *d*). Again, D_{Ni} remains constant at approximately 10 across the range of Mg#'s, whereas Zr shows slight variation, but defines no particular trend with Mg# (*Figure 7.8d*). The constant partition coefficient of approximately 10 for Ni means that it is preferentially partitioned into clinopyroxene in the presence of co-existing garnet. Trace element partitioning was not found to be dependent on the Mg# of clinopyroxene at all. The Mg# of garnet clearly does determine the partitioning of trace elements between garnet and clinopyroxene to some extent, but does not exert the influence that the Ca content of garnet does.

Figures 7.9a and *b* show partition coefficients for Sr, Sm, Gd and Nd as a function of Al in the 6-fold clinopyroxene cation site. Trace element partitioning in the Roberts Victor eclogites has been observed to be dependent on $Al^{[6]}$ and the correlation with this variable is thought to arise from the correlation of D_i and jadeite components with $Ca/(Ca+Mg)_{cpx}$ (Harte & Kirkley, 1997). A similar correlation may be present in the Rietfontein eclogites. Clinopyroxenes from kyanite eclogites are more jadeite-rich (*Chapter 4*) and hence have a greater proportion of $Al^{[6]}$ than the remaining eclogites, which are more likely to contain a greater proportion of $Al^{[4]}$. It is thus easy to distinguish the different eclogite groups and thereby identify partitioning trends or groupings on the basis of $Al^{[6]}$. There is significantly more scatter on these diagrams than on the Ca plots (*Figure 7.8*), indicating that the Ca content of garnet exerts a bigger influence over trace element partitioning than the Al content of clinopyroxene. Whilst very broad inverse correlations may be identified, the bimineralic and orthopyroxene-bearing eclogites seem to form groupings, whereas the kyanite eclogites exhibit tidier trends for Sm and Nd (*Figure 7.9 a* and *b*). Sr, Sm (*Figure 7.9 a*), Nd and Gd (*Figure 7.9b*) all show broad partitioning trends as a function of $Al^{[6]}$.

Figures 7.9c and *d* illustrate partition coefficients plotted as a function of equilibration temperatures. Again, the partitioning of Ni (*Figure 7.9d*) remains fairly constant and no dependence of partitioning on temperature can be observed in any of the trace elements. This is in contrast to results obtained by O'Reilly & Griffin (1995), who found that in on-craton Southern African eclogites, Ni partitioning for clinopyroxene/garnet is moderately dependent on X_{Mg}, and strongly dependent on temperature. O'Reilly & Griffin (1995) and Harte & Kirkley (1997) noted that Zr partitioning between garnet and clinopyroxene in eclogites from on-craton localities is mostly temperature controlled, and is mildly influenced by the jadeite component of clinopyroxene and the Ca content of garnet. However, no such temperature dependence is observed in the Rietfontein eclogites. On-craton eclogite suites thus seem to be more temperature dependent with regards to trace element partitioning than an off-craton locality such as Rietfontein.

Figure 7.10 illustrates Ln $D_i^{cpx/gt}$ of selected trace elements (Nd, Sm and Gd) against the natural logarithms of the molar partition coefficients for Ca and good linear trends are defined. Marked correlations exist for most elements, irrespective of the valency and abundance of the elements. This can be seen in the regression values for the correlations, where $r^2_{Nd} = 0.92$, $r^2_{Sm} = 0.94$, and

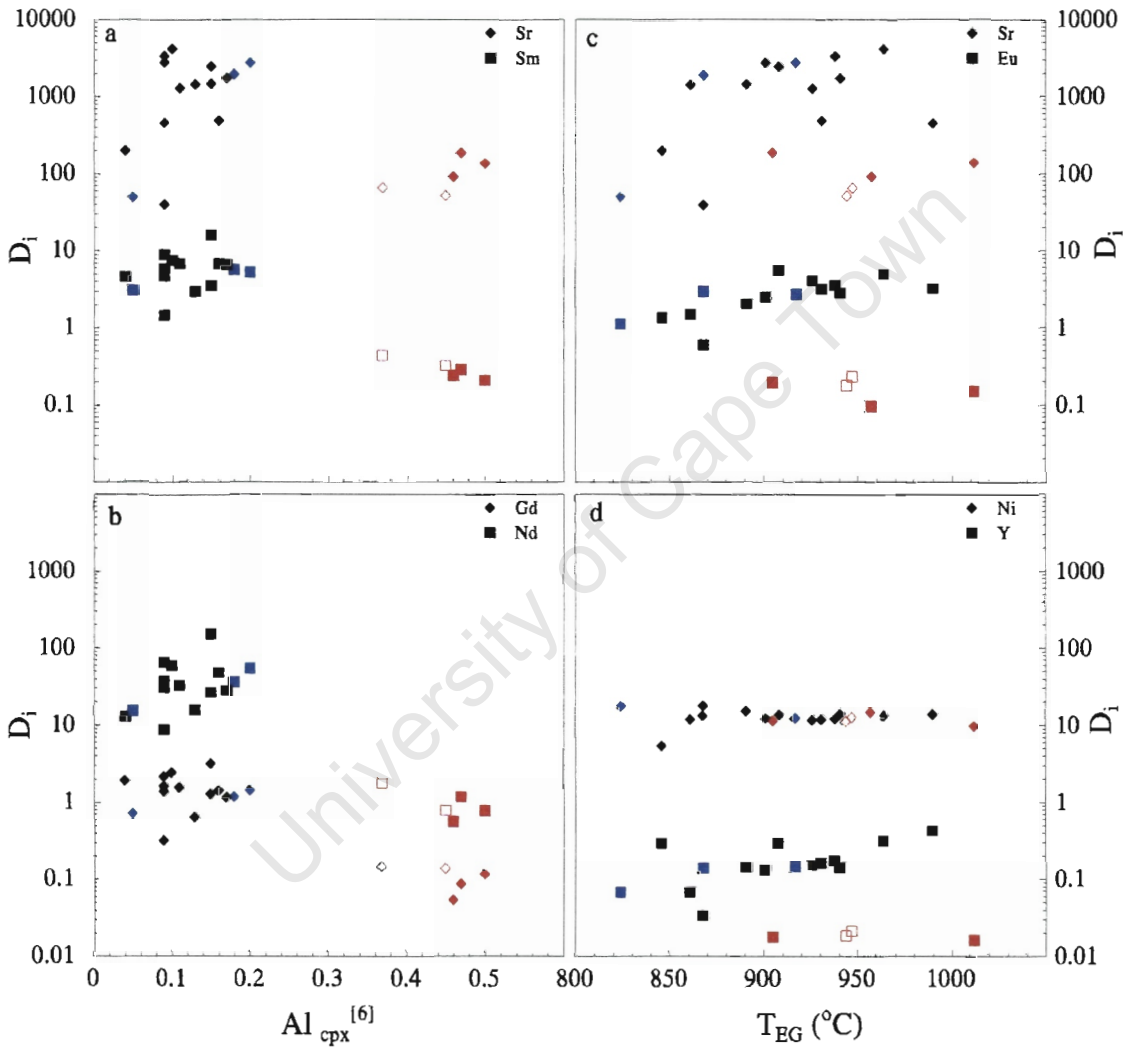

Figure 7.9 *Further partition coefficient diagrams for the Rietfontein eclogites. Colours as are those in Figure 7.8.* ***a)*** *D_{Sr} and D_{Sm} vs [6]-fold coordinated Al in clinopyroxene;* ***b)*** *partition coefficients for Gd and Nd as a function of $Al_{cpx}^{[6]}$;* ***c)*** *D_{Sr} and D_{Eu} vs equilibration temperatures of Ellis & Green (1979);* ***d)*** *partition coefficients for Ni and Y vs equilibration temperatures of Ellis & Green (1979).*

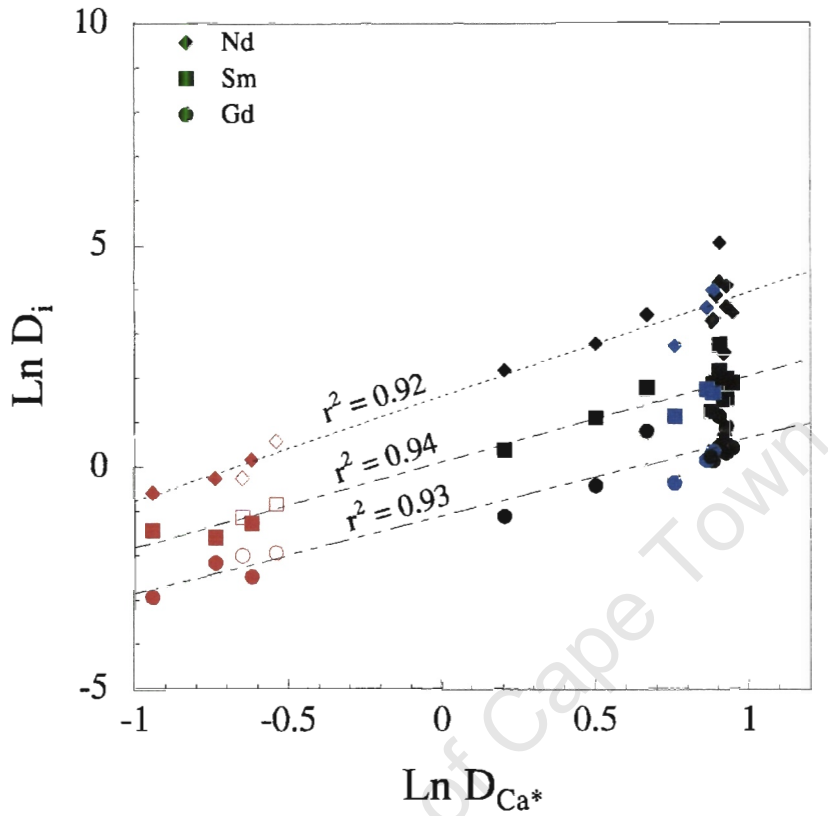

Figure 7.10 *Natural logarithms of partition coefficients for Nd, Sm and Gd plotted as a function of the natural logarithm of* D_{Ca*}, *where* $D_{Ca*} = Ca_{cpx}/Ca_{gt}$.

$r^2_{Gd} = 0.93$. Trace element partitioning in eclogites from the Roberts Victor kimberlite was investigated by Harte & Kirkley (1997), who also observed good correlations between LnD_i and LnD_{Ca*} for Nd ($r^2 = 0.93$) and Sm ($r^2 = 0.96$). Harte & Kirkley (1997) used linear regression analyses to derive the equation

$$LnD_i^{cpx/gt} = A(LnD_{Ca*}^{cpx/gt}) + B$$

Calculated constants A and B for the Roberts Victor eclogites are as follows: $A^{Nd} = 2.28$, $B^{Nd} = 0.78$, $A^{Sm} = 1.99$ and $B^{Sm} = -0.45$. These are subtly different to those calculated for the Rietfontein eclogites, where $A^{Nd} = 2.35$, $B^{Nd} = 1.58$, $A^{Sm} = 1.93$ and $B^{Sm} = 0.103$. Similar results were obtained by Harte & Kirkley (1997), who noted that the best correlation exists between LnD_{i*} and Ln D_{Ca*}, but weaker correlations could be observed between LnD_i and Ln D_{Mg*}, and Ln D_i and Ln $D_{[Al]6*}$.

To summarise, trace element partitioning within the Rietfontein eclogites appears to be controlled mainly by the major element compositions, most notably the Ca content in garnet, although Mg contents in garnet and Ca contents in clinopyroxene also play a role. $Al^{[6]}$ in clinopyroxene is also seen to influence the partitioning of some trace elements. Equilibration temperatures of the eclogites have no effect on trace element partitioning and Ni and Zr show very little response to any of the possible partitioning controls.

7.6 Discussion

7.6.1 REE elements

Figure 7.11 provides comparative diagrams for REE patterns for garnet and clinopyroxene from the Rietfontein eclogites and from Siberian and Roberts Victor eclogites. All three groups of Rietfontein eclogites exhibit garnet REE patterns (*Figure 7.11a*) very similar to those observed in on-craton eclogites. The extreme depletion noted in some of the Rietfontein eclogite garnets is also noted in garnets analysed from Udachnaya and Roberts Victor eclogite samples. Positive Eu anomalies are not uncommon either, having been noted from both comparative localities, and Bellsbank (Smyth & Caporuscio, 1984; Taylor & Neal, 1990). The garnet REE patterns exhibited by the bimineralic and orthopyroxene-bearing eclogites from Rietfontein are not unusual, and can be matched to similar patterns from most on-craton localities, including Roberts Victor and Udachnaya. *Figure 7.11c* illustrates the large range in LREE abundances found within clinopyroxenes from the Rietfontein eclogites. Similarly large ranges are observed in eclogite clinopyroxene from South African and Siberian localities (*Figure 7.11d*). Bimineralic and orthopyroxene-bearing eclogites from Rietfontein do not exhibit unusual patterns, and similar patterns have been reported from most South African localities (*eg.* Taylor & Neal, 1989; Harte & Kirkley, 1997). However, the unusual patterns represented by clinopyroxenes of the Rietfontein kyanite eclogites have been reported from Siberian localities (turquoise blue marker on *Figure 7.11d*) (*eg.* Jerde *et al.*, 1993*a*; Sobolev *et al.*, 1994; Snyder *et al.*, 1997). These clinopyroxenes show a convex upwards pattern in the light to middle REE range. Thus, whilst the clinopyroxenes from the Rietfontein eclogites exhibit different REE patterns, it is not the first time that such patterns have been recorded. The REE mineral patterns of the Rietfontein eclogites are thus very similar to patterns recorded in on-craton eclogites, from both South African and Siberian localities. Comparisons with trace-elements from off-craton eclogites could

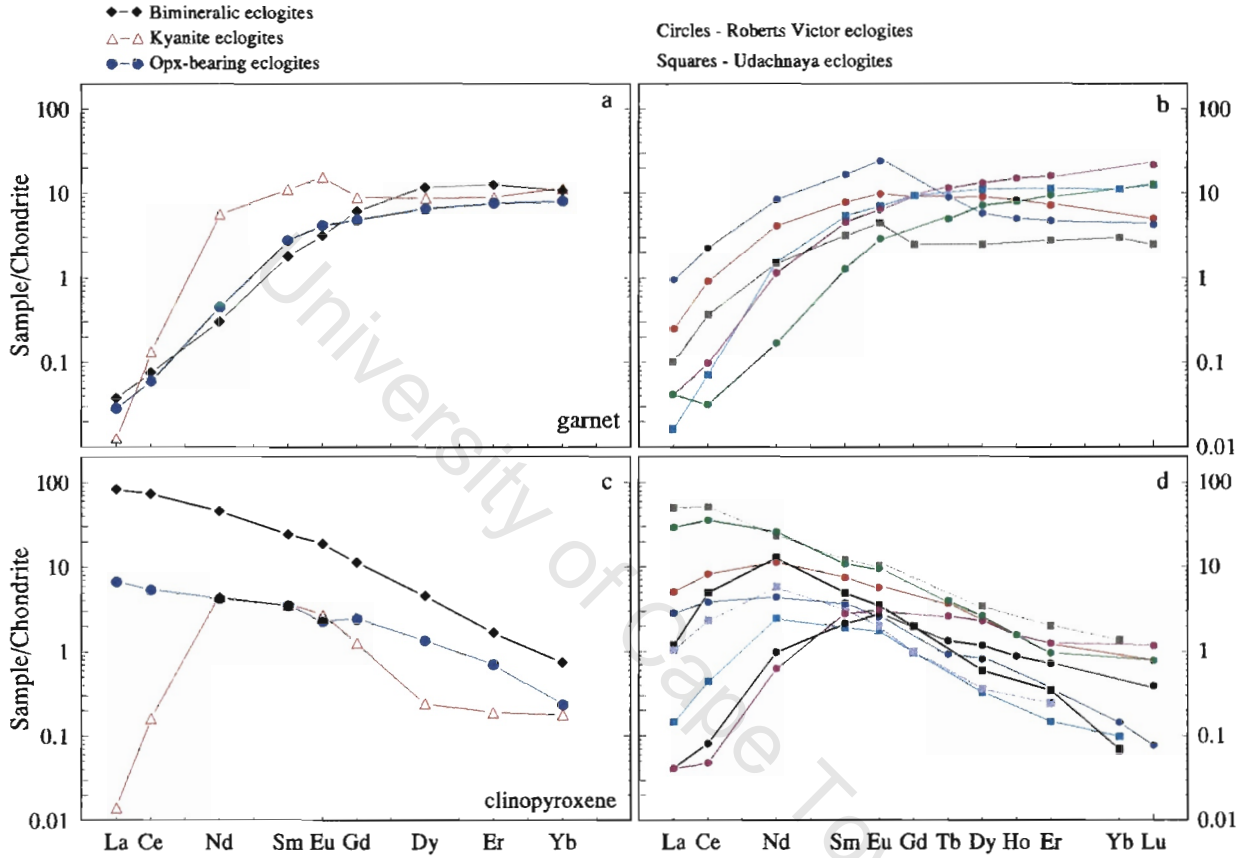

Figure 7.11 *REE patterns for selected garnets* ***(a)*** *and clinopyroxenes* ***(b)*** *from the Rietfontein eclogites, compared to data from on-craton eclogites* ***(b & d)****. Square symbols in b & d refer to Udachnaya eclogites (Sobolev et al., 1994; Snyder et al., 1997), circles represent Roberts Victor eclogites (Caporuscio & Smyth, 1990; Harte & Kirkley, 1997). REE abundances are normalised using chondrite values of Sun & McDonough (1989).*

not be made, due to a lack of such data in the literature. The significant REE differences between the kyanite and bimineralic/orthopyroxene-bearing eclogites suggest different protoliths and/or petrogenetic histories for the kyanite eclogites. On the basis of major elements the bimineralic and orthopyroxene-bearing eclogites of Rietfontein can be grouped as Group A and B eclogites (after Taylor & Neal, 1989). Although REE patterns are similar, the Rietfontein Group A eclogites show much greater LREE enrichment in clinopyroxene ($100 < [La/Yb]_{cpx} < 263$) than Group B eclogites ($[La/Yb]_{cpx} = 6\text{-}60$). Group A clinopyroxenes also have higher MgO contents, and lower Na_2O contents than Group B eclogites, and these chemical differences, combined with differences in REE concentrations, may imply different protoliths for the two groups, despite the similarity in REE patterns. Neal *et al.* (1990) believe that Group A eclogite xenoliths may be the result of crystallisation from a Group II kimberlite magma within the upper mantle, and are thus true mantle cumulates. Taylor & Neal (1989) also believe that clinopyroxene/garnet partition coefficients for Group B eclogites are not consistent with an origin by fractional crystallisation of a magma and must thus have a crustal protolith. Neither Group A nor Group B eclogites from Rietfontein show chemical signatures associated with crustal rocks, although crustal involvement in the formation of these eclogites cannot yet be discounted. However, the higher MgO contents of both garnets and clinopyroxenes from Group A eclogites, together with lower Na_2O_{cpx} abundances and higher clinopyroxene REE abundances suggest that crystallisation of the eclogites from a primary, basaltic magma at high pressures and temperatures cannot be discounted. The higher Na_2O_{cpx} contents of Group B clinopyroxenes could imply a less primary origin than the Group A eclogites, and the suggestion that Group B eclogites may represent metamorphosed basaltic oceanic crust (Taylor & Neal, 1989) is a possibility. Should the Rietfontein Group B eclogites have formed by the metamorphism of oceanic crust, this crust would not necessarily have been plagioclase-rich, as no positive Eu anomalies are recorded in either garnet or clinopyroxene from this eclogite group.

An initial depleted source region or protolith for the kyanite eclogites could be implied by the LREE depletion and overall low REE abundances, or it may imply partial melting after eclogite formation. The positive Eu anomalies in garnets from the Rietfontein kyanite eclogites provide strong evidence for a plagioclase-rich protolith for these rocks. Plagioclase is known to possess a strong positive Eu anomaly and LREE depletion (Pallister & Knight, 1981), and this chemical

signature may be retained during metamorphism and is hence exhibited by minerals comprising the resulting rock. Subduction of plagioclase-rich oceanic crust and subsequent metamorphism at high pressures and high temperatures, could result in eclogites yielding the mineral REE patterns observed in the Rietfontein kyanite eclogites. Metamorphism of ancient subducted oceanic crust is proposed to account for Group C (or kyanite) eclogites from a number of on-craton localities, such as Roberts Victor and Bellsbank (*eg.* MacGregor & Manton, 1986; Shervais *et al.*, 1988; Taylor & Neal, 1989). If melting of an eclogite were to occur, garnet and clinopyroxene would both begin to melt at the same time, in cotectic proportions. LREE have a large ionic radius and are thus incompatible (Rollinson, 1993), and would be preferentially incorporated into the melt at the onset of melting, depleting the co-existing crystals in LREE. The subduction of plagioclase-rich oceanic crust, followed by partial melting of the resulting eclogite are processes which could lead to the positive Eu anomalies and extreme LREE depletion observed in minerals of the kyanite eclogites. Such partial melting processes have also been suggested to account for convex-upward REE profiles (Jerde *et al.*, 1993*a*).

7.6.2 Trace element partitioning

Partitioning of trace elements between two mineral phases is known to be affected by a series of variables such as pressure, temperature, and mineral composition (Harte & Kirkley, 1997). However, trace element partitioning in the Rietfontein eclogites shows no evidence for any dependence on temperature. It is difficult to ascertain whether or not there is any pressure dependence, as pressure estimates were only available for the six orthopyroxene-bearing eclogites and only three of these were selected for trace element analysis. The Ca content of the Rietfontein eclogites exerts the most control on clinopyroxene/garnet trace element partitioning, with garnet compositions having a greater effect than clinopyroxene compositions. Weaker controls are found to be exerted by [6]-fold Al in clinopyroxene and, to an even lesser extent, by the Mg content of garnet which affects only select trace elements (Sr, Nd, Eu, Gd and Y). The Mg content of clinopyroxene has no effect on partitioning whatsoever. The dominant partitioning control exerted by Ca suggests that most trace elements substitute in the [8]-fold Ca site of garnet and [6]-fold Ca site of clinopyroxene, with a lesser preference for the [6]-fold site of Al in clinopyroxene. The abundance of an element does not affect its partitioning at all. Zr and Ni are two trace elements that do not seem to be affected by either temperature or composition, although

Ni partitioning shows slightly more variability than Zr. It has been suggested that the smaller ionic radius of Zr, compared to the REE, may lead to substitution in the [6]-fold sites in clinopyroxene and garnet, rather than the Ca-bearing [8]-fold sites (Harte & Kirkley, 1997). The partition coefficients for the kyanite eclogites are always lower than those for the bimineralic and orthopyroxene-bearing eclogites. Trace elements progressively favour garnet over clinopyroxene as increasing amounts of Ca are strongly partitioned into garnet, leading to lower cpx/gt partition coefficients for kyanite eclogites (Harte & Kirkley, 1997). This is due to the favouring of garnet over clinopyroxene by trace elements as increasing amounts of Ca are strongly partitioned into garnet rather than clinopyroxene (Harte & Kirkley, 1997). The higher partition coefficients for the Group A and Group B eclogites once again indicate different petrogenetic processes or environmental mantle conditions for the Group A/B eclogites and the Group C (kyanite) eclogites.

8. WHOLE ROCK CHEMISTRY

8.1 Introduction

One of the major hindrances to the study of the upper mantle is the lack of *in situ* exposures of mantle material. Eclogites, together with ultra-mafic xenoliths, are direct samples of the upper mantle, and the bulk chemistry of xenolith suites has received considerable interest in efforts to characterise the bulk composition of the upper mantle (Haggerty, 1995). The geochemical signatures of eclogite protoliths (such as subducted oceanic crust) may be retained within the xenoliths themselves, thus providing the opportunity to investigate prior mantle processes.

Eclogites are rocks that have a broadly basaltic whole-rock composition (*Figure 8.1*), and Yoder & Tilley (1962) proposed that "for each and every basalt there is an equivalent eclogite of the same bulk composition". Whilst the whole-rock chemistry of eclogite suites is variable, in general an eclogite will have either a komatiitic- or mid-ocean ridge basalt (MORB)-like composition (Haggerty, 1995). Eclogites with low MgO contents approach basaltic compositions, whereas high MgO eclogites show more similarity to komatiites (Haggerty, 1995). The bulk major element compositional similarities of eclogites to both basalts and komatiites is not surprising, considering that ancient komatiites may have originated from the same deep, depleted mantle reservoir as modern picrites and MORB (Anderson, 1994). Similarities of eclogites to basaltic rocks can also (and most importantly) be seen in the REE patterns of eclogites. Many eclogites exhibit relatively flat REE patterns at abundance levels of 5-15x those seen in chondrites, similar to those observed in some MORB (Smyth *et al.*, 1990; Jerde *et al.*, 1993*a*; Beard *et al.*, 1996). Gabbroic rocks often exhibit a positive Eu anomaly, similar to the distinctive positive Eu anomalies in kyanite-bearing and Group C (Taylor & Neal, 1989) eclogites.

The existence of three groups of eclogites *viz.* Groups A, B & C (Taylor & Neal, 1989) was discussed in *Chapters 4* and *7*, and each group has a characteristic whole-rock composition. Group A eclogites (possible mantle cumulates) have high whole-rock Mg #'s, SiO_2 and Cr_2O_3 contents (Sobolev *et al.*, 1994) and low Al_2O_3, CaO and TiO_2 contents; Group B eclogites have major element compositions similar to that of Archaean basalts, high FeO, with moderate Al_2O_3, MgO and CaO contents and low concentrations of incompatible trace elements; Group C

eclogites have high Al_2O_3 and CaO, low MgO, FeO and low REE abundances, often with positive Eu anomalies (Taylor & Neal, 1989). These differing bulk rock compositions are often used to infer contrasting geological histories and protoliths for the different eclogite groups (*eg.* Taylor & Neal, 1989).

8.2 Aims

This chapter aims to address a number of issues relating to the whole-rock composition of the Rietfontein eclogites. These can be summarized as follows:

- to reconstruct the whole rock composition using analysed mineral compositions (both major elements and trace elements) and modal abundances,
- to compare the bulk rock compositions of the Rietfontein eclogites with respect to established compositional ranges for Group A, B and C eclogites,
- to compare the major and trace element bulk rock compositions with fields for mafic igneous rocks with a view to determining likely protoliths and petrogenetic origin and
- to compare REE patterns for mafic igneous rocks with those of the Rietfontein eclogites.

8.3 Reconstructing whole-rock compositions

8.3.1 Procedure

Many of the Rietfontein eclogites examined in this study are small, being less than 2cm in diameter. This meant that it was impossible to perform whole-rock compositional analyses on the samples themselves and whole-rock compositions have thus been reconstructed using the known compositions of the primary minerals. However, sample size and degree of alteration also meant that it was difficult to obtain representative modal proportion estimates in some samples. In these samples, it is necessary to assume an equal garnet:clinopyroxene ratio, whereas in some of the larger samples, a representative modal estimate could be obtained. Taking into account those for which estimated modal proportions were determined, it was found that the average garnet:clinopyroxene ratio for the suite of xenoliths is 48.8:51.2. It is thus fairly representative of the suite as a whole to use equal proportions of garnet and clinopyroxene to reconstruct whole-rock compositions.

The effect of varying garnet:clinopyroxene proportions on calculated major and trace element compositions is illustrated in *Figure 8.1*. It is clear that there is no marked effect for the largely incompatible trace elements (*eg.* REE) (*Figure 8.1a*), but significant variations can occur in the major stoichiometric components such as Al, Fe and Ca (*Figure 8.1b*) for garnet:clinopyroxene ratios ranging from 60:40 to 40:60. Some major elements are more affected by changes in modal proportions than others and the largest variation is seen in elements which show vastly different abundances between garnet and clinopyroxene, such as Al and Ca. Elements such as Mg, which can show similar concentrations in garnet and clinopyroxene, are not as greatly affected by modal proportion changes.

A number of samples contained a third primary mineral, either kyanite, or orthopyroxene. In reconstructing the whole-rock composition of these samples, it was essential to include this third

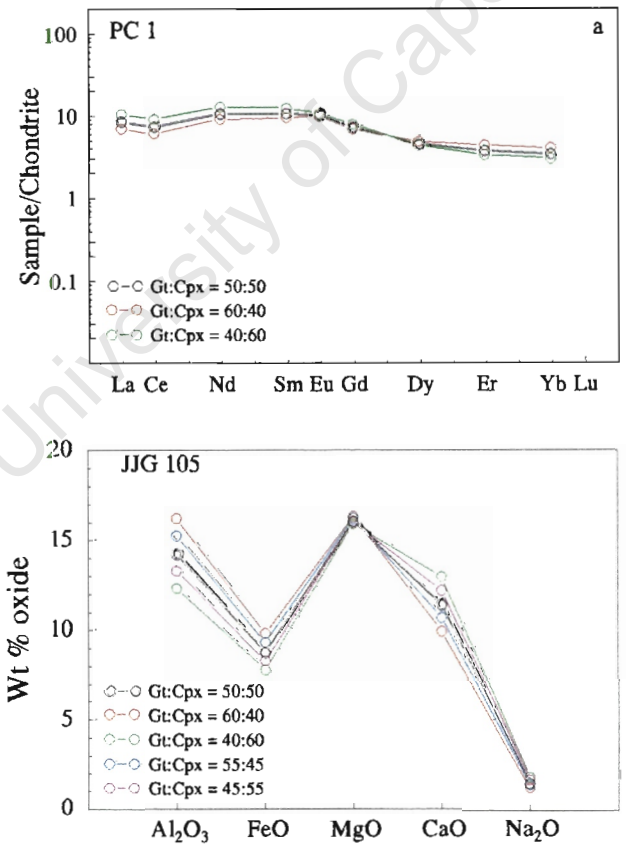

Figure 8.1 *Effect of varying garnet and clinopyroxene modal proportions on REE* ***(a)*** *and major elements* ***(b)*** *for samples PC1 and JJG 105, respectively.*

primary mineral. In such samples equal proportions of garnet and clinopyroxene were assumed and the appropriate modal proportion of either kyanite or orthopyroxene was accounted for in the major element reconstruction. Rutile was a common accessory mineral in some samples, and for these samples 1% rutile was assumed to be present and this too was accounted for in the whole-rock major element reconstruction. Trace element compositions were measured on garnet and clinopyroxene only, so whole-rock trace element chemistry is based on equal garnet and clinopyroxene proportions.

8.3.2 Advantages and disadvantages

There are certain advantages to reconstructing whole-rock chemistry, one of which is the exclusion of contributions from secondary minerals (phlogopite, amphiboles, oxides), which could commonly enrich the rock in elements such as K and Ti. Metasomatism would also affect mineral and hence whole-rock composition, as it introduces elements such as K, Na, Fe, Ti, Rb, Ba, Sr, Zr, Nb and LREE (Erlank *et al.*, 1987). Analyses of whole-rocks may thus lead to whole-rock compositions which are significantly enriched in particular elements, when compared to reconstructed whole-rock compositions. Analysed whole-rock chemical compositions are also known to be depleted in Na_2O relative to reconstructed whole-rocks (Sobolev *et al.*, 1994). A disadvantage of reconstructing whole-rock compositions is that possible errors could occur as a result of misjudged modal mineral proportions and the presence of widely distributed accessory phases.

Samples containing very large mineral grains, significant amounts of alteration or samples that are very small may lead to erroneous estimates of modal proportions, variations in which would affect the resultant calculated composition. It has been shown though, that for REE at least, varying the modal proportions within accepted eclogite limits does not significantly affect REE patterns or concentrations (*Figure 8.1* and Jerde *et al.*, 1993*a*). As REE and isotopic signatures are considered more useful than bulk major element compositions in unravelling the petrogenesis of eclogites (Neal & Taylor, 1990), this is an important point to note. The usefulness of major or trace elements in unravelling eclogite petrogenesis is still a source of debate. Neal & Taylor (1990) believe that REE signatures are most useful, whereas Ireland *et al.* (1994) and Rudnick (1995) caution against the use of trace element data because of the complex evolutionary history

of eclogites and the susceptibility of trace elements to metasomatic alteration. Using reconstructed whole-rock patterns limits the metasomatic influences though, and much information can still be gathered from the trace element chemistry.

8.4 Major element compositions

Table 8.1 presents reconstructed whole-rock major element compositions for selected Rietfontein eclogites. Distinct differences in major element compositions can be observed between the kyanite eclogites and the bimineralic/orthopyroxene-bearing eclogites from Rietfontein. SiO_2 contents for the eclogites range between 45 and 49 wt%, which, together with the Na_2O contents (0.4-3.1 wt%), confirms the overall basaltic nature of the eclogites (*Figure 8.2*). According to the Basaltic Volcanism Study Project (1981), "basalts are characterised by Fe, Ca and Mg contents in the range 5-15 wt%, and SiO_2 contents generally in the range 38-53 wt%", although some MORB from the Southern Mid-Atlantic Ridge have reported MgO contents greater than 15 wt% (le Roex *et al.*, 1987). Most MORB have Na_2O contents greater than 1.5 wt%, although concentrations as low as 0.2% have been reported (le Roex *et al.*, 1989). A number of bimineralic eclogites exhibit FeO contents just under 5 wt%, although CaO contents for all eclogites are mostly within the defined basaltic field. The kyanite and high Na-Al eclogites have MgO contents within the defined basaltic range, but the remaining eclogites (bimineralic and opx-bearing) all have contents greater than 15 wt%. Overall though, the whole-rock compositions of the Rietfontein eclogites are broadly basaltic.

8.4.1 Inter-group variation

Kyanite eclogites have Al_2O_3 contents that exceed those of the remaining eclogites, a direct consequence of the presence of up to 20% modal kyanite. Al_2O_3 contents range from 22-27 wt% and Na_2O contents range from 2.1-3.19 wt%. The high Na-Al eclogites, which do not contain kyanite, have lower Al_2O_3 contents of 16-17.8 wt%. The presence of kyanite in only five of the high Al-Na eclogites suggests the existence of a threshold amount of Al_2O_3 in the protolith for these rocks, above which the final product will contain primary kyanite (Jerde *et al.*, 1993*a*). TiO_2 in the kyanite eclogites shows a factor of 10 variation, from 0.07-1.16 wt%. These higher

Table 8.1 *Reconstructed major element compositions of selected Rietfontein eclogites.*

	Bimineralic eclogites							
	JJG 105	**PC1**	**Rtfn 31-3**	**Rtfn 55-4**	**Rtfn 43-10**	**CMA 1**	**CMA 6**	**CMA 9**
SiO_2	47.62	48.30	47.25	47.30	46.85	47.90	47.80	47.73
TiO_2	0.22	0.15	1.15	0.10	0.24	0.10	0.08	0.17
Al_2O_3	14.20	13.04	13.57	12.56	14.02	12.91	11.88	12.92
Cr_2O_3	0.31	0.17	0.11	0.36	0.10	0.31	0.98	0.47
FeO	8.74	5.36	5.91	7.41	9.02	6.80	6.24	5.36
MnO	0.19	0.17	0.22	0.24	0.20	0.23	0.26	0.20
MgO	16.05	18.79	18.14	16.12	14.78	15.48	17.80	18.43
CaO	11.38	13.84	12.26	15.08	12.81	15.85	13.95	13.62
Na_2O	1.50	0.43	1.16	0.64	1.46	0.66	0.44	0.84
K_2O	0.01	0.00	0.00	0.01	0.00	0.00	0.00	0.00
Total	**100.22**	**100.26**	**99.76**	**99.83**	**99.47**	**100.24**	**99.42**	**99.75**
Mg#	76.60	86.20	84.55	79.51	74.49	80.23	83.57	85.96

	Kyanite eclogites				Opx-bearing eclogites			
	JJG 2104	**Rtfn 54-1**	**Rtfn 54-4**	**Rtfn 55-3**	**PC 5.2/1**	**CMA 3**	**CMA 12**	**CMA13**
SiO_2	44.92	45.65	45.07	46.61	48.61	49.00	48.85	47.93
TiO_2	0.07	0.17	1.13	0.32	0.16	0.07	0.23	1.00
Al_2O_3	26.71	23.08	22.25	17.31	13.72	9.62	13.06	11.71
Cr_2O_3	0.02	0.02	0.06	0.03	0.29	0.49	0.18	0.67
FeO	5.34	7.98	7.72	8.59	8.34	10.68	8.06	6.97
MnO	0.08	0.12	0.12	0.14	0.19	0.36	0.19	0.23
MgO	6.29	7.62	8.31	9.77	16.95	18.54	17.97	17.92
CaO	14.24	12.88	12.07	13.67	10.22	10.63	9.98	12.94
Na_2O	2.11	2.67	2.79	3.19	1.77	0.52	1.63	0.51
K_2O	0.00	0.00	0.00	0.01	0.01	0.00	0.01	0.00
Total	**99.79**	**100.19**	**99.52**	**99.64**	**100.26**	**99.91**	**100.14**	**99.88**
Mg#	67.73	62.98	65.75	66.97	78.37	75.59	79.90	82.10

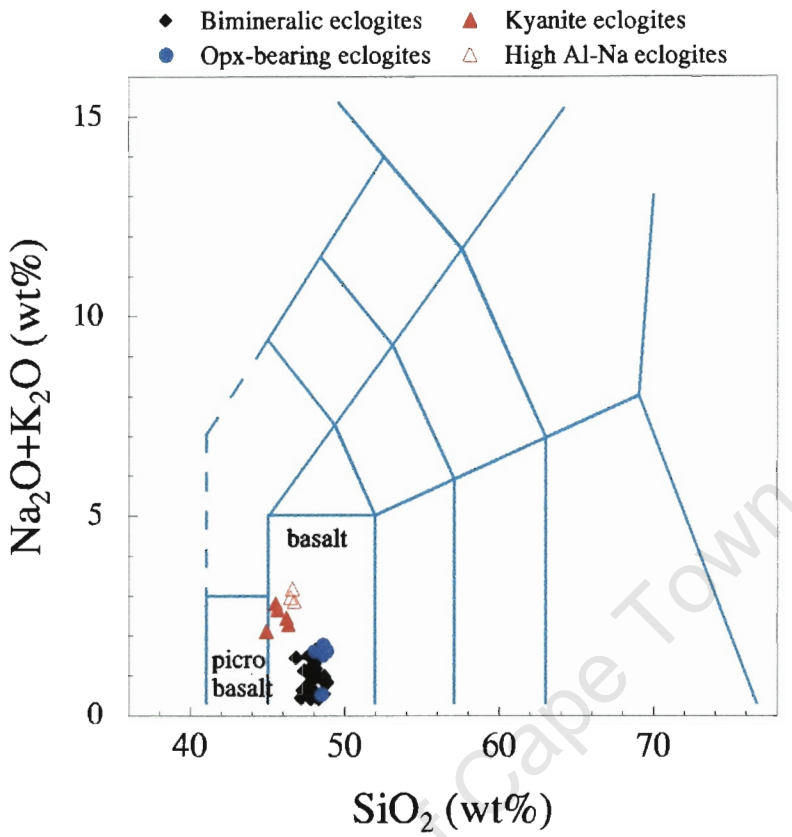

Figure 8.2 *Chemical classification of the Rietfontein eclogites, using the total alkali vs silica (TAS) diagram of Le Maitre (1989), based on reconstructed whole rock compositions.*

Ti eclogites are those that contain visible rutile, but the abundance of Ti in the remaining eclogites is low for a basaltic rock. It is likely that rutile is present in most of the eclogites, but was not present in the limited sample available for study, and was thus not accounted for when reconstructing the whole rock compositions. FeO and MgO contents in the kyanite eclogites range from 5.3-9.6 wt% and 6.3-10 wt%, respectively. CaO contents are more restricted, from 12-15 wt%. SiO_2 abundances in the kyanite eclogites are lower than those of the bimineralic and orthopyroxene-bearing eclogites and they also exhibit the lowest Mg#'s (< 72). The effect of lower MgO contents on the Rietfontein kyanite eclogites can be seen in *Figure 8.3a*, where they form a distinct group at higher Ca/(Ca+Mg) and lower Mg/(Mg+Fe) ratios. *Figure 8.3b* illustrates the lower Cr and higher Al abundances in the kyanite eclogites, compared to the bimineralic and orthopyroxene-bearing eclogites. The kyanite and high Na-Al eclogite groups all have Cr-ratios ≤ 1 and, whereas a number of bimineralic and kyanite eclogites have similar values,

most are greater than 1. In *Figure 8.3*, error bars on sample JJG 105 further illustrate the consequences of variable garnet:clinopyroxene modal proportions, where garnet:clinopyroxene proportions of 60:40 and 40:60 were accounted for.

The orthopyroxene-bearing and bimineralic eclogites are very similar in terms of major element whole-rock compositions. Mg#'s range upwards of 74, Al_2O_3 = 9-14%, FeO = 4-10 wt%, CaO = 10-16 wt%, and MgO contents are all greater than 15 wt%. The higher average Cr_2O_3 concentrations of the bimineralic and orthopyroxene-bearing eclogites are illustrated in *Figure 8.3b*, where the bimineralic eclogites form a distinct group at higher Mg/(Mg+Fe) ratios. Variation in the TiO_2 contents of the bimineralic and orthopyroxene-bearing eclogites is similar to that of the kyanite eclogites, with the visibly rutile-bearing eclogites exhibiting higher TiO_2 abundances (*Figure 8.4a*). The bimineralic and orthopyroxene-bearing eclogites have higher MgO and Cr_2O_3, and lower Na_2O and Al_2O_3 than the kyanite eclogites.

8.4.2 Mafic rock similarities

The compositional differences between the Rietfontein eclogite groups, and their relationship to the compositional fields of some mafic igneous rocks and boninites are illustrated in *Figure 8.4a-d*. The kyanite and bimineralic/orthopyroxene-bearing eclogites are compositionally distinct from each other and similarities can be seen between the Rietfontein eclogites and a number of igneous rock groups. One of the major differences between MORB and eclogites is the average lower TiO_2 content in eclogites. This is illustrated in *Figure 8.4a*, where most of the Rietfontein eclogites can be seen to have much lower TiO_2 abundances than MORB or komatiites, although the kyanite eclogites fall within the oceanic gabbro field. The rutile-bearing eclogites have higher TiO_2 contents and thus plot within both the MgO and TiO_2 MORB compositional fields. The kyanite eclogites have similar CaO, NaO and Al_2O_3 contents to both oceanic gabbros and MORB (*Figure 8.4b-d*), but for the most part can be represented entirely by the gabbroic field. A significant amount of overlap with boninites can be noted for many of the kyanite eclogite major element components.

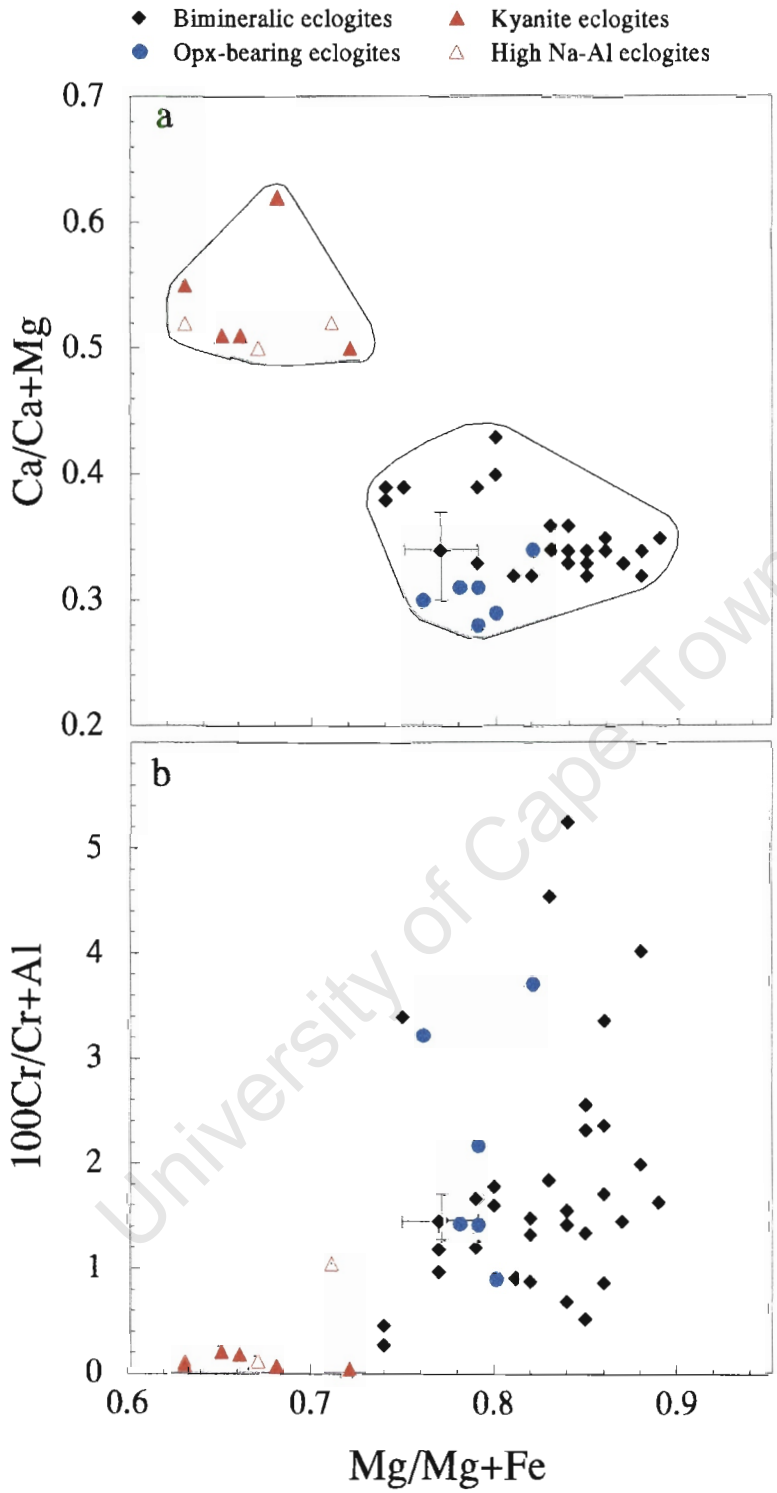

Figure 8.3 *Major element ratios for the Rietfontein eclogites plotted as a function of Mg# (Mg/(Mg+Fe)).* ***a)*** *Ca/(Ca+Na) vs Mg/(Mg+Fe) and* ***b)*** *Cr/(Cr+Al) vs Mg/(Mg+Fe). In a), the distinction between the kyanite and remaining eclogite groups is clearly visible. Figure 8.3b illustrates the overall lower Cr contents in eclogitic garnets. The error bars in each diagram represent the compositional differences that variable garnet:cpx (60:40 - 40:60) proportions makes on sample JJG 105.*

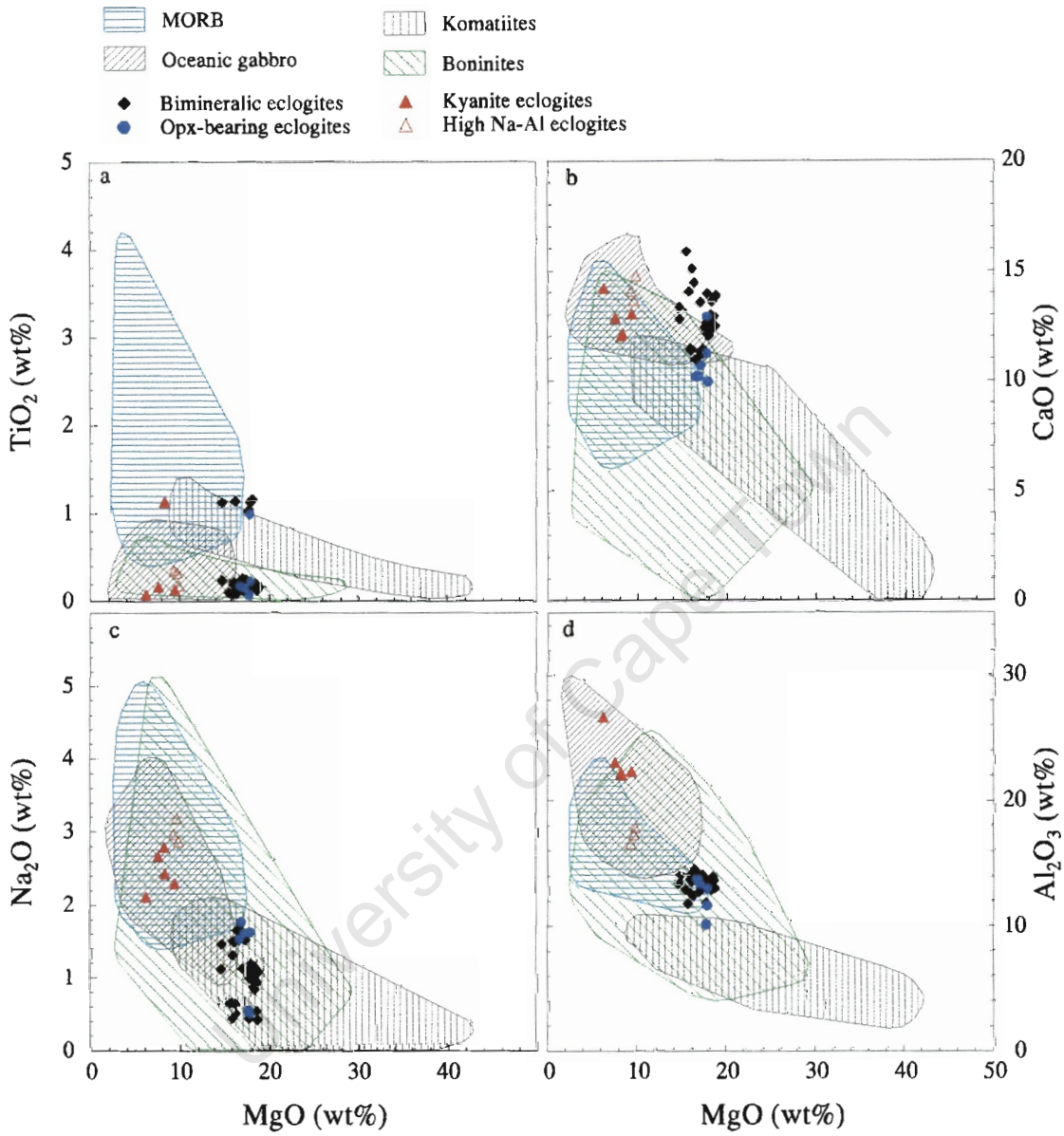

Figure 8.4 *Comparative whole-rock major element diagrams for the Rietfontein eclogites.* ***a)*** *TiO_2 vs MgO;* ***b)*** *CaO vs MgO;* ***c)*** *Na_2O vs MgO; and* ***d)*** *Al_2O_3 vs MgO. MORB data from le Roex et al., 1983; le Roex et al., 1985; le Roex et al., 1987; le Roex et al., 1996; le Roex et al., 1989; Mahoney et al., 1992. Gabbro data represents oceanic and olivine gabbros from the South West Indian Ridge (Meyer et al., 1989; Dick et al., 1999). Komatiite data from Smith & Erlank, 1982; Jahn et al., 1982; Parman et al., 1997; Byerly, 1999; Venneman & Smith, 1999; Polat et al., 1999. Boninite data from Bloomer, 1989; Brown & Jenner, 1989; Cameron, 1989; Crawford et al., 1989; Coish, 1989; Hickey-Vargas, 1989; van der Laan et al., 1989; Sobolev & Danyushevsky, 1994; Kerrich et al., 1998.*

The Rietfontein bimineralic and orthopyroxene-bearing eclogites show strong compositional similarities, as well as compositional overlap with a number of igneous rocks. TiO_2 contents are variable, depending on the presence of rutile, and the high-Ti eclogites fall within the MORB compositional field (*Figure 8.4a*). Compositional similarities to boninites on the basis of TiO_2 and MgO may also be noted. Many of the Rietfontein bimineralic eclogites exhibit CaO contents (*Figure 8.4b*) greater than those observed in boninites, komatiites or basaltic rocks, but the lower Ca eclogites overlap into the boninite, komatiite and oceanic gabbro fields. Igneous rocks show a large range in Na_2O contents (*Figure 8.4c*) and the bimineralic and orthopyroxene-bearing eclogites show compositions most similar to boninites and low-Mg (basaltic) komatiites. Al_2O_3 abundances in the bimineralic and orthopyroxene-bearing eclogites plot well within the boninite defined field (*Figure 8.4d*), but also show similarities to MORB.

8.5 Trace element compositions

8.5.1 General observations

Reconstructed whole-rock trace element compositions of the Rietfontein eclogites are presented in *Table 8.2*. As with the major element chemistry, the kyanite eclogites show significant differences to the bimineralic and orthopyroxene-bearing eclogites with regard to their trace element chemistry. On average, the kyanite eclogites have lower Sc, Zr, Ce and Nd concentrations than the other eclogites (illustrated in Figure *8.5a, b & d*), but the rest of the trace element concentrations are similar between all the petrographic groups. The relative abundances of the trace elements Nd, Sc, Ni, Ce and Zr are illustrated in *Figure 8.5a-d*. Calculated Ni (88-274ppm) and Sr (13-208ppm) concentrations in the eclogites are both highly variable and Sc shows a very wide concentration range (11-99ppm). *Figure 8.5b* shows that the higher Sc abundances are distinct outliers when considering the remaining eclogites. Both garnet and clinopyroxene from these two samples (CMA 1 and CMA 3) have higher Sc contents than other samples, resulting in a higher whole-rock Sc abundance. These higher Sc contents are thus not anticipated to be the result of analytical error. Broad positive correlations are evident between Sc, Nd, Ce and Zr (*Figure 8.5*), whereas Ni in bimineralic eclogites decreases with increasing Zr. As was the case with the major element mineral chemistry, a group of seven eclogites (six bimineralic and one orthopyroxene-bearing eclogite) contain slightly higher Zr concentrations than the other eclogites, although this is to be expected after reconstructing the whole-rock chemistry

Table 8.2 *Reconstructed whole-rock trace element compositions of the Rietfontein eclogites. All data reported in ppm.*

	Kyanite & high Na-Al eclogites					Opx-bearing eclogites		
	JJG 2104	Rtfn 54.1	Rtfn 54.4	CMA 4	CMA 17	PC 5.2/1	CMA 3	CMA 12
Sc	10.9	17.1	24.5	19.8	35.8	32.4	96.2	37.8
Ni	223	162	123	244	96.7	274	202	157
Sr	69.6	145	187	94.4	54.1	164	17.2	120
Y	4.17	8.11	10.9	6.68	8.75	6.63	9.17	15.3
Zr	2.77	7.35	9.12	6.61	6.34	11.3	6.56	21.4
La	0.00	0.01	0.03	0.00	0.67	4.52	0.80	5.61
Ce	0.13	0.32	0.54	0.09	2.12	10.2	1.68	14.2
Nd	1.00	3.04	3.01	2.40	2.08	5.90	1.07	7.13
Sm	0.57	1.96	1.64	1.13	1.01	1.40	0.36	1.79
Eu	0.44	0.93	0.82	0.53	0.45	0.46	0.12	0.62
Gd	0.66	1.83	1.81	1.07	1.40	1.25	0.60	2.26
Dy	0.72	1.63	2.14	1.16	1.64	1.15	1.33	2.67
Er	0.50	0.79	1.17	0.77	0.93	0.70	1.22	1.56
Yb	0.43	0.63	0.98	1.01	0.99	0.72	1.30	1.84

	Bimineralic eclogites							
	JJG 105	PC 1	Rtfn 31.1	Rtfn 43.1	Rtfn 48.2	Rtfn 55.1	Rtfn 55.2	Rtfn 57.1
Sc	32.5	23.9	35.9	51.8	51.9	43.8	35.0	33.9
Ni	186	87.9	186	115	174	152	169	189
Sr	194	84.3	89.2	163	209	107	111	104
Y	6.62	6.00	5.50	12.2	4.43	11.3	4.17	6.05
Zr	23.7	6.66	8.67	32.8	32.5	33.2	15.3	9.27
La	7.86	2.04	1.51	9.97	12.6	5.52	3.48	3.90
Ce	21.5	4.54	4.64	22.8	31.4	13.0	9.94	9.65
Nd	11.4	4.99	3.50	11.0	14.3	7.17	8.96	5.13
Sm	2.03	1.64	1.00	2.09	2.27	1.53	2.04	1.09
Eu	0.63	0.59	0.37	0.70	0.64	0.47	0.43	0.36
Gd	1.62	1.49	0.98	1.88	1.62	1.49	1.01	1.04
Dy	1.29	1.16	0.98	2.04	0.94	1.91	0.78	1.13
Er	0.68	0.63	0.58	1.33	0.42	1.38	0.50	0.69
Yb	0.69	0.59	0.59	1.40	0.42	1.44	0.46	0.64

	Bimineralic eclogites			
	CMA 1	CMA 5	CMA 8	CMA 14
Sc	98.9	35.9	56.4	45.9
Ni	233	162	175	158
Sr	13.3	83.2	108	105
Y	9.42	14.1	8.49	9.22
Zr	2.81	23.7	31.9	5.83
La	0.57	3.43	5.47	2.23
Ce	1.26	9.18	13.5	4.03
Nd	0.69	6.25	8.34	2.67
Sm	0.34	1.73	2.29	0.84
Eu	0.15	0.61	0.77	0.33
Gd	0.84	2.24	2.43	1.07
Dy	1.62	2.60	1.76	1.48
Er	1.07	1.54	0.86	1.17
Yb	0.94	1.70	0.70	1.18

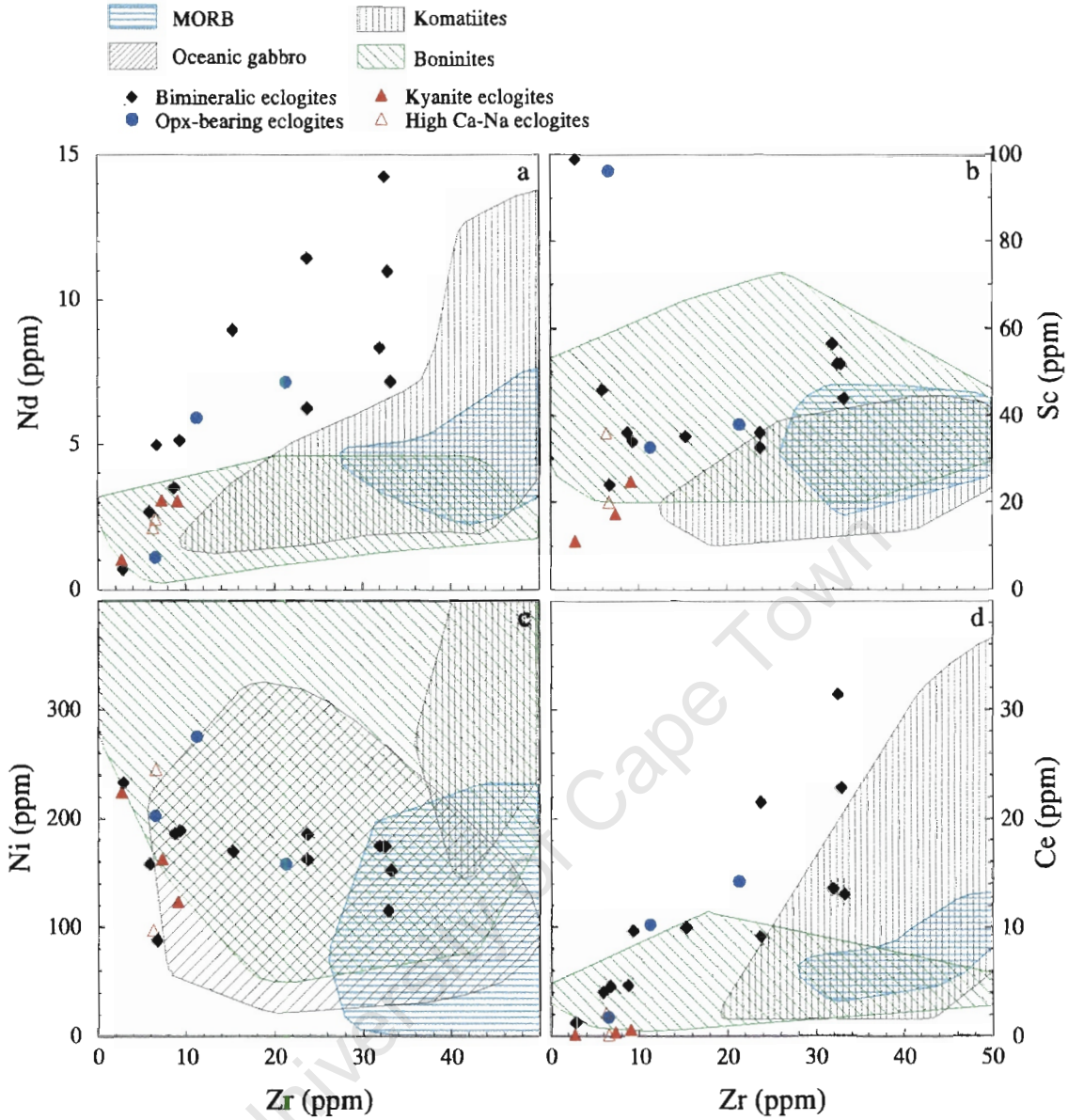

Figure 8.5 *Selected trace element abundances in Rietfontein eclogites, compared to abundances in a variety of igneous rocks. MORB data from le Roex & Dick, 1981; le Roex et al., 1983; Humphris et al., 1985; le Roex et al., 1985; Price, 1986; le Roex et al., 1987; le Roex et al., 1989; le Roex et al., 1996. Gabbro data from Dick et al., 1999. Komatiite data from Jahn et al., 1982; Parman et al., 1987; Polat et al., 1999. Boninite data from Bloomer, 1989; Brown & Jenner, 1989; Cameron, 1989; Coish, 1989; Crawford et al., 1989; Sobolev & Danyushevsky, 1994; Kerrich et al., 1998.*

from the mineral chemistry. These higher Zr-eclogites all have Zr contents > 30ppm, whereas the remaining eclogite groups all have abundances < 15ppm. Zr contents for the entire eclogite suite range from 3-33ppm.

8.5.2 REE patterns

Figure 8.6 presents REE patterns for selected Rietfontein eclogites, reconstructed using garnet:clinopyroxene ratios of 50:50. Kyanites from the kyanite eclogites were analysed for REE concentrations but no significant concentrations were measured and orthopyroxenes were not analysed due to sample shortages. REE patterns for both the kyanite and orthopyroxene-bearing eclogites were thus constructed in the same manner as those for the bimineralic eclogites, using only garnet and clinopyroxene.

A number of REE patterns are exhibited by the bimineralic and orthopyroxene-bearing eclogites (*Figure 8.6, top and middle*). A number of these eclogites exhibit relatively flat REE patterns, with REE concentrations of 10-20x chondrite. A common pattern exhibited by the Rietfontein eclogites (both bimineralic and orthopyroxene-bearing) is one that decreases from LREE to HREE (*eg.* Rtfn 48.2, PC 5.2/1). The enrichment of LREE in these decreasing REE patterns ranges between 15-60x chondrite, whereas HREE concentrations vary between 2-10x chondrite. It is interesting to note that the sample showing the greatest LREE enrichment (Rtfn 48.2), also shows the greatest HREE depletion. Although some of the REE patterns decrease smoothly from LREE to HREE, some eclogites (*eg.* Rtfn 43.1, Rtfn 57.1) show relatively flat HREE patterns. Slightly more unusual REE patterns are exhibited by samples CMA 1 and CMA 3, which show a pattern of decreasing REE concentrations from La to Nd and La to Eu respectively, and then an increasing pattern from the MREE onwards. CMA 1 exhibits a relatively flat HREE (from Dy to Yb) pattern, whereas the pattern of CMA 3 smoothly increases from Eu through to Yb. Once again, it can be seen that the REE patterns of the bimineralic and orthopyroxene-bearing eclogites show a number of similarities. The LREE concentrations of these two samples varies between 1.5-4x chondrite, whereas the HREE show enrichment levels of up to 10x chondrite.

The kyanite eclogites exhibit vastly different calculated bulk rock REE patterns and are strongly LREE depleted (0.03-1x chondrite) (*Figure 8.6, bottom*). A distinctive feature of these eclogites

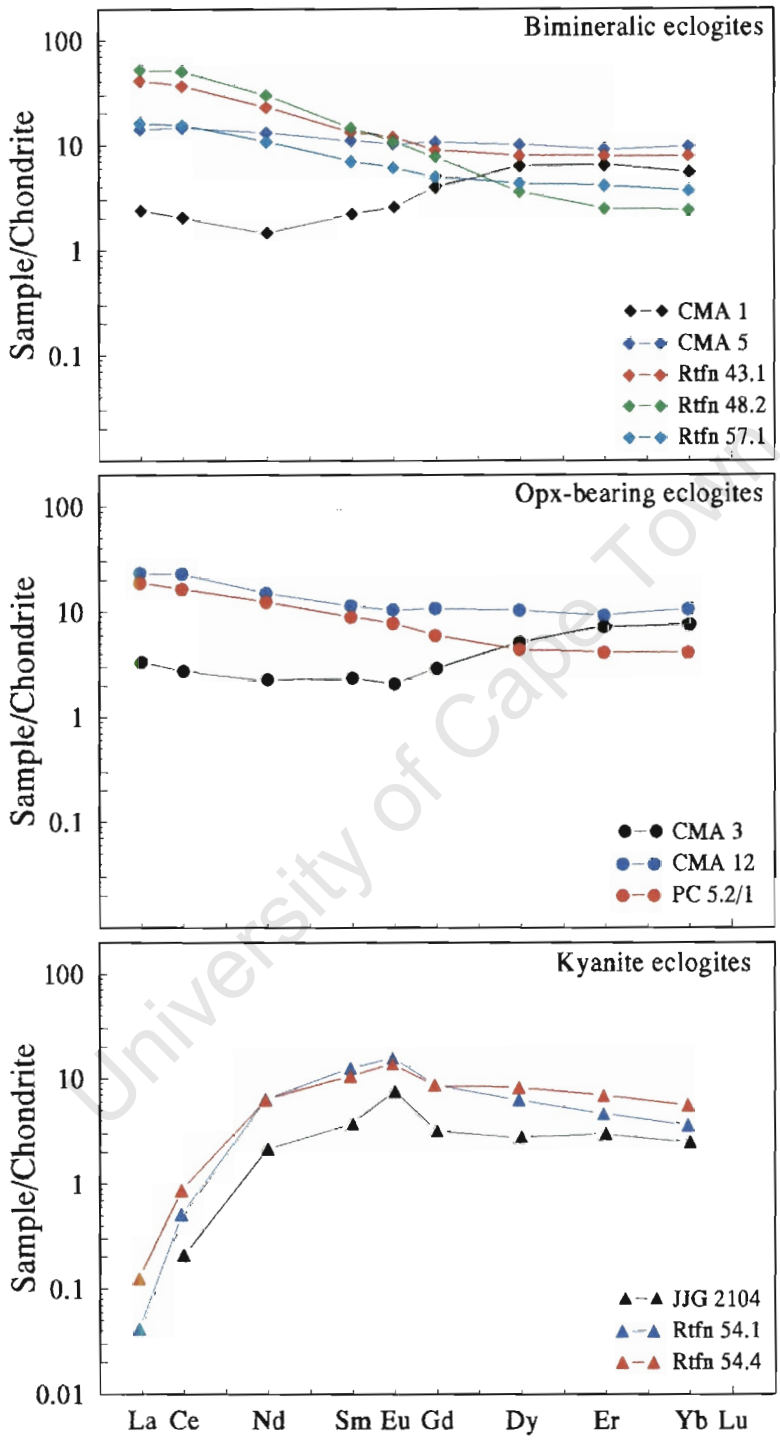

Figure 8.6 *Whole-rock REE abundances of selected bimineralic (top), opx-bearing (middle) and kyanite eclogites (bottom) from Rietfontein, reconstructed using equal garnet and clinopyroxene proportions. Concentrations are chondrite normalised after Sun & McDonough (1989).*

is the presence of a positive Eu anomaly, most pronounced in sample JJG 2104, which contains the most calcic garnet and the highest modal proportion of kyanite. The HREE enrichment of these samples is moderate, at concentrations of 2-4x chondrite. The concave upward patterns of the light and middle REE are a characteristic feature of these kyanite eclogites, and echoes the patterns observed in the garnets and clinopyroxenes of these samples. The middle to heavy REE transition is seen to be a decreasing pattern in a number of the kyanite eclogites, but sample JJG 2104 exhibits an almost flat middle to heavy REE pattern. The kyanite eclogites have extremely low $[La/Yb]_N$ values (< 0.05).

8.5.3 Mafic rock similarities

Compositional fields for trace elements from select igneous rocks are illustrated in *Figure 8.5*. The Rietfontein eclogites often show a compositional spread outside fields of mafic igneous rocks. The kyanite eclogites have Zr contents far lower than those found in MORB (*Figure 8.5*), although Ni contents are similar to those reported in oceanic gabbros. The only other igneous field into which the kyanite eclogites overlap is the boninite field, where similar Nd, Sc and Ni abundances can be seen (*Figure 8.5 a-c*).

The bimineralic and orthopyroxene-bearing eclogites also show trace element compositional similarities to boninites. Ni, Zr and Sc abundances are all very similar (*Figure 8.5 b-c*) but most of the bimineralic and orthopyroxene-bearing eclogites have Nd and Ce abundances much higher than those in boninites. Very little compositional overlap can be seen between the eclogites and either MORB or komatiites. There are however, similarities between the Ni and Zr contents of oceanic gabbros and the bimineralic and orthopyroxene-bearing eclogites (*Figure 8.5c*).

Figure 8.7 compares REE patterns for a number of igneous rock types (gabbro, basalts, MORB, komatiite and boninite) with REE patterns exhibited by the Rietfontein eclogites. Gabbros are often characterised by positive Eu anomalies, a result of plagioclase accumulation in the source region, although negative Eu anomalies may also be present, produced when plagioclase is removed from a system (Pallister & Knight, 1981). Both positive and negative Eu anomalies have also been noted in MORB (*eg.* Puchelt *et al.*, 1977; Dostal & Muecke, 1978). These positive Eu anomalies in MORB and ophiolitic gabbros compare favourably with the positive Eu

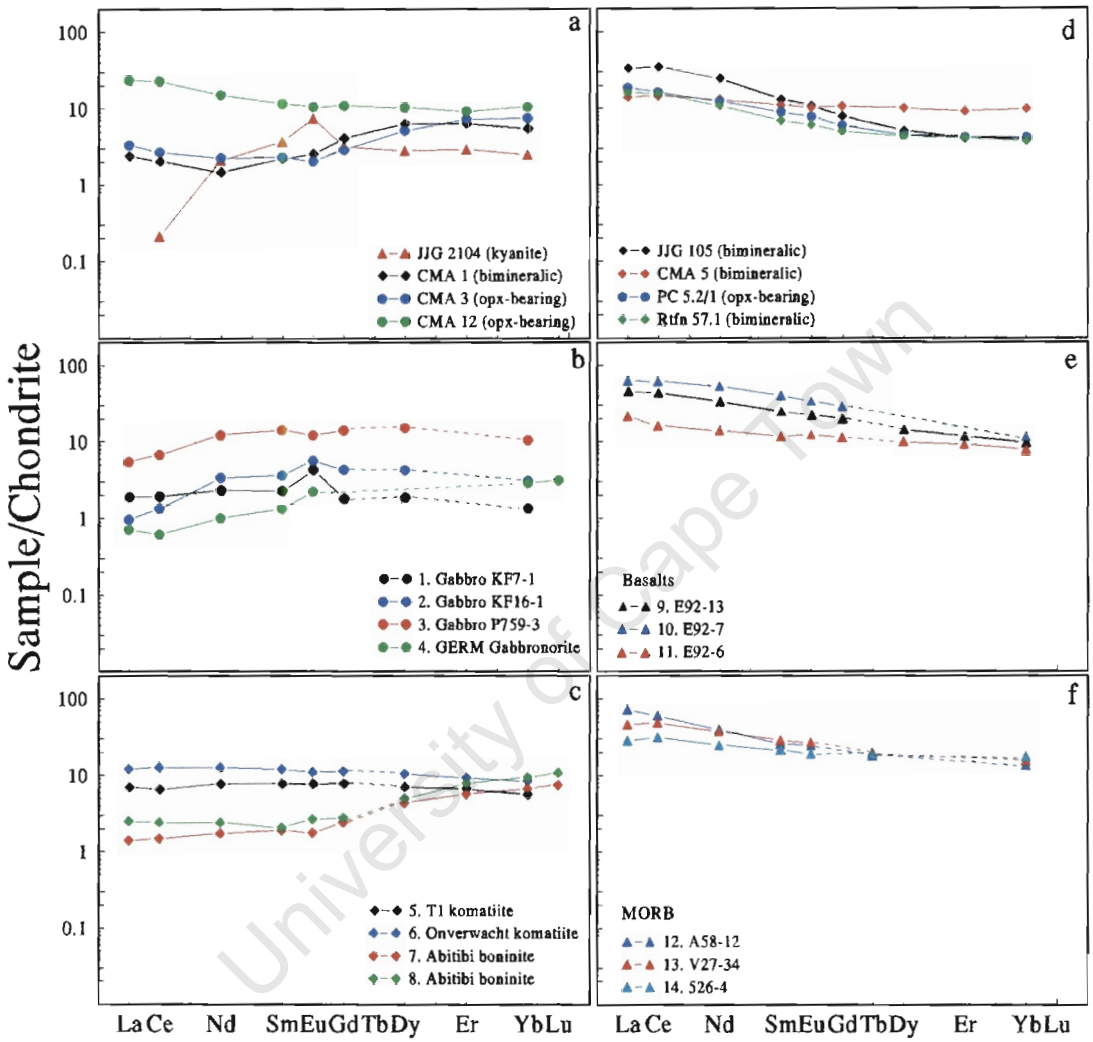

Figure 8.7 *Whole-rock REE patterns for select igneous rocks, compared to patterns of the Rietfontein eclogites (**a** & **d**). **1,2** & **3**: Gabbro (Pallister & Knight, 1981); **4**: Oceanic gabbronorite (Booij & Staudigel, 1996); **5**: Al-undepleted komatiite (Xie et al., 1993); **6**: Basaltic komatiite (Jahn et al., 1982); **7** & **8**: Boninites (Kerrich et al., 1998); **9-11**: Basalts (Kerr et al., 1996); **12**: MORB (le Roex et al, 1983); **13**: MORB (le Roex et al., 1985); **14** MORB (le Roex et al., 1983).*

anomalies observed in the kyanite eclogites from Rietfontein (*Figure 8.7a*), although the LREE depletion in the Rietfontein eclogites is far more extreme. Abundances of HREE are however similar to those of the gabbros.

A number of Rietfontein bimineralic and orthopyroxene-bearing eclogites exhibit REE patterns with a slight negative Eu anomaly (*Figure 8.7a*), a pattern which is not unusual, having been recorded in boninites (*eg.* Kerrich *et al.*, 1998), gabbros (*eg.* Pallister & Knight, 1981) and MORB (*eg.* Puchelt *et al.*, 1977). Flat REE patterns, such as those found in some basaltic komatiites (*Figure 8.7c*) and MORB (*Figure 8.7f*), are very similar to the flatter whole-rock REE patterns of the Rietfontein bimineralic and orthopyroxene-bearing eclogites (*Figure 8.7a & d*). The smoothly decreasing REE patterns of basalts from Gorgona (*Figure 8.7e*) and MORB (*Figure 8.7f*) show an overall similarity to the bimineralic and orthopyroxene-bearing eclogites of Rietfontein.

On the basis of REE patterns alone, it is strongly suggested that many of the Rietfontein eclogites may be the result of metamorphism of subducted oceanic crust. This crust may be the basaltic upper layers and sheeted dykes, or the underlying gabbroic layers, and both may be represented by the eclogites. Some of the eclogites exhibit the flat REE patterns that are characteristic of komatiites, whereas others show marked REE similarities to boninites, implying crust with boninitic affinities.

8.6 Discussion

8.6.1 Major elements

The Rietfontein kyanite eclogites show striking compositional similarities to both oceanic gabbros and MORB (*Figure 8.4*). The kyanite eclogites are also seen to show a number of major element correlations with boninites, although the kyanite eclogites extend to higher Al_2O_3 concentrations. The Mg#'s of the kyanite eclogites (63-72) correlate with the Mg#'s of MORB (35-79; le Roex & Dick, 1981; le Roex *et al.*, 1987) and oceanic gabbros (up to 86; Dick *et al.*, 1999). In all geochemical aspects, with the exception of TiO_2 contents, the kyanite eclogites are similar to basaltic (MORB and oceanic gabbro) rocks. The similarities of the bimineralic and orthopyroxene-bearing eclogites to basaltic and gabbroic oceanic crust are not quite as

convincing. A small amount of compositional overlap occurs in the fields of MORB and gabbros, depending on the component, but similarities to boninites seem to be more striking. Some overlap with komatiites can be observed, but these tend to be with the lower-Mg, basaltic komatiites, again substantiating the basaltic nature of these rocks. The Rietfontein eclogites do have a broadly basaltic composition (*Figure 8.2*), but the Mg#'s of the bimineralic eclogites can reach 88, greater than that found in MORB or gabbro (le Roex *et al.*, 1987; Dick *et al.*, 1999). These Mg#'s could be too high to represent metamorphosed oceanic crust and the primary compositions may imply derivation directly from a cumulate basaltic magma chamber.

The low Mg#'s and similarities of the kyanite and high Na-Al eclogites to oceanic crustal material (gabbroic and basaltic) suggests derivation of these eclogites from such igneous protoliths. The kyanite and high Na-Al eclogites are compositionally distinct from the bimineralic and orthopyroxene-bearing eclogites and it is thus unlikely that these groups are petrogenetically related in any way. These kyanite and high Na-Al eclogites most likely represent subducted, and subsequently metamorphosed oceanic crust. Based on major element compositional similarities, it seems plausible that basaltic oceanic crust was subducted and metamorphosed to eclogite. A more aluminous and more plagioclase-rich crustal section may have resulted in the kyanite eclogites than the crust which gave rise to the high Na-Al eclogites, which lack kyanite and are thus not as aluminous. The boninitic affinities of the bimineralic and orthopyroxene-bearing eclogites suggests generation of boninite magmas, which may occur during ocean-floor spreading at a mid-ocean ridge spreading centre (Crawford *et al.*, 1989), resulting in oceanic crust with both basaltic and boninite similarities.

8.6.2 Trace elements

The large positive Eu anomalies in the Rietfontein kyanite eclogites provide compelling evidence that these eclogites had protoliths that were relatively enriched in plagioclase. Gabbroic rocks commonly possess positive Eu anomalies and are thus a logical protolith for the Rietfontein kyanite eclogites. The high Na-Al eclogites (kyanite absent) show similar REE patterns to the kyanite eclogites, although the Eu anomaly is not as pronounced and in one case the REE pattern is much flatter, similar to the bimineralic eclogites. MORB and gabbros can both exhibit positive or negative Eu anomalies (Puchelt *et al.*, 1977; Pallister & Knight, 1981), or neither. Plagioclase-

rich oceanic crust (gabbro) is the most likely crustal protolith of the Rietfontein kyanite eclogites, based on the presence of a positive Eu anomaly. The similarities of many of the eclogite REE patterns to MORB suggests that these eclogites may represent the metamorphosed upper portion of oceanic crust, despite the fact that the eclogites have higher, more primary Mg#'s. The LREE depletion of the Rietfontein kyanite eclogites may be the result of partial melting of the eclogites after metamorphism from oceanic crust. Partial melting has been suggested as a method of fractionating LREE (to the melt) from the HREE (left in the residue), to account for extreme LREE depletion and flat HREE patterns in eclogites from other localities (Taylor & Neal, 1989; Jerde *et al.*, 1993*a*). Such processes may also add or remove Eu anomalies, making Eu a poor indicator on which to base universal eclogite classifications (Jerde *et al.*, 1993*a*).

Absolute trace element abundances of the Rietfontein eclogites are sometimes higher than those observed in MORB, komatiites and boninites (*Figure 8.5*). These relative enrichments may be due to metasomatic or alteration processes, known to enrich rocks in such incompatible elements such as LREE (Erlank *et al.*, 1987). MORB from the FAMOUS Valley, on the Mid-Atlantic ridge have lower Zr contents than average MORB (le Roex *et al.*, 1996), and these values are similar to the low Zr abundances observed in the Rietfontein eclogites. Despite the higher trace element abundances in some cases, it is still feasible for the eclogites to have been derived from oceanic crustal rocks. Ni contents greater than 300ppm, together with $Mg/(Mg+0.85Fe^*) > 0.68$ are two criteria used to classify basic liquids as primitive (*i.e.* unfractionated) upper mantle liquids (Dawson & Carswell, 1990). Ni contents in the Rietfontein eclogites are all less than 300ppm, and the similarities of the bimineralic and orthopyroxene eclogites to basaltic rocks and boninites again implies the involvement of oceanic crust. The similar trace element patterns of boninites and MORB with many of the bimineralic and orthopyroxene-bearing eclogites provides further evidence for a link between the three rock types, in an oceanic crustal environment.

8.6.3. Summary

The whole rock composition of the Rietfontein eclogites indicates that the three different eclogite groups from Rietfontein probably represent differing protoliths. The kyanite and high Na-Al eclogites correlate with the Group C eclogites of Taylor & Neal (1989) and, like the Bellsbank Group C eclogites, probably represent subducted and metamorphosed fragments of

ancient oceanic crust rich in plagioclase. It has been suggested that eclogites from many localities were derived in such a manner (*eg.* Helmstaedt & Doig, 1975; Jagoutz *et al.*, 1984; MacGregor & Manton, 1986; Beard *et al.*, 1996). The low Mg#'s, and the major and trace element similarities of the kyanite and high Na-Al eclogites to oceanic crustal material (gabbroic and basaltic) suggests derivation of these eclogites from such igneous protoliths. The exact type and composition of oceanic crust may have resulted in two different types of eclogites, those containing kyanite, and those compositionally similar, but lacking kyanite. More aluminous and plagioclase rich crust could account for the presence of kyanite and the stronger positive Eu anomalies in the kyanite eclogites.

The kyanite and high Na-Al eclogites are compositionally distinct from the bimineralic and orthopyroxene-bearing eclogites and it is thus unlikely that these groups are petrogenetically related in any way. A number of the bimineralic and orthopyroxene-bearing eclogites also show distinct similarities to basaltic oceanic crust and may represent the basaltic portions of the crust, as opposed to the derivation of kyanite eclogites from possible gabbroic sections. Unlike the kyanite eclogites though, the link between oceanic crust and the bimineralic/orthopyroxene-bearing eclogites is not as well defined. Beard *et al.* (1996) suggested that in the case of Siberian (Mir) eclogites, low-Ca group eclogites represent the upper section of oceanic crust, consisting mostly of pillow lavas, whereas high-Ca group eclogites represent lower sections of oceanic crust, consisting mostly of massive and layered gabbros. This may be applicable to the Rietfontein eclogites, where some bimineralic and orthopyroxene-bearing eclogites with flat REE patterns represent the upper oceanic crustal section, and the kyanite eclogites represent the lower, gabbroic section of the crust. The boninitic affinities of many of the bimineralic eclogites implies the generation of boninitic magmas at some stage during oceanic crustal production, or during subduction processes. The only ambiguous compositional feature of the bimineralic and orthopyroxene-bearing eclogites is the high Mg#'s of some samples, which could be used to argue against an oceanic crustal protolith imply derivation as a cumulate from a primary basaltic magma chamber. The majority of evidence however, seems to indicate metamorphism of subducted oceanic crust, compositionally different (not as plagioclase-rich) to that which gave rise to the kyanite eclogites.

9. OXYGEN ISOTOPES

9.1 Introduction

Oxygen isotopes may provide information regarding the introduction of crustal-derived material into mantle source regions or the occurrence of crustal contamination of ascending mantle-derived magmas (Graham & Harmon, 1983). They provide a powerful tool for the examination of fluid-rock interactions (Lowry *et al.*, 1999). The usefulness of oxygen isotopes in unravelling petrogenetic histories stems from the knowledge that rocks that have equilibrated with the hydrosphere or atmosphere, and rocks that formed from magmas derived by partial melting of pristine mantle, have greatly differing stable isotope compositions (Graham & Harmon, 1983). Taylor & Sheppard (1986) conclude that "all relatively ^{18}O-depleted ($\delta^{18}O < 4.5‰$) or ^{18}O-rich ($\delta^{18}O > 7.5‰$) silicate melts on earth must have, in part been derived from, or have exchanged with, precursor material that once resided on, or near, the Earth's surface". By inference then, rocks with $\delta^{18}O$ values between 4.5‰ and 7.5‰ may not show evidence of crustal involvement and may thus be mantle derived. The great abundance of oxygen in most fluids and rocks, together with substantial differences in the $\delta^{18}O$ values of various reservoirs, makes it a useful geochemical tracer (Kyser, 1986) which can be used to place constraints on processes such as sediment recycling, differentiation and metasomatism.

Various surface, crustal and mantle oxygen isotope reservoirs have differing and distinctive ranges in $\delta^{18}O$ values, with sedimentary and crustal rocks exhibiting higher values and much larger $\delta^{18}O$ ranges than mantle derived rocks (Graham & Harmon, 1983). In a study of eclogites from the Orapa kimberlite pipe in Botswana, Deines *et al.* (1991) defined a "normal" mantle $\delta^{18}O$ range of 5-6.5‰. Mantle mineral phases are often unstable at the low pressure and temperature environment of the Earth's surface and reactions with surficial fluids will alter the original oxygen isotope compositions. Variable $\delta^{18}O$ values in the mantle may result from a number of processes, such as subduction of material with variable $\delta^{18}O$ values into the mantle, high temperature fractionation of oxygen isotopes between phases and ^{18}O enrichment by fluids rich in CO_2 or H_2O (Kyser, 1986).

A diverse range in oxygen isotopic compositions has been recorded in eclogites, with whole-rock $\delta^{18}O$ values of 2.2-9.2‰, a range almost twice that found in other mantle xenoliths (Kyser, 1990). Such anomalous $\delta^{18}O$ values in eclogites were first detected at Roberts Victor (Garlick *et al.*, 1971) and have subsequently been noted at many other localities such as Mir (Beard *et al.*, 1996), Bellsbank (Shervais *et al.*, 1988; Neal *et al.*, 1990), Orapa (Deines *et al.*, 1991) and Udachnaya (Jerde *et al.*, 1993; Jacob *et al.*, 1994). Whereas many localities exhibit $\delta^{18}O$ values that greatly deviate both above and below mantle values, Bellsbank eclogites all deviate towards lower $\delta^{18}O$ values and Udachnaya eclogites extend only 0.5‰ either side of the accepted mantle range. This lack of lower $\delta^{18}O$ values in the Udachnaya kimberlite pipe implies either that this branch of the eclogite suite is not preserved in the Siberian mantle under this particular area, or that it is simply not sampled by the Udachnaya kimberlite (Jacob *et al.*, 1994). It may also be possible that the oceanic crust, which essentially gave rise to the Bellsbank eclogites, experienced more intense hydrothermal alteration than the area from which oceanic crust forming the Udachnaya eclogites originated.

Deviations from mantle $\delta^{18}O$ values in mantle eclogites have previously been taken as unambiguous evidence of a crustal protolith for eclogites *i.e.* that eclogites may represent metamorphosed fragments of oceanic crust (Jagoutz *et al.*, 1984; MacGregor & Manton, 1986; Neal *et al.*, 1990). An earlier interpretation that the range in values could be due to fractional crystallisation (Garlick *et al.*, 1971) has been discounted (Clayton *et al.*, 1975). In order to test the possibility of crustal involvement in the petrogenesis of the Rietfontein eclogites, oxygen isotope compositions of representative samples from different compositional groups were determined. It has been shown that $\delta^{18}O$ commonly varies with eclogite chemistry (MacGregor & Manton, 1986; Neal *et al.*, 1990; Beard *et al.*, 1996), hence the analysis of garnets from different compositional population groups. If the eclogite has equilibrated internally at mantle temperatures, garnets and clinopyroxenes of a sample will have similar $\delta^{18}O$ values. The petrography of the eclogites (*Chapter 3*), together with their major and trace element data (*Chapters 4 & 7*), indicate that the Rietfontein eclogites are well equilibrated, and the garnet isotopic data is thus assumed to be representative of the samples as a whole.

9.2 Methods

Garnets from the Rietfontein eclogites were analysed by Dr C. Harris at the University of Cape Town using a laser flourination vacuum line. Details of the analytical technique can be found in *Appendix I, Section Ic*. Mineral picking of coarsely crushed eclogites resulted in garnets from five samples being selected for oxygen isotope analysis. All grains were angular fragments of larger garnet grains and the freshest, unfractured grains were selected. These grains were first cleaned in warm, dilute HF, and then acetone, in order to remove any surface weathering or alteration material. The cleanest 1-2mg grains were then selected for analysis. The results presented in *Section 9.3* were those obtained after a second set of analyses had been performed on the Rietfontein eclogites. The first set of results was unsatisfactory, having shown poor reproducibility and a wide spread of results. In the second run, samples were more carefully selected, reproducibility on the garnet standard (MON GT) was good *(Appendix I)* and more satisfactory results were obtained. For one of the samples on which replicate analyses were performed, reproducibility was better than that of the garnet standard. For the other two samples however, reproducibility was worse than that of the standard. The differences between analyses on the Ca-rich garnets of JJG 2104 were larger than those on other garnets, and could be due to the armouring effects of calcium flouride on the garnets. Each garnet analysed was derived from a different grain, and it is therefore possible that differing $\delta^{18}O$ values may indicate heterogeneities within samples.

9.3 Results

Results of the oxygen isotope analyses performed on garnets from the Rietfontein eclogites are presented in *Table 9.1*. Samples JJG 2104, CMA 4 and CMA 14 were each analysed twice in order to check analytical accuracy. Samples Rtfn 43.2 and 55.1 were only analysed once due to a shortage of material. Whereas the two oxygen isotope analyses for each of samples CMA 4 and 14 are similar (within ~0.3‰), JJG 2104 shows a greater difference between analyses (~0.9‰). This sample contained the freshest garnet grains and the large difference therefore cannot be due to the effects of alteration, but may be a result of analytical uncertainties.

Sample	$\delta^{18}O$(‰)
JJG 2104	6.84
	5.95
CMA 4	5.58
	5.82
CMA 14	5.99
	5.61
Rtfn 43.2	5.24
Rtfn 55.1	5.16

Table 9.1 *Oxygen isotope data for garnets from the Rietfontein eclogites.*

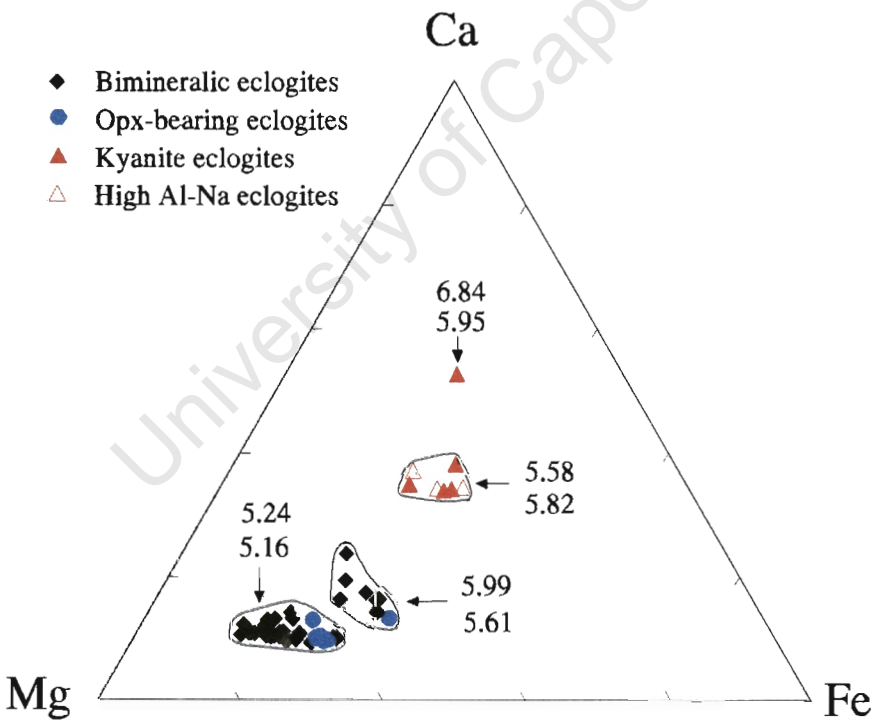

Figure 9.1 *Molar Ca-Mg-Fe diagram for garnets from the Rietfontein eclogites, together with the recorded $\delta^{18}O$ values (reported in ‰) associated with each garnet group.*

Figure 9.1 illustrates the oxygen isotope values (all reported in ‰) relative to the molar Ca, Mg and Fe compositions of the garnets. The most Ca-rich sample, JJG 2104, exhibits the highest $\delta^{18}O$ values, 6.84 and 5.95‰. The most Mg-rich samples, Rtfn 43.2 and Rtfn 55.1 contain garnets with the lowest $\delta^{18}O$ values, 5.24 and 5.16‰ respectively. The garnet groups with Mg and Ca contents intermediate to these two above-mentioned groups have intermediate $\delta^{18}O$ contents. If one disregards the outlier value of 6.84‰, all data for the Rietfontein garnets fall within the "normal" mantle range of 5-6.5‰, defined by Deines *et al.* (1991), as well as the range for ultramafic upper mantle xenoliths of 5.5±0.7‰ (Mattey *et al.*, 1994).

Figure 9.2 illustrates the variation in the cation proportions of garnet major elements relative to $\delta^{18}O$. Broad linear trends are discernable in all the diagrams. $Ca/(Ca+Mg)_{gt}$ is positively correlated with $\delta^{18}O$ (*Figure 9.2a*), whereas $Mg/(Mg+Fe)_{gt}$ and $Cr/(Cr+Al)_{gt}$ are inversely correlated with $\delta^{18}O$. No other trends or groupings were observed between $\delta^{18}O$ and any of the other major elements, trace elements or equilibration temperatures.

9.4 Discussion

Figure 9.3 illustrates the range of $\delta^{18}O$ values found in garnets from the Rietfontein eclogites, compared to eclogitic garnets analysed from southern African (Finsch, Orapa, Roberts Victor and Bellsbank) and Russian (Mir and Udachnaya) localities. $\delta^{18}O$ values from peridotitic garnets and clinopyroxenes have also been included for comparative purposes. This graph illustrates the range of $\delta^{18}O$ values observed in eclogitic garnets (2.2-9.2 ‰), and it can be seen that the most frequently reported $\delta^{18}O$ values are 5-7‰. The range of oxygen isotopes defined by Rietfontein garnets is small in comparison to other localities and lies close to the range of accepted mantle values (Deines *et al.*, 1991), with only one analysis offset to higher values. The oxygen isotope data therefore provides no clear evidence of a crustal precursor. However, the small oxygen isotope sample size must be kept in mind, as it is possible that a larger sample population may lead to a greater spread of $\delta^{18}O$ values.

Previous studies (MacGregor & Manton, 1986; Jacob *et al.*, 1994) have noted that the chemical composition of eclogite minerals can vary systematically with oxygen isotope compositions and these variations may be similar to those produced during hydrothermal alteration of oceanic crust.

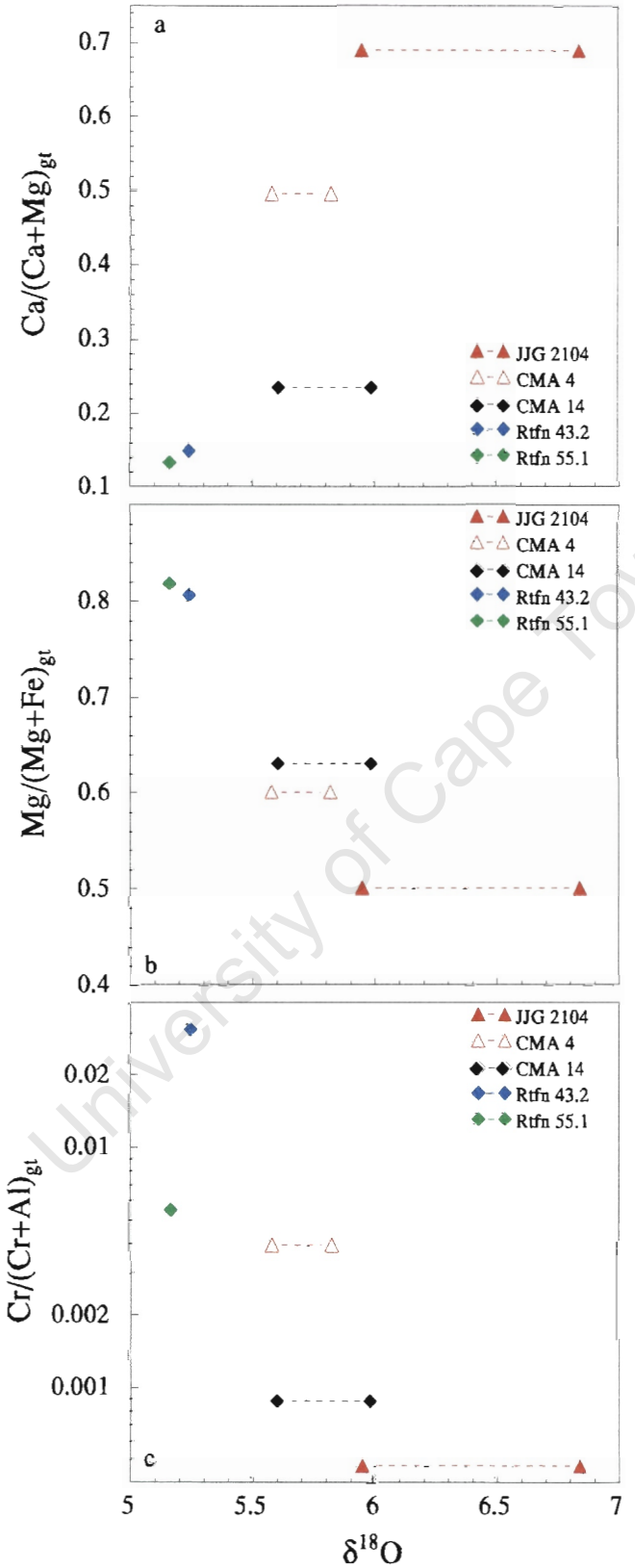

Figure 9.2 *Major element proportions plotted as a function of $\delta^{18}O$ (‰). **a)** Ca/(Ca+Mg) vs $\delta^{18}O$, **b)** Mg/(Mg+Fe) vs $\delta^{18}O$ and c) Cr/(Cr+Al) vs $\delta^{18}O$. For the samples on which replicate analyses were performed, values have been joined by a dotted line.*

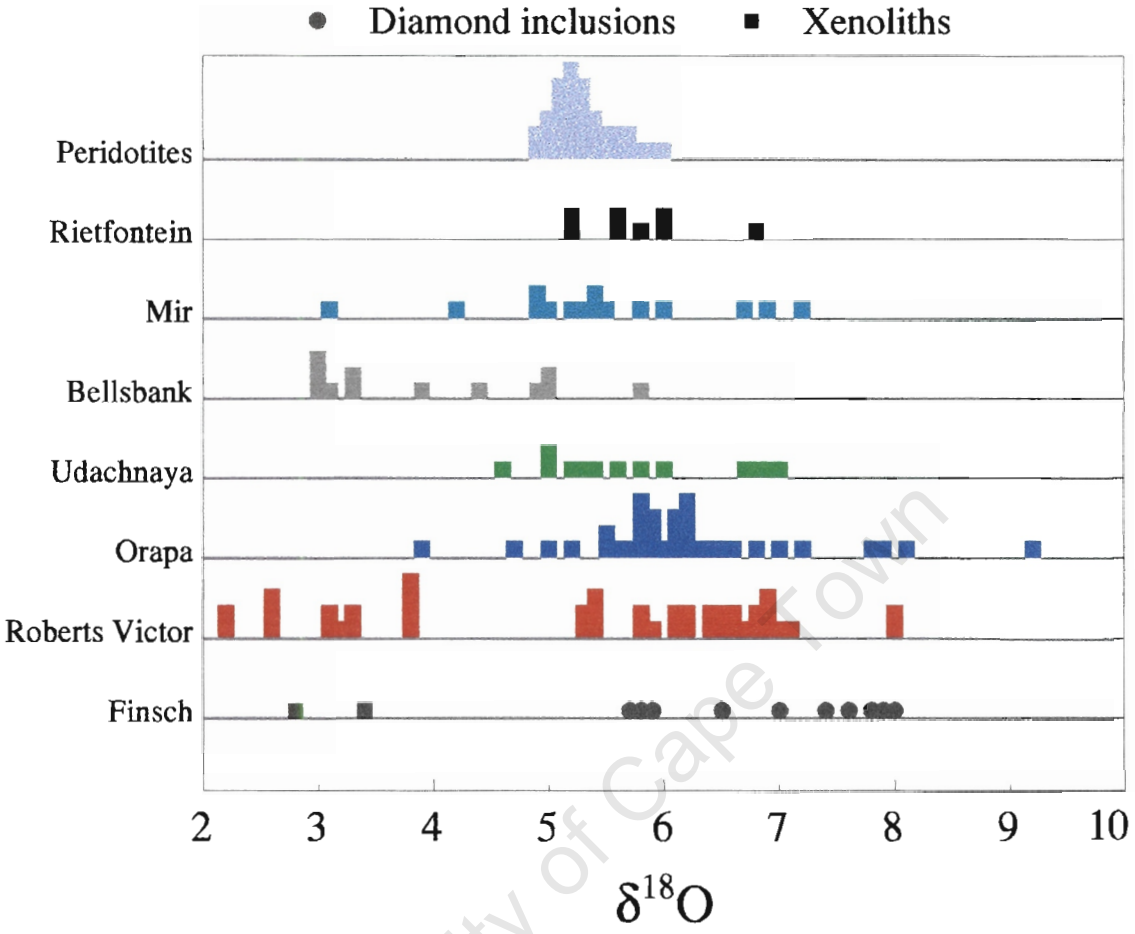

Figure 9.3 *$\delta^{18}O$ values of eclogitic garnets from xenoliths and diamond inclusions from various on-craton localities. All $\delta^{18}O$ values are reported in ‰; diamond inclusions are plotted as open circles and xenoliths are plotted as closed squares. Eclogite data from Garlick et al. (1971), Jagoutz et al. (1984), Ongley et al. (1987), Shervais et al. (1988), Neal et al. (1990), Deines et al. (1991), Jacob et al. (1994), Jerde et al. (1994), Beard et al. (1996) and Lowry et al. (1999). Peridotite data from Mattey et al. (1994), Ionov et al. (1994) and Lowry et al. (1999).*

Jacob *et al.* (1994) showed that FeO can increase and CaO can decrease with an increasing degree of low temperature alteration, as measured by increasing $\delta^{18}O$ values. These negative trends of CaO and $\delta^{18}O$ provide support for the involvement of oceanic crust in the eclogite protolith (Snyder *et al.*, 1997). Correlations of MgO, Na_2O and whole-rock K_2O have also been noted (MacGregor & Manton, 1986; Deines *et al.*, 1991) and such direct correlations are consistent with hydrothermal alteration of the protolith (Kyser, 1990). Broad correlations of CaO, MgO and

FeO with $\delta^{18}O$ were observed in the Rietfontein eclogites, although there were no noted Na_2O or K_2O correlations. High temperature magma fractionation processes may also be responsible for compositional and isotopic correlations, as may be garnet-clinopyroxene fractionation. Equilibrium oxygen isotope fractionations between clinopyroxene and garnet depend significantly on the major element chemical compositions of both phases (Beard *et al.*, 1996), with an increased jadeite component increasing clinopyroxene-garnet fractionation and an increased pyrope content decreasing the fractionation (Matthews *et al.*, 1983). These two effects act in the same direction in eclogites from Mir, giving larger isotopic fractionations for Ca-rich rocks (Beard *et al.*, 1996), and a similar process may have occurred in the Rietfontein eclogites. However, the major element correlations show most consistency with alteration of basalt by sea-water and this is the most likely explanation for the oxygen isotope characteristics of the Rietfontein eclogites.

9.5 Conclusion

Information derived from the oxygen isotopes of the Rietfontein eclogites is thus inconclusive. Whereas evidence such as the correlation of major elements with oxygen isotopes and an oxygen isotope value outside of the mantle range may be indicative of the involvement of hydrothermally altered oceanic crust in the genesis of the Rietfontein eclogites, direct derivation of the eclogites from primary melts or magmas cannot be ruled out on the basis of oxygen isotope values alone.

10. Discussion And Conclusions

The Rietfontein off-craton kimberlite, located at 26.75°S, 20.04°E, hosts a suite of eclogite xenoliths that can be subdivided into three petrographically distinct groups, *viz.* bimineralic, orthopyroxene-bearing and kyanite eclogites. The bimineralic eclogites are by far the most common variety, with only six orthopyroxene-bearing and five kyanite eclogites occurring in the sample suite. Both Group I and Group II eclogites (following the classification of MacGregor & Carter, 1970) can be identified, although small sample sizes and abundant alteration made it difficult to characterise some samples according to this scheme. All samples are texturally well-equilibrated, although many of the bimineralic and orthopyroxene-bearing eclogites show signs of alteration and/or metasomatism. This is evidenced by the presence of such secondary and alteration minerals as amphibole, phlogopite, chlorite and spongy reaction rims surrounding clinopyroxene grains (Taylor & Neal, 1989). The surfaces of some of the kyanite eclogites are covered by a white alteration product, this is however not visible in thin sections and is thus unidentifiable. The overall fresh nature of the kyanite eclogites when compared to the remaining eclogites means that they were not subjected to a metasomatic event, implying a different entrainment period or a different mantle derivation area. The presence of kyanite in some of the eclogites alludes to an Al_2O_3 rich protolith, which, when subjected to progressively increasing pressures, may exsolve kyanite (Jerde *et al.*, 1993*a*). The exsolution of garnet from clinopyroxene in one sample indicates that this particular eclogite, if not the others, was cooled at depth from higher temperatures, possibly being subjected to increasing pressure at the same time (Harte & Gurney, 1975).

Major element mineral compositions can also be used to identify three groups within the Rietfontein eclogite suite. The kyanite eclogites form a distinct group and included with these eclogites are three bimineralic eclogites, in which the mineral compositions match those of the kyanite eclogites, although they lack modal kyanite. Garnets from the kyanite eclogites are the most calcic and are depleted in Cr_2O_3 and MgO relative to the bimineralic and orthopyroxene-bearing eclogites. Clinopyroxenes from the kyanite eclogites are the most sodic and have the lowest MgO and CaO contents. There is much compositional overlap between the bimineralic and orthopyroxene-bearing eclogites, although two groups can be identified based on the Na_2O-MgO_{cpx} classification scheme of Taylor & Neal (1989). Most of the bimineralic eclogites

classify as Group A eclogites, whereas a number of orthopyroxene-bearing eclogites fall in the Group B compositional field. Increased Cr_2O_3 contents in some of the bimineralic eclogites indicate a tendency towards a peridotitic signature (Snyder *et al.*, 1997). Despite petrographic groupings of the eclogites as Group I and Group II eclogites, compositionally only Group II (McCandless & Gurney, 1989) eclogites can be identified on the basis of Na_2O_{gt} and K_2O_{cpx} contents. The minerals are all compositionally well-equilibrated, including the garnet exsolution lamellae in CMA 1, indicating a substantial mantle residence period prior to kimberlite entrainment. Despite compositional similarities to both on- and off-craton eclogites, trends exhibited by the Rietfontein eclogites show a greater similarity to those of on-craton (Group II) eclogites.

A mantle origin, rather than a lower crustal origin, for the Rietfontein eclogites is indicated by equilibration temperatures and pressures. Temperatures range from 733-1000°C, calculated using the geothermometer of Krogh (1988), whereas equilibration pressures for the orthopyroxene eclogites range between 24 and 39kbar, using Brey & Köhler's (1990) geobarometer in association with the Krogh (1988) geothermometer. Comparisons of these temperatures with on- and off-craton eclogitic temperatures indicate that the range of temperatures and the most common equilibration temperatures of the Rietfontein eclogites are most similar to those of off-craton eclogites (Robey, 1981; Pearson *et al.*, 1995*a*). On-craton eclogites generally show higher equilibration temperatures than the Rietfontein eclogites. The pressure range exhibited by the Rietfontein eclogites represents a large range in mantle stratigraphy, of approximately 40-50km. A comparison of geotherms for the Rietfontein area, based on equilibration pressures and temperatures of the orthopyroxene-bearing eclogites, reveal a heat flow of approximately 41-44mW.m^{-2}. This is significantly less than heat flow measured in off-craton mobile belts such as the Namaqua-Natal Belt (Jones, 1999) and it bears a greater similarity to geotherms for established on-craton areas such as Lesotho. Despite the similarity of Rietfontein equilibration temperatures to those of off-craton eclogites, the geotherms suggest lower heat flow than other off-craton areas, indicative of a thicker lithospheric setting (Nyblade & Pollack, 1993).

The trace element compositions of the kyanite eclogites are distinctly different from the remaining eclogite groups, as are the major element compositions. Garnets of the kyanite

eclogites have higher Sr, Eu and Sm abundances than the orthopyroxene-bearing or bimineralic eclogites, whereas clinopyroxenes from the kyanite eclogites have the lowest Sc, Y and REE abundances. Orthopyroxene-bearing and bimineralic eclogites exhibit similar abundances of all trace elements in both garnet and clinopyroxene. REE patterns for the kyanite eclogite minerals are distinctly different to patterns for the bimineralic and orthopyroxene-bearing eclogites. Garnets from the kyanite eclogites are extremely depleted in LREE, exhibit positive Eu anomalies and have relatively flat middle to heavy REE patterns. Garnets from the bimineralic and orthopyroxene-bearing eclogites have very similar REE patterns, being depleted in LREE with flat to smoothly increasing middle to heavy REE patterns. Clinopyroxenes from the kyanite eclogites have an overall convex upwards appearance and are depleted in LREE, with mostly flat MREE patterns, decreasing towards HREE. Bimineralic and orthopyroxene-bearing eclogitic clinopyroxenes show smoothly decreasing REE patterns from the light to heavy REE, some with a slight negative Eu anomaly. These REE patterns are similar to those exhibited by eclogites from a number of on-craton localities, such as Roberts Victor and Udachnaya. Trace element partitioning between garnet and clinopyroxene within the Rietfontein eclogites is strongly dependent on the Ca content of garnet, with $D^{cpx/gt}$ for most elements decreasing with increasing Ca content. The Mg content of garnet and $Al^{[6]}$ in clinopyroxene are seen to exert moderate controls on trace element partitioning and there is no temperature dependence of partitioning at all.

The main differences between the calculated major element whole rock compositions, based on modal mineralogy of the kyanite, orthopyroxene-bearing and bimineralic eclogites are illustrated by the Al_2O_3, MgO and Na_2O contents. The kyanite and high Na-Al eclogites all have Al_2O_3 contents greater than 17 wt%, MgO < 10 wt% and Na_2O > 2 wt%, whereas the bimineralic and orthopyroxene-bearing eclogites have Al_2O_3 < 15 wt%, MgO > 15 wt% and Na_2O < 2 wt%. The Mg#'s of the kyanite eclogites are all lower (< 68) than those of the remaining eclogites (all > 75). Major element compositional similarities between oceanic gabbros and boninites can be noted. The Sc, Zr and Ce abundances within the kyanite eclogites are also lower, on average, than the abundances found in the bimineralic and orthopyroxene-bearing eclogites. The eclogites have a basaltic whole-rock composition, with the kyanite eclogites showing many major element compositional similarities to oceanic gabbros and MORB. Whole-rock REE patterns of the kyanite eclogites can be distinguished from those of the bimineralic and

orthopyroxene-bearing eclogites by way of extreme LREE depletion and positive Eu anomalies. These positive Eu anomalies are similar to those expressed by many gabbros, whereas the flatter REE patterns of the bimineralic and orthopyroxene-bearing eclogites are more similar to MORB, komatiite and, for some samples, even boninite REE patterns. The positive Eu anomalies observed within the kyanite eclogites provide convincing evidence of a plagioclase-rich precursor rock.

Garnets from the Rietfontein eclogites yield $\delta^{18}O$ values of 5.16-6.84‰, which, disregarding the outlier value of 6.84‰, fall within the mantle range of Deines *et al.* (1991). These data provide no clear evidence of a crustal precursor for the Rietfontein eclogites, although it must be remembered that the sample size is small and a larger data set may indicate $\delta^{18}O$ values offset from "normal" mantle values. Correlations of $\delta^{18}O$ values with the Cr, Ca and Mg contents of garnet could be indicative of high-temperature fractionation (magmatic) processes or hydrothermal alteration of a basaltic precursor. High temperature fractionation processes were initially suggested to account for the large ranges in oxygen isotope compositions observed in the Roberts Victor eclogites (Garlick *et al.*, 1971) and it was only at a later stage that hydrothermal alteration was suggested as the mechanism responsible for the $\delta^{18}O$ values in these eclogites (MacGregor & Manton, 1986). Considering the nature of the Rietfontein eclogites - mantle derived, with mineral and whole-rock compositions suggesting a possible basaltic, oceanic crustal precursor - it seems likely that the correlations of major element compositional trends with $\delta^{18}O$ values are due to hydrothermal alteration. Such a hypothesis has been suggested for compositional correlations within the on-craton eclogites of Roberts Victor (MacGregor & Manton, 1986).

Two main hypotheses for the origin of mantle eclogites now exist. The first petrogenetic model postulates a magmatic origin as mantle cumulates or melts, involving igneous fractionation processes (*eg.* MacGregor & Carter, 1970; Hatton, 1978; Smyth *et al.*, 1989; Caporuscio & Smyth, 1990) within the garnet stability field in the upper mantle. More recently, models proposing an origin for eclogites as subducted oceanic crust have been suggested (*eg.* Helmstaedt & Doig, 1975; Jagoutz *et al.*, 1984; MacGregor & Manton, 1986; Shervais *et al.*, 1988; Taylor & Neal, 1989; Neal *et al.*, 1990; Jerde *et al.*, 1993*a*; Snyder *et al.*, 1997). Both

models should be taken into account when considering an origin and possible protoliths for the Rietfontein eclogites.

The Rietfontein kyanite eclogites most likely represent subducted, metamorphosed, plagioclase-rich, basaltic oceanic crust. A number of characteristics observed in the eclogites support this theory. The overall major element characteristics of the kyanite eclogites are very similar to those of oceanic gabbros and MORB. The positive Eu anomalies, observed in both the garnet and whole-rock REE kyanite eclogite patterns, are known to be indicative of plagioclase accumulation in a magma chamber (Pallister & Knight, 1981) and can be expressed by both gabbros and MORB (*eg.* Puchelt *et al.*, 1977). Despite noted LREE depletion in MORB (le Roex *et al.*, 1996), it does not reach the extreme depletion observed in the Rietfontein kyanite eclogites. This depletion could be accounted for by partial melting within the system after eclogite formation. The interlocking textures and triple junctions observed in the kyanite eclogites imply metamorphic recrystallisation and the relatively higher (although still within the mantle range) $\delta^{18}O$ values (> 5.5‰) suggest possible low-temperature hydrothermal alteration (Muehlenbachs & Clayton, 1972) of protoliths at crustal levels.

The possibility exists that Rietfontein bimineralic and orthopyroxene-bearing eclogites are a high pressure crystallisation product of a mantle melt or magma. Unlike the kyanite eclogites, these eclogites exhibit no positive Eu anomalies and derivation from a plagioclase-rich protolith is thus not directly implied. A magma chamber situated within the garnet stability field in the mantle could crystallise garnet and clinopyroxene directly from the magma (O'Hara *et al.*, 1975). Accumulation of these garnet and clinopyroxene crystals would result in the formation of an eclogite with a basaltic composition. Primary magmas would have high Mg#'s ($Mg/(Mg+0.85Fe^*) > 0.68$) (Dawson & Carswell, 1990) and crystallisation of the Rietfontein eclogites from such magmas would result in eclogites with high Mg#'s.

The kyanite eclogites are extremely depleted in LREE (incompatible elements) and they all have low (< 70) Mg#'s, thus making it possible to discount the kyanite eclogites as having a high pressure crystal cumulate origin. All of the bimineralic and orthopyroxene-bearing eclogites however, have Mg#'s > 70, although the compositional similarities (of both the major and rare earth elements) to MORB are a good indication that they may represent a basaltic oceanic crustal

protolith. The lack of Eu anomalies in the bimineralic and orthopyroxene-bearing eclogites mean that these eclogites cannot be directly linked to plagioclase-rich crust. However, many of the REE patterns of these eclogites are flat and show trends similar to those of MORB. These eclogites tend to have higher Mg#'s than average MORB. If however, a MORB was a picritic cumulate basalt, it would be olivine-rich and, as a result, would have a high whole-rock Mg#. MORB therefore cannot be discounted as a possible protolith for the Rietfontein bimineralic and orthopyroxene-bearing eclogites.

Major element compositions of the bimineralic and orthopyroxene-bearing eclogites show some overlap with major element compositional fields of MORB and oceanic gabbros and also show compositional similarities to boninites. REE patterns for some of the eclogites show strong similarities to boninitic rocks. Magma segregation at increasing depths from 20-100km in subduction-zone settings may generate a range of primary magma compositions, ranging from high-Si, high-Mg boninitic compositions, to low-Si, high-Mg picritic or olivine tholeiite end-members (Crawford *et al.*, 1989). The association of boninitic-type magmas, gabbros, and basalts in ophiolite complexes (Crawford *et al.*, 1989; Kelemen *et al.*, 1997) implies that all three rock types may be associated with, or form oceanic crust. Most of the bimineralic and orthopyroxene-bearing eclogites from Rietfontein have interlocking metamorphic type textures and triple junctions that suggest recrystallisation. Such textures would be in agreement with a proposed origin as subducted and metamorphosed oceanic crust. The characteristics observed in the bimineralic and orthopyroxene-bearing eclogites of Rietfontein are thus not inconsistent with these eclogites being remnants of subducted oceanic crust. If a section of basaltic oceanic crust that was not plagioclase-rich but contained magmas of boninitic affinities, was initially hydrothermally altered, subducted to lithospheric depths and subsequently metamorphosed to eclogite, eclogites of the Rietfontein bimineralic and orthopyroxene-bearing varieties may result.

Magmas with boninitic affinities are known to be important constituents of some greenstone belts and ophiolites (Crawford *et al.*, 1989). Ophiolites are generally recognised as representing transported slabs of oceanic crust and upper mantle that have been emplaced upon continental margins (*eg.* McCulloch *et al.*, 1981; Serri, 1981). This indicates that even though modern-day boninites appear to be restricted to intra-oceanic arcs (Coish, 1989), processes conducive to the generation of boninite magmas may have been active in other tectonic settings as recently as the

Mesozoic (McCulloch *et al.*, 1981). Crawford *et al.* (1989) believe that ocean-floor spreading at a mid-ocean ridge spreading centre can generate the type of boninites incorporated into ophiolites. If this is the case, it would thus be possible to generate a slab of oceanic crustal material exhibiting boninitic affinities, together with the basalt and gabbro crustal components. Movement of this crustal material away from the mid-ocean ridge at which it was generated, towards a subduction zone would lead to eventual subduction of the slab of oceanic crust. Subsequent metamorphism of this crust may generate eclogites showing the compositional characteristics observed in the Rietfontein eclogites. This model is proposed to account for the generation of the bimineralic and orthopyroxene-bearing eclogites sampled by the Rietfontein kimberlite.

The temperatures and pressures of equilibration of the Rietfontein eclogites indicate equilibration within a mantle setting. Not only are the kyanite eclogites compositionally distinct from the remaining Rietfontein eclogites but they also have higher average equilibration temperatures, indicating a greater depth of origin. This suggests that the oceanic crust which yielded the kyanite eclogites was subducted to deeper mantle levels than the oceanic crust which gave rise to the bimineralic and orthopyroxene-bearing eclogites. The equilibration pressures indicated by the orthopyroxene-bearing eclogites represent a large vertical mantle range, of almost 50km. It is unlikely that this range represents a single large eclogitic body. What may be possible however, is that the Rietfontein kimberlite has sampled a number of eclogite bodies, all of which formed by the metamorphism of subducted oceanic crust. The metasomatic effects visible in the bimineralic and orthopyroxene-bearing eclogites but not the kyanite eclogites suggest different petrogenetic histories for the different eclogite bodies. If these kyanite eclogites originated at deeper lithospheric levels, they should logically have been entrained in the kimberlite before the bimineralic and orthopyroxene-bearing eclogites. Kimberlite-related metasomatism would have affected all entrained xenoliths, not just one particular eclogite group. A kyanite eclogite body, separate to the eclogite body which yielded the bimineralic and orthopyroxene-bearing eclogites, thus seems to be indicated.

The nature and characteristics of the Rietfontein eclogites therefore seem to imply derivation from two different sources, one giving rise to the kyanite and high Na-Al eclogites, the other yielding the bimineralic and orthopyroxene-bearing eclogites. Slight low-temperature,

hydrothermal alteration of oceanic crust consisting of basalt and gabbro, followed by subduction into the lithosphere and subsequent metamorphism to eclogite probably gave rise to the kyanite eclogites. A similar process of subduction and metamorphism of both low- and high-temperature hydrothermally altered oceanic crust with boninitic, gabbroic and basaltic affinities could have resulted in the formation of an eclogite body yielding the bimineralic and orthopyroxene-bearing eclogites. Each of these eclogite bodies may have, at different times, separately under plated the continental lithosphere in the Rietfontein area. These bodies would then have been sampled at different stages in the ascension of the Rietfontein kimberlite. It is possible that the crustal section which eventually gave rise to the bimineralic and orthopyroxene-bearing eclogites was subducted first and the resultant eclogite body was the first to under plate the Rietfontein continental lithosphere. This initial under plating may then have been followed by welding of the kyanite eclogite body to the lithosphere, accounting for their greater depths of equilibration. In this way the Rietfontein kimberlite would sample the kyanite eclogites first and then, as the kimberlite proceeded towards the surface, go on to sample the bimineralic and orthopyroxene-bearing eclogites.

11. REFERENCES

(1981) *Basaltic Volcanism Study Project*. Pergamon Press.

Ai, Y. (1994) A revision of the garnet-clinopyroxene Fe^{2+}-Mg exchange thermometer. *Contributions to Mineralogy and Petrology* **115**, 467-473.

Anderson, D.L. (1994) Komatiites and picrites: evidence that the "plume" source is depleted. *Earth and Planetary Science Letters* **128**, 303-311.

Aranovich, L.Y. & Pattison, D.R.M. (1995) Reassessment of the garnet-clinopyroxene Fe-Mg exchange thermometer: I. Evaluation of the Pattison and Newton (1989) experiments. *Contributions to Mineralogy and Petrology* **119**, 16-29.

Ater, P.C., Eggler, D.H. & McCallum, M.E. (1984) Petrology and geochemistry of mantle eclogite xenoliths from the Colorado-Wyoming kimberlites: recycled oceanic crust? In *Kimberlites II: The mantle and crust-mantle relationships.* (ed. J. Kornprobst), pp. 309-318. Elsevier.

Ballard, S., Pollack, H.N. & Skinner, N.J. (1987) Terrestrial heat flow in Botswana and Namibia. *Journal of Geophysical Research* **92**, 6291-6300.

Basu, A.R., Ongley, J.S. & MacGregor, I.D. (1986) Eclogites, pyroxene geotherm, and layered mantle convection. *Science* **233**, 1303-1305.

Beard, B.L., Fraracci, K.N., Taylor, L.A., Snyder, G.A., Clayton, R.A., Mayeda, T.K. & Sobolev, N.V. (1996) Petrography and geochemistry of eclogites from the Mir kimberlite, Yakutia, Russia. *Contributions to Mineralogy and Petrology* **125**, 293-310.

Beck (1899) Neues von den Afrikanischen Diamantlagerstatten. *Zeit fur Prackt. Geologie*, 417-419.

Bell, D.R. (1981) Ultramafic xenoliths from the Koffiefontein kimberlite pipe, South Africa. Unpublished Honours Project, University of Cape Town.

Bell, D.R. & Rossman, G.R. (1992) The distribution of hydroxyl in garnets from the subcontinental mantle of Southern Africa. *Contributions to Mineralogy and Petrology* **111**, 161-178.

Berman, R.G., Aranovich, L.Y. & Pattison, D.R.M. (1995) Reassessment of the garnet-clinopyroxene Fe-Mg exchange thermometer: II. Thermodynamic analysis. *Contributions to Mineralogy and Petrology* **119**, 30-42.

Bertrand, P. & Mercier, J-C.C. (1985) The mutual solubility of coexisting ortho- and clinopyroxene: toward an absolute geothermometer for the natural system? *Earth and Planetary Science Letters* **76**, 109-122.

Bloomer, A. G. & Nixon, P.H. (1973) The geology of the Letseng-la-terae kimberlite pipes. In *Lesotho Kimberlites* (ed. P. H. Nixon), pp. 20-37. Lesotho National Development Corporation.

Bloomer, S. H. (1989) Geochemical characteristics of boninite- and tholeiite-series rocks of the Mariana forearc and the role of an incompatible element-enriched fluid in arc petrogenesis. In *Mantle metasomatism and alkaline magmatism*, (ed. E. M. Morris, & Pasteris, J.D.), pp. 151-164. Geological Society of America Special Paper **215**.

Blundy, J. D. & Wood, B.J. (1991) Crystal chemical controls on partitioning of Sr and Ba between plagioclase feldspar, silicate melts and hydrothermal solutions. *Geochimica et Cosmochimica Acta* **55**, 193-209.

Booij, E. & Staudigel, H. (1996) Bulk composition estimates of mature oceanic crust: arc input constraints and seawater-ocean crust fluxes. *EOS* , Transactions AGU **77**, 781.

Boyd, F. R. (1973) A pyroxene geotherm. *Geochimica et Cosmochimica Acta* **37**, 2533-2546.

Boyd, F. R., Gurney, J.J. & Richardson, S.H. (1985) Evidence for a 150-200-km thick Archaean lithosphere from diamond inclusion thermobarometry. *Nature* **315**, 387-389.

Boyd, F. R. & Gurney, J.J. (1986) Diamonds and the African Lithosphere. *Science* **232**, 472-477.

Brey, G. P., Köhler, T. & Nickel, K.G. (1990) Geothermobarometry in Four-phase Lherzolites I. Experimental results from 10 to 60kb. *Journal of Petrology* **31**, 1313-1352.

Brey, G. P. & Köhler, T. (1990) Geothermobarometry in Four-phase Lherzolites II. New Thermobarometers, and Practical Assessment of Existing Thermobarometers. *Journal of Petrology* **31**, 1353-1378.

Brown, A. V. & Jenner, G.A. (1989) Geological setting, petrology and chemistry of Cambrian boninite and low-Ti tholeiite lavas in western Tasmania. In *Boninites* (ed. A. J. Crawford), pp. 232-263. Unwin Hyman.

Bucher, K. & Frey, M. (1994) *Petrogenesis of metamorphic rocks* pp318. Springer-Verlag.

Byerly, G. R. (1999) Komatiites of the Mendon Formation: Late-stage ultramafic volcanism in the Barberton Greenstone Belt. In *Geological evolution of the Barberton Greenstone Belt, South Africa* (ed. D. R. Lowe & Byerly,G.R.), pp. 189-211. Geological Society of America Special Publication **329**.

Cameron, W. E. (1989) Contrasting boninite-tholeiite associations from New Caledonia. In *Boninites* (ed. A. J. Crawford), pp. 314-338. Unwin Hyman.

Caporuscio, F. A. & Smyth, J.R. (1986) Rare earth signatures of garnet and clinopyroxene from mantle eclogites. *EOS,* Transactions **67,** AGU 1986 Fall meeting, 1253.

Caporuscio, F. A. & Smyth, J.R. (1987) Variable LREE enrichment in mantle eclogites from South Africa by MARID fluid. *Geological Society of America Annual Meeting*, 610-611.

Caporuscio. F.A. & Smyth, J.R. (1990) Trace element crystal chemistry of mantle eclogites. *Contributions to Mineralogy and Petrology* **105**, 550-561.

Carswell, D.A. (1975) Primary and secondary phlogopites and clinopyroxenes in garnet lherzolite xenoliths. In *Physics and Chemistry of the Earth* **9** (ed. L. H. Ahrens, Dawson, J.B., Duncan, A.R. & Erlank, A.J.), pp. 471-429. Pergamon Press.

Carswell, D.A. (1990) Eclogites and the eclogite facies: definitions and classification. In *Eclogite facies rocks* (ed. D. A. Carswell), pp. 1-13. Blackie.

Chapman, D.S. (1986) Thermal gradients in the continental crust. In *The nature of the lower continental crust*, Geological Society Special Publication No.**24** (ed. J. B. Dawson, Carswell, D.A., Hall, J. & Wedepohl, K.H.), pp. 63-70. Blackwell Scientific Publications.

Clayton, R. N., Goldsmith, J.R., Karel, K.J., Mayeda, T.K. & Newton, R.C. (1975) Limits on the effect of pressure on isotopic fractionation. *Geochimica et Cosmochimica Acta* **39**, 1197-1201.

Coish, R.A. (1989) Boninitic lavas in Appalachian ophiolites: a review. In *Boninites* (ed. A. J. Crawford), pp. 264-287. Unwin Hyman.

Coleman, R.G., Lee, D.E., Beatty, L.B. & Brannock, W.W. (1965) Eclogites and eclogites: their differences and similarities. *Geological Society of America Bulletin* **76**, 483-508.

Cox, K.G., Gurney, J.J. & Harte, B. (1973) Xenoliths from the Matsoku pipe. In *Lesotho Kimberlites* (ed. P. H. Nixon), pp. 76-100. Lesotho National Development Corporation.

Crawford, A.J., Falloon, T.J. & Green, D.H. (1989) Classification, petrogenesis and tectonic setting of boninites. In *Boninites* (ed. A. J. Crawford), pp. 2-44. Unwin Hyman.

Davis, B.T.C. & Boyd, F.R. (1966) The join $Mg_2Si_2O_6$-$CaMgSi_2O_6$ at 30 kilobars and its application to pyroxenes from kimberlites. *Journal of Geophysical Research* **71**, 3567-3576.

Davis, G. L. (1977) The ages and uranium contents of zircons from kimberlites and associated rocks. *Proceedings of the 2nd International Kimberlite Conference, Extended abstracts*.

Dawson, J. B. & Stephens, W.E. (1975) Statistical classification of garnets from kimberlite and associated xenoliths. *Journal of Geology* **83**, 589-607.

Dawson, J.B. (1980) *Kimberlites and their xenoliths*. Springer-Verlag.

Dawson, J.B. (1989) Geographic and time distribution of kimberlites and lamproites: relationships to tectonic processes. In *Kimberlites and related rocks: their composition, occurrence, origin and emplacement*, Vol. 1 (ed. J. Ross, Jaques, A.L., Ferguson, J., Green,

D.H., O'Reilly, S.Y., Danchin, R.V. & Janse, A.J.A.), pp. 323-342. Geological Society of Australia Special Publication No.**14**.

Dawson, J. B. & Carswell, D.A. (1990) High temperature and ultra-high pressure eclogites. In *Eclogite facies rocks* (ed. D.A. Carswell), pp. 315-349. Blackie.

de Wit, M.J., Roering, C., Hart, R.J., Armstrong, R.A., de Ronde, C.E.J., Green, R.W.E., Tredoux, M., Peberdy, E. & Hart, R.A. (1992) Formation of an Archaean continent. *Nature* **357**, 553-562.

Deines, P., Harris, J.W., Robinson, D.N., Gurney, J.J. & Shee, S.R. (1991) Carbon and oxygen isotope variations in diamond and graphite eclogites from Orapa, Botswana, and the nitrogen content of their diamonds. *Geochimica et Cosmochimica Acta* **55**, 515-524.

Dick, H.J.B., Natland, J.H., Miller, D.J. *et al.* (1999) Proceedings of the Ocean Drilling Program, Initial Reports 176 (CD-ROM).

Dostal, J. & Muecke, G.K. (1978) Trace element geochemistry of the peridotite-gabbro-basalt suite from DSDP Leg 37. *Earth and Planetary Science Letters* **40**, 415-422.

Droop G.T.R. (1987) A general equation for estimating Fe^{3+} concentrations in ferromagnesian silicates and oxides from microprobe analyses, using stoichiometric criteria. *Mineralogical magazine* **51**, 431-435.

Ellis, D.J. & Green, D.H. (1979) An experimental study of the effect of Ca upon garnet-clinopyroxene Fe-Mg exchange equilibria. *Contributions to Mineralogy and Petrology* **71**, 13-22.

Erlank, A. J., Waters, F.G., Hawkesworth, C.J., Haggerty, S.E., Allsopp, H.L., Rickard, R.S. & Menzies, M. (1987) Evidence for mantle metasomatism in peridotite nodules from the Kimberley Pipes, South Africa. In *Mantle Metasomatism* (ed. M. A. H. Menzies, Hawkesworth, C.J.). Academic Press Geology Series.

Finnerty, A. A. & Boyd, F.R. (1984) Evaluation of thermobarometers for garnet peridotites. *Geochimica et Cosmochimica Acta* **48**, 15-27.

Franz, L., Brey, G.P. & Okrusch, M. (1996a) Reequilibration of ultramafic xenoliths from Namibia by metasomatic processes at the mantle boundary. *Journal of Geology* **104**, 599-615.

Franz, L., Brey, G. & Okrusch, M. (1996b) Steady state geotherm, thermal disturbances, and tectonic development of the lower lithosphere underneath the Gibeon Kimberlite Province, Namibia. *Contributions to Mineralogy and Petrology* **126**, 181-198.

Frey, F. A. (1984) Rare Earth Element abundances in upper mantle rocks. In *Rare Earth Element Geochemistry* (ed. P. Henderson), pp. 153-203. Elsevier.

Ganguly, J. (1979) Garnet and clinopyroxene solid solutions, and geothermometry based on Fe-Mg distribution coefficient. *Geochimica et Cosmochimica Acta* **43**, 1021-1029.

Ganguly, J., Cheng, W. & Tirone, M. (1996) Thermodynamics of aluminosilicate garnet solid solution: new experimental data, an optimized model, and thermometric applications. *Contributions to Mineralogy and Petrology* **126**, 137-151.

Garlick, G. D., MacGregor, I.D. & Vogel, D.E. (1971) Oxygen isotope ratios in eclogites from kimberlites. *Science* **172**, 1025-1026.

Germs, G.J.B. (1983) Implications of a sedimentary facies and depostional environmental analysis of the Nama Group in South West Africa/Namibia. *Special Publication of the Geological Society of South Africa* **11**, 89-114.

Giaramita, J. & Day, H. (1990) Error propagation in calculations of structural formulas. *American Mineralogist* **75**, 170-182.

Graham, C.M. & Harmon, R.S. (1983) Stable isotope evidence on the nature of crust-mantle interactions. In *Continental basalts and mantle xenoliths* (ed. C.J.N. Hawkesworth, Norry, M.J.), pp. 20-45. Shiva.

Griffin, W.L., Carswell, D.A. & Nixon, P.H. (1979) Lower crustal granulites from Lesotho, South Africa. In *The mantle sample: Inclusions in kimberlites and other volcanics*, Vol 1. Proceedings of the Second International Kimberlite Conference (ed. F. R. M. Boyd, Meyer, H.O.A.), pp. 59-86. American Geophysical Union.

Griffin, W.L. & O'Reilly, S.Y. (1986) The lower crust in eastern Australia: Xenolith evidence. In *The Nature of the Lower Continental Crust* (ed. J. B. Dawson, Carswell, D.A. Hall, J. & Wedepohl, K.H.), pp. 363-374. Geological Society Special Publication Vol. 24.

Griffin, W.L., & O'Reilly, S.Y. (1987) The composition of the lower crust and the nature of the continental Moho - xenolith evidence. In *Mantle Xenoliths* (ed. P. H. Nixon), pp. 413-430. John Wiley & Sons.

Griffin, W.L., O 'Reilly, S.Y. & Pearson, N.J. (1990) Eclogite stability near the crust-mantle boundary. In *Eclogite Facies Rocks* (ed. D. A. Carswell), pp. 291-314. Blackie.

Gurney, J.J., Mathias, M., Siebert, C., Moseley, G. (1971) Kyanite eclogites from the Rietfontein Kimberlite Pipe, Mier Coloured Reserve, Gordonia, Cape Province, South Africa. *Contributions to Mineralogy and Petrology.* **30**, 46-52.

Gurney, J.J. & Harte, B. (1980) Chemical variations in upper mantle nodules from southern African kimberlites. *Phil.Trans.R.Soc.Lond.* **297**, 273-293.

Gurney, J.J., Harris, J.W., Rickard, R.S. & Moore, R.O. (1985) Inclusions in Premier Mine diamonds. *Transactions of the Geological Society of South Africa* **88**, 301-310.

Gurney, J.J. (1989) Diamonds. In *Kimberlites and related rocks* (ed. J. Ross, Jaques, A.L., Ferguson, J., Green, D.H., O'Reilly, S.Y., Danchin, R.V. & Janse, J.A.), pp. 935-965. Special Publication Geological Society of Australia **14**.

Gurney, J.J. (1990) The diamondiferous roots of our wandering continent. *South African Journal of Geology* **93**, 424-437.

Gurney, J.J., Moore, R.O., Otter, M.L., Kirkley, M.B., Hops, J.J. & McCandless, T.E. (1991) Southern African kimberlites and their xenoliths. In *Magmatism in extensional structural settings* (ed. A. B. Kampunzu & Lubala, R.T.). Springer-Verlag.

Haggerty, S.E. (1991) Oxide mineralogy of the upper mantle. In *Oxide Minerals: Petrologic and magnetic significance*, Reviews in Mineralogy **25** (ed. D. H. Lindsley), pp. 355-416. Mineralogical Society of America.

Haggerty, S.E. (1995) Upper Mantle Mineralogy. *Journal of Geodynamics* **20**, 331-364.

Harley, S.L. (1984a) An experimental study of the partitioning of Fe and Mg between garnet and orthopyroxene. *Contributions to Mineralogy and Petrology* **86**, 359-373.

Harley, S.L. (1984b) The solubility of alumina in orthopyroxene coexisting with garnet in FeO-MgO-Al_2O_3-SiO_2 and CaO-FeO-MgO-Al_2O_3-SiO_2. *Journal of Petrology* **25**, 665-696.

Harris, C., Smith, H.S. & le Roex, A.P. (1999) Oxygen isotope composition of phenocrysts from Tristan da Cunha and Gough Island lavas: variation with fractional crystallisation and evidence for assimilation. *Contributions to Mineralogy and Petrology* In press.

Harte, B. & Gurney, J.J. (1975) Evolution of clinopyroxene and garnet in an eclogite nodule from the Roberts Victor kimberlite pipe, South Africa. In *Physics and Chemistry of the Earth*, Vol. **9** (ed. L. H. Ahrens, Dawson, J.B., Duncan, A.R. & Erlank, A.J.), pp. 367-387. Pergamon Press.

Harte, B. (1977) Rock nomenclature with particular relation to deformation and recrystallisation textures in olivine-bearing xenoliths. *Journal of Geology* **85**, 279-288.

Harte, B. (1983) Mantle peridotites and processes - the kimberlite sample. In *Continental basalts and mantle xenoliths* (ed. C. J. N. Hawkesworth, Norry, M.J.), pp. 46-91. Shiva Publishing.

Harte, B. & Hawkesworth, C.J. (1989) Mantle domains and mantle xenoliths. In *Kimberlites and related rocks: Their mantle/crust setting, diamonds and diamond exploration*. Geological Society of Australia Special Publication, Vol. **14** (ed. J. Ross), pp. 649-686. Carlton.

Harte, B. & Kirkley, M.B. (1997) Partitioning of trace elements between clinopyroxene and garnet: data from mantle eclogites. *Chemical Geology* **136**, 1-24.

Hartnady, C., Joubert, P. & Stowe, C. (1985) Proterozoic crustal evolution in Southwestern Africa. *Episodes* **8**, 236-244.

Hatton ,C. J. (1978) The geochemistry and origin of xenoliths from the Roberts Victor Mine. Unpublished Ph.D. thesis, University of Cape Town.

Hatton, C. J. & Gurney, J.J. (1987) Roberts Victor eclogites and their relation to the mantle. In *Mantle Xenoliths* (ed. P. H. Nixon), pp. 453-463. Wiley.

Hauy, R. J. (1822) *Traite de Mineralogie, 2nd edition*. Bachelier, Paris Delance, IV.

Helmstaedt, H. & Doig, R. (1975) Eclogite nodules from kimberlite pipes of the Colorado Plateau - samples of subducted Franciscan-type oceanic lithosphere. In *Physics and Chemistry of the Earth*, Vol. **9** (ed. L. H. Ahrens, Dawson, J.B., Duncan, A.R. & Erlank, A.J.), pp. 95-111. Pergamon Press.

Hickey-Vargas, R. (1989) Boninites and tholeiites from DSDP Site 458, Mariana forearc. In *Boninites* (ed. A. J. Crawford), pp. 339-356. Unwin Hyman.

Hill, S.J. (1989) A study of the diamonds and xenoliths from the Star kimberlite, Orange Free State, South Africa. Unpublished M.Sc. thesis, University of Cape Town.

Hops, J.J. (1989) Some aspects of the geochemistry of high temperature peridotites and megacrysts from the Jagersfontein kimberlite pipe, South Africa. Unpublished Ph.D. thesis, University of Cape Town.

Humphris, S.E., Thompson, G., Schilling, J.G. & Kingsley, R.H. (1985) Petrological and chemical variations along the Mid-Atlantic Ridge between 46°S and 32°S: influence of the Tristan da Cunha mantle plume. *Geochimica et Cosmochimica Acta* **49**, 1445-1464.

Ionov, D.A., Harmon, R.S., France-Lanord, C., Greenwood, P.B. & Aschhepkov, I.V. (1994) Oxygen isotope composition of garnet and spinel peridotites in the continental mantle: Evidence from the Vitim xenolith suite, southern Siberia. *Geochimica et Cosmochimica Acta* **58**, 1463-1470.

Ireland, T.R., Rudnick, R.L. & Spetsius, Z. (1994) Trace elements in diamond inclusions from eclogites reveal link to Archean granites. *Earth and Planetary Science Letters* **128**, 199-213.

Jacob, D., Jagoutz, E., Lowry, D., Mattey, D. & Kudrjavtseva, G. (1994) Diamondiferous eclogites from Siberia: Remnants of Archaean oceanic crust. *Geochimica et Cosmochimica Acta* **58**, 5191-5207.

Jagoutz, E., Dawson, J.B., Hoernes, S., Spettel, B. & Wanke, H. (1984) Anorthositic oceanic crust in the Archaean Earth. *15th Lunar and Planetary Science Conference, Houston*, 395-396.

Jahn, B., Gruau, G. & Glickson, A.Y. (1982) Komatiites of the Onverwacht Group, South Africa: REE geochemistry, Sm/Nd age and mantle evolution. *Contributions to Mineralogy and Petrology* **80**, 25-40.

Jerde, E.A., Taylor, L.A., Crozaz, G., Sobolev, N.V. & Sobolev, V.N. (1993a) Diamondiferous eclogites from Yakutia, Siberia: evidence for a diversity of protoliths. *Contributions to Mineralogy and Petrology* **114**, 189-202.

Jerde, E.A., Taylor, L.A., Crozaz, G. & Sobolev, N.V. (1993b) Exsolution of garnet within clinopyroxene of mantle eclogites: major- and trace-element chemistry. *Contibutions to Mineralogy and Petrology* **114**, 148-159.

Jones, M.Q.W. (1999) A review of heat flow in Southern Africa and the thermal structure of the lithosphere. *SA Geophysical Review*, in press.

Kelemen, P.B., Koga, K. & Shimizu, N. (1997) Geochemistry of gabbro sills in the crust-mantle transition zone of the Oman ophiolite: implications for the origin of the oceanic lower crust. *Earth and Planetary Science Letters* **146**, 475-488.

Kennedy, C.S. & Kennedy, G.C. (1976) The equilibrium boundary between graphite and diamond. *Journal of Geophysical Research* **81**, 2467-2470.

Kerr, A.C., Marriner, G.F., Arndt, N.T., Tarney, J., Nivia, A., Saunders, A.D. & Duncan, R.A. (1996) The petrogenesis of Gorgona komatiites, picrites and basalts: new field, petrographic and geochemical constraints. *Lithos* **37**, 245-260.

Kerrich, R., Wyman, D., Fan, J. & Bleeker, W. (1998) Boninite series: low Ti-tholeiite associations from the 2.7Ga Abitibi greenstone belt. *Earth and Planetary Science Letters* **164**, 303-316.

Kirkley, M.B., Gurney, J.J. & Levinson, A.A. (1991) Age, origin, and emplacement of diamonds: Scientific advances in the last decade. *Gems & Gemology* **27**(No.1), 2-25.

Krogh, E.J. (1988) The garnet-clinopyroxene Fe-Mg geothermometer - a reinterpretation of existing experimental data. *Contributions to Mineralogy and Petrology* **99**, 44-48.

Kyser, T.K. (1986) Stable isotope variations in the mantle. In *Stable Isotopes in high temperature geologic processes*, Reviews in Mineralogy **16** (ed. J. W. Valley), pp. 141-164.

Kyser, T.K. (1990) Stable isotopes in the continental lithospheric mantle. In *Continental Mantle* (ed. M. A. Menzies), pp. 127-156.

Lappin, M.A. & Dawson, J.B. (1975) Two Roberts Victor cumulate eclogites and their re-equilibration. In *Physics and Chemistry of the Earth* **9** (ed. L. H. Ahrens, Dawson, J.B., Duncan, A.R. & Erlank, A.J.), pp. 351-365. Pergamon Press.

Lappin, M.A. (1978) The evolution of a grospydite from the Roberts Victor Mine, South Africa. *Contributions to Mineralogy and Petrology* **66**, 229-241.

Lawless, P.J. (1978) Some aspects of mineral chemistry of the peridotite xenolith suite from the Bultfontein diamond mine, Kimberley, South Africa. Unpublished Ph.D. thesis, University of Cape Town.

Le Maitre, R.W. (1989) *A classification of igneous rocks and glossary of terms*. Blackwell Scientific Publications.

le Roex, A.P., Frey, F.A. & Richardson, S.H. (1996) Petrogenesis of lavas from the AMAR Valley and Narrowgate region of the FAMOUS Valley, 36°-37°N on the Mid-Atlantic Ridge. *Contributions to Mineralogy and Petrology* **124**, 167-184.

le Roex, A P. & Dick, H.J.B. (1981) Petrography and geochemistry of basaltic rocks from the Conrad fracture zone on the America-Antarctica Ridge. *Earth and Planetary Science Letters* **54**, 117-138.

le Roex, A.P., Dick, H.J.B., Erlank, A.J., Reid, A.M., Frey, F.A. & Hart, S.R. (1983) Geochemistry, mineralogy and petrogenesis of lavas erupted along the South-West Indian Ridge between the Bouvet triple junction and 11°E. *Journal of Petrology* **24**, 267-318.

le Roex, A.P., Dick, H.J., Reid, A.M., Frey, F.A. & Erlank, A.J. (1985) Petrology and geochemistry of basalts from the American-Antarctic Ridge, Southern Ocean: implications for the west-ward influence of the Bouvet mantle plume. *Contributions to Mineralogy and Petrology* **90**, 367-380.

le Roex, A.P., Dick, H.J.B., Gullen, L., Reid, A.M. & Erlank, A.J. (1987) Local and regional heterogeneity in MORB from the Mid-Atlantic Ridge between 54.5°S and 51°S: evidence for geochemical enrichment. *Geochimica et Cosmochimica Acta* **51**, 541-555.

le Roex, A.P., Dick, H.J.B. & Fisher, R.L. (1989) Petrology and geochemisty of MORB from 25°E-46°E along the South-West Indian Ridge: evidence for contrasting styles of mantle enrichment. *Journal of Petrology* **30**, 947-986.

Lee, H.Y. & Ganguly, J. (1988) Equilibrium compositions of coexisting garnet and orthopyroxene: experimental determinations in the system FMAS & applications. *Journal of Petrology* **29**, 93-113.

Lenardic, A. (1997) On the heat flow variation from Archaean cratons to Proterozoic mobile belts. *Journal of Geophysical Research* **102**, 709-721.

Lindsley, D.H. & Dixon, S.A. (1976) Diopside-enstatite equilibria at 850-1400°C, 5-35kb. *American Journal of Science* **276**, 1285-1301.

Lowry, D., Mattey, D.P. & Harris, J.W. (1999) Oxygen isotope composition of syngenetic inclusions in diamond from the Finsch Mine, RSA. *Geochmica et Cosmochimica Acta* **63**, 1825-1836.

MacGregor, I. D. & Carter, J.L. (1970) The chemistry of clinopyroxenes and garnets of eclogite and peridotite xenoliths from the Roberts Victor Mine, South Africa. *Phys. Earth Planet. Interiors* **3**, 391-397.

MacGregor, I. D. (1974) The system $MgO-Al_2O_3-SiO_2$: solubility of Al_2O_3 in enstatite for spinel and garnet peridotite compositions. *American Mineralogist* **59**, 110-119.

MacGregor, I. D. (1975) Petrologic and thermal structure of the upper mantle beneath South Africa in the Cretaceous. In *Physics and chemistry of the Earth* **9** (ed. L. H. Ahrens, Dawson, J.B., Duncan, A.R. & Erlank, A.J.), pp. 455-466. Pergamon Press.

MacGregor, I. D. & Manton, W.I. (1986) Roberts Victor eclogites: ancient oceanic crust. *Journal of Geophysical Research* **91**, 14063-14079.

Mahoney, J., le Roex, A.P., Peng, Z., Fisher, R.L. & Natland, J.H. (1992) Southwestern limits of Indian Ocean Ridge mantle and the origin of low $^{206}Pb/^{204}Pb$ mid-ocean ridge basalt: isotope systematics of the central South West Indian Ridge 17°-50°E. *Journal of Geophysical Research* **97**, 19771-19790.

Mattews, A., Goldsmith, J.R. & Clayton, R.N. (1983) Oxygen isotope fractionations involving pyroxenes: the calibration of mineral-pair geothermometers. *Geochimica et Cosmochimica Acta* **47**, 631-644.

Mattey, D., Lowry, D. & MacPherson, C. (1994) Oxygen isotope composition of mantle peridotite. *Earth and Planetary Science Letters* **128**, 231-241.

McCandless, T.E. & Gurney, J.J. (1989) Sodium in garnet and potassium in clinopyroxene: criteria for classifying mantle eclogites. In *Kimberlites and related rocks. Vol 2. Their mantle/crust setting, diamonds and diamond exploration.* Geological Society Australia Special Publication **14** (ed. J. Ross), pp. 827-832. Blackwell, Carlton.

McCulloch, M.T., Gregory, R.T., Wasserburg, G.J. & Taylor, H.P., Jr. (1981) Sm-Nd, Rb-Sr and $^{18}O/^{16}O$ isotopic systematics in an oceanic crustal section: evidence from the Samail Ophiolite. *Journal of Geophysical Research* **86**, 2721-2735.

McDonough, W.F., & Frey, F.A. (1989) Rare earth elements in upper mantle rocks. In *Geochemistry and mineralogy of rare earth elements*, Reviews in Mineralogy **21** (ed. B. R. M. Lipin, McKay, G.A.), pp. 99-145. Mineralogical Society of America.

McDonough, W.F. (1994) Chemical and isotopic systematics of continental lithospheric mantle. In *Kimberlites, related rocks and mantle xenoliths* (ed. H. O. A. L. Meyer, Leonardos, O.H.), pp. 478-485.

Mitchell, R.H. (1984) Garnet lherzolites from the Hanaus-I and Louwrensia kimberlites of Namibia. *Contributions to Mineralogy and Petrology* **86**, 178-188.

Moore, R.O. (1986) A study of the kimberlites, diamonds and associated rocks and minerals from the Monastery Mine, South Africa. Unpublished Ph.D. thesis, University of Cape Town.

Mori T. & Green, D.H. (1978) Laboratory duplication of phase equilibria observed in natural garnet lherzolites. *Journal of Geology* **86**, 83-97.

Morimoto, N. (1988) Nomenclature of pyroxenes. *American Mineralogist* **73**, 1123-1133.

Muehlenbachs, K. & Clayton, R.N. (1972) Oxygen isotope geochemistry of submarine greenstones. *Canadian Journal of Earth Sciences* **9**, 471-478.

Neal, C.R. & Taylor, L.A. (1990) Comment on "Mantle eclogites: evidence of igneous fractionation in the mantle" by J.R. Smyth, F.A. Caporuscio and T.C. McCormick. *Earth and Planetary Science Letters* **101**, 112-112.

Neal, C.R., Taylor, L.A., Davidson, J.P., Holden, P., Halliday, A.N., Nixon, P.H., Paces, J.P., Clayton, R.N. & Mayeda, T.K. (1990) Eclogites with oceanic crustal and mantle signatures from the Bellsbank kimberlite, South Africa, part 2: Sr, Nd, and O isotope geochemistry. *Earth and Planetary Science Letters* **99**, 362-379.

Nickel, K.G. & Green, D.H. (1985) Empirical geothermobarometry for garnet peridotites and implications for the nature of the lithosphere, kimberlites and diamonds. *Earth and Planetary Science Letters* **73**, 158-170.

Nixon, P.H. & Boyd, F.R. (1973) Petrogenesis of the granular and sheared ultrabasic nodule suite in kimberlite. In *Lesotho Kimberlites* (ed. P. H. Nixon), pp. 48-56. Lesotho National Development Corporation.

Nixon, P.H. (1980) Kimberlites in the South-west Pacific. *Nature* **287**, 718-720.

Nowicki, T.E. (1990) Mantle xenoliths from the Abrahamskraal kimberlite: A craton-margin geotherm. Unpublished M.Sc. thesis, Rhodes University.

Nyblade, A.A. & Pollack, H.N. (1993) A global analysis of heat flow from Precambrian terrains: Implications for the thermal structure of Archean and Proterozoic lithosphere. *Journal of Geophysical Research* **98**, 12207-12218.

O'Hara, M.J. & Yoder, H.S. (1967) Formation and fractionation of basic magmas at high pressures. *Scottish Journal of Geology* **3**, 67-117.

O'Hara, M.J., Saunders, M.J. & Mercy, E.L.P. (1975) Garnet peridotite, primary ultrabasic magma and eclogite; interpretation of upper mantle processes in kimberlite. In *Physics and chemistry of the earth 9*, Vol. **9** (ed. L. H. Ahrens, Dawson, J.B., Duncan, A.R. & Erlank, A.J.), pp. 571-604. Pergamon Press.

O'Neill, H.S.C. & Wood, B.J. (1979) An experimental study of Fe-Mg partitioning between garnet and olivine and its calibration as a geothermometer. *Contributions to Mineralogy and Petrology* **70**, 59-70.

Ongley, J.S., Basu, A.R. & Kyser, T.K. (1987) Oxygen isotopes in coexisting garnets, clinopyroxenes and phlogopites of Roberts Victor eclogites: implications for petrogenesis and mantle metasomatism. *Earth and Planetary Science Letters* **83**, 80-84.

O'Reilly, S.Y. & Griffin, W.L. (1995) Trace-element partitioning between garnet and clinopyroxene in mantle-derived pyroxenites and eclogites: P-T-X controls. *Chemical Geology* **121**, 105-130.

Pallister, J.S., & Knight, R.J. (1981) Rare-Earth element geochemistry of the Samail Ophiolite near Ibra, Oman. *Journal of Geophysical Research* **86**, 2673-2697.

Parman, S.W., Dann, J.C., Grove, T.L. & de Wit, M.J. (1997) Emplacement conditions of komatiite magmas from the 3.49Ga Komati Formation, Barberton Greenstone Belt, South Africa. *Earth and Planetary Science Letters* **150**, 303-323

.

Pattison, D.R.M. & Newton, R.C. (1989) Reversed experimental calibration of the garnet-clinopyroxene Fe-Mg exchange thermometer. *Contributions to Mineralogy and Petrology* **101**, 87-103.

Pearson, D.G., Boyd, F.R., Hoal, K.E.O., Nixon, P.H. & Rogers, N.W. (1994a) A Re-Os isotopic and petrological study of Namibian peridotites: contrasting petrogenesis and composition of on- and off-craton lithospheric mantle. *Mineralogical Magazine* **58A**, 703-704.

Pearson, D.G., Snyder, G.A., Shirey, S.B., Taylor, L.A. & Sobolev, N.V. (1994b) Re-Os isotope evidence for a mid-Archaean age of diamondiferous eclogite xenoliths from the Udachnaya kimberlite, Siberia: constraints on eclogite petrogenesis and Archaean tectonics. *Mineralogical Magazine* **58A**, 705-706.

Pearson, D.G., Kelley, S.P., Poklilenko, N.P. & Boyd, F.R. (1997) Laser $^{40}Ar/^{39}Ar$ dating of phlogopites from southern Africa and Siberian kimberlites and their xenoliths: constraints on eruption ages, melt degassing and mantle volatile compositions. In *Kimberlites, related rocks and mantle xenoliths* (ed. Mitchell, R.H. & Sobolev, N.V.), pp. 106-117.

Pearson, N. J., O'Reilly, S.Y. & Griffin, W.L. (1995) The crust-mantle boundary beneath cratons and craton margins: a transect across the south-west margin of the Kaapvaal craton. *Lithos* **36**, 257-287.

Polat, A., Kerrich, R. & Wyman, D.A. (1999) Geochemical diversity in oceanic komatiites and basalts from the late Archaean Wawa Greenstone Belts, Superior Province, Canada: trace element and Nd isotope evidence for a heterogeneous mantle. *Precambrian Research* **94**, 139-173.

Pollack, H.N. & Chapman, D.S. (1977) On the regional variation of heat flow, geotherms, and lithospheric thickness. *Tectonophysics* **38**, 279-296.

Pouchez, J.L. & Pichoir, F. (1984) A new model for quantitative X-ray microanalysis. Part I: application to the analysis of homogeneous samples. *Res. Aerosp.* **3**.

Price, R.C., Kennedy, A.K., Riggs-Sneeringer, M. & Frey, F.A. (1986) Geochemistry of basalts from the Indian Ocean triple junction: implications for generation and evolution of Indian Ocean ridge basalts. *Earth and Planetary Science Letters* **78**, 379-396.

Puchelt H., Emmermann, R. & Srivastava, R.K. (1977) Rare earth and other trace elements in basalts from the Mid-Atlantic Ridge 36°N, DSDP Leg 37. In *Initial Reports of the Deep Sea Drilling Project*, Vol. 37 (ed. F. Aumento, Melson, W.G. *et al.*), pp. 581-589. US Government Printing Office.

Råheim, A. & Green, D.H. (1974) Experimental determination of the temperature and pressure dependence of the Fe-Mg partition coefficient for co-existing garnet and clinopyroxene. *Contributions to Mineralogy and Petrology* **48**, 179-203.

Reid, A.M., Brown, R.W., Dawson, J.B., Whitfield, G.G. & Siebert, J.C. (1976) Garnet and pyroxene compositions in some diamondiferous eclogites. *Contributions to Mineralogy and Petrology* **58**, 203-220.

Reid, D.L. (1997) Sm-Nd age and REE geochemistry of Proterozoic arc-related igneous rocks in the Richtersveld Subprovince, Namaqua mobile belt, southern Africa. *Journal of African Earth Sciences* **24**, 621-6333.

Rickwood, P.C., Gurney, J.J. & White-Cooper, D.R. (1969) The nature and occurrences of eclogite xenoliths in the kimberlites of Southern Africa. In *The Upper Mantle Project*, pp. 371-394. Geological Society of South Africa Special Publication No.2.

Ringwood, A.E. & Green, D.H. (1967) An experimental investigation of the gabbro-eclogite transformation and some geophysical implications. In *International Council of Scientific Unions, Upper Mantle Project; 2nd Australian Progress Report 1965-1967* (ed. A. E. Ringwood), pp. 90-91. Australian Academy of Science.

Robey, J.v.A. (1981) Kimberlites of the Central Cape Province, R.S.A. Unpublished Ph.D. thesis, University of Cape Town.

Robinson, D.N., Gurney, J.J. & Shee, S.R. (1984) Diamond eclogite and graphite eclogite xenoliths from Orapa, Botswana. In *Kimberlites II: The mantle and crust-mantle relationships* (ed. J. Kornprobst), 11-24. Elsevier Science.

Rolfe, D.G. (1973) The geology of the Kao kimberlite pipes. In *Lesotho Kimberlites* (ed. P. H. Nixon), pp. 101-109. Lesotho National Development Corporation.

Rollinson, H.R. (1993) *Using Geochemical Data: Evaluation, presentation and interpretation.* Longman Scientific & Technical.

Rudnick, R.L. (1995) Eclogite xenoliths: Samples of Archaean ocean floor. *Extended Abstracts of the 6th International Kimberlite Conference* , 473-475.

Rudnick, R.L., McDonough, W.F. & O'Connell, R.J. (1998) Thermal structure, thickness and composition of continental lithosphere. *Chemical Geology* 145, 395-411.

Sachtleben, T. & Seck, H.A. (1981) Chemical control of Al-solubility in orthopyroxene and its implications on pyroxene geothermometry. *Contributions to Mineralogy and Petrology* **78**, 157-165.

Sautter, V. & Harte, B. (1988) Diffusion gradients in an eclogite xenolith from the Roberts Victor Kimberlite Pipe: 1. Mechanism and evolution of garnet exsolution in Al_2O_3-rich clinopyroxene. *Journal of Petrology* **29**(6), 1325-1352.

Saxena, S.K. (1979) Garnet-clinopyroxene geothermometer. *Contributions to Mineralogy and Petrology* **70**, 229-235.

Schulze, D.J. (1989) Constraints on the abundance of eclogite in the upper mantle. *Journal of Geophysical Research* **94**, 4205-4212.

Serri, G. (1981) The petrochemistry of ophiolite gabbroic complexes: a key for the classification of ophiolites into low-Ti and high-Ti types. *Earth and Planetary Science Letters* **52**, 203-212.

Sharp, Z. D. (1990) A laser based microanalytical method for the in situ determination of oxygen isotope ratios of silicates and oxides. *Geochimica et Cosmochimica Acta* **54**, 1353-1357.

Shee, S. R. (1978) The mineral chemistry of xenoliths from the Orapa kimberlite pipe, Botswana. Unpublished M.Sc. thesis, University of Cape Town.

Shee, S. R. & Gurney, J.J. (1979) The mineralogy of xenoliths from Orapa, Botswana. *Proceedings of the 2nd International Kimberlite Conference*, 37-49.

Shervais, J. W., Taylor, L.A., Lugmair, G.W., Clayton, R.N., Mayeda, T.K. & Korotev, R.L. (1988) Early Proterozoic oceanic crust and the evolution of subcontinental mantle: Eclogites and related rocks from southern Africa. *Geological Society of America Bulletin* **100**, 411-423.

Simakov, S. K. (1999) Garnet-clinopyroxene geobarometry of deep mantle eclogites and eclogite paleogeotherms. *Proceedings of the Seventh International Kimberlite Conference* (ed. J.J. Gurney, Gurney, J.L., Pascoe, M.D. & Richardson, S.R.), 783-787.

Smith, C. B. (1983) Pb, Sr and Nd isotopic evidence for sources of southern African Cretaceous kimberlites. *Nature* **304**, 51-54.

Smith, D. (1999) Temperatures and pressures of mineral equilibration in peridotites xenoliths: Review, discussion and implications. In *Mantle Petrology: Field observations and high pressure experimentation: A tribute to Francis R. (Joe) Boyd*, Vol. **6** (ed. B. Fei, Mysen). Geochemical Society Special Publication No. 6.

Smith, H.S., & Erlank, A.J. (1982) Geochemistry and petrogenesis of komatiites from the Barberton Greenstone Belt, South Africa. In *Komatiites* (ed. N. T. Arndt & Nisbet, E.G.), pp. 347-397. George Allen & Unwin.

Smyth, J.R., McCormick, T.C. & Caporuscio, F.A. (1984) Petrology of a suite of eclogite inclusions from the Bobbejaan Kimberlite I. Two unusual corundum-bearing kyanite eclogites. In *Kimberlites II: The mantle and crust-mantle relationships.* (ed. J. Kornprobst), pp. 109-119. Elsevier.

Smyth, J.R. & Caporuscio, F.A. (1984) Petrology of a suite of eclogite inclusions from the Bobbejaan Kimberlite II: Primary phase compositions and origin. In *Kimberlites II: The mantle and crust-mantle relationships.* (ed. J. Kornprobst), pp. 121-131. Elsevier.

Smyth, J.R., Caporuscio, F.A. & McCormick, T.C. (1989) Mantle eclogites: evidence of igneous fractionation in the mantle. *Earth and Planetary Science Letters* **93**, 133-141.

Smyth, J.R., Caporuscio, F.A. & McCormick, T.C. (1990) Reply to comment of C.R.Neal and L.A.Taylor on "Mantle eclogites: evidence of igneous fractionation in the mantle". *Earth and Planetary Science Letters* **101**, 120-124.

Snyder, G.A., Taylor, L.A., Crozaz, G., Halliday, A.N., Beard, B.L., Sobolev, V.N. & Sobolev, N.V. (1997) The origins of Yakutian eclogite xenoliths. *Journal of Petrology* **38**(Number 1), 85-113.

Sobolev, A.V. & Danyushevsky, L.V. (1994) Petrology and geochemistry of boninites from the North Termination of the Tonga Trench: constraints on the generation conditions of primary high-Ca boninite magmas. *Journal of Petrology* **35**, 1183-1211.

Sobolev, V.N., Taylor, L.A. & Snyder, G.A. (1994) Diamondiferous eclogites from the Udachnaya Kimberlite Pipe, Yakutia. *International Geology Review* **36**, 42-64.

Stephens, W.E. & Dawson, J.B. (1977) Statistical comparison between pyroxenes from kimberlites and their associated xenoliths. *Journal of Geology* **85**, 433-449.

Stowe, C. W. (1983) The Upington geotraverse and its implications for craton margin tectonics. *Special Publication of the Geological Society of South Africa* **10**, 147-171.

Stowe, C.W. (1986) Synthesis and interpretation of structures along the north-eastern boundary of the Namaqua Tectonic Province, South Africa. *Transactions of the Geological Society of South Africa* **89**, 185-198.

Sun, S.-s. & McDonough, W.F. (1989) Chemical and isotope systematics of oceanic basalts: implications for mantle composition and processes. In *Magmatism in the ocean basins* (ed. A.D.N. Saunders & Norry, M.J.), pp. 313-345. Geological Society Special Publication **42**.

Tankard, A.J., Jackson, M.P.A., Eriksson, K.A., Hobday, D.K., Hunter, D.R. & Minter, W.E.L. (1982) *Crustal Evolution of Southern Africa*. Springer-Verlag.

Taylor, H.P. & Sheppard, S.M.F. (1986) Igneous rocks: I. Processes of isotopic fractionation and isotope systematics. In *Stable isotopes in high temperature geological processes*, Reviews in Mineralogy Vol. **16** (ed. J.W. Valley, Taylor, H.P. Jr. & O'Neil, J.R.), pp. 227-271. Mineralogical Society of America.

Taylor, L.A. & Neal, C.R. (1989) Eclogites with oceanic crustal and mantle signatures from the Bellsbank kimberlite, South Africa, Part 1: mineralogy, petrography, and whole-rock chemistry. *Journal of Geology* **97**, 551-567.

Taylor, L.A. & Neal, C.R. (1993) Comment on "Trace-element crystal chemistry of mantle eclogites by F.A. Caporuscio and J.R. Smyth. *Contributions to Mineralogy and Petrology* **113**, 280-284.

van der Laan, S. R., Flower, M.F.J. & van Groos, A.F.K. (1989) Experimental evidence for the origin of boninites: near-liquidus phase relations to 7.5kb. In *Boninites* (ed. A. J. Crawford), pp. 112-147. Unwin Hyman.

Venneman, T. W. & Smith, H.S. (1999) Geochemistry of mafic and ultramafic rocks in the type section of the Kromberg Formation, Barberton Greenstone Belt, South Africa. In *Geologic evolution of the Barberton Greenstone Belt, South Africa*, (ed. D. R. Lowe & Byerly, G.R.), pp. 133-149. Geological Society of America Special Publication **329**.

Viljoen, K. S. (1994) The petrology and geochemistry of a suite of mantle-derived eclogite xenoliths from the Kaalvallei kimberlite, South Africa. Unpublished Ph.D. thesis, University of the Witwatersrand.

Viljoen, K.S. (1995) Graphite and diamond-bearing eclogite xenoliths from the Bellsbank kimberlites, Northern Cape, South Africa. *Contributions to Mineralogy and Petrology* **121**, 414-423.

Wagner, P.A. (1914) *The diamond fields of Southern Africa*. The Transvaal Leader.

Waters, F.G. (1987) A geochemical study of metasomatised peridotite and MARID nodules from the Kimberley pipes, South Africa. Unpublished Ph.D.thesis, University of Cape Town.

Wells, P.R.A. (1977) Pyroxene thermometry in simple and complex systems. *Contributions to Mineralogy and Petrology* **62**, 129-139.

Whitelock, T.K. (1973) The Monastery Mine kimberlite pipe. In *Lesotho Kimberlites* (ed. P. H. Nixon), pp. 214-220. Lesotho National Development Corporation.

Winterburn, P.A. (1987) Geochemical studies of peridotite xenoliths from southern African kimberlites. Ph.D., unpublished, University of Edinburgh.

Wood, B.J. & Banno, S. (1973) Garnet-orthopyroxene and orthopyroxene-clinopyroxene relationships in simple and complex systems. *Contributions to Mineralogy and Petrology* **42**, 109-124.

Wood, B.J. (1974) The solubility of alumina in orthopyroxene co-existing with garnet. *Contributions to Mineralogy and Petrology* **46**, 1-15.

Xie, Q., Kerrich, R. & Fan, J. (1993) HFSE/REE fractionations recorded in three komatiite-basalt sequences, Archean Abitibi greenstone belt: Implications for multiple plume sources and depths. *Geochimica et Cosmochimica Acta* **57**, 4111-4118.

Yoder, H. S. J. & Tilley, C.E. (1962) Origin of basalt magmas: An experimental study of natural and synthetic rock systems. *Journal of Petrology* **3**, 342-532.

Appendix I:

Analytical Techniques

Ia: Electron Microprobe (EMP)

Major element mineral analyses were determined on double-polished, 60μm thick probe sections. Analyses were carried out using the Cameca Camebax electron microprobe at the University of Cape Town (UCT). For the purposes of analyses, the beam current was set at approximately 40nA, and an accelerating voltage of 15kV was used. The size of the incident electron beam can be focussed to a diameter of approximately 0.1μm, whilst the flourescent x-ray beam has a diameter of 2-5μm, depending on the nature of the matrix. Ten second counting times at peak and background positions were used for all elements, except Na in garnet, and K in clinopyroxene, for which counting times of 30 seconds were used. Na, Mg, Si and Al were analysed using the TLAP analysing crystal; Fe and Mn using LIF200, and Ca, K, Ti and Cr using the PET analysing crystal. Data was reduced online using the PAP reduction method, as described by Pouchouz & Pichoir (1984).

Lower limits of detection (LLD) and 1σ errors for EMP analyses are presented in *Table I.1*

Ib: Laser Ablation Inductively Coupled Plasma Mass Spectrometry (LA-ICP-MS)

Trace element concentrations of garnet and clinopyroxene grain mounts were analysed using a Perkin Elmer ELAN6000 ICP-MS and CETAC LSX-200 laser ablation system at UCT. The laser is a frequency-quadrupled Nd-YAG laser, operating at a pulse repetition rate of 5Hz, resulting in an ablation pit approximately 100μm in diameter. The main gas flow in the ICP-MS was approximately 15L/min, whilst the nebuliser and auxiliary gas flows were set at 1.10 and 0.75 L/min respectively. The vacuum operated under a pressure of 2.38×10^{-5} Torr, and the autolens (set at ^{48}Ti: 5.0V, ^{88}Sr: 5.2V and ^{174}Yb: 6.0V) manipulated the ion beam.

Recommended values for NIST 610 and 612 glass standards (Pearce *et al.*, 1997) were used to standardise the instrument every hour, and isobaric interference corrections were automatically made using ^{144}Sm on ^{144}Nd, ^{152}Gd on ^{152}Sm, ^{160}Dy on ^{160}Gd and ^{174}Hf on ^{174}Yb. After an initial read delay of 40s, counts were accumulated for three replicates each of 100 readings, for a total counting time of 55.08s. ^{44}Ca was used as the internal standard during analyses.

LLD and 1σ and 2σ errors for trace elements measured using LA ICP-MS are presented in *Table I.1*. Graphical representations of the 2σ errors for garnet and clinopyroxene for two representative samples (Rtfn 54.1 and CMA 8) are illustrated in *Figure I.1*.

Ic: Laser Flourination Oxygen Isotope Analysis

Garnets from the Rietfontein eclogites were analysed at UCT using a laser flourination vacuum line, based originally on the system described by Sharp (1990). Garnet grains were cleaned first in warm HF, and then acetone, and 1-3 grains of each sample, collectively weighing 1-2mg, were loaded into pure Ni sample holders. Samples were directly loaded into the reaction chamber from a 110°C oven to prevent moisture absorption. Details of the analytical method are given in Harris *et al.* (*in press*). The laser is a 40mW Synrad CO_2 laser with an exit beam diameter of approximately 4mm, which, after passing through a 7x beam expander, is combined with a He-Ne sighting laser.

Each sample was reacted in the presence of approximately 15kPa ClF_3, and once the reaction had been completed, any excess ClF_3 and Cl_2 that formed as a result of dissociation was frozen out of the system. The remaining gas was then expanded into the stainless steel double-U trap, and the purified O_2 was expanded into the glass line and converted to CO_2. The yield of CO_2 is then measured, and is transferred to "break-seal tubes" for mass spectrometric analysis. The standard in use at UCT for laser flourination analyses is MON GT, garnet derived from a garnet megacryst retrieved from the Monastery Kimberlite (Moore, 1986). For the Rietfontein sample run, the garnet standard (MON GT) was run three times, resulting in values of 5.57‰, 5.69‰ and 5.40‰. This gave an average value of 5.55±0.15‰. All data was normalised so that MON GT = 5.55‰ relative to SMOW (Standard Mean Ocean Water).

Table I.1 *Lower limits of detection (LLD) and 1 σ errors for garnet and clinopyroxene. Major element values for EMP in wt%, trace element values for LA-ICP-MS in ppm*

EMP	Garnet		Clinopyroxene	
	LLD	1σ	LLD	1σ
SiO_2	0.04	0.20	0.05	0.20
TiO_2	0.01	0.01	0.02	0.02
Al_2O_3	0.04	0.16	0.04	0.10
Cr_2O_3	0.01	0.02	0.02	0.01
FeO	0.06	0.18	0.06	0.07
MnO	0.03	0.03	0.01	0.01
MgO	0.04	0.13	0.05	0.11
CaO	0.03	0.11	0.03	0.14
Na_2O	0.01	0.01	0.09	0.11
K_2O			0.02	0.00

LA-ICP-MS	Garnet		Clinopyroxene	
	LLD	1σ	LLD	1σ
Sc	0.58	0.34	0.33	0.33
Ni	1.9	0.73	1.2	9.5
Sr	0.17	0.070	0.072	8.4
Y	0.14	0.31	0.060	0.078
Zr	0.30	0.080	0.13	1.4
La	0.020	0.013	0.046	0.47
Ce	0.060	0.013	0.048	0.57
Nd	0.22	0.047	0.040	0.18
Sm	0.20	0.066	0.14	0.094
Eu	0.099	0.039	0.15	0.056
Gd	0.31	0.11	0.067	0.048
Dy	0.32	0.095	0.18	0.094
Er	0.20	0.032	0.15	0.031
Yb	0.22	0.085	0.089	0.018

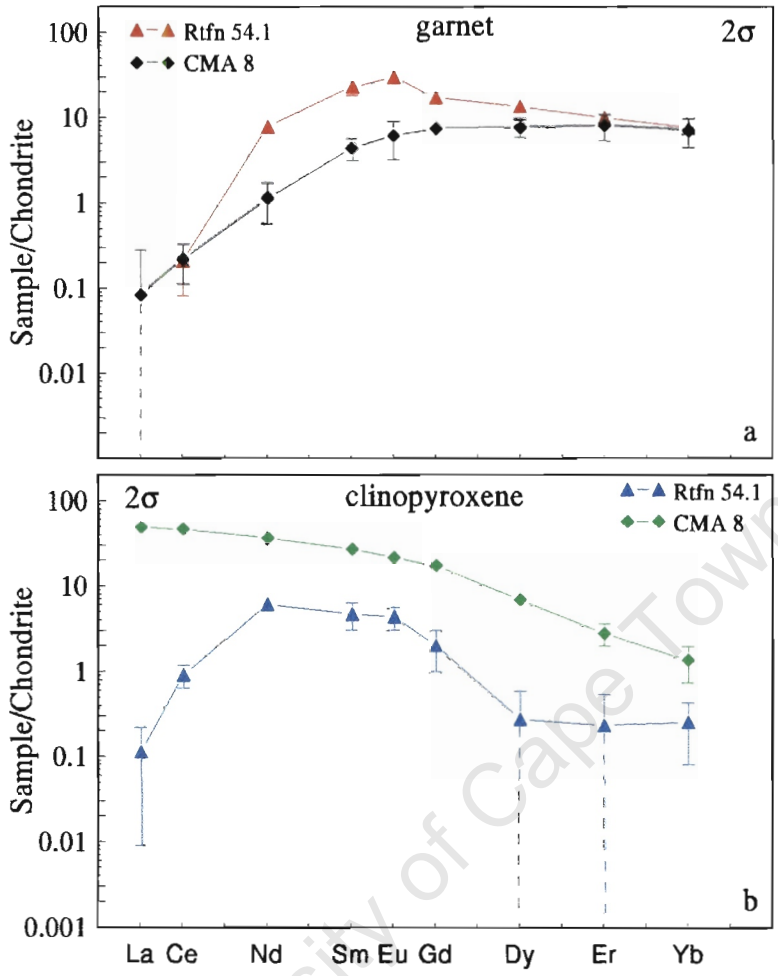

Figure I.1 *2σ errors on REE measurements by LA-ICP-MS for garnet* ***(a)*** *and clinopyroxene* ***(b)*** *from the Rietfontein eclogites.*

Appendix II:

Petrography

JJG 105

Bimineralic Eclogite. Group I. Gt:Cpx = 60:40

Coarse textured rock, garnet grains reach 1.5cm in diameter. Grains are cloudy and extensively fractured. Garnets are irregular and vary in size, as do the clinopyroxene grains. Serpentinization is found along grain boundaries. Phlogopite is present in the rock, mostly as fine grained laths along grain boundaries. Signs of strain can be seen within some of the clinopyroxene grains. Disaggregated pieces of clinopyroxene occur along grain boundaries. Accessory pyrite and chalcopyrite blebs are found within the sample.

JJG 2104

Kyanite eclogite. Group II. Gt:Cpx:Ky = 20:60:20.

Equigranular rock - garnet, kyanite and clinopyroxene grains are all 1-2mm in diameter. Most of the kyanite grains are rounded to euhedral, and simple twinning is common. Garnet grains range from rounded to elongate. Most are fractured and some have kyanite inclusions. Grains are fresh-looking, with small amounts of alteration occurring along grain boundaries. Clinopyroxene grains are irregular and seem to be interstitial to the garnet and kyanite grains. Clinopyroxenes also fractured, but fresh looking. Triple junctions are common. Grain sizes vary from 0.5 - 6mm in diameter.

PC 1

Bimineralic eclogite. Gt:Cpx = 70:30.

Fractured, altered rock with serpentinization along fractures and grain boundaries. Both garnet and clinopyroxene are cloudy. Clinopyroxene grains show strain in the form of undulose extinction and are small and irregular, with large amounts of serpentinization. Garnet grains reach a maximum of 1cm in diameter. Triple junctions are observed.

PC 3

Bimineralic eclogite. Group II. Gt:Cpx = 60:40.

Much serpentinization and alteration in the sample. Strained clinopyroxene grains. Garnets are all fractured, but still fresh looking. Clinopyroxene seems to be interstitial between garnet grains. Garnet grains are fractured, but seem to have an overall subhedral to rounded shape. Some clinopyroxene grains are completely serpentinized. Clinopyroxene grains are irregular and anhedral. Spinel (or rutile) needles are enclosed in some garnets. Secondary phlogopite is present as a metasomatic alteration product.

PC 5.2/1

Orthopyroxene eclogite. Gt:Cpx:Opx = 60:35:5.

Garnets are fractured with some alteration, but relatively fresh garnets are also present. Fractures are generally serpentinized with traces of mica. Very irregular grain boundaries occur between clinopyroxene and garnet. Small amounts of fresh-looking orthopyroxene occur in the sample. Clinopyroxene is cloudy and pale green in colour, with diameters of 0.5 - 4mm. Garnet grains reach 1-5mm in diameter. Serpentinization occurs along grain boundaries. A small amount of clinopyroxene is surrounded by garnet in one case. Interstitial sulphide is found within the sample.

PC 5.2/2

Bimineralic eclogite. Group II. Gt:Cpx = 40:60.

Garnet grains range in diameter from 2-8mm. Garnet grains are fresh, some clinopyroxene is cloudy, whilst other grains are fresh. Clinopyroxene grains are 0.5-5mm diameter, anhedral, and irregularly shaped. Grain edges are embayed and grain boundaries are curved to irregular. Grains are fractured with serpentinization along fractures.

PC 12

Bimineralic eclogite. Group II. Gt:Cpx = 30:70.

Fresh sample, although garnet is fresher than the clinopyroxene. All grains are fractured. Triple junctions exist between some of the clinopyroxene grains. Small amounts of serpentinization occur around some of the clinopyroxene grains (undulose extinction). Clinopyroxenes are anhedral and irregularly shaped. Clinopyroxene seems to be interstitial around the garnet grains. Grains sizes are 1-4mm in diameter.

Rtfn 31.1

Bimineralic eclogite. Gt:Cpx = 45:55.

Entirely garnet, with only small amounts of clinopyroxene along the edges of the sample. Small amount of phlogopite. Garnet is fractured, with both fresh and cloudy areas. Accessory amphibole also observed in the sample, forming fine-grained irregular interlocking plates. It is pale green in colour, pleiochroic and occurs mostly around garnet grain boundaries.

Rtfn 31.2

Bimineralic eclogite. Group II. Assumed Gt:Cpx = 50:50.

Most of the sample is garnet, with a small amount of clinopyroxene around the edge of the grain. Garnets are fractured, with serpentinization and alteration along the fractures. Clinopyroxene is altered and cloudy. Garnets are angular and anhedral, with diameters of 1.5 - 3mm.

Rtfn 31.3

Bimineralic eclogite. Group II. Gt:Cpx = 45:55.

Clinopyroxene grains have embayed edges and undulose extinction is visible in some grains. Garnet grains reach 6mm in diameter, clinopyroxene grains 4mm. Garnet and clinopyroxene grains seem to be interlocking. Triple junctions are visible in the rock. Garnet grains are subhedral, clinopyroxene grains are more anhedral. Curved and irregular grain boundaries occur between garnet and clinopyroxene. Garnets are fractured, but fresh, with inclusions of microscopic rutile needles. Clinopyroxene is also fractured with embayed edges. Ilmenite and rutile occur as interstitial accessory minerals.

Rtfn 43.1

Bimineralic eclogite. Group II. Gt:Cpx = 60:40.

Garnet grains reach 3mm in diameter. Clinopyroxene grains are irregularly shaped, smaller (1-3mm) and not as fresh as the garnet. Clinopyroxene also occurs as an inclusion in garnet. Curved and irregular grain boundaries are observed between clinopyroxene grains. Garnets are fractured, but fresh looking. Sericitization is found within clinopyroxene grains and along fractures. Accessory rutile and ilmenite occur interstitially.

Rtfn 43.7

Bimineralic eclogite. Gt:Cpx = 40:60.

Large mica (phlogopite) in sample, 3mm in diameter, with a tabular, plate-like habit. Cumulus textured rock, with euhedral/subhedral garnets set in a clinopyroxene matrix. Garnets are large, up to 5mm in diameter and are fractured but look fresh. Clinopyroxenes are irregular in shape, also reaching 5mm in diameter. Clinopyroxene is not as fresh as the garnet, grains are cloudy and show undulose extinction (strain). Serpentinization occurs in the rock, along grains boundaries and within clinopyroxene. Small rutile grains occur interstitially.

Rtfn 43.9

Bimineralic eclogite. Group II. Gt:Cpx = 40:60.

Fresh, well-equilibrated rock with straight grain boundaries and triple junctions between grains. Possibly a cumulus textured rock where garnet grains have sunk into clinopyroxene. Clinopyroxene is not quite as fresh as the garnet and all grains are fractured. Garnet contains inclusions of small rutile or spinel

needles. Disintegration of clinopyroxene occurs along some of the grain boundaries. Garnet grains reach 4mm in diameter, whilst clinopyroxene grains are slightly smaller at approximately 3mm. A small amount of kimberlite matrix occurs at the edge of the sample.

Rtfn 43.10

Bimineralic eclogite. Gt:Cpx = 45:55.

Much alteration is found along grain boundaries (calcite, chlorite, phlogopite and amphibole). Garnet grains are irregular, fractured and reach 5mm in diameter. Clinopyroxene grain enclosed by garnet in one part of the sample. Grains in sample are not particularly fresh looking, most show some degree of clouding. Garnet-clinopyroxene grain boundaries are curved to irregular.

Rtfn 48.1

Bimineralic eclogite. Group II. Gt:Cpx = 55:45.

Fractured, but very fresh garnet and clinopyroxene grains. All mineral grains are anhedral. Sericitization and serpentinization occurs along fractures. The alteration product in the sample includes chlorite, calcite, serpentine and phlogopite, and is found as patches between grains. Some garnets contain rutile or spinel needles. Embayed edges are visible in some of the grains. The rock is coarse grained with 1-5mm diameter grains. Rutile is an interstitial accessory mineral.

Rtfn 48.2

Bimineralic eclogite. Group I. Assumed Gt:Cpx = 50:50.

Coarse grained rock where rounded garnet grains are set in clinopyroxene. Altered rock, with much phlogopite in areas of alteration. Garnets are fractured, but relatively fresh looking, whilst the clinopyroxene is cloudy. Clinopyroxene grains are irregular and strained. Much serpentinization is found within the sample. Garnets reach 5mm in diameter.

Rtfn 54.1

Kyanite eclogite. Group II. Gt:Cpx:Ky = 60:30:10.

Equigranular texture. Mostly anhedral grains, but some kyanites are euhedral or rounded. Some serpentine replacement of minerals has occurred, but most are fresh looking, if not fractured. Irregular and rounded garnet grains are surrounded by clinopyroxene. Garnets are fresh, some fractures within garnet contain calcite and chlorite. Kyanites are mostly twinned. Medium grained rock, with grains reaching a maximum of 1.5 - 2mm. Most grain boundaries are regular with some triple junctions.

Rtfn 54.2

Kyanite eclogite. Group II. Gt:Cpx:Ky = 30:60:10.

Rounded garnets are set in kyanite and clinopyroxene. Clinopyroxene grains are irregularly shaped, and twinning occurs in some of the kyanite grains. Most grains are fresh, but some do show signs of alteration. Garnets are all fresh, but fractured. Clinopyroxene encloses garnet in one instance. Grain sizes vary from 0.5-3mm in diameter. Kyanite grains are subhedral. Grain boundaries are straight, curved and irregular, and some triple junctions can be observed. Rutile occurs as an accessory mineral with a golden brown colour and high relief.

Rtfn 54.3

Kyanite eclogite. Group II. Gt:Cpx:Ky = 45:45:10.

Euhedral, angular garnet grains. Garnets are fresh, but fractured. Garnet-garnet grain boundaries are straight, whilst garnet-clinopyroxene/kyanite boundaries are curved. Carbonate and clinopyroxene inclusions can be found in some garnet grains. Kyanite and clinopyroxene grains are rounded to subhedral. Some grains have embayed edges and twinning is common in the kyanite grains. Garnet grains reach 2-4mm in diameter, whilst clinopyroxene and kyanite grains average 2mm.

Rtfn 54.4

Kyanite eclogite. Group II. Gt:Cpx:Ky = 30:60:10.

Subhedral to rounded kyanite grains. One kyanite grain occurs as an inclusion in clinopyroxene. Grain boundaries are curved and irregular, and are often embayed and altered. Grains are fractured, but mostly fresh looking (with the exception of some cloudy clinopyroxene grains). Clinopyroxene grains are irregular, possibly of a cumulate texture. Some garnets are irregularly shaped, others are rounded. Clinopyroxene occurs as inclusions in some of the garnet grains. Serpentinization occurs along fractures in the rock. Kyanite grains range in size from 0.5-1.5mm in diameter, whilst clinopyroxene grains reach a maximum of 6mm. Interstitial rutile and a sulphide inclusion in clinopyroxene are accessory minerals.

Rtfn 55.1

Bimineralic eclogite. Group I. Gt:Cpx = 60:40.

Grains in this rock are fractured, and the sample shows much alteration. Garnet and clinopyroxene grains are both fractured and cloudy, but overall the garnet grains have a fresher appearance. Garnet grains are fractured and disaggregated. Much interstitial alteration is found between grains. Sericitization and serpentinization occurs along fractures in the minerals. Grains are anhedral with clinopyroxene grains showing undulose extinction and embayed grain boundaries. Grains reach 5mm in diameter.

Rtfn 55.2

Bimineralic eclogite. Group I. Gt:Cpx = 80:20.

Altered sample. Garnets are large (3-6mm diameter) and angular, enclosing smaller (1.5mm) clinopyroxene grains. Rock is very fractured, and minerals have a cloudy appearance. Clinopyroxene is also serpentinized with undulose extinction. Grain boundaries are both straight and curved, with a few triple junctions. Phlogopite occurs as an alteration product.

Rtfn 55.3

Bimineralic eclogite. Assumed Gt:Cpx = 50:50.

Garnets are orange-brown in colour, whilst clinopyroxenes have a murky green appearance. Garnets are slightly clouded and fractured. Mica is common along grain boundaries. Clinopyroxenes are fractured, but overall have a relatively fresh looking appearance. Garnet grains are large (5mm and greater) and seem to be rounded. Clinopyroxene grains are much smaller (1-2mm), although one grain is approximately 5mm in diameter. Clinopyroxene grains are irregularly shaped, fractured and altered. Chlorite is present along grain boundaries, as part of the alteration material, and occurs as irregular laths and subhedral grains. Small, fine-grained fragments of clinopyroxene also occur in this matrix.

Rtfn 55.4

Bimineralic eclogite. Group II. Gt:Cpx = 30:70.

Sample consists of small (1-2mm, max 3mm) garnet grains set in clinopyroxene. Clinopyroxene is intercumulus to the garnet grains, and triple junctions can be found between the clinopyroxene grains. Some garnets are subhedral with some relatively well-formed crystal faces whilst other garnets are rounded. Clinopyroxene grains are both irregular and euhedral, with diameters of 0.5 - 5mm. Clinopyroxenes are clouded, whilst garnet grains are relatively fresh but fractured. Serpentinization occurs around the edge of the sample and along some grain boundaries.

Rtfn 56.1

Orthopyroxene eclogite. Group II. Gt:Cpx:Opx = 58:37:5.

Both garnet and clinopyroxene range from cloudy to fresh in appearance. Grains are irregular and anhedral. There is a moderate amount of alteration within the rock, serpentinization has affected the clinopyroxene to varying extents - almost entirely replacing one grain, and causing embayed grain boundaries in other instances. Phlogopite is visible along grain boundaries. Undulose extinction occurs in some clinopyroxenes. Grain boundaries are relatively straight, and garnets are dark coloured.

Rtfn 57.1

Bimineralic eclogite. Group II. Gt:Cpx = 50:50.

Irregularly shaped clinopyroxene grains. Triple junctions are visible, but scarce. Garnets are fresher than the clinopyroxene. Some serpentinization of grains has taken place. Clinopyroxene-garnet grain boundaries are irregular. Clinopyroxene grains are irregular and cloudy, and up to 3mm in diameter.

Rtfn 57.2

Bimineralic eclogite. Group II. Gt:Cpx = 40:60.

Angular garnet grains with straight grain boundaries occur in this sample, but there are also rounded grains, set in clinopyroxene. Garnets are fractured and very fresh looking. Clinopyroxenes are fractured, but more cloudy in appearance. Grain boundaries between clinopyroxene grains are irregular. Much serpentinization occurs in the rock, along with alteration products (phlogopite, brucite, calcite). A coarse grained rock, with grain sizes 1-3mm in diameter.

Rtfn 57.3

Bimineralic eclogite. Group II. Gt:Cpx = 50:50.

Garnet grains are rounded and 2-3mm in diameter. Triple junctions are visible between some of the clinopyroxene grains. Clinopyroxenes are mostly fresh, with one or two clouded by small amounts of alteration. Cumulus textured rock – rounded garnets with interstitial clinopyroxene. Clinopyroxene - garnet grain boundaries are curved. Sulphides occur as interstitial accessory minerals, and also as an inclusion in garnet.

CMA 1

Bimineralic eclogite. Group II. Gt:Cpx = 30:70.

Garnets are rounded, up to 2mm diameter, and form linear necklaces in some parts of the rock. Garnet exsolution is visible in 2 clinopyroxene grains – relatively fresh garnet laths, approximately 0.25-0.5mm in diameter, run parallel through large, optically continuous clinopyroxene grains. Clinopyroxene grains are large in some instances, up to 5mm diameter. Some garnets also have irregular shapes, whilst others are rounded, and up to 2mm in diameter. Clinopyroxene is rounded with curved grain boundaries. Grains are fractured with small amounts of clouding and some triple junctions are present. Garnets are fractured, but mostly fresh looking. Serpentinization and sericitization occurs along fractures and within grains. Pale green pleiochroic amphibole is found along some grain boundaries.

CMA 2

Bimineralic eclogite. Group II. Gt:Cpx = 40:60.

Garnets are rounded, often with irregular shapes, 0.5-5mm in diameter. Garnet grain boundaries are occasionally straight, whilst clinopyroxenes have both curved and straight boundaries. Clinopyroxene grains are on average larger than the garnets, and are 1-5mm in diameter. All grains are fractured, with clouding, although the garnets are generally fresher than the clinopyroxene. Schillerisation can be seen in clinopyroxene, and along grain boundaries. Triple junctions are visible in some areas. Secondary amphibole is observable along grain boundaries.

CMA 3

Orthopyroxene eclogite. Group II. Gt:Cpx:Opx = 30:50:20.

Grain sizes range from 0.5-5mm in diameter. Garnets are subhedral to rounded, fractured, but overall they are remarkably fresh. Pyroxenes reach diameters of 5mm. Clinopyroxenes are fresh, but the orthopyroxene is very altered – brown alteration along the edges of grains and replacing opx. Clinopyroxene grains are irregularly shaped with curving grain boundaries, sometimes showing serpentinization. Fine grained, green pleiochroic amphibole occurs interstitially. Decompression melting veins with carbonate-filled vesicles are present.

CMA 4

Bimineralic eclogite. Gt:Cpx = 40:60.

Garnets are fractured, but relatively fresh, as is the clinopyroxene in this sample. Coarse grained rock, complete anhedral grains up to 5mm diameter. Fine to medium grained secondary alteration comprises brucite, calcite, pyroxene and phlogopite.

CMA 5

Bimineralic eclogite. Gt:Cpx = 50:50.

Coarse textured rock – garnets up to 1.5cm diameter, but most are smaller. Garnets look rounded and irregularly shaped. Clinopyroxenes are also large, reaching diameters of 5mm. Garnets are fractured, and are both fresh and clouded. Clinopyroxene grains show more alteration than garnet. Most grain boundaries are curved, but some are straight. Patches of alteration material consisting of phlogopite, amphibole, calcite and brucite observed.

CMA 6

Bimineralic eclogite. Group II. Gt:Cpx = 35:65.

Garnets are subhedral to rounded but can also be irregular. Medium sized grains – 1-3mm diameter. Clinopyroxene grains have irregular shapes with curving grain boundaries. Garnets are both relatively fresh and cloudy. Clinopyroxenes are more altered than garnet, and show serpentinization in areas.

CMA 7

Bimineralic eclogite. Group I. Gt:Cpx = 50:50.

Very coarse grained rock with rounded garnets reaching diameters of 1.5cm. Grain boundaries are curved, and in one case, garnet is enclosed within clinopyroxene. Some clinopyroxenes have embayed grain boundaries. Interstitial rutile is an accessory mineral.

CMA 8

Bimineralic eclogite. Group II. Gt:Cpx = 50:50.

Garnet grains are both anhedral and irregularly shaped and 4-5mm in diameter. Very altered rock, all grains are "cloudy". Large amount of serpentinization and sericitization in the rock. Clinopyroxene grains are irregularly shaped, some grains however have euhedral outlines. Grain boundaries are both curved and straight, and embayments are common. Alteration is found along grain boundaries and fractures, and accessory amphibole occurs along grain boundaries.

CMA 9

Bimineralic eclogite. Group I. Gt:Cpx = 70:30.

Garnets are rounded, some irregularly shaped, up to 1cm in diameter. Clinopyroxene seems largely interstitial and grains can be subhedral, rounded or irregular, and up to 3mm diameter. Some grains show strain in the form of undulose extinction. Garnet and clinopyroxene are both fresh, despite evidence for pervasive fluid movement through the rock. Garnets are fractured with fine grained alteration products along fractures and grain boundaries. Ilmenite blebs occur interstitially in the rock, and fine grained amphibole or chlorite is visible along grain boundaries.

CMA 10

Bimineralic eclogite. Gt:Cpx = 50:50.

Garnets range in size from 1mm to 1cm, and are irregularly shaped. Rock is very altered, clinopyroxene and garnet are both cloudy and altered. Clinopyroxene reaches 6mm in diameter, and grains are mostly irregularly rounded with curving boundaries. There are also some straight boundaries, complete serpentinization of some clinopyroxene grains has occurred and undulose extinction is common. Alteration of minerals has occurred along fractures and grain boundaries. Garnets contain small needles of rutile. Ilmenite and rutile occur interstitially.

CMA 11

Orthopyroxene eclogite. Gt:Cpx:Opx = 60:35:5.

Large (1cm) rounded garnets with smaller clinopyroxene grains (2mm - 1cm) occur. Garnets are fractured, but fresh looking, as are the clinopyroxenes. Orthopyroxene grains are intensely altered around rims and along fractures to a reddish-brown material, only the cores remain and it is impossible to see the original grain outline. Clinopyroxene grains are rounded, although some are irregular, and show undulose extinction.

CMA 12

Orthopyroxene eclogite. Group II. Gt:Cpx:Opx = 45:45:10.

Garnets up to 7mm in diameter occur here, with rounded to irregular outlines. All grains are very fractured. Garnets are fresh looking, whilst the clinopyroxene is cloudy. Orthopyroxene is altered to a reddish brown product around grain edges. Serpentinization of pyroxene grains is common. Grain boundaries mostly seem to be curving. Clinopyroxene grains have rounded edges but are irregularly shaped and show undulose extinction. Decompression melting veins with carbonate-filled vesicles occur.

CMA 13

Orthopyroxene eclogite. Group II. Gt:Cpx:Opx = 35:60:5.

Finer grained rock, with garnet grains reaching a maximum diameter of approximately 2mm, orthopyroxene grains are about the same size. Clinopyroxene grains are larger, up to 5mm in diameter. Garnets are subhedral to rounded. Some clinopyroxene grains are very euhedral, others have a more rounded irregular shape. Grain boundaries are both curved and straight. Serpentinization and alteration has mostly affected orthopyroxene grains. Clinopyroxene and garnet grains are both clouded – garnets are slightly fresher though. Some clinopyroxene edges are embayed, with grains showing partial replacement by alteration minerals. Carbonate filled vesicles form decompression melting veins. Rutile is present as an accessory phase.

CMA 14

Bimineralic eclogite. Gt:Cpx = 40:60.

Very altered rock. Garnets are rounded and up to 1cm in diameter. Garnet is fractured but relatively fresh looking. Clinopyroxenes show sizes varying from 1-6mm. Some clinopyroxene is relatively fresh, others are more clouded. Clinopyroxene has been most affected by alteration – grains have been fractured and alteration occurs along fracture zones, and grains show undulose extinction. Accessory interstitial rutile is present.

CMA 15

Bimineralic eclogite. Group II. Gt:Cpx = 40:60.

Very altered. Small rounded garnets, 1-2mm in diameter, with clinopyroxenes varying between 1 and 6mm. Small tablet shaped garnet grains can also be observed. All grains are fractured, and much of the clinopyroxene is serpentinized. Clinopyroxene grains are irregular, embayed with curving grain boundaries. Slight clouding is seen in both clinopyroxene and garnet. Interstitial ilmenite blebs are present.

CMA 16

Bimineralic eclogite. Gt:Cpx = 50:50.

Very little clinopyroxene in sample, most of which is a huge (1.5cm) garnet grain. Very altered rock, garnet is fractured and very cloudy, as is the clinopyroxene. Irregularly shaped clinopyroxene has curving grain boundaries, is 3mm in diameter and shows undulose extinction. Embayed grains have irregular grain boundaries. Clinopyroxene is much finer grained in areas of alteration. Fine grained secondary amphibole is present in altered areas.

CMA 17

Bimineralic eclogite. Group II. Gt:Cpx = 70:30.

Coarse grained garnet and clinopyroxene grains set in a medium grained matrix of metasomatic material (brucite, amphibole, calcite, chlorite). Garnet and clinopyroxene grains themselves are relatively fresh. Most grains are irregularly shaped, sometimes with rounded outlines.

CMA 18

Bimineralic eclogite. Group II. Gt:Cpx = 60:40.

Subhedral to rounded garnets, approximately 5mm in diameter, although some are as small as 1mm. Clinopyroxene grains also reach 5mm in diameter, and are rounded, but with irregular outlines. Grain boundaries are both straight and curved. Garnets are fresher than the clinopyroxenes, which show undulose extinction.

Appendix III:
Geochemical Data

Table III.1 *Major element composition of garnets from the Rietfontein eclogites*

Sample	Eclogite type	Grain	SiO_2	TiO_2	Al_2O_3	Cr_2O_3	FeO	MnO	MgO	CaO	Na_2O	Total	Mg#
JJG 2104	Kyanite-bearing	Gt 1 rim	39.88	0.13	22.64	0.04	11.33	0.15	6.19	20.32	0.04	**100.71**	49.3
		Gt 2 core	39.88	0.09	22.66	0.02	11.03	0.20	6.59	19.56	0.06	**100.11**	51.6
		Gt 3	39.76	0.09	22.64	0.00	11.46	0.19	6.33	19.35	0.05	**99.88**	49.6
Rtfn 54.1	Kyanite-bearing	Gt 1 core	39.15	0.09	23.39	0.01	15.02	0.25	8.47	14.20	0.06	**100.64**	50.1
		Gt 2 core	39.77	0.06	23.30	0.00	14.76	0.28	8.90	13.76	0.07	**100.89**	51.8
		Gt 2 rim	39.17	0.10	22.80	0.01	15.06	0.25	7.22	15.48	0.05	**100.16**	46.1
		Gt 3 core	39.19	0.09	23.07	0.00	15.08	0.28	7.18	15.08	0.08	**100.05**	45.9
Rtfn 54.2	Kyanite-bearing	Gt 1 core	39.39	0.10	22.14	0.04	15.90	0.27	9.22	12.97	0.03	**100.07**	50.8
		Gt 2 rim	39.99	0.10	22.26	0.06	16.10	0.26	9.21	12.96	0.04	**100.98**	50.5
		Gt 3 core	39.47	0.09	22.23	0.05	15.57	0.24	9.88	12.10	0.05	**99.70**	53.1
		Gt 3 rim	39.53	0.12	22.30	0.03	15.50	0.27	9.73	12.30	0.02	**99.79**	52.8
Rtfn 54.3	Kyanite-bearing	Gt 1 rim	40.63	0.06	23.42	0.00	12.54	0.16	10.56	12.96	0.03	**100.35**	60.0
		Gt 2 rim	39.61	0.05	22.93	0.00	12.61	0.15	10.71	12.72	0.02	**98.80**	60.2
Rtfn 54.4	Kyanite-bearing	Gt 1 core	39.44	0.10	22.71	0.04	15.09	0.25	9.29	12.81	0.05	**99.78**	52.3
		Gt 1 rim	39.13	0.11	22.71	0.05	14.95	0.28	9.37	13.08	0.04	**99.71**	52.8
		Gt 2 rim	39.15	0.09	22.75	0.06	14.99	0.22	9.72	12.43	0.05	**99.46**	53.6
		Gt 2 core	39.33	0.08	22.52	0.08	15.13	0.26	9.79	12.38	0.05	**99.61**	53.6
PC 5.2/1	Opx-bearing	Gt 1 core	41.43	0.09	23.51	0.23	13.21	0.34	18.29	3.71	0.06	**100.86**	71.2
		Gt 2	41.46	0.11	23.65	0.28	13.40	0.34	17.78	3.57	0.07	**100.65**	70.3
Rtfn 56.1	Opx-bearing	Gt 1	41.68	0.11	22.81	0.31	13.10	0.27	17.72	3.58	0.02	**99.62**	70.7
		Gt 1 rim	41.21	0.11	23.26	0.30	13.39	0.25	17.28	3.67	0.03	**99.50**	69.7
		Gt 2 core	41.80	0.11	23.08	0.27	13.16	0.27	17.41	3.65	0.02	**99.76**	70.2
CMA 3	Opx-bearing	Gt 1 core	40.16	0.07	22.12	0.81	16.48	0.68	14.43	4.91	0.01	**99.68**	61.0
		Gt 2 core	40.10	0.05	22.29	0.78	16.21	0.65	14.20	4.91	0.01	**99.22**	61.0
CMA 11	Opx-bearing	Gt 1	40.58	0.07	23.45	0.45	12.70	0.32	17.87	3.81	0.05	**99.30**	71.5
		Gt 2 core	40.92	0.06	23.52	0.46	12.74	0.33	17.85	3.81	0.05	**99.74**	71.4
CMA 12	Opx-bearing	Gt 1 core	40.73	0.13	23.64	0.18	12.82	0.39	18.12	3.84	0.06	**99.91**	71.6
		Gt 1 rim	41.63	0.11	23.95	0.14	12.27	0.36	18.37	3.85	0.04	**100.72**	72.7
		Gt 2 core	41.39	0.11	24.10	0.17	12.61	0.36	17.87	3.79	0.06	**100.46**	71.6
		Gt 2 rim	40.81	0.08	23.70	0.17	12.44	0.34	18.22	3.88	0.05	**99.69**	72.3
CMA 13	Opx-bearing	Gt 1 core	40.94	0.08	22.76	1.01	11.66	0.40	17.29	5.03	0.02	**99.19**	72.5
		Gt 1 rim	41.14	0.06	23.29	0.92	11.50	0.41	17.45	4.83	0.03	**99.63**	73.0
		Gt 2 rim	40.99	0.03	23.02	0.93	11.47	0.38	17.52	4.93	0.03	**99.31**	73.1
		Gt 3 rim	41.03	0.09	22.92	1.00	11.51	0.50	17.27	5.03	0.05	**99.39**	72.8
JJG 105	Bimineralic	Gt 1	41.01	0.13	23.80	0.29	13.77	0.31	16.87	3.92	0.04	**100.14**	68.6
		Gt 2 rim	41.13	0.15	23.85	0.35	14.00	0.28	16.99	3.88	0.05	**100.68**	68.4
		Gt 2 rim	41.13	0.15	23.85	0.35	14.00	0.28	16.99	3.88	0.05	**100.68**	68.4

Table III.1 *continued.*

Sample	Eclogite type	Grain	SiO_2	TiO_2	Al_2O_3	Cr_2O_3	FeO	MnO	MgO	CaO	Na_2O	Total	Mg#
PC 1	Bimineralic	Gt 1	42.36	0.12	24.78	0.24	8.81	0.29	19.88	4.46	0.02	**100.96**	80.1
		Gt 2	42.16	0.12	24.39	0.23	8.63	0.32	19.99	4.55	0.07	**100.45**	80.5
PC 3	Bimineralic	Gt 1	42.01	0.14	24.70	0.34	7.81	0.34	20.64	4.26	0.05	**100.29**	82.5
		Gt 2	42.12	0.12	24.52	0.34	7.84	0.39	20.65	4.14	0.05	**100.16**	82.4
		Gt 3	41.65	0.13	24.59	0.35	8.03	0.34	20.64	4.14	0.04	**99.91**	82.1
PC 5.2/2	Bimineralic	Gt 1	41.38	0.12	23.56	0.31	10.48	0.33	19.55	3.83	0.02	**99.59**	76.9
		Gt 2	41.61	0.12	23.63	0.35	10.80	0.34	19.47	3.78	0.06	**100.17**	76.3
PC 12	Bimineralic	Gt 1 rim	41.49	0.12	24.03	0.24	11.27	0.37	18.40	4.34	0.03	**100.29**	74.4
		Gt 1 core	41.69	0.16	23.84	0.25	11.09	0.37	18.37	4.24	0.03	**100.03**	74.7
		Gt 2 core	41.62	0.16	24.00	0.18	11.54	0.37	18.49	4.34	0.04	**100.74**	74.1
		Gt 2 rim	41.50	0.13	24.24	0.22	11.42	0.37	18.46	4.16	0.03	**100.54**	74.2
Rtfn 31.1	Bimineralic	Gt 1	40.86	0.14	23.22	0.22	13.94	0.32	16.81	3.95	0.04	**99.49**	68.3
		Gt 2	40.82	0.10	23.46	0.21	13.78	0.30	16.73	3.82	0.04	**99.27**	68.4
		Gt 3	40.77	0.12	23.19	0.23	14.08	0.34	17.58	3.97	0.21	**100.49**	69.0
Rtfn 31.2	Bimineralic	Gt 1 core	41.19	0.08	23.94	0.28	12.54	0.26	18.31	3.63	0.03	**100.27**	72.3
		Gt 1 rim	41.10	0.09	23.81	0.29	12.12	0.36	18.17	3.62	0.03	**99.60**	72.8
		Gt 2 rim	41.34	0.08	23.59	0.29	12.36	0.26	18.12	3.54	0.03	**99.61**	72.3
		Gt 2 core	41.44	0.09	24.11	0.33	12.48	0.25	18.51	3.51	0.03	**100.74**	72.6
Rtfn 31.3	Bimineralic	Gt 1 rim	41.51	0.12	23.97	0.10	9.50	0.40	20.04	4.00	0.04	**99.66**	79.0
		Gt 1 core	41.68	0.10	23.84	0.11	9.46	0.35	19.84	3.99	0.02	**99.39**	78.9
		Gt 2 rim	41.57	0.19	23.78	0.12	9.71	0.37	19.91	4.29	0.05	**99.99**	78.5
		Gt 2 core	41.53	0.19	23.75	0.15	9.52	0.37	19.63	4.12	0.05	**99.31**	78.6
Rtfn 43.1	Bimineralic	Gt 1 core	41.97	0.10	23.51	0.30	9.78	0.33	19.27	4.24	0.04	**99.54**	77.8
		Gt 1 rim	42.08	0.13	23.91	0.29	9.94	0.33	19.10	4.25	0.04	**100.07**	77.4
Rtfn 43.2	Bimineralic	Gt 1 rim	41.79	0.11	22.65	2.05	8.63	0.45	19.62	4.66	0.03	**99.98**	80.2
		Gt 1 core	42.12	0.10	22.88	2.08	8.69	0.38	19.64	4.69	0.03	**100.62**	80.1
		Gt 2 rim	41.95	0.12	22.67	2.09	8.44	0.37	19.90	4.75	0.03	**100.32**	80.8
		Gt 2 core	41.92	0.10	22.56	2.10	8.47	0.38	19.63	4.67	0.03	**99.85**	80.5
Rtfn 43.7	Bimineralic	Gt 1 core	41.98	0.11	23.74	0.20	9.34	0.43	19.77	4.18	0.04	**99.79**	79.1
		Gt 1 rim	41.86	0.14	23.70	0.19	9.59	0.39	19.78	4.21	0.04	**99.89**	78.6
		Gt 2 core	42.00	0.11	23.97	0.27	9.23	0.38	19.72	4.11	0.04	**99.83**	79.2
		Gt 2 rim	42.17	0.12	24.03	0.32	9.34	0.38	19.72	4.13	0.04	**100.23**	79.0
Rtfn 43.9	Bimineralic	Gt 1 core	41.40	0.12	23.78	0.37	9.95	0.41	19.12	4.05	0.04	**99.24**	77.4
		Gt 1 rim	41.81	0.13	24.09	0.35	9.94	0.41	19.34	4.04	0.04	**100.15**	77.6
Rtfn 43.10	Bimineralic	Gt 1 core	40.62	0.13	23.06	0.03	14.05	0.34	14.74	6.68	0.05	**99.71**	65.2
		Gt 1 rim	40.81	0.12	23.28	0.02	14.11	0.35	14.68	6.73	0.05	**100.14**	65.0
		Gt rim	40.25	0.13	23.03	0.02	14.14	0.37	14.83	6.73	0.05	**99.54**	65.2

Table III.1 *continued*

Sample	Eclogite type	Grain	SiO_2	TiO_2	Al_2O_3	Cr_2O_3	FeO	MnO	MgO	CaO	Na_2O	Total	Mg#
Rtfn 48.1	Bimineralic	Gt 1 rim	42.17	0.10	24.02	0.56	8.89	0.31	19.87	4.08	0.03	**100.03**	79.9
		Gt 2 rim	42.12	0.12	23.94	0.48	8.78	0.33	19.96	4.01	0.04	**99.78**	80.2
		Gt 2 core	41.79	0.12	23.84	0.50	9.14	0.34	19.97	3.98	0.04	**99.73**	79.6
		Gt 3	42.13	0.19	23.62	0.46	9.01	0.35	19.80	4.26	0.05	**99.87**	79.7
Rtfn 48.2	Bimineralic	Gt 1 core	42.19	0.10	24.34	1.08	7.34	0.32	20.92	4.18	0.04	**100.51**	83.6
		Gt 1 rim	41.78	0.09	24.18	1.04	6.99	0.37	20.98	4.10	0.04	**99.57**	84.3
		Gt 2	41.53	0.10	24.13	1.05	7.13	0.43	20.92	4.07	0.05	**99.41**	84.0
Rtfn 55.1	Bimineralic	Gt 1 core	42.97	0.12	23.70	0.36	8.28	0.38	20.44	4.22	0.04	**100.50**	81.5
		Gt 1 rim	43.13	0.13	24.14	0.42	7.99	0.34	20.46	4.35	0.04	**100.99**	82.0
		Gt 2 core	42.92	0.10	23.99	0.41	8.06	0.35	20.21	4.16	0.03	**100.25**	81.7
		Gt 3 core	42.96	0.14	23.80	0.39	8.08	0.35	19.87	4.18	0.04	**99.82**	81.4
		Gt 3 rim	42.73	0.11	23.86	0.36	8.03	0.37	19.84	4.08	0.03	**99.40**	81.5
Rtfn 55.2	Bimineralic	Gt 1	43.19	0.11	23.72	0.43	7.20	0.25	20.42	4.36	0.02	**99.71**	83.5
		Gt 1	43.93	0.12	24.83	0.49	7.10	0.26	19.20	4.32	0.03	**100.28**	82.8
		Gt 1	43.04	0.14	24.35	0.41	7.27	0.30	20.15	4.38	0.04	**100.06**	83.2
		Gt 2 core	42.67	0.13	24.18	0.48	7.19	0.28	20.05	4.41	0.02	**99.39**	83.3
Rtfn 55.3	Bimineralic	Gt 1 core	39.56	0.25	22.59	0.02	14.76	0.27	9.66	12.72	0.07	**99.90**	53.8
		Gt 1 rim	39.46	0.20	22.75	0.00	14.43	0.22	9.64	12.75	0.05	**99.49**	54.4
		Gt 1 core	40.01	0.17	22.59	0.00	14.24	0.25	9.57	12.61	0.04	**99.47**	54.5
Rtfn 55.4	Bimineralic	Gt 1	40.70	0.07	23.00	0.45	12.42	0.42	15.48	7.51	0.02	**100.09**	69.0
		Gt 2	40.52	0.08	22.69	0.47	12.24	0.48	15.20	7.57	0.09	**99.35**	68.9
		Gt 3	40.48	0.07	23.11	0.42	12.18	0.39	15.44	7.19	0.02	**99.31**	69.3
Rtfn 57.1	Bimineralic	Gt 1	41.07	0.08	23.59	0.18	13.80	0.30	17.64	3.92	0.01	**100.58**	69.5
		Gt 1	40.79	0.07	23.38	0.16	13.72	0.34	17.34	3.92	0.02	**99.74**	69.3
		Gt 1	40.95	0.05	22.88	0.16	13.86	0.29	17.40	3.90	0.01	**99.49**	69.1
Rtfn 57.2	Bimineralic	Gt 1 core	42.42	0.09	24.30	0.43	7.22	0.21	20.87	4.84	0.02	**100.40**	83.7
		Gt 1 rim	42.25	0.08	24.19	0.44	7.30	0.21	20.61	4.84	0.01	**99.93**	83.4
		Gt 1 core	42.36	0.07	24.22	0.43	7.12	0.18	20.76	4.93	0.02	**100.10**	83.9
		Gt 2 core	42.52	0.09	23.92	0.37	7.06	0.19	20.71	4.79	0.04	**99.69**	84.0
Rtfn 57.3	Bimineralic	Gt 1	41.26	0.10	23.70	0.64	8.85	0.36	20.45	4.47	0.11	**99.94**	80.5
		Gt 2	41.29	0.13	23.70	0.64	9.32	0.34	20.16	4.33	0.06	**99.97**	79.4
CMA 1	Bimineralic	Gt 1 lamellae	40.37	0.07	22.98	0.41	11.39	0.45	14.52	8.94	0.01	**99.14**	69.4
		Gt 2 lamellae	41.08	0.06	23.25	0.43	11.60	0.44	14.61	9.10	<0.01	**100.58**	69.2
		Gt 3 core	40.58	0.07	23.14	0.39	11.11	0.41	14.51	9.09	<0.01	**99.31**	70.0
		Gt 3 rim	40.69	0.06	23.00	0.41	11.25	0.46	14.68	9.01	0.01	**99.58**	69.9
		Gt 4	41.03	0.07	23.21	0.40	11.28	0.43	14.62	9.12	0.01	**100.17**	69.8
CMA 2	Bimineralic	Gt 1	40.49	0.05	22.93	0.40	12.79	0.46	15.78	6.46	0.01	**99.37**	68.7
		Gt 2 core	40.83	0.06	23.19	0.47	12.84	0.41	16.03	6.20	0.01	**100.03**	69.0
		Gt 3	40.31	0.05	22.90	0.44	12.83	0.38	15.88	6.19	0.01	**99.00**	68.8

Table III.1 *continued*

Sample	Eclogite type	Grain	SiO_2	TiO_2	Al_2O_3	Cr_2O_3	FeO	MnO	MgO	CaO	Na_2O	Total	Mg#
CMA 4	Bimineralic	Gt 1 rim	40.12	0.12	22.58	0.27	12.29	0.22	9.95	14.56	0.08	**100.18**	59.1
		Gt 2 core	40.20	0.10	22.59	0.25	12.32	0.24	10.56	13.97	0.06	**100.30**	60.4
		Gt 2 rim	40.11	0.10	22.61	0.24	12.44	0.24	10.66	14.06	0.04	**100.49**	60.4
CMA 5	Bimineralic	Gt 1 core	41.48	0.11	23.37	0.18	11.41	0.32	19.03	3.76	0.04	**99.69**	74.8
		Gt 2 core	41.53	0.16	23.52	0.20	11.11	0.34	18.80	3.88	0.02	**99.57**	75.1
CMA 6	Bimineralic	Gt 1 core	41.23	0.06	22.37	1.46	10.50	0.40	18.72	5.19	0.03	**99.94**	76.1
		Gt 1 rim	40.75	0.09	22.35	1.45	10.40	0.46	18.73	5.19	0.02	**99.43**	76.2
CMA 7	Bimineralic	Gt 1 core	42.04	0.10	23.94	0.18	9.56	0.33	20.25	4.04	0.04	**100.48**	79.1
		Gt 2 rim	40.90	0.11	23.88	0.17	9.24	0.38	20.37	4.14	0.03	**99.21**	79.7
		Gt 2	41.61	0.09	24.07	0.11	9.55	0.35	20.29	4.01	0.05	**100.13**	79.1
CMA 8	Bimineralic	Gt 1 core	41.19	0.09	22.49	1.13	9.88	0.65	18.51	5.58	0.08	**99.59**	77.0
		Gt 2 core	40.66	0.11	22.98	1.11	9.31	0.45	19.87	4.48	0.03	**99.00**	79.2
		Gt 3	41.45	0.10	23.01	1.12	9.64	0.45	19.28	4.58	0.04	**99.67**	78.1
CMA 9	Bimineralic	Gt 1 rim	42.22	0.11	23.47	0.58	8.56	0.32	20.24	5.12	0.03	**100.65**	80.8
		Gt 1 core	41.31	0.10	23.15	0.52	8.59	0.32	19.92	5.13	<0.01	**99.04**	80.5
		Gt 2 core	41.80	0.11	23.50	0.55	8.66	0.32	19.91	5.24	0.01	**100.11**	80.4
		Gt 2 rim	41.09	0.13	23.04	0.56	8.79	0.37	19.86	5.30	0.04	**99.18**	80.1
CMA 10	Bimineralic	Gt 1	41.75	0.12	23.84	0.51	10.02	0.36	19.36	4.44	0.09	**100.48**	77.5
		Gt 2	41.07	0.15	24.00	0.26	10.19	0.36	19.65	4.38	0.10	**100.16**	77.5
CMA 14	Bimineralic	Gt 1	40.13	0.17	23.03	0.08	14.89	0.33	14.24	6.18	0.05	**99.10**	63.0
		Gt 1	40.46	0.18	23.25	0.07	14.96	0.35	14.24	6.31	0.04	**99.85**	62.9
		Gt 2 core	40.40	0.16	23.13	0.06	15.04	0.34	14.43	6.19	0.04	**99.79**	63.1
		Gt 2 rim	40.35	0.14	23.14	0.05	15.08	0.37	14.30	6.01	0.04	**99.45**	62.8
CMA 15	Bimineralic	Gt 1 rim	40.59	0.06	22.69	0.87	15.27	0.60	14.96	5.20	0.04	**100.26**	63.6
		Gt 1 core	40.32	0.07	22.57	1.00	15.81	0.59	14.80	5.41	0.04	**100.61**	62.5
CMA 16	Bimineralic	Gt 1 core	41.74	0.16	23.31	0.35	10.62	0.34	19.28	3.74	0.06	**99.58**	76.4
		Gt 2 core	41.78	0.16	23.63	0.24	10.60	0.32	19.18	3.93	0.06	**99.89**	76.3
CMA 17	Bimineralic	Gt 1 core	39.19	0.25	22.38	0.02	15.71	0.28	8.39	12.90	0.09	**99.21**	48.8
		Gt 1 rim	39.48	0.27	22.66	0.04	16.04	0.35	8.68	12.49	0.11	**100.12**	49.1
		Gt 2 rim	39.14	0.24	22.75	0.04	15.80	0.34	8.44	12.76	0.09	**99.59**	48.8
CMA 18	Bimineralic	Gt 1 core	42.11	0.11	23.59	0.63	8.50	0.38	20.15	4.39	0.06	**99.91**	80.9
		Gt 1 core	41.91	0.13	23.38	0.77	8.57	0.34	19.89	4.45	0.04	**99.50**	80.5
		Gt 2 core	42.20	0.12	23.54	0.69	8.52	0.34	19.85	4.36	0.04	**99.64**	80.6

Table III.2 Major element composition of clinopyroxenes from the Rietfontein eclogites

Sample	Eclogite type	Grain	SiO_2	TiO_2	Al_2O_3	Cr_2O_3	FeO	MnO	MgO	CaO	Na_2O	K_2O	Total	Mg#
JJG 2104	Kyanite-bearing	Cpx 1	54.04	0.12	13.35	0.02	1.98	0.00	9.32	16.08	5.30	<0.02	**100.21**	89.3
		Cpx 2	54.20	0.12	13.18	0.01	1.99	0.00	9.52	16.25	5.15	<0.02	**100.42**	89.5
		Cpx 3	53.76	0.12	12.97	0.01	1.78	0.00	9.29	16.41	5.23	<0.02	**99.60**	90.3
Rtfn 54.1	Kyanite-bearing	Cpx 1	53.63	0.27	13.96	0.04	2.85	0.02	8.47	14.17	5.94	<0.02	**99.35**	84.1
		Cpx 2	53.52	0.28	14.55	0.03	2.77	0.02	8.43	14.28	5.92	<0.02	**99.80**	84.4
		Cpx 3	53.61	0.29	14.04	0.03	2.96	0.03	8.36	14.29	5.87	<0.02	**99.48**	83.4
Rtfn 54.2	Kyanite-bearing	Cpx 1 rim	54.75	0.26	13.25	0.08	2.41	0.03	9.77	14.45	5.55	<0.02	**100.54**	87.9
		Cpx 1 core	54.76	0.23	12.92	0.08	2.44	0.03	9.61	14.40	5.26	<0.02	**99.74**	87.6
		Cpx 2 core	54.78	0.24	12.89	0.08	2.43	0.03	9.40	14.34	5.63	<0.02	**99.82**	87.3
		Cpx 2 rim	55.20	0.27	13.14	0.06	2.50	0.04	9.47	14.56	5.35	<0.02	**100.57**	87.1
Rtfn 54.3	Kyanite-bearing	Cpx 1 core	54.24	0.22	12.07	0.00	1.90	0.05	10.50	15.96	5.19	<0.02	**100.13**	90.8
		Cpx 1 rim	54.37	0.24	12.31	0.02	1.91	0.02	10.42	15.94	5.01	<0.02	**100.24**	90.7
		Cpx 2 core	53.99	0.22	12.08	0.03	1.99	0.00	10.46	16.16	5.16	<0.02	**100.10**	90.4
		Cpx 2 rim	54.00	0.21	12.13	0.02	1.94	0.06	10.44	16.17	4.95	<0.02	**99.93**	90.6
Rtfn 54.4	Kyanite-bearing	Cpx 1 core	53.61	0.26	13.23	0.06	2.36	0.05	9.33	14.46	6.29	<0.02	**99.65**	87.6
		Cpx 1 rim	53.57	0.23	13.27	0.05	2.38	0.02	9.20	14.52	6.35	<0.02	**99.61**	87.3
		Cpx 2 core	54.17	0.25	13.39	0.08	2.25	0.00	9.07	14.52	6.01	<0.02	**99.76**	87.8
		Cpx 2 rim	53.38	0.26	13.31	0.08	2.28	0.00	9.08	14.59	6.09	<0.02	**99.09**	87.6
PC 5.2/1	Opx-bearing	Cpx 1	55.12	0.24	5.30	0.36	3.36	0.05	14.28	17.81	3.64	<0.02	**100.16**	88.3
		Cpx 1 core	54.98	0.23	5.42	0.36	3.30	0.05	14.41	17.89	3.68	0.02	**100.34**	88.6
		Opx 1	56.51	0.03	0.71	0.05	9.34	0.06	32.54	0.31	0.16	<0.02	**99.69**	86.1
		Opx 1	57.09	0.06	0.73	0.02	9.32	0.09	32.46	0.32	0.10	0.02	**100.20**	86.1
Rtfn 56.1	Opx-bearing	Cpx 1	55.04	0.25	5.68	0.34	3.22	0.07	14.61	18.00	3.05	<0.02	**100.26**	89.0
		Cpx 1	54.85	0.28	5.62	0.30	3.12	0.07	14.62	17.78	3.21	<0.02	**99.84**	89.3
		Opx 1	57.41	0.04	0.78	0.05	8.95	0.08	32.26	0.31	0.10	0.03	**99.99**	86.5
		Opx 1	57.39	0.05	0.80	0.04	8.98	0.07	32.28	0.32	0.18	<0.02	**100.13**	86.5
CMA 3	Opx-bearing	Cpx 1	54.20	0.10	1.66	0.35	4.21	0.11	16.74	21.56	1.33	<0.02	**100.26**	87.6
		Cpx 1	54.03	0.08	1.63	0.38	4.09	0.14	16.57	21.42	1.20	<0.02	**99.54**	87.8
		Opx 1	55.82	0.06	0.58	0.04	11.99	0.19	30.47	0.32	0.04	<0.02	**99.52**	81.9
		Opx 2	56.42	0.05	0.57	0.07	12.14	0.20	30.60	0.34	0.08	<0.02	**100.47**	81.8
CMA 11	Opx-bearing	Cpx 2 core	54.55	0.23	4.67	0.46	3.11	0.05	14.69	18.62	3.27	<0.02	**99.66**	89.4
		Cpx 2 core	54.49	0.24	4.66	0.45	3.09	0.08	14.94	18.65	3.37	<0.02	**99.98**	89.6
		Opx 1	55.72	0.06	0.70	0.04	8.80	0.09	33.92	0.28	0.12	0.02	**99.74**	87.3
CMA 12	Opx-bearing	Cpx 1 core	54.69	0.38	4.98	0.22	3.40	0.06	14.63	18.43	3.64	<0.02	**100.44**	88.5
		Cpx 1 rim	54.93	0.36	4.89	0.22	3.50	0.05	14.57	18.32	3.51	<0.02	**100.37**	88.1
		Cpx 2 core	54.23	0.37	4.90	0.21	3.67	0.04	14.37	18.25	3.50	<0.02	**99.55**	87.5
		Opx 1	56.95	0.09	0.70	0.00	8.31	0.12	33.53	0.31	0.17	0.03	**100.21**	87.8
		Opx 2	57.34	0.12	0.70	0.01	8.18	0.08	32.91	0.30	0.12	<0.02	**99.77**	87.8

Table III.2 continued

Sample	Eclogite type	Grain	SiO_2	TiO_2	Al_2O_3	Cr_2O_3	FeO	MnO	MgO	CaO	Na_2O	K_2O	Total	Mg#
CMA 13	Opx-bearing	Cpx 1 core	54.25	0.11	1.55	0.43	2.33	0.06	16.90	22.68	1.05	<0.02	**99.36**	92.8
		Cpx 2 core	54.22	0.09	1.49	0.45	2.41	0.06	16.74	22.74	1.03	<0.02	**99.23**	92.5
		Cpx 1	57.54	0.08	0.73	0.11	7.32	0.10	34.10	0.27	0.02	<0.02	**100.27**	89.3
		Opx 1	57.77	0.07	0.72	0.10	7.57	0.11	33.79	0.28	0.09	<0.02	**100.49**	88.8
JJG 105	Bimineralic	Cpx 1	54.34	0.30	4.50	0.32	3.84	0.04	14.97	18.95	3.01	<0.02	**100.27**	87.4
		Cpx 2	54.10	0.25	4.37	0.25	3.68	0.00	14.93	18.79	2.91	<0.02	**99.27**	87.9
PC 1	Bimineralic	Cpx 1	54.70	0.14	1.54	0.13	1.86	0.00	17.83	23.07	0.74	<0.02	**100.04**	94.5
		Cpx 2	54.19	0.17	1.53	0.09	1.92	0.06	17.71	22.80	0.85	<0.02	**99.33**	94.3
		Cpx 3	54.50	0.17	1.61	0.09	2.00	0.04	17.82	22.82	0.87	<0.02	**99.94**	94.1
PC 3	Bimineralic	Cpx 1	54.14	0.29	3.23	0.33	1.56	0.02	16.46	21.59	1.88	<0.02	**99.51**	95.0
		Cpx 1	54.32	0.28	3.23	0.31	1.59	0.03	16.60	21.37	1.79	<0.02	**99.53**	94.9
PC 5.2/2	Bimineralic	Cpx 1 rim	54.65	0.40	4.79	0.37	2.59	0.05	15.36	18.95	3.15	<0.02	**100.31**	91.4
		Cpx 1 core	54.15	0.40	4.69	0.36	2.53	0.06	15.21	18.95	3.14	<0.02	**99.48**	91.5
		Cpx 2 core	54.37	0.39	4.70	0.36	2.58	0.04	15.30	19.14	3.16	<0.02	**100.04**	91.4
PC 12	Bimineralic	Cpx 1 core	54.74	0.23	3.22	0.16	2.88	0.08	16.52	20.57	1.80	<0.02	**100.19**	91.1
		Cpx 1 rim	54.67	0.24	3.28	0.11	2.94	0.07	16.84	20.38	2.00	<0.02	**100.51**	91.1
		Cpx 2	54.63	0.21	3.23	0.12	2.86	0.08	16.74	20.59	2.02	<0.02	**100.49**	91.2
		Cpx 3 rim	54.49	0.22	3.23	0.16	2.67	0.06	16.70	20.67	1.95	<0.02	**100.14**	91.8
Rtfn 31.1	Bimineralic	Cpx 1	54.32	0.27	4.11	0.25	3.49	0.05	15.18	19.09	2.88	<0.02	**99.65**	88.6
Rtfn 31.2	Bimineralic	Cpx 1	54.83	0.31	5.26	0.17	3.30	0.02	14.71	18.32	3.28	<0.02	**100.21**	88.8
		Cpx 2	54.03	0.26	5.54	0.26	3.77	0.03	13.83	17.65	3.64	<0.02	**99.00**	86.7
		Cpx 3	53.67	0.16	3.25	0.37	4.33	0.07	14.68	20.30	2.22	<0.02	**99.07**	85.8
Rtfn 31.3	Bimineralic	Cpx 1 rim	53.76	0.28	3.56	0.10	2.22	0.06	16.71	20.62	2.26	<0.02	**99.57**	93.1
		Cpx 1 core	54.07	0.32	3.50	0.11	2.32	0.05	16.62	20.62	2.32	<0.02	**99.93**	92.7
Rtfn 43.1	Bimineralic	Cpx 1	54.35	0.27	2.93	0.26	2.89	0.04	16.25	20.51	2.07	<0.02	**99.57**	90.9
		Cpx 2	54.15	0.27	2.78	0.24	2.65	0.08	16.68	20.83	2.00	<0.02	**99.68**	91.8
		Cpx 3	54.43	0.21	2.66	0.23	2.51	0.06	16.70	21.16	1.88	<0.02	**99.84**	92.2
Rtfn 43.7	Bimineralic	Cpx 1 core	54.31	0.28	3.20	0.29	2.29	0.06	16.85	20.71	2.25	<0.02	**100.24**	92.9
		Cpx 1 rim	53.85	0.26	3.10	0.30	2.57	0.03	16.50	20.63	2.24	<0.02	**99.50**	92.0
		Cpx 2 core	54.35	0.25	3.17	0.25	2.31	0.07	16.41	20.69	2.19	<0.02	**99.69**	92.7
		Cpx 2 rim	54.07	0.27	3.15	0.27	2.34	0.06	16.39	20.73	2.03	<0.02	**99.31**	92.6
Rtfn 43.9	Bimineralic	Cpx 1 core	53.87	0.26	3.64	0.30	2.49	0.05	16.14	20.19	2.19	<0.02	**99.13**	92.0
		Cpx 1 rim	54.16	0.27	3.58	0.29	2.51	0.06	16.38	20.33	2.49	<0.02	**100.08**	92.1
		Cpx 2 core	54.23	0.27	3.58	0.31	2.42	0.06	16.32	20.23	2.36	<0.02	**99.78**	92.3
		Cpx 2 rim	54.41	0.28	3.62	0.34	2.42	0.06	16.16	19.97	2.37	<0.02	**99.62**	92.2
Rtfn 43.10	Bimineralic	Cpx 1 core	53.92	0.33	5.76	0.04	3.10	0.04	14.18	18.70	3.49	<0.02	**99.56**	89.1
		Cpx 2 core	54.46	0.32	5.71	0.04	3.13	0.06	14.10	18.78	3.64	<0.02	**100.25**	88.9
Rtfn 48.1	Bimineralic	Cpx 1	54.40	0.28	3.53	0.46	2.27	0.06	16.02	20.23	2.18	<0.02	**99.44**	92.6
		Cpx 2	54.06	0.28	3.27	0.46	2.29	0.07	16.42	20.38	2.34	<0.02	**99.56**	92.7
		Cpx 3	53.73	0.27	3.36	0.42	2.35	0.03	16.30	20.55	2.28	<0.02	**99.29**	92.5

Table III.2 continued

Sample	Eclogite type	Grain	SiO_2	TiO_2	Al_2O_3	Cr_2O_3	FeO	MnO	MgO	CaO	Na_2O	K_2O	Total	Mg#
Rtfn 48.2	Bimineralic	Cpx 1 core	54.25	0.18	3.51	0.64	1.97	0.07	16.40	20.60	2.03	<0.02	**99.65**	93.7
		Cpx 1	54.15	0.14	3.02	0.63	1.98	0.05	16.48	21.02	2.09	<0.02	**99.58**	93.7
		Cpx 2	54.43	0.19	3.14	0.67	1.91	0.09	16.52	20.83	2.18	<0.02	**99.95**	93.9
		Cpx 3	54.47	0.15	3.20	0.70	1.95	0.06	16.51	20.84	2.09	<0.02	**99.98**	93.8
Rtfn 55.1	Bimineralic	Cpx 1	54.78	0.27	3.18	0.30	1.93	0.05	16.16	21.10	1.64	<0.02	**99.42**	93.7
		Cpx 2 core	54.74	0.28	3.16	0.30	2.08	0.07	15.90	21.22	1.71	<0.02	**99.47**	93.2
		Cpx 3 core	54.90	0.27	3.19	0.29	1.92	0.08	16.27	20.92	1.79	<0.02	**99.63**	93.8
Rtfn 55.2	Bimineralic	Cpx 1	53.84	0.26	3.13	0.40	1.88	0.07	16.70	21.58	1.64	<0.02	**99.50**	94.1
		Cpx 2	54.64	0.27	3.07	0.36	1.68	0.07	16.82	21.72	1.67	<0.02	**100.29**	94.7
		Cpx 3	54.48	0.26	3.06	0.37	1.63	0.06	16.85	21.79	1.66	<0.02	**100.16**	94.9
Rtfn 55.3	Bimineralic	Cpx 1 core	53.21	0.44	11.96	0.05	2.69	0.06	9.91	14.51	6.42	<0.02	**99.24**	86.8
		Cpx 1 rim	53.75	0.45	11.84	0.06	2.74	0.02	10.00	14.75	6.21	<0.02	**99.82**	86.7
		Cpx 2 core	53.54	0.42	11.99	0.05	2.75	0.05	9.85	14.77	6.43	<0.02	**99.84**	86.5
Rtfn 55.4	Bimineralic	Cpx 1 core	53.87	0.14	2.25	0.24	2.40	0.05	16.83	22.55	1.26	<0.02	**99.61**	92.6
		Cpx 1 rim	53.78	0.14	2.18	0.24	2.38	0.01	16.82	22.46	1.18	0.02	**99.21**	92.6
		Cpx 2 core	53.46	0.14	2.18	0.24	2.52	0.06	16.86	22.67	1.22	<0.02	**99.35**	92.3
		Cpx 2 rim	54.04	0.14	2.28	0.25	2.53	0.02	16.69	22.71	1.21	<0.02	**99.88**	92.2
Rtfn 57.1	Bimineralic	Cpx 1 core	54.47	0.28	4.26	0.21	3.78	0.07	14.84	19.00	2.68	<0.02	**99.60**	87.5
		Cpx 2 core	55.27	0.29	4.22	0.21	3.77	0.04	14.51	19.06	2.59	<0.02	**99.96**	87.3
		Cpx 2 rim	55.14	0.28	4.17	0.21	3.72	0.01	14.27	18.94	2.58	<0.02	**99.33**	87.3
		Cpx 3 core	55.00	0.28	4.28	0.24	3.72	0.06	14.29	18.77	2.62	<0.02	**99.28**	87.2
Rtfn 57.2	Bimineralic	Cpx 1 core	55.24	0.16	1.93	0.22	1.37	0.00	16.70	22.75	1.07	<0.02	**99.44**	95.6
		Cpx 2 core	55.01	0.16	2.14	0.23	1.37	0.04	16.58	22.58	1.11	<0.02	**99.23**	95.6
		Cpx 2 rim	55.20	0.17	2.15	0.22	1.43	0.00	16.54	22.83	1.07	<0.02	**99.60**	95.4
Rtfn 57.3	Bimineralic	Cpx 1 rim	53.99	0.22	2.76	0.44	2.07	0.05	16.63	21.41	1.83	<0.02	**99.40**	93.5
		Cpx 1 core	53.91	0.24	2.81	0.43	2.10	0.06	16.68	21.47	1.69	<0.02	**99.41**	93.4
		Cpx 2 core	54.04	0.23	2.78	0.41	2.28	0.02	16.84	21.32	1.80	<0.02	**99.71**	92.9
		Cpx 2 rim	53.96	0.21	2.75	0.40	2.11	0.04	16.81	21.56	1.85	<0.02	**99.69**	93.4
CMA 1	Bimineralic	Cpx 1	54.94	0.12	2.66	0.21	2.32	0.06	16.37	22.52	1.35	<0.02	**100.55**	92.6
		Cpx 2	53.32	0.13	2.75	0.25	2.37	0.02	16.38	22.71	1.38	<0.02	**99.30**	92.5
CMA 2	Bimineralic	Cpx 1	54.85	0.08	1.85	0.21	2.55	0.06	16.81	22.84	1.02	<0.02	**100.27**	92.1
		Cpx 2	54.76	0.12	1.87	0.24	2.68	0.04	16.63	22.50	0.95	<0.02	**99.79**	91.7
		Cpx 3	54.71	0.11	1.85	0.18	2.75	0.04	16.75	22.39	1.08	<0.02	**99.86**	91.6
CMA 4	Bimineralic	Cpx 1 core	53.99	0.25	12.74	0.24	1.91	0.04	10.02	15.98	5.54	<0.02	**100.73**	90.3
		Cpx 1 rim	54.02	0.22	12.75	0.25	1.86	0.02	9.90	15.85	5.66	<0.02	**100.53**	90.5
		Cpx 2 core	54.05	0.25	13.78	0.35	1.84	0.03	9.14	15.16	5.93	<0.02	**100.54**	89.8
		Cpx 2 rim	53.60	0.24	13.81	0.32	1.88	0.02	9.08	15.13	5.77	<0.02	**99.86**	89.6
CMA 5	Bimineralic	Cpx 1	54.28	0.40	4.50	0.20	2.91	0.03	15.39	18.57	3.09	<0.02	**99.36**	90.4
		Cpx 1	54.79	0.40	4.49	0.22	3.03	0.07	15.26	18.81	3.15	<0.02	**100.22**	90.0
		Cpx 1	54.84	0.40	4.49	0.17	2.86	0.04	14.85	18.81	3.00	<0.02	**99.46**	90.2

Table III.2 continued

Sample	Eclogite type	Grain	SiO_2	TiO_2	Al_2O_3	Cr_2O_3	FeO	MnO	MgO	CaO	Na_2O	K_2O	Total	Mg#
CMA 6	Bimineralic	Cpx 1	54.59	0.09	1.35	0.53	2.13	0.09	16.84	22.75	0.84	<0.02	**99.22**	93.4
CMA 7	Bimineralic	Cpx 1 rim	54.68	0.27	3.46	0.14	2.59	0.04	16.29	20.99	2.43	<0.02	**100.89**	91.8
		Cpx 1 core	54.23	0.29	3.38	0.14	2.34	0.06	16.11	21.03	2.22	<0.02	**99.80**	92.5
		Cpx 2 core	54.21	0.28	3.39	0.14	2.65	0.07	16.12	20.91	2.32	<0.02	**100.09**	91.6
		Cpx 3	54.30	0.29	3.41	0.13	2.64	0.03	15.95	20.85	2.37	<0.02	**99.98**	91.5
CMA 8	Bimineralic	Cpx 1	54.45	0.17	2.86	0.69	2.75	0.11	15.50	21.65	2.10	<0.02	**100.29**	90.9
		Cpx 2	54.19	0.12	2.93	0.76	2.81	0.09	15.45	21.33	2.27	<0.02	**99.96**	90.8
CMA 9	Bimineralic	Cpx 1 core	53.72	0.23	2.60	0.36	2.09	0.08	16.96	21.96	1.70	<0.02	**99.69**	93.5
		Cpx 1 rim	53.68	0.24	2.47	0.35	2.17	0.06	16.84	21.95	1.66	<0.02	**99.43**	93.3
		Cpx 2 core	54.29	0.23	2.59	0.35	2.21	0.06	16.73	22.18	1.63	<0.02	**100.28**	93.1
		Cpx 2 rim	54.10	0.24	2.54	0.40	2.20	0.07	16.90	22.06	1.65	<0.02	**100.16**	93.2
		Cpx 3 core	54.10	0.24	2.62	0.42	2.17	0.06	16.69	22.03	1.61	<0.02	**99.94**	93.2
		Cpx 3 rim	53.84	0.23	2.56	0.37	2.08	0.03	16.89	21.96	1.71	<0.02	**99.69**	93.5
CMA 10	Bimineralic	Cpx 1 core	54.03	0.23	2.77	0.33	2.57	0.01	16.45	21.12	2.01	<0.02	**99.54**	91.9
CMA 14	Bimineralic	Cpx 1 core	54.13	0.23	3.66	0.03	3.54	0.03	15.17	20.68	2.17	<0.02	**99.66**	88.4
		Cpx 1 rim	54.62	0.23	3.71	0.05	3.48	0.03	15.45	20.87	2.34	<0.02	**100.78**	88.8
		Cpx 2 core	54.13	0.22	3.64	0.05	3.57	0.04	15.11	20.74	2.26	<0.02	**99.77**	88.3
		Cpx 2 rim	54.62	0.20	3.69	0.04	3.48	0.03	15.32	20.55	2.20	<0.02	**100.15**	88.7
CMA 15	Bimineralic	Cpx 1 core	54.18	0.07	1.21	0.29	3.60	0.08	16.73	22.73	0.86	<0.02	**99.74**	89.2
		Cpx 1 core	53.68	0.07	1.14	0.28	3.79	0.06	16.91	22.57	0.86	<0.02	**99.37**	88.8
CMA 16	Bimineralic	Cpx 1	54.99	0.36	4.61	0.37	2.99	0.05	14.64	18.31	3.22	<0.02	**99.54**	89.7
		Cpx 2 core	54.12	0.36	4.61	0.35	2.61	0.05	14.98	18.78	3.19	<0.02	**99.04**	91.1
CMA 17	Bimineralic	Cpx 1 rim	53.68	0.46	10.41	0.00	3.40	0.03	10.17	15.60	5.84	<0.02	**99.59**	84.2
		Cpx 2 core	53.94	0.49	10.47	0.04	3.39	0.00	10.04	15.40	5.67	<0.02	**99.43**	84.1
		Cpx 3 core	53.61	0.49	10.23	0.03	3.39	0.00	10.16	15.70	5.81	<0.02	**99.43**	84.3
CMA 18	Bimineralic	Cpx 1	55.26	0.20	2.71	0.55	2.48	0.06	15.91	20.83	1.84	<0.02	**99.84**	92.0
		Cpx 2	55.32	0.26	2.73	0.58	2.35	0.08	15.92	20.35	1.94	<0.02	**99.54**	92.4
		Cpx 3	55.16	0.22	2.76	0.56	2.48	0.05	15.89	20.68	1.97	<0.02	**99.77**	92.0

Table III.3 *Major element composition of kyanite from the Rietfontein kyanite eclogites*

Kyanite	Grain	SiO_2	TiO_2	Al_2O_3	Cr_2O_3	FeO	MnO	MgO	CaO	Na_2O	Total
JJG 2104	Ky 1	37.15	0.01	62.55	0.07	0.12	0.03	0.02	0.02	0.01	**99.97**
	Ky 2	37.26	0.01	61.53	0.05	0.17	0.03	0.04	0.19	0.06	**99.35**
	Ky 3	36.76	0.00	62.21	0.02	0.14	0.00	0.02	0.00	0.00	**99.16**
Rtfn 54.1	Ky 1	36.63	0.01	62.67	0.08	0.20	0.00	0.02	0.00	0.00	**99.60**
	Ky 2	36.11	0.00	61.26	0.07	0.14	0.01	0.01	0.00	0.00	**97.61**
Rtfn 54.2	Ky 1	36.49	0.01	62.90	0.11	0.19	0.03	0.00	0.07	0.00	**99.79**
	Ky 2	36.48	0.03	62.22	0.08	0.17	0.01	0.02	0.00	0.00	**99.03**
Rtfn 54.3	Ky 1	36.76	0.02	63.24	0.05	0.16	0.02	0.00	0.00	0.02	**100.29**
	Ky 2	36.19	0.01	61.85	0.03	0.12	0.00	0.01	0.00	0.00	**98.20**
Rtfn 54.4	Ky 1	36.30	0.00	62.65	0.06	0.13	0.00	0.01	0.00	0.00	**99.15**
	Ky 2	36.00	0.01	62.52	0.08	0.11	0.00	0.00	0.00	0.00	**98.73**

Table III.4 *Major element composition of accessory ilmenites. Fe_2O_3 calculated on the basis of stoichiometry, using the method of Droop (1987).*

Ilmenite	Grain	SiO_2	TiO_2	Al_2O_3	Cr_2O_3	FeO	Fe_2O_3	MnO	MgO	CaO	Total
CMA 10	Ilm 1	0.01	54.11	0.38	0.52	27.43	4.22	0.37	11.74	0.01	**98.79**
	Ilm 2	0.01	54.27	0.33	0.47	26.19	5.34	0.45	12.41	0.10	**99.57**
	Ilm 2	0.00	54.49	0.35	0.47	25.93	5.05	0.28	12.83	0.00	**99.40**
	Ilm 3	0.01	54.16	0.37	0.51	25.64	5.02	0.40	12.70	0.08	**98.89**
	Ilm 4	0.02	54.90	0.31	0.52	25.37	5.38	0.43	13.25	0.04	**100.22**
	Ilm 5	0.02	53.39	1.04	0.51	26.73	5.30	0.41	11.74	0.04	**99.18**
CMA 15	Ilm 1	0.00	48.95	0.29	1.22	32.06	9.36	0.37	6.64	0.00	**98.90**
	Ilm 1	0.00	48.98	0.26	1.19	31.86	9.59	0.37	6.77	0.00	**99.03**
CMA 9	Ilm 1	0.01	56.02	0.34	0.59	25.20	3.56	0.37	13.92	0.02	**100.03**
	Ilm 2	0.02	56.31	0.38	0.61	24.03	3.56	0.25	14.81	0.01	**99.99**
	Ilm 3	0.00	54.85	0.32	0.56	27.45	3.90	0.65	11.92	0.02	**99.66**
	Ilm 4	0.02	56.05	0.37	0.53	24.88	3.57	0.32	14.16	0.01	**99.91**
Rtfn 31.3	Ilm 1	0.00	55.66	0.20	0.13	27.90	3.21	0.36	12.22	0.03	**99.71**
	Ilm 2	0.00	55.60	0.21	0.14	28.47	2.89	0.46	11.81	0.03	**99.61**
Rtfn 43.1	Ilm 1	0.00	55.36	0.32	0.36	28.03	3.89	0.39	11.99	0.02	**100.37**
	Ilm 2	0.00	55.71	0.25	0.30	27.33	3.77	0.30	12.60	0.04	**100.30**

Table III.5 *Major element composition of accessory rutile*

Sample	Grain	SiO_2	TiO_2	Al_2O_3	Cr_2O_3	FeO	MnO	MgO	CaO	Total
CMA 10	Rut 1	0.03	89.78	0.38	1.78	1.13	0.02	0.06	0.37	**93.55**
	Rut 2	0.02	84.22	0.85	1.71	3.99	0.00	0.51	0.00	**91.29**
CMA 13	Rut 1	0.00	93.25	0.17	2.65	0.82	0.04	0.01	0.04	**96.98**
	Rut 1	0.00	88.92	0.06	2.54	4.64	0.07	0.83	0.08	**97.13**
	Rut 1 rim	0.02	94.63	0.67	2.64	2.01	0.00	0.05	0.02	**100.04**
CMA 14	Rut 1	0.00	92.98	0.25	0.16	4.19	0.05	0.57	0.14	**98.33**
CMA 7	Rut 1	0.01	94.70	0.12	0.56	2.96	0.01	0.16	0.24	**98.75**
	Rut 2	0.00	93.45	2.19	0.55	1.92	0.00	0.16	0.00	**98.27**
	Rut 3	0.02	96.27	0.40	0.55	1.51	0.01	0.08	0.10	**98.95**
	Rut 3	0.05	97.22	0.09	0.57	2.33	0.00	0.14	0.16	**100.56**
Rtfn 31.1	Rut 1	0.01	94.83	0.08	0.45	3.02	0.01	0.64	0.05	**99.09**
Rtfn 31.3	Rut 1	0.00	92.76	0.26	0.44	3.45	0.00	0.19	0.03	**97.14**
Rtfn 43.1	Rut 1	0.01	85.06	0.79	1.21	3.61	0.02	0.17	0.04	**90.91**
	Rut 1 core	0.02	84.36	0.82	1.17	3.92	0.00	0.32	0.02	**90.63**
	Rut 1	0.00	83.45	1.05	1.23	3.98	0.02	0.37	0.03	**90.15**
	Rut 2	0.01	84.92	0.82	1.19	4.05	0.00	0.43	0.01	**91.43**
	Rut 2	0.02	83.64	0.80	1.16	4.85	0.01	0.62	0.05	**91.14**
	Rut 2	0.00	84.88	0.86	1.24	4.38	0.00	0.39	0.03	**91.78**
	Rut 2 core	0.02	84.24	0.88	1.21	4.86	0.00	0.51	0.07	**91.79**
Rtfn 43.7	Rut 1	0.00	93.89	0.38	0.70	2.56	0.00	0.14	0.01	**97.68**
	Rut 1	0.01	93.99	0.36	0.77	2.83	0.00	0.16	0.00	**98.13**
	Rut 2	0.02	92.84	0.34	0.74	3.39	0.01	0.38	0.05	**97.77**
Rtfn 48.1	Rut 1	0.00	94.55	1.75	1.42	1.02	0.00	0.00	0.02	**98.76**
	Rut 1	0.00	93.98	0.58	1.43	0.65	0.00	0.00	0.01	**96.66**
	Rut 1 core	0.02	91.75	1.45	1.46	3.35	0.03	0.08	0.02	**98.17**
	Rut 1 rim	0.01	95.16	0.50	1.46	1.97	0.06	0.48	0.10	**99.76**
Rtfn 54.2	Rut 1	0.03	98.26	1.60	0.10	0.49	0.02	0.03	0.02	**100.54**
	Rut 1	0.01	96.44	2.39	0.14	0.78	0.00	0.06	0.10	**99.92**
	Rut 1 core	0.01	98.38	0.99	0.15	0.52	0.02	0.01	0.02	**100.09**
	Rut 1 rim	1.19	95.38	0.94	0.14	0.93	0.03	0.04	1.44	**100.09**
Rtfn 54.4	Rut 1	0.00	97.30	0.78	0.20	0.79	0.02	0.00	0.01	**99.11**
	Rut 2	0.00	97.64	0.85	0.16	0.57	0.04	0.01	0.00	**99.28**

Table III.6 *Major element composition of secondary amphibole and mica in the Rietfontein eclogites*

Sample	Grain	SiO_2	TiO_2	Al_2O_3	Cr_2O_3	FeO	MnO	MgO	CaO	Na_2O	K_2O	F	Total
CMA 1	Amph 1	40.31	0.05	17.01	0.19	10.59	0.53	15.01	9.74	3.63	0.24	-	**97.30**
	Amph 2	43.31	0.17	15.41	0.37	7.50	0.16	16.15	10.46	3.88	0.97	-	**98.38**
CMA 14	Amph 1	53.21	0.25	1.42	0.08	3.86	0.08	16.34	21.07	1.66	0.00	-	**97.97**
	Amph 1	52.94	0.25	1.34	0.11	3.70	0.03	16.52	21.27	1.62	0.00	-	**97.78**
	Amph 2	53.66	0.21	3.82	0.07	3.56	0.03	15.38	20.71	2.13	0.00	-	**99.56**
CMA 16	Amph 1	46.15	0.59	11.73	0.26	5.05	0.07	18.64	8.59	4.26	1.13	-	**96.47**
	Amph 2	47.27	0.52	10.36	0.30	4.76	0.06	19.33	8.67	4.47	1.02	-	**96.75**
CMA 2	Amph 1	42.77	0.24	15.12	0.41	8.92	0.20	15.57	9.89	4.06	0.68	-	**97.85**
	Amph 2	41.00	0.26	16.40	0.42	8.58	0.10	14.76	9.62	4.17	0.59	-	**95.89**
CMA 8	Amph 1	45.61	0.37	12.21	0.80	4.10	0.07	19.87	10.22	4.36	1.10	-	**98.71**
	Amph 2	45.47	0.41	11.77	0.75	4.03	0.07	19.57	10.29	4.23	1.13	-	**97.74**
	Amph 3	45.56	0.45	11.60	0.86	4.14	0.08	19.54	10.20	4.12	1.14	-	**97.68**
Rtfn 31.1	Amph 1	45.45	0.56	11.70	0.25	6.11	0.05	17.23	9.16	4.12	1.23	-	**95.85**
	Amph 2	46.98	0.43	9.57	0.17	6.27	0.06	18.36	8.56	4.34	0.76	-	**95.49**
	Amph 2	46.87	0.49	10.98	0.18	6.06	0.06	18.09	8.64	4.14	0.75	-	**96.26**
Rtfn 43.2	Amph 1	43.15	0.37	16.36	1.41	4.83	0.12	17.05	9.27	4.26	0.73	-	**97.55**
	Amph 2	42.30	0.20	17.68	1.23	4.91	0.18	16.52	8.85	4.79	0.70	-	**97.36**
Rtfn 55.3	Mica 1	39.08	0.88	18.81	0.03	8.54	0.01	20.43	0.03	1.11	8.27	0.43	**97.62**
	Mica 2	42.09	1.19	13.99	0.20	5.56	0.00	23.86	0.09	0.50	9.43	0.50	**97.39**

Table III.7 *Compositions of accessory sulphide minerals in the Rietfontein eclogites*

Sulphides	Grain	S	Fe	Cu	Ni	Zn	Co	Total
JJG 105	$S^{=}1$ rim	32.99	33.28	16.35	14.60	0.00	0.06	**97.27**
	$S^{=}1$ rim	30.37	34.92	14.94	12.58	0.00	0.10	**92.91**
	$S^{=}1$ core	32.38	48.76	0.00	14.22	0.00	0.17	**95.53**
	$S^{=}1$ core	30.45	45.39	0.00	16.70	0.21	0.95	**93.70**
	$S^{=}1$ rim	26.72	32.12	23.85	4.42	0.00	2.39	**89.50**
	$S^{=}1$ rim	31.75	34.13	14.21	16.58	0.00	0.20	**96.87**
	$S^{=}2$ core	32.71	33.59	16.55	14.91	0.10	0.23	**98.10**
	$S^{=}2$ rim	16.43	19.58	36.98	5.53	0.02	4.39	**82.93**
	$S^{=}3$ core	33.82	47.95	0.07	18.00	0.29	0.17	**100.32**
	$S^{=}3$ rim	30.59	34.07	15.24	15.51	0.10	0.36	**95.87**
PC 5.2/1	$S^{=}1$ core	22.06	0.68	2.33	57.55	0.46	1.13	**84.21**
	$S^{=}1$ core	19.86	1.25	3.23	55.42	0.53	2.62	**82.90**
	$S^{=}2$ core	25.80	2.89	0.52	70.90	0.16	0.12	**100.39**
	$S^{=}3$ (incl.)	30.72	1.60	0.55	55.74	0.37	1.06	**90.03**
PC 3	$S^{=}1$(incl.)	29.06	3.07	27.07	30.45	0.28	1.39	**91.33**
Rtfn 31.1	$S^{=}1$ core	22.46	21.76	11.38	20.30	0.53	2.57	**79.00**
	$S^{=}2$	27.45	27.48	5.18	20.67	0.82	0.67	**82.28**
Rtfn 54.4	$S^{=}1$ core	6.25	20.30	0.46	12.66	0.17	10.53	**50.37**
Rtfn 57.3	$S^{=}1$ rim	33.96	7.11	5.45	53.18	0.18	0.02	**99.89**
	$S^{=}1$ core	24.90	6.21	0.87	46.36	0.35	3.89	**82.58**
	$S^{=}2$ core	27.83	24.53	7.57	28.02	0.48	2.02	**90.44**
	$S^{=}2$ rim	15.59	22.94	1.05	21.28	0.41	7.20	**68.48**

Table III.8 *Trace element abundances in garnets from the Rietfontein eclogites*
n.d. = not determined

Garnet	CMA 1	CMA 3	CMA 4	CMA 5	CMA 8	CMA 12	CMA 14	CMA 17
Sc	157	145	32.5	51.4	89.8	53.5	66.8	53.8
Ni	24.3	21.2	39.5	24.7	23.1	21.2	24.0	14.2
Sr	0.65	0.67	3.51	0.33	0.46	0.12	0.15	1.62
Y	18.2	17.2	13.1	24.2	11.8	26.9	17.2	17.1
Zr	3.37	6.83	5.7	11.2	19.9	10.1	4.5	5.95
La	0.009	n.d.	0.003	0.011	0.020	n.d.	0.008	0.034
Ce	0.046	0.028	0.083	0.071	0.13	0.063	0.047	0.32
Nd	0.14	0.13	2.67	0.25	0.53	0.38	0.31	1.49
Sm	0.28	0.17	1.70	0.45	0.67	0.52	0.42	1.40
Eu	0.18	0.12	0.91	0.29	0.36	0.31	0.26	0.73
Gd	1.26	0.69	1.87	1.83	1.52	2.05	1.29	2.44
Dy	3.00	2.32	2.26	3.91	1.89	4.08	2.58	3.14
Er	2.09	2.32	1.51	2.79	1.28	2.88	2.24	1.84
Yb	1.83	2.57	1.98	3.19	1.18	3.56	2.33	1.97

Garnet	JJG 105	JJG 2104	PC 1	PC 5.2/1	Rtfn 31.1	Rtfn 43.1	Rtfn 48.2	Rtfn 54.1
Sc	47.1	17.2	32.2	48.5	51.3	77.5	79.4	27.9
Ni	25.5	28.1	26.8	40.8	22.4	17.4	24.4	30.1
Sr	0.16	1.49	0.82	0.12	0.12	0.097	0.099	2.10
Y	10.2	8.26	9.23	11.6	9.60	20.8	6.70	16.0
Zr	4.71	2.24	3.48	4.26	5.84	21.8	20.2	6.147
La	0.014	n.d.	n.d.	0.007	0.009	0.006	0.016	n.d
Ce	0.070	0.072	0.071	0.037	0.053	0.075	0.11	0.12
Nd	0.15	1.27	0.71	0.21	0.25	0.33	0.48	3.40
Sm	0.24	0.92	0.58	0.44	0.44	0.42	0.53	3.24
Eu	0.19	0.80	0.50	0.25	0.24	0.30	0.21	1.62
Gd	0.77	1.26	1.02	1.02	0.86	1.43	0.94	3.28
Dy	1.58	1.40	1.49	1.70	1.46	2.93	1.12	3.20
Er	1.15	0.95	1.05	1.29	1.06	2.39	0.65	1.54
Yb	1.23	0.84	1.04	1.40	1.10	2.68	0.78	1.23

Garnet	Rtfn 54.4	Rtfn 55.1	Rtfn 55.2	Rtfn 57.1
Sc	39.3	65.3	53.4	48.7
Ni	19.8	23.4	25.4	24.7
Sr	1.98	0.17	0.079	0.12
Y	21.4	19.7	7.37	10.6
Zr	6.64	23.5	11.0	4.48
La	n.d.	0.006	n.d.	0.003
Ce	0.14	0.11	0.033	0.064
Nd	2.75	0.43	0.47	0.35
Sm	2.55	0.39	0.72	0.29
Eu	1.37	0.18	0.24	0.19
Gd	3.33	1.16	0.84	0.95
Dy	4.14	2.85	1.17	1.79
Er	2.30	2.50	0.91	1.27
Yb	1.94	2.78	0.86	1.23

Table III.9 *Trace element abundances in clinopyroxenes from the Rietfontein eclogites*
n.d. = not determined

Cpx	CMA 1	CMA 3	CMA 4	CMA 5	CMA 8	CMA 12	CMA 14	CMA 17
Sc	41.3	47.7	7.1	20.5	23.0	22.0	24.9	17.7
Ni	442	382	449	299	327	293	292	179
Sr	26.0	33.6	185	166	215	241	210	107
Y	0.62	1.17	0.24	3.98	5.16	3.82	1.19	0.37
Zr	2.25	6.30	7.57	36.2	43.9	32.7	7.18	6.73
Nb	0.01	0.37	0.00	0.23	2.22	0.09	0.09	0.03
Th	0.06	0.15	0.00	0.42	0.82	0.45	0.36	0.11
La	1.13	1.60	0.003	6.85	10.9	11.2	4.45	1.30
Ce	2.48	3.33	0.100	18.3	26.9	28.3	8.02	3.92
Nd	1.24	2.02	2.13	12.2	16.2	13.9	5.02	2.67
Sm	0.40	0.55	0.56	3.01	3.92	3.06	1.26	0.62
Eu	0.11	0.13	0.16	0.93	1.18	0.93	0.39	0.17
Gd	0.41	0.50	0.26	2.65	3.34	2.48	0.84	0.36
Dy	0.24	0.35	0.063	1.30	1.64	1.27	0.37	0.13
Er	0.062	0.12	0.032	0.29	0.43	0.23	0.112	0.025
Yb	0.050	0.041	0.031	0.21	0.21	0.13	0.027	0.017

Cpx	JJG 105	JJG 105	JJG 2104	PC 1	PC 5.2/1	Rtfn 31.1	Rtfn 43.1	Rtfn 48.2
Sc	17.9	20.9	4.57	15.5	16.4	20.6	26.1	24.4
Ni	346	334	419	149	508	350	213	324
Sr	388	211	138	168	328	178	327	417
Y	3.05	2.25	0.074	2.77	1.70	1.39	3.72	2.16
Zr	42.7	20.9	3.30	9.84	18.3	11.5	43.9	44.7
Nb	2.4	n.d.	0.44	0.53	0.7	0.1	0.9	n.d.
Th	0.5	n.d.	0.00	0.26	0.5	0.1	1.1	n.d.
La	15.7	8.56	0.008	4.09	9.03	3.01	19.9	25.3
Ce	42.9	21.5	0.184	9.02	20.3	9.22	45.5	62.7
Nd	22.7	12.5	0.72	9.28	11.6	6.74	21.6	28.0
Sm	3.81	2.38	0.22	2.71	2.37	1.57	3.76	4.00
Eu	1.06	0.76	0.078	0.68	0.68	0.50	1.09	1.06
Gd	2.47	1.76	0.068	1.97	1.49	1.11	2.33	2.30
Dy	0.99	0.66	0.041	0.83	0.60	0.50	1.16	0.77
Er	0.21	0.19	0.053	0.21	0.11	0.10	0.28	0.20
Yb	0.14	0.070	0.021	0.15	0.045	0.074	0.13	0.069

Cpx	Rtfn 54.1	Rtfn 54.4	Rtfn 55.1	Rtfn 55.2	Rtfn 57.1	Rtfn 57.1
Sc	6.32	9.76	22.3	16.7	19.2	18.6
Ni	294	226	281	313	353	388
Sr	288	372	215	221	208	274
Y	0.26	0.38	3.03	0.98	1.52	3.14
Zr	8.56	11.6	42.9	19.6	14.1	34.6
Nb	0.36	0.0	0.6	0.2	1.0	n.d.
Th	0.00	0.0	0.8	0.6	0.3	n.d.
La	0.026	0.069	11.0	6.96	7.80	11.3
Ce	0.52	0.93	25.9	19.8	19.2	33.6
Nd	2.68	3.28	13.9	17.4	9.91	19.7
Sm	0.68	0.73	2.67	3.37	1.89	3.74
Eu	0.24	0.27	0.76	0.62	0.54	1.03
Gd	0.39	0.29	1.83	1.18	1.13	2.41
Dy	0.065	0.13	0.98	0.38	0.47	0.91
Er	0.036	0.038	0.25	0.087	0.10	0.20
Yb	0.041	0.017	0.090	0.058	0.051	0.044

Table III.10 *Calculated whole-rock major element chemistry of the Rietfontein eclogites, reconstructed using equal proportions of garnet and clinopyroxene, and appropriate amounts of kyanite or orthopyroxene where appropriate*

Sample	Type	SiO_2	TiO_2	Al_2O_3	Cr_2O_3	FeO	MnO	MgO	CaO	Na_2O	K_2O	Total	Mg#
JJG 2104	Kyanite	44.92	0.07	26.71	0.02	5.34	0.08	6.29	14.24	2.11	0.00	**99.79**	67.73
Rtfn 54.1	Kyanite	45.46	0.16	22.94	0.03	7.95	0.12	7.66	12.88	2.64	0.00	**99.84**	63.22
Rtfn 54.2	Kyanite	45.76	1.13	22.04	0.07	8.11	0.13	8.41	12.19	2.43	0.00	**100.26**	64.90
Rtfn 54.3	Kyanite	45.97	0.13	22.07	0.01	6.53	0.09	9.45	12.99	2.29	0.00	**99.54**	72.07
Rtfn 54.4	Kyanite	45.07	1.13	22.25	0.06	7.72	0.12	8.31	12.07	2.79	0.00	**99.52**	65.75
Rtfn 55.3	High Na-Al	46.43	0.31	17.25	0.03	8.52	0.12	9.74	13.57	3.19	0.00	**99.16**	67.10
CMA 4	High Na-Al	46.74	0.18	17.82	0.28	7.13	0.13	9.95	14.80	2.87	0.01	**99.91**	71.31
CMA 17	High Na-Al	46.24	0.37	16.36	0.03	9.59	0.17	9.27	14.14	2.92	0.00	**99.08**	63.26
PC 5.2/1	Opx	49.01	0.15	13.04	0.28	8.35	0.18	17.71	9.70	1.68	0.01	**100.11**	79.08
Rtfn 56.1	Opx	48.39	0.17	13.74	0.30	8.26	0.17	16.60	10.18	1.46	0.00	**99.28**	78.18
CMA 3	Opx	48.24	0.08	9.64	0.48	10.49	0.32	18.19	10.77	0.53	0.00	**98.73**	75.55
CMA 11	Opx	47.81	0.15	13.30	0.44	7.92	0.19	17.16	10.62	1.59	0.01	**99.19**	79.43
CMA 12	Opx	48.79	0.23	13.05	0.18	8.03	0.20	17.94	9.98	1.62	0.01	**100.02**	79.93
CMA13	Opx	47.93	1.00	11.71	0.67	6.97	0.23	17.92	12.94	0.51	0.00	**99.88**	82.10
JJG 105	Bimineralic	47.62	0.22	14.20	0.31	8.74	0.19	16.05	11.38	1.50	0.01	**100.22**	76.60
PC1	Bimineralic	48.30	0.15	13.04	0.17	5.36	0.17	18.79	13.84	0.43	0.00	**100.26**	86.20
PC12	Bimineralic	48.07	0.18	13.60	0.18	6.99	0.22	17.59	12.42	1.00	0.00	**100.26**	81.77
PC3	Bimineralic	47.98	0.20	13.98	0.31	4.74	0.20	18.46	12.84	0.94	0.00	**99.64**	87.41
PC 5.2/2	Bimineralic	47.83	0.20	14.07	0.28	6.51	0.20	17.11	11.40	1.50	0.00	**99.11**	82.40
Rtfn 31.1	Bimineralic	47.19	1.14	13.53	0.24	8.72	0.20	16.21	11.41	1.49	0.00	**100.14**	76.83
Rtfn 31.2	Bimineralic	47.72	0.17	14.33	0.26	7.97	0.16	16.35	10.99	1.58	0.00	**99.52**	78.52
Rtfn 31.3	Bimineralic	47.25	1.15	13.57	0.11	5.91	0.22	18.14	12.26	1.16	0.00	**99.76**	84.55
Rtfn 43.1	Bimineralic	47.65	1.03	13.15	0.28	6.22	0.21	17.68	12.41	1.00	0.00	**99.63**	83.53
Rtfn 43.10	Bimineralic	46.85	0.24	14.02	0.10	9.02	0.20	14.78	12.81	1.46	0.00	**99.47**	74.49
Rtfn 43.7	Bimineralic	47.55	1.13	13.39	0.27	5.83	0.21	17.92	12.28	1.09	0.00	**99.68**	84.56
Rtfn 43.9	Bimineralic	47.70	0.20	13.63	0.32	6.24	0.24	17.75	12.10	1.20	0.00	**99.37**	83.53
Rtfn 48.1	Bimineralic	47.61	1.14	13.43	0.48	5.62	0.18	18.07	12.06	1.17	0.00	**99.76**	85.15
Rtfn 48.2	Bimineralic	47.65	0.12	13.77	0.86	4.59	0.23	18.64	12.43	1.03	0.00	**99.33**	87.86
Rtfn 55.1	Bimineralic	48.53	0.20	13.46	0.35	4.99	0.22	17.93	12.63	0.92	0.00	**99.23**	86.49
Rtfn 55.2	Bimineralic	48.55	0.19	13.53	0.41	4.44	0.17	18.32	12.99	0.09	0.00	**98.68**	88.04
Rtfn 55.4	Bimineralic	46.91	0.10	12.46	0.34	7.26	0.22	16.07	14.88	0.61	0.01	**98.85**	79.79
Rtfn 57.1	Bimineralic	47.95	0.18	13.74	0.20	8.75	0.18	15.99	11.44	1.30	0.00	**99.75**	76.51
Rtfn 57.2	Bimineralic	48.45	0.12	13.15	0.33	4.24	0.11	18.59	13.72	0.55	0.00	**99.27**	88.67

Table III.10 *continued*

Sample	Type	SiO_2	TiO_2	Al_2O_3	Cr_2O_3	FeO	MnO	MgO	CaO	Na_2O	K_2O	Total	Mg#
Rtfn 57.3	Bimineralic	47.74	0.16	13.14	0.52	5.57	0.17	18.14	12.86	0.93	0.00	**99.22**	85.32
CMA 1	Bimineralic	47.08	0.10	12.92	0.31	6.77	0.24	15.33	15.80	0.67	0.00	**99.22**	80.14
CMA 2	Bimineralic	46.94	0.06	12.43	0.31	7.67	0.22	16.28	14.47	0.53	0.00	**98.93**	79.10
CMA 5	Bimineralic	47.27	0.26	13.90	0.19	7.00	0.18	16.94	11.26	1.59	0.00	**98.58**	81.19
CMA 6	Bimineralic	47.13	0.09	11.81	0.98	6.23	0.23	17.80	14.17	0.46	0.00	**98.88**	83.59
CMA 7	Bimineralic	47.62	1.15	13.59	0.14	6.00	0.19	18.06	12.42	1.16	0.00	**100.34**	84.29
CMA 8	Bimineralic	47.59	0.12	12.81	0.91	6.21	0.33	17.29	13.36	1.12	0.00	**99.75**	83.22
CMA 9	Bimineralic	47.73	0.17	12.92	0.47	5.36	0.20	18.43	13.62	0.84	0.00	**99.75**	85.96
CMA 10	Bimineralic	47.24	1.05	13.22	0.37	6.30	0.18	17.80	12.64	1.04	0.00	**99.85**	83.43
CMA 14	Bimineralic	46.89	1.12	13.38	0.05	9.24	0.20	14.68	13.32	1.12	0.00	**99.99**	73.91
CMA 15	Bimineralic	46.93	0.07	11.76	0.62	9.58	0.34	15.75	13.97	0.45	0.00	**99.47**	74.55
CMA 16	Bimineralic	47.62	0.24	14.01	0.32	6.70	0.19	17.13	11.32	1.63	0.00	**99.15**	82.00
CMA 18	Bimineralic	47.88	0.17	13.06	0.68	5.40	0.20	18.04	12.77	0.99	0.00	**99.19**	85.62

Table III.11 *Calculated whole rock trace element abundances for the Rietfontein eclogites, reconstructed using equal proportions of garnet and clinopyroxene. N.d. = not determined*

Sample	CMA 1	CMA 3	CMA 4	CMA 5	CMA 8	CMA 12	CMA 14	CMA 17
Sc	98.9	96.2	19.8	35.9	56.4	37.8	45.9	35.8
Ni	233	202	244	162	175	157	158	96.7
Sr	13.3	17.2	94.4	83.2	108	120	105	54.1
Y	9.42	9.17	6.68	14.1	8.49	15.3	9.22	8.75
Zr	2.81	6.56	6.61	23.7	31.9	21.4	5.83	6.34
Nb	0.006	0.183	0.002	0.115	1.11	0.045	0.043	0.015
Th	0.030	0.075	n.d.	0.210	0.409	0.226	0.182	0.053
La	0.569	0.801	0.003	3.43	5.47	5.61	2.23	0.668
Ce	1.26	1.68	0.092	9.18	13.5	14.2	4.03	2.12
Nd	0.692	1.07	2.40	6.25	8.34	7.13	2.67	2.08
Sm	0.338	0.360	1.13	1.73	2.29	1.79	0.839	1.01
Eu	0.148	0.125	0.534	0.613	0.767	0.619	0.326	0.451
Gd	0.836	0.599	1.07	2.24	2.43	2.26	1.07	1.40
Dy	1.62	1.33	1.16	2.60	1.76	2.67	1.48	1.64
Er	1.07	1.22	0.771	1.54	0.858	1.56	1.17	0.935
Yb	0.940	1.30	1.01	1.70	0.695	1.84	1.18	0.994

Sample	JJG 105	JJG 2104	PC 1	PC 5.2/1	Rtfn 31.1	Rtfn 43.1	Rtfn 48.2	Rtfn 54.1
Sc	32.5	10.9	23.9	32.4	35.9	51.8	51.9	17.1
Ni	186	223	87.90	274	186	115	174	162
Sr	194	69.63	84.27	164	89.20	163	209	145
Y	6.62	4.17	6.00	6.63	5.50	12.2	4.43	8.11
Zr	23.7	2.77	6.66	11.27	8.67	32.8	32.47	7.354
Nb	1.20	0.220	0.267	0.375	0.056	0.433	n.d.	0.181
Th	0.244	n.d.	0.131	0.245	0.075	0.538	n.d.	n.d.
La	7.86	n.d.	2.04	4.52	1.51	9.97	12.6	0.007
Ce	21.5	0.128	4.54	10.18	4.64	22.8	31.4	0.323
Nd	11.4	0.997	4.99	5.90	3.50	11.0	14.3	3.04
Sm	2.03	0.571	1.64	1.40	1.00	2.09	2.27	1.96
Eu	0.626	0.441	0.587	0.465	0.372	0.699	0.638	0.928
Gd	1.62	0.664	1.49	1.25	0.984	1.88	1.62	1.83
Dy	1.29	0.719	1.16	1.15	0.980	2.04	0.945	1.63
Er	0.679	0.503	0.629	0.699	0.580	1.33	0.422	0.786
Yb	0.685	0.430	0.591	0.724	0.587	1.40	0.424	0.635

Sample	Rtfn 54.4	Rtfn 55.1	Rtfn 55.2	Rtfn 57.1
Sc	24.5	43.8	35.0	33.9
Ni	123	152	169	189
Sr	187	107	111	104
Y	10.9	11.3	4.17	6.05
Zr	9.12	33.2	15.3	9.27
Nb	n.d.	0.278	0.094	0.498
Th	n.d.	0.418	0.324	0.132
La	0.027	5.52	3.48	3.90
Ce	0.535	13.0	9.94	9.65
Nd	3.01	7.17	8.96	5.13
Sm	1.642	1.53	2.04	1.09
Eu	0.820	0.470	0.433	0.364
Gd	1.81	1.49	1.01	1.04
Dy	2.14	1.91	0.778	1.13
Er	1.17	1.38	0.498	0.687
Yb	0.978	1.44	0.460	0.642